



2053159

*External*

**Council for National Academic Awards**

DR. JAMES

President: HRH The Prince of Wales KG, GCB

Chairman: Sir Michael Clapham KBE, MA

Chief Officer: Edwin Kerr BSc, PhD

344-354 Gray's Inn Road, London WC1X 8BP  
Telephone: 01-278 4411



*With compliments*

Thesis returned as stated in letter  
of 21st December 1976



THE APPLICATION OF COMMUNICATION  
PRINCIPLES TO PULSE-WIDTH-  
MODULATED INVERTERS.

By

M.G.JAYNE, M.Sc.(Wales).

A dissertation submitted to the C.N.A.A. in support  
of an application for the degree of Doctor of Philosophy  
in Electrical Engineering.

AUGUST,1976.

Department of Electrical Engineering,  
University of Bristol.

Department of Electrical Engineering,  
Gwent College of Higher Education.

## MEMORANDUM

The accompanying dissertation - THE APPLICATION OF COMMUNICATION PRINCIPLES TO PULSE-WIDTH-MODULATED INVERTERS- is based on the work carried out by the author during fourteen months full-time research in the Engineering Laboratories of the University of Bristol between July, 1973 and September, 1974, and sixteen months part-time research in the Faculty of Science and Technology at the Gwent College of Higher Education, between September, 1974 and July, 1976.

All work and ideas are original unless otherwise acknowledged in the text or by reference. This work has not been submitted for another degree of the C.N.A.A., nor for the award of a degree or diploma at any other institution.

The main contributions that the author claims to have made to the subject of variable voltage/variable frequency inverters include:

- 1). An analysis of pulse modulation processes which concludes that the pulse-width-modulation process is best suited to inverters intended for cage rotor induction motor variable speed drives.
- 2). An investigation into prior-art harmonic elimination techniques which concludes that such techniques are only applicable to constant voltage/constant frequency inverters without incurring added power components and transformers.
- 3). Identification of the sampling process in prior-art inverters as natural sampling, which is a well known concept in communications engineering but which has not previously been referred to in power inverters.

- 4). Theoretical and experimental investigations into natural sampled pulse-width-modulated inverters, which concluded that at low values of carrier frequency to modulating frequency ratio, undesirable harmonic distortion occurs.
- 5). The application of the concept of regular sampling to pulse-width-modulated inverter systems which proved to be entirely novel.
- 6). Theoretical and experimental investigation into regular sampled pulse-width-modulated systems, which concluded that regular sampling techniques eradicated the many undesirable features present in prior-art natural sampled pulse-width-modulated inverter systems.
- 7). The construction of a practical thyristor pulse-width-modulated inverter which incorporated regular sampling techniques in its control circuits at very little extra cost.
- 8). An experimental investigation into the harmonic spectra of the output voltage from the thyristor pulse-width-modulated inverter, which concluded that the incorporation of regular sampling techniques in the control circuits, significantly increases the usable frequency range of the inverter without increasing the switching frequency of the power devices.

*Marcel Fayre*

## LIST OF SYMBOLS

- V = amplitude of pulse  
T = periodic Time  
t = time  
N, n, m = integers  
A = amplitude of wave  
 $\omega$  = angular frequency  
 $\phi$  = phase angle  
 $J_n$  = Bessel function of order n  
k = integer ratio  
R = resistance  
L = inductance  
C = capacitance  
 $\gamma$  = conduction angle  
V(t), U(t), f(t) = functions of time  
 $\alpha$  = firing angle  
Z = impedance  
E = direct supply voltage  
e = instantaneous values of time functions  
v = instantaneous voltage

### Suffices

- c - pertaining to carrier wave  
m - pertaining to modulating wave  
s - pertaining to sampling  
r - pertaining to repetition wave  
a - pertaining to phase of 3-phase system  
b - pertaining to phase of 3-phase system  
c - pertaining to phase of 3-phase system

## SUMMARY

The object of this dissertation is to show that communication principles may be usefully applied to pulse-width-modulated inverters to increase their useable frequency range, without increasing the switching frequency of the power devices.

The prior-art techniques of reducing harmonic distortion in pulse-width-modulated inverters is investigated, and it is shown that such techniques are mainly applicable to constant voltage/constant frequency inverters.

It is shown that the sampling process inherent in existing pulse-width-modulated inverters is natural sampling. The results of theoretical and experimental analysis shows that this sampling process is the cause of considerable unwanted harmonic distortion at low values of carrier frequency to modulating frequency ratio when operating in both the synchronous mode and asynchronous mode.

The concept of regular sampling which is common in communication engineering but which has not previously been used in power inverters, is applied to the pulse-width-modulation process, and it is shown that such techniques eradicate the many undesirable features introduced by natural sampling.

The construction of a practical thyristor pulse-width-modulated inverter whose control circuits incorporate regular sampling techniques is described. A harmonic spectral analysis of the output voltage waveforms from the power inverter, shows that the useable frequency range of the inverter is considerably increased by the application of regular sampling techniques to the control circuit, without increasing the switching frequency of the power devices.

CONTENTS

Page No.

(1.) INTRODUCTION	1
(1.1) Modulation	1
(1.2) The Need for Variable Frequency Supplies	1
(1.3) Variable-Frequency/Variable-Voltage Power Convertors	2
(1.3.1) Introduction	2
(1.3.2) The Cycloconverter	2
(1.3.3) The d.c. link inverter	3
(1.4) Infinitely-Variable Speed Control Systems	3
(2) THE FUNDAMENTAL THEORY OF PULSE MODULATED POWER CONVERTORS	7
(2.1) Introduction	7
(2.2) Principles of Modulation	7
(2.2.1) Types of Modulation	7
(2.2.2) The Unmodulated Pulse Carrier Wave	8
(2.2.3) Pulse Amplitude Modulation (P.A.M.)	8
(2.2.4) Pulse Position Modulation (P.P.M.)	11
(2.2.5) Pulse Width Modulation (P.W.M.)	15
(2.2.6) Trailing-Edge Pulse Width Modulation	15
(2.2.7) Leading-Edge Pulse Width Modulation	19
(2.2.8) Double-Edge Pulse Width Modulation	21
(2.2.9) Amplitude Modulated P.P.M. (A.M.P.P.M.)	24
(2.2.10) Amplitude Modulated P.W.M. (A.M.P.W.M.)	27
(2.3) Requirements of a Practical Pulse-Modulated Power-Convertor	31
(2.3.1) Introduction	31
(2.3.2) Choice of Modulation Device	31



CONTENTS (Cont'd)Page No.

(2.3.3) The Use of Thyristors as Pulse Modulating Devices	32
(2.3.4) Forced Commutation	32
(2.3.5) The Need for Feedback Diodes	38
(2.3.6) Requirement for Variation of Frequency and Magnitude of Output Voltage Waveform from Modulator	41
(2.3.7) Frequency Control	41
(2.3.8) Voltage Control	42
(2.4) Elimination of Unwanted Frequency Components	48
(2.4.1) Introduction	48
(2.4.2) Control of the Modulation Process	49
(2.4.2.1) Use of a Bipolar Carrier Wave	49
(2.4.2.2) Width Control of the Output Waveform	53
(2.4.2.3) Width Control of Multiple Pulse Output Waveform	55
(2.4.2.4) Changing the waveform of the Modulating Wave	58
(2.4.2.5) Increasing the Ratio of Carrier- Frequency to Modulating Frequency	58
(2.4.3) Modulation and Summation by means of a Transformer	59
(2.4.4) Modulation and Cancellation by supplying a 3-wire, 3-phase load	67
(2.5) Interim Conclusions	71

CONTENTS (CONT'D)Page No.

(3) THE GENERATION AND REALISATION OF P.W.M.	
WAVEFORMS	73
(3.1) Introduction	73
(3.2) The choice of Carrier Waveform	74
(3.3) Modulation Depth or Modulation Index	76
(3.4) The Generation of Leading-Edge P.W.M. Waveforms	78
(3.5) The Generation of Trailing-Edge P.W.M. Waveforms	78
(3.6) The Generation of Double-Edge P.W.M. Waveforms	81
(3.7) Identification of the Sampling Process in Existing P.W.M. Power Convertors	83
(3.8) The Generalised Sampling Theorem	84
(3.8.1) Limitation of the Generalised Sampling Theorem when Applied to The Natural Sampled P.W.M. Process	86
(3.9) Regular Sampling	90
(3.9.1) Regular Sampled Leading-Edge P.W.M.	92
(3.9.2) Regular Sampled Trailing-Edge P.W.M.	94
(3.9.3) Regular Sampled Symmetrical Double- Edge Modulation	94
(3.9.4) Regular Sampled Asymmetrical Double- Edge Modulation	96
(3.9.5) Limitations of the Regular Sampling Process in P.W.M. Systems	98
(3.10) Interim Conclusions	100

CONTENTS (CONT'D)Page No.

(4)	IMPROVEMENTS IN THE P.W.M. POWER CONVERTOR WHEN OPERATING IN THE SYNCHRONISED MODE.	102
(4.1)	Introduction	102
(4.2)	Prior-Art P.W.M. Systems	102
(4.2.1)	Analytical Investigation into Natural Sampled P.W.M. Systems	103
(4.2.1.1)	Details of Computed Harmonic Spectra	104
(4.2.1.2)	Leading-Edge P.W.M.	106
(4.2.1.3)	Trailing-Edge P.W.M.	111
(4.2.1.4)	Double-Edge P.W.M.	111
(4.2.1.5)	Choice of Natural <sup>1</sup> Sampled P.W.M. System	117
(4.2.2)	Experimental Investigation Into Natural Sampled Double-Edge P.W.M.	118
(4.2.2.1)	Measurements Technique	120
(4.2.2.2)	Experimental Results	122
(4.2.2.3)	Discussion of Results and Interim Conclusions	122
(4.3)	The Application of Regular Sampling to P.W.M. Power Convertors Operating in the Synchronised Mode.	137
(4.3.1)	Analytical Investigation Into Regular Sampled, Double-Edge P.W.M. Systems	139
(4.3.1.1)	Odd Triple-Integer Values of Frequency Ratio	140

CONTENTS (CONT'D)Page No.

(4.3.1.2)	Even Triple-Integer Values of Frequency Ratio	145
(4.3.1.3)	Odd Non-triple-Integer Values of Frequency Ratio	146
(4.3.1.4)	Even Non-triple-Integer Values of Frequency Ratio	147
(4.3.1.5)	Interim Conclusions	148
(4.3.2)	Experimental Investigation Into The regular Sampled Asymmetrical Double-edge P.W.M. Process	148
(4.3.2.1)	Control Circuit for Regular Sampled Asymmetrical Double-Edge P.W.M.	148
(4.3.2.2)	Harmonic Spectra	153
(4.3.2.2a)	Odd Triple-Integer Frequency Ratio's	155
(4.3.2.2b)	Even Triple-Integer Frequency Ratio's	155
(4.3.2.2c)	Odd Non-Triple- Integer Frequency Ratio's	161
(4.3.2.2d)	Even Non-Triple- Integer Frequency Ratio's	164
(4.3.3)	Amplitude Control of the Fundamental Harmonic Components	164
(4.4)	Interim Conclusions	167
(5)	A NOVEL ASYNCHRONOUS MODE CONTROL SCHEME FOR A P.W.M. POWER CONVERTOR	170

CONTENTS (CONT'D)Page No.

(5.1) Introduction	170
(5.2) The Natural Sampled Asynchronous Mode of Generating P.W.M. Control Waveforms	171
(5.2.1) Relationship Between Fundamental Repetition Frequency and Frequency Ratio	175
(5.2.2) Analytical Investigation Into the Natural Sampled Asynchronous Mode of Generating Double-Edge P.W.M. Waveforms	179
(5.2.2.1) Effects of Random Time- Phase Displacement Between Carrier Wave and Modulating Waves	180
(5.2.2.2) Desirability for Balanced Harmonic Spectra	183
(5.2.2.2a) D.C. Components	186
(5.2.2.2b) Sub-Harmonic Components	190
(5.2.2.2c) Wanted Harmonic Components	196
(5.2.2.2d) Super-Harmonic Components	197
(5.2.3) Interim Conclusions	198
(5.3) The Application of Regular Sampling Techniques to the Asynchronous Mode of Generating P.W.M. Control Waveforms	199
(5.3.1) Analytical Investigation Into the Application of Regular Sampling Techniques to the Asynchronous Mode of Generating Double-Edge P.W.M. Waveforms	199
(5.3.1.1) D.C. Components	199

CONTENTS (CONT'D)Page No.

(5.3.1.2)	Sub-Harmonic Components	200
(5.3.1.3)	Wanted Harmonic Components	202
(5.3.1.4)	Super-Harmonic Components	203
(5.3.1.5)	Interim Conclusions	202
(5.3.2)	Experimental Investigation Into the Three Double-Edge P.W.M. Control Schemes	204
(5.3.2.1)	Light Electronic Control System Which Simulated the Three P.W.M. Processes	204
(5.3.2.2)	Measurements Technique	210
(5.3.2.3)	Beat Effect Phenomenon	210
(5.3.2.4)	Experimental Results	213
(5.3.3)	Interim Conclusions	217
(6)	POWER CONVERTOR AND TRIGGER PULSE CIRCUITS	218
(6.1)	Introduction	218
(6.2)	Design Details of the Practical P.W.M. Power Convertor	218
(6.2.1)	Three-Phase Uncontrolled A.C. to D.C. Power Convertor	221
(6.2.2)	Three-Phase Auxiliary Impulse Commutated Thyristor Inverter	221
(6.2.3)	Inhibition Circuits and Steering Circuits	224
(6.2.4)	Trigger Pulse Amplifiers	228
(6.3)	Experimental Results	231
(6.3.1)	Synchronous-Mode of Operation	231

CONTENTS (CONT'D)Page No.

(6.3.1.1)	$f_m = 20 \text{ Hz}, \frac{f_c}{f_m} = 3,$ Mod.Index = 0.5	232
(6.3.1.2)	$f_m = 30 \text{ Hz}, \frac{f_c}{f_m} = 4,$ Mod.Index = 0.5	232
(6.3.1.3)	$f_m = 40 \text{ Hz}, \frac{f_c}{f_m} = 5,$ Mod.Index = 0.5	235
(6.3.1.4)	Relationship Between Amplitude of Fundamental Component and Modulation Index	235
(6.3.2)	Asynchronous-Mode of Operation	237
(6.3.2.1)	$f_m = 40 \text{ Hz},$ Mod.Index = 0.95	237
(6.3.2.2)	$f_m = 90 \text{ Hz},$ Mod.Index = 0.95	239
(6.3.2.3)	$f_m = 140 \text{ Hz},$ Mod.Index 0.95	239
(6.3.3)	Interim Conclusions	239
(7)	CONCLUSIONS	243
(8)	ACKNOWLEDGEMENTS	248
(9)	REFERENCES	249

## (1) INTRODUCTION

### (1.1) Modulation

This thesis is based upon the philosophy that frequency conversion whether in communication systems or in power electronic systems, can only be achieved by modulation.<sup>(1)</sup> All frequency changers can therefore be identified as modulators. Although this philosophy has been fully exploited in the development of communication systems, there appears to be little evidence to suggest that it has influenced the development of power frequency convertors. The possibility therefore existed, that the concepts and principles which have been used in the development of communications, could also be applied to power electronic convertors. This cross-fertilization of ideas between communication technology and power technology, could therefore provide, the basis for analysis and improvement of existing power convertors and the development of new power convertors. This thesis investigates the application of communication techniques to existing and new forms of pulse-modulated power electronic convertors.

### (1.2) The Need for Variable Frequency Supplies.

Much of the electrical energy produced at the present time is converted to mechanical energy for utilization. The energy conversion process is generally achieved by means of an electrical motor. Such motors are *often* required to be variable speed, of high efficiency, mechanically robust and require little maintenance. Most of these requirements are met by the 3-phase, squirrel-cage induction motor, with the exception of the requirement for speed variation.



The method used to control the speed of a cage rotor induction motor depends very much upon the application. If the motor is driving a fan or pump for example, the speed of the motor can be varied by varying the magnitude of the applied stator voltage only,<sup>(2)</sup> whereas, if the motor is required to have discrete changes in speed, pole-changing methods can be used.<sup>(3)</sup> Applications which require variation of speed and control of torque are best achieved by variation of the magnitude and frequency of the applied stator voltage. It is into this class of application which most infinitely variable systems of cage rotor induction motor speed control fall.

### (1.3) Variable-Frequency/Variable-Voltage Power Convertors.

#### (1.3.1) Introduction

As a result of the introduction of the thyristor in the 1950's and the present day cost of maintenance most electro/mechanical rotary convertors have been or are being replaced by static convertors which employ semi-conductor devices such as the thyristor. Convertors employing such semi-conductor devices can be made highly reliable and require no maintenance. Basically there are two types of thyristor power convertor: the cycloconvertor and the d.c. link inverter.

#### (1.3.2) The Cycloconvertor

The cycloconvertor principle of operation is not new, in fact, it was used as early as 1930 in Germany for producing a  $16\frac{2}{3}$  Hz. supply from a 50 Hz. supply for traction applications. This particular application utilized multi-anode, steel tank

mercury arc rectifiers. The use of the cycloconverter for the speed control of a single induction motor only became an economically attractive proposition as a result of the introduction of the thyristor. The cycloconverter converts a.c. directly to a.c. and allows power flow in both directions.<sup>(4)</sup> The frequency and magnitude of the output voltage can be varied, and commutation of the thyristors is inherent in the convertor.

### (1.3.3) The d.c. link Inverter.

This method of converting a.c. to a.c. basically entails two processes: (1) the conversion of a.c. at one particular value of frequency and voltage to either a constant or variable d.c. voltage, and (2) the conversion of a d.c. voltage to a.c. of variable frequency and variable voltage. The process of converting d.c. to a.c. is known as inversion,<sup>(5)</sup> and the convertor which achieves this process is known as an inverter. Inverters can be divided into two classes: those which rely upon the a.c. supply voltage to commutate the thyristors, and those which utilize circuit techniques to obtain forced commutation.<sup>(5)</sup> It is normally the latter class of inverter which is applied to variable speed cage rotor induction motor drives.

### (1.4) Infinitely-Variable Speed Control Systems

The main requirement of an infinitely variable system of speed control which utilizes squirrel-cage induction motors, is that the magnitude and frequency of the output voltage applied to the stator windings, be independently variable over a wide range. This allows the torque-speed characteristic of

the induction motor to match any required load characteristic. It is also important that the overall efficiency of the power convertor and induction motor remain above an acceptable level throughout the range of speed variation. These requirements are not easily met in practice. The cycloconvertor-squirrel-cage induction motor combination does not fulfill these requirements for two reasons: (1) The upper limit of output frequency is approximately only 50% of the input supply frequency. Above this limit considerable harmonic distortion is introduced in the output waveform which can cause the induction motor to crawl. (2) The overall efficiency of the convertor and induction motor falls off rapidly when the output frequency approaches or exceeds its upper limit. The range of output frequency variation has recently been increased by the application of communication techniques to the control circuit of the cycloconvertor.<sup>(6)</sup> Although this new control technique has significantly increased the upper limit of output frequency, the combining of the cycloconvertor with an off the shelf squirrel-cage induction motor does not satisfy the requirement of an infinitely variable system of speed control. Therefore, the conventional cycloconvertor-cage rotor induction motor speed control system, is only suitable for applications which have a restricted speed range.

Two new types of a.c. to a.c. power convertor were recently introduced, whose theory of operation is based entirely upon the communication principles of amplitude modulation.<sup>(7)</sup> These new convertors have a much wider range of output frequency

than the conventional cycloconverter. The main disadvantages of the new converters are: (1) they require special machines which are more costly than the conventional cage rotor induction motor, and (2) the overall efficiency of the converter and motor falls off rapidly when the output frequency of the converter approaches that of the mains supply frequency.

The d.c. link inverter driving a squirrel-cage induction motor can be made to satisfy many of the requirements of an infinitely variable system of speed control, although many problems still remain to be solved. For example, varying the frequency of the output voltage from the inverter can cause a change in the harmonic distortion of the output waveform. Similarly, changing the magnitude of the output voltage can create commutation problems, if such a change is brought about by varying the d.c. link voltage to the inverter. Therefore, the inverter must be capable of maintaining low harmonic distortion of the output waveform when the frequency is varied, and provide a means of controlling the magnitude of the output voltage, whilst the d.c. link voltage to the inverter remains constant. The overall efficiency of the inverter and squirrel-cage induction motor must be maintained at as high a level as possible, throughout the entire range of speed. Although the squirrel-cage induction motor is considerably less costly than a d.c. motor of equivalent rating, the cost of the inverter which drives the induction motor can be considerably greater than the cost of the a.c. to d.c. converter which drives the d.c. motor. It is therefore

most important that the cost of the inverter and its control circuitry be maintained at as low a value as possible, if the inverter-induction motor drive system is to be competitive with the d.c. motor - a.c. to d.c. convertor system.

It was felt that the application of communication principles and concepts to thyristor power inverters might form the basis for an induction motor variable speed drive, which would satisfy the many requirements of a viable infinitely-variable speed control system.

## (2) THE FUNDAMENTAL THEORY OF PULSE MODULATED POWER CONVERTORS.

### (2.1) Introduction

Pulse-modulation techniques have been used extensively in communications for the transmission of information signals.<sup>(8)</sup> It is only in the past decade that this form of modulation has been applied to power convertors. This has been brought about by the availability of high-power, fast switching transistors and thyristors. The conversion of d.c. to variable frequency a.c. which is commonly known as 'inversion', can only be achieved by pulse-modulation. It is therefore instructive to demonstrate that the communication principles of pulse-modulation apply to such power inverters.

### (2.2) Principles of Modulation

#### (2.2.1) Types of modulation

The unmodulated carrier-wave of a pulse-modulated system, is generally considered to consist of a series of regularly recurrent pulses. Such a waveform can be completely defined by three parameters. The three parameters are :

- (1) The amplitude of the pulses,  $V_p$ .
- (2) The duration between pulses,  $T$ .
- (3) The duration of the pulses,  $t_o$ .

Normally the three parameters are constant. Modulation is the process of varying one or more of the three parameters, while the remaining parameters are held constant. Variation of the amplitude of the pulses while the duration between pulses and the duration of the pulses are held constant is

termed - 'amplitude-modulation'. When the amplitude and duration of the pulses are held constant, and the duration between the pulses is made to vary, 'pulse-position-modulation' is achieved. The variation of the duration or width of the pulses, while the amplitude of the pulses and duration between the pulses are held constant, is known as 'pulse-width-modulation'. The above modulation processes are illustrated in the time domain in Fig.(2.1). Although pulse-modulation normally infers the variation of one parameter while the remaining two parameters are held constant, the possibility of simultaneously varying two of the three parameters or all three parameters cannot be ruled out.

### (2.2.2) The Unmodulated Pulse Carrier Wave

The zero on the time-axis of the unmodulated pulse-carrier wave may be positioned as shown in Fig.(2.2) The carrier-wave can then be expressed by the following time function:

$$U(t) = k + k \sum_{m=1}^{m=\infty} \frac{\sin m k \pi}{m k \pi} \cos m \omega_c t \quad \text{---- (2.1)}$$

where  $k = \frac{t_0}{T}$ .

### (2.2.3) Pulse Amplitude Modulation (P.A.M)

This method of modulation basically entails the varying of the amplitude of the pulses according to the modulating signal, so that instead of the pulses having unit height, they have a height varying as  $V(t)$ , where  $V(t)$  is the modulating function. Therefore, if the modulating function

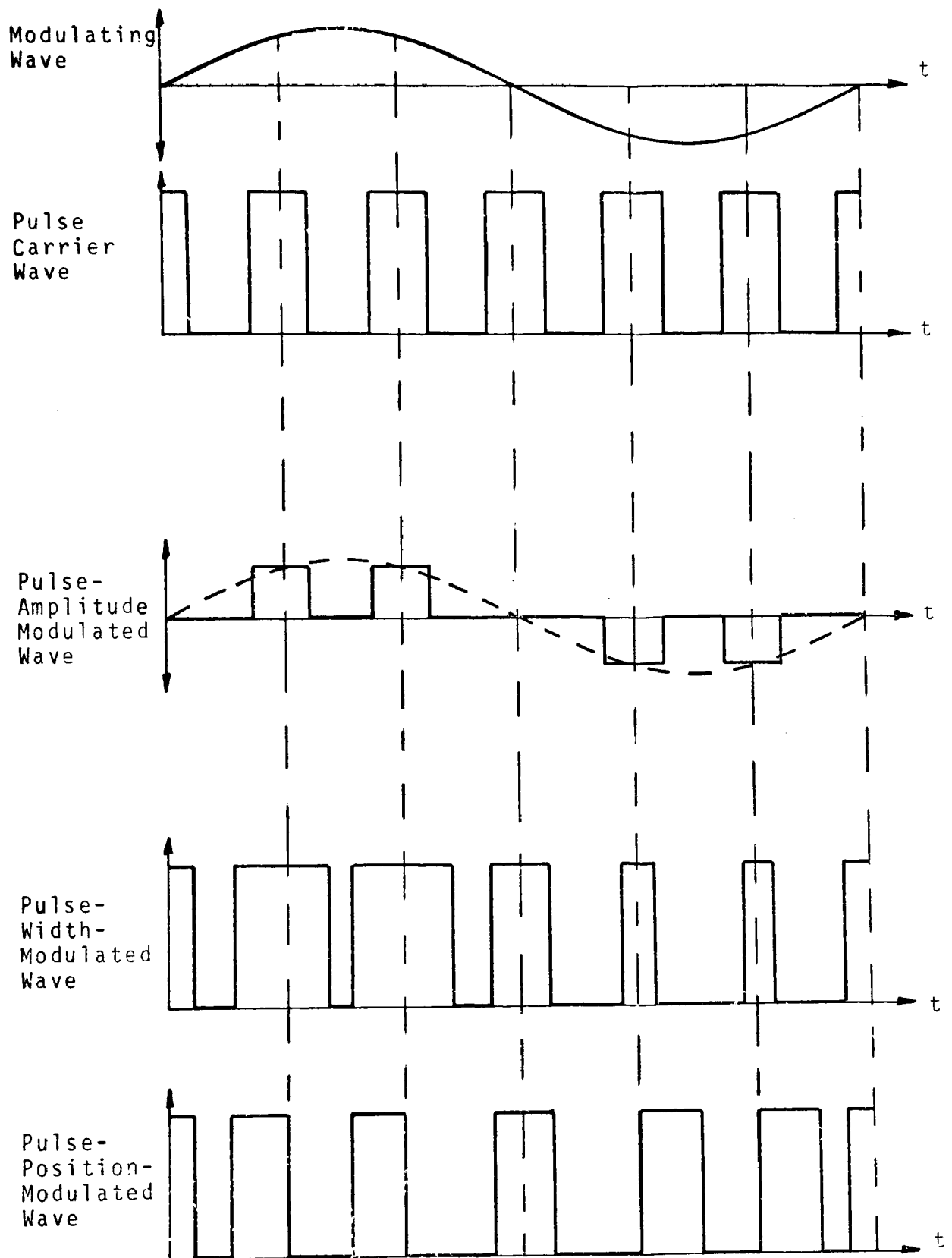


FIG.(2.1) TIME DOMAIN REPRESENTATION OF PULSE-MODULATION



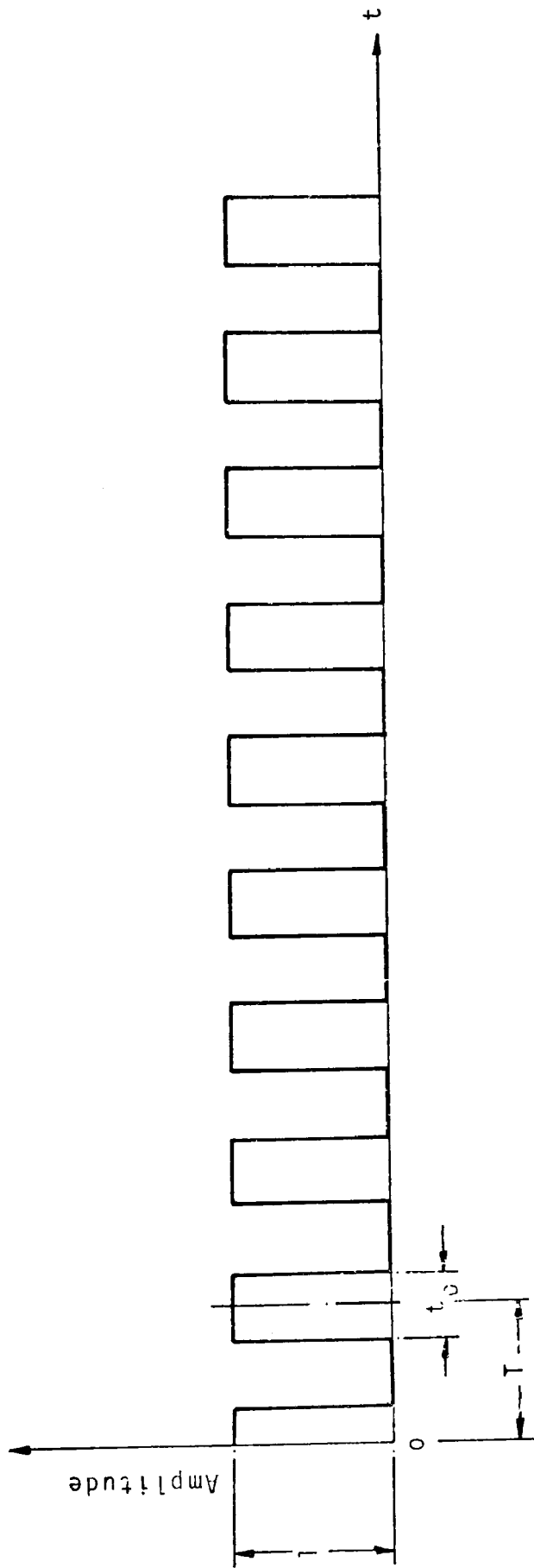


FIG.(2.2) UNMODULATED PULSE CARRIER WAVE OF UNITY AMPLITUDE

is defined by:

$$V(t) = A_m \cos(\omega_m t + \phi_m) \quad \text{---- (2.2)}$$

then the process of amplitude modulation is given by:

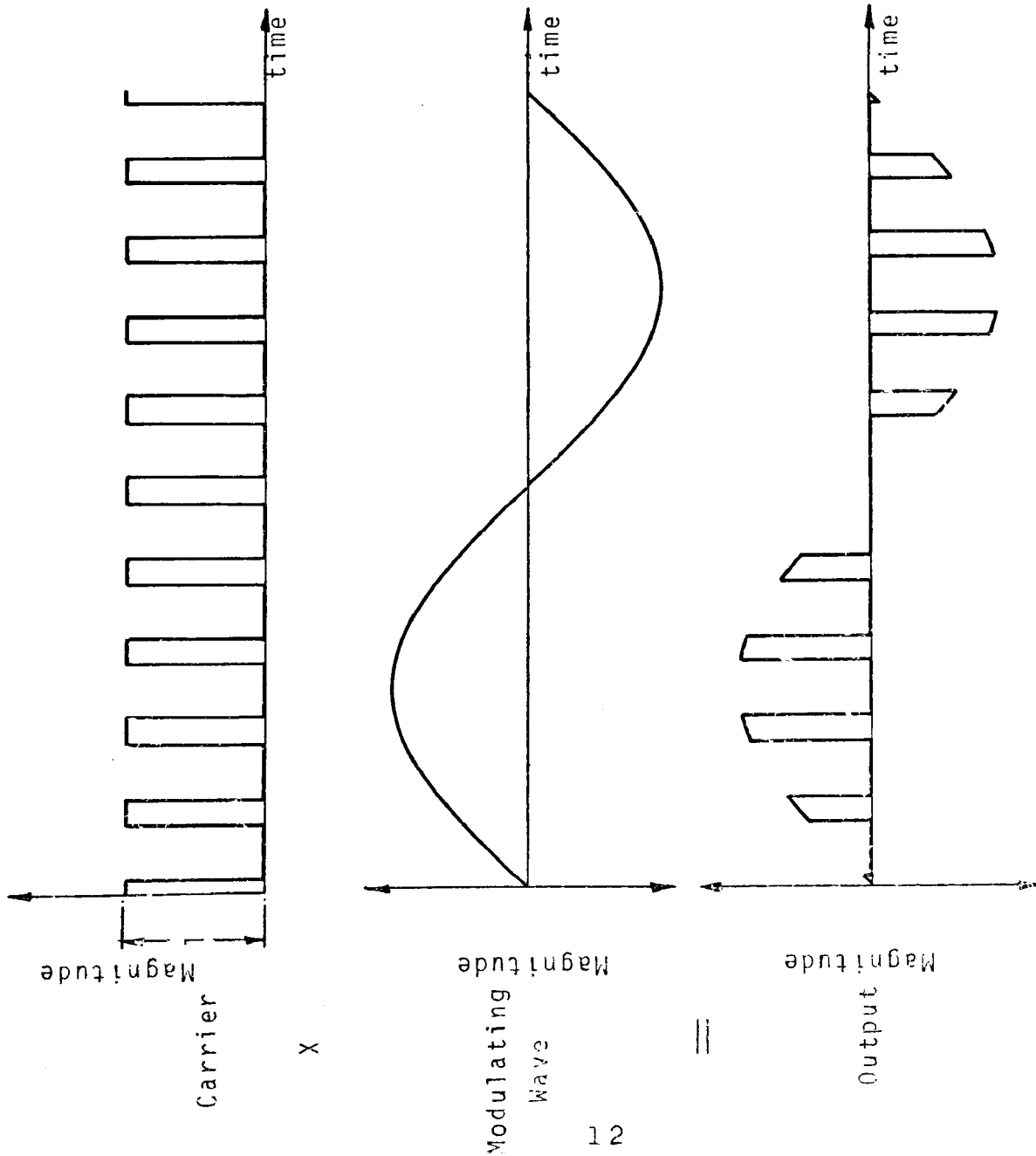
$$\begin{aligned} V U &= [A_m \cos(\omega_m t + \phi_m)] \left[ k + k \sum_{m=1}^{m=\infty} \frac{\sin m k \pi}{m k \pi} \cos m \omega_c t \right] \\ &= k A_m \cos(\omega_m t + \phi_m) + \\ &\quad k A_m \sum_{m=1}^{m=\infty} \frac{\sin m k \pi}{2 m k \pi} \cos [(m \omega_c \pm \omega_m) t \pm \phi_m] \quad \text{--(2.3)} \end{aligned}$$

This process is illustrated in both the time and frequency domains in Fig.(2.3). It will be seen from equation(2.3) that the products of modulation are upper and lower side bands of frequencies:  $(m \omega_c + \omega_m)$  and  $(m \omega_c - \omega_m)$  around the carrier of frequency,  $\omega_c$ , and its harmonics, plus a remanent of the modulating wave of frequency,  $\omega_m$ . The amount of modulating wave remaining, will depend on the magnitude of  $A_m$ . and the value of  $k$ .

#### (2.2.4) Pulse Position Modulation (P.P.M)

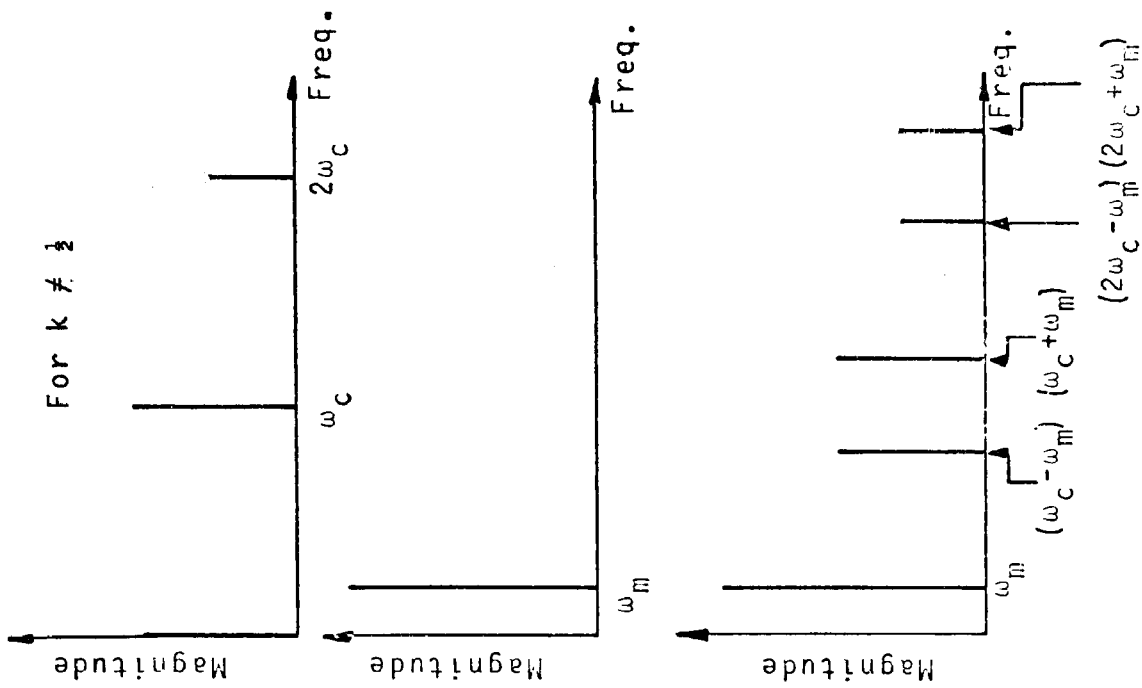
P.P.M.causes the pulses illustrated in Fig.(2.2) to be displaced in time according to instantaneous values of the modulating wave, the height and duration of the pulses being maintained constant. The unmodulated pules which have a repetition period,  $T$ , and mid-time values at  $0, T, 2T, 3T$ ----, are described by the time function:

$$U(t) = k + k \sum_{m=1}^{m=\infty} \frac{\sin m k \pi}{m k \pi} \cos m \omega_c t \quad \text{----(2.1)}$$



(a)

TIME DOMAIN REPRESENTATION.



(b) FREQUENCY DOMAIN REPRESENTATION

FIG. (2.3) PULSE AMPLITUDE MODULATION.

If the pulse centre lines are varied in time according to the function:

$$T A_m \cos(\omega_m t + \phi_m)$$

and  $t_0 \ll T$ , then the pulse-position-modulated pulses are described by the time-function<sup>(9)</sup>:

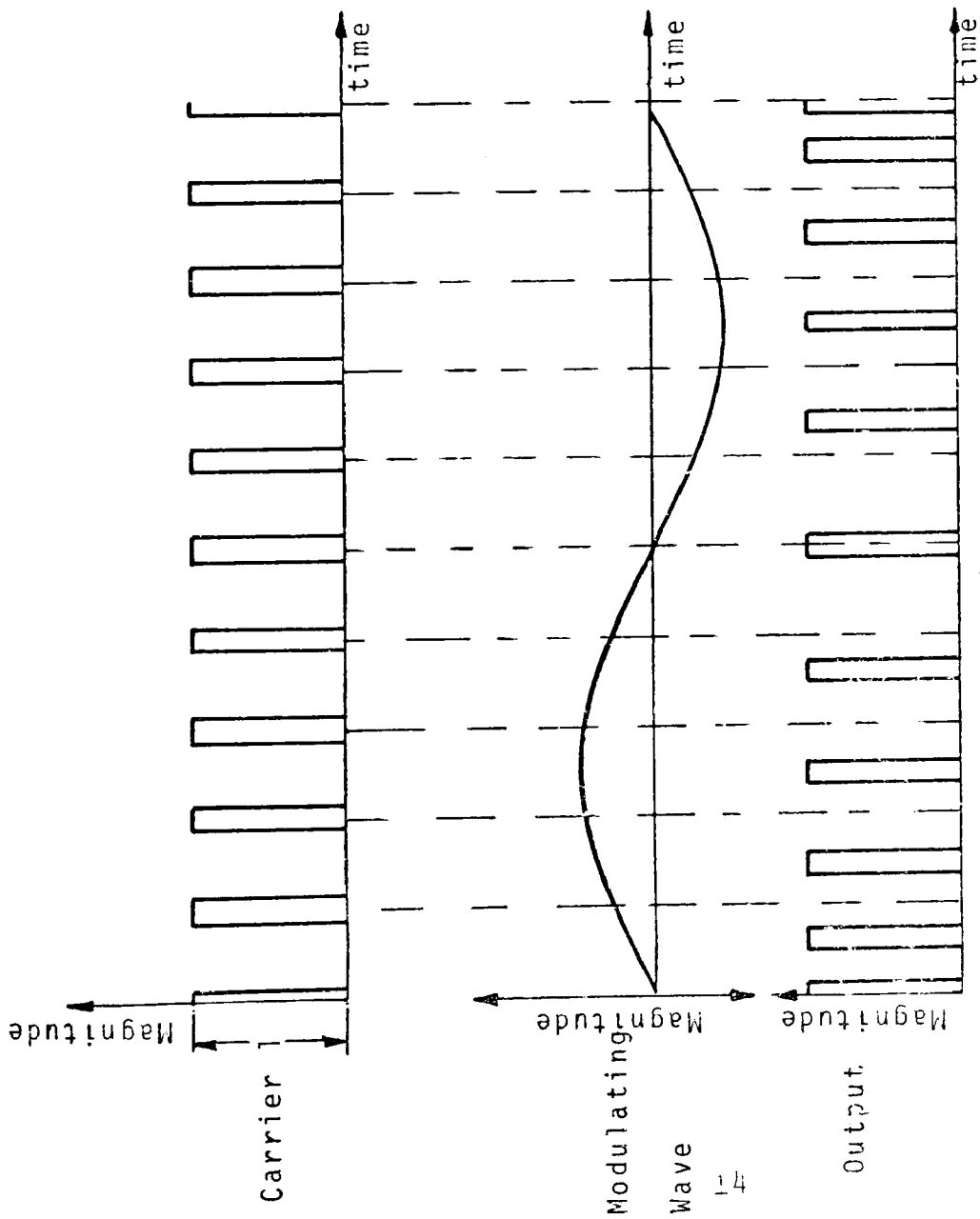
$$f(t) = k + 2k \sum_{m=1}^{m=\infty} \frac{\sin m k \pi}{m k \pi} \cos m \omega_c \left[ t - \frac{T A_m \cos(\omega_m t + \phi_m)}{T A_m \cos(\omega_m t + \phi_m)} \right] \quad \text{-----(2.4)}$$

Equation (2.4) can be further expanded in terms of Bessel functions as follows :

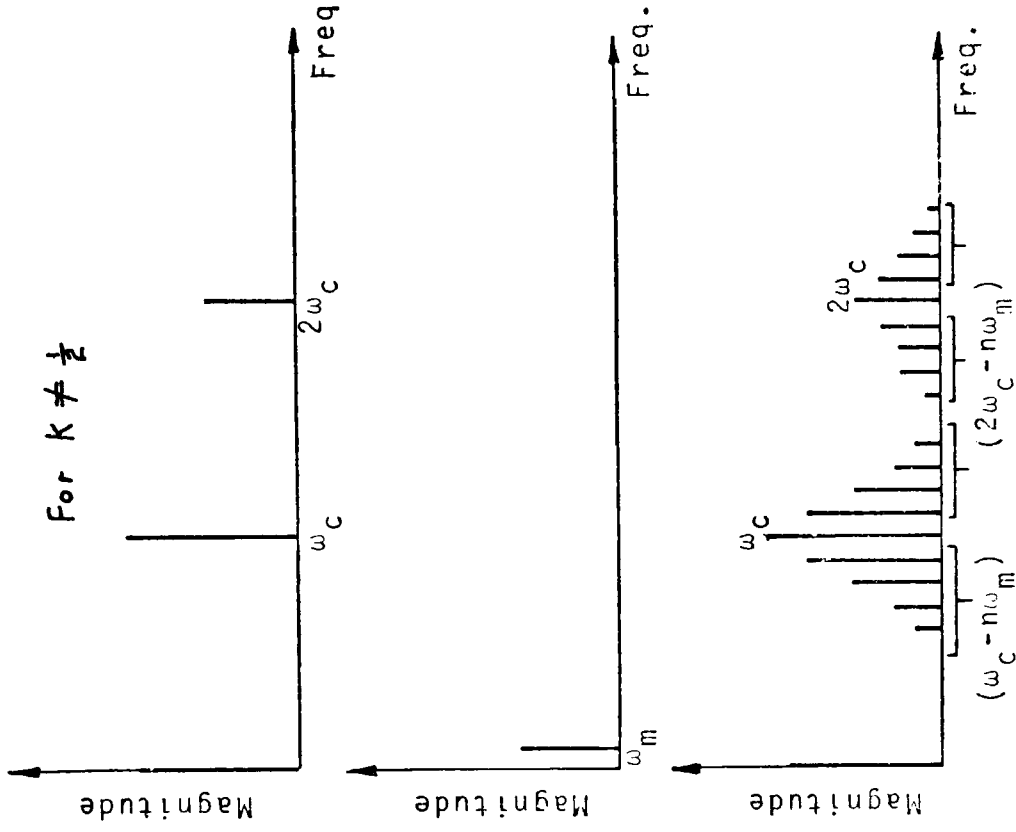
$$\begin{aligned} f(t) = k + 2k \sum_{m=1}^{m=\infty} \frac{\sin m k \pi}{m k \pi} \{ & J_0(x) \cos m \omega_c t \\ & + J_1(x) [\sin[(m\omega_c - \omega_m)t - \phi_m] - \sin[(m\omega_c + \omega_m)t + \phi_m]] \\ & - J_2(x) [\cos[(m\omega_c - 2\omega_m)t - 2\phi_m] + \cos[(m\omega_c + 2\omega_m)t + 2\phi_m]] \\ & - J_3(x) [\sin[(m\omega_c - 3\omega_m)t - 3\phi_m] - \sin[(m\omega_c + 3\omega_m)t + 3\phi_m]] \\ & + \dots \} \quad \text{-----(2.5)} \end{aligned}$$

where  $x = 2\pi A_m$ .

Fig (2.4) illustrates the P.P.M process in both the time and frequency domains. Equation (2.5) illustrates that the products of modulation are the carrier signal and its harmonics which have amplitudes of  $\frac{2 \sin m k \pi}{m \pi} J_0(x)$ , and side-bands around the carrier and its harmonics of frequencies:  $m(\omega_c - \omega_m)$  and  $m(\omega_c + \omega_m)$  and amplitudes of  $\frac{2 \sin m k \pi}{m \pi} J_n(x)$ . It is important to note that equation



(a) TIME DOMAIN REPRESENTATION



(b) FREQUENCY DOMAIN REPRESENTATION

FIG.(2.4) PULSE POSITION MODULATION

(2.5) does not contain a harmonic component of modulating frequency whose amplitude is proportional to the amplitude of the modulating wave. This suggests that no linear means of voltage control of the wanted harmonic component is provided.

#### (2.2.5) Pulse-Width-Modulation (P.W.M)

This method of modulation causes the widths of the pulses illustrated in Fig.(2.2) to vary. The degree of variation in the width of each pulse, is dependent upon instantaneous values of the modulating wave. The three possible ways by which the duration of the pulses can be varied are:

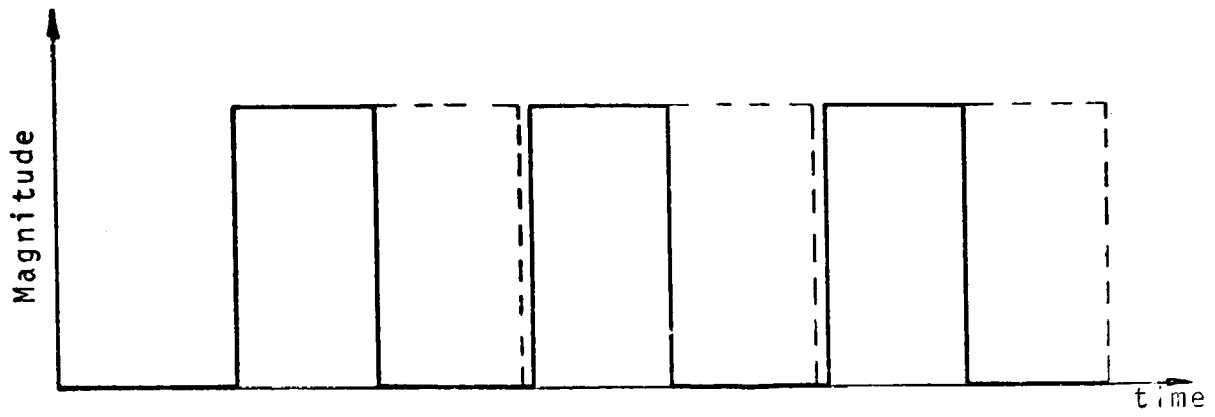
- (1) leading-edge fixed, trailing-edge varied,
- (2) trailing-edge fixed, leading-edge varied,
- (3) centre line of pulses fixed, both edges varied.

These three methods of varying the widths of the pulses are used to define the type of pulse-width-modulation, and are illustrated in Fig.(2.5)

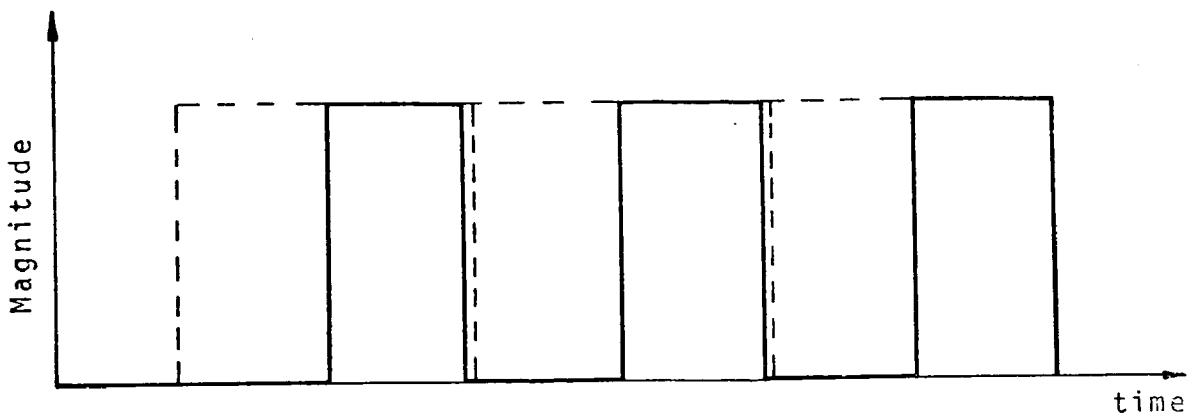
#### (2.2.6) Trailing-Edge Pulse-Width-Modulation

This particular form of P.W.M. causes the leading-edges of the pulses to be fixed, whilst the trailing-edges are modulated, the degree of modulation being dependent upon instantaneous values of the modulating wave. This process is illustrated in Fig.(2.6). The unmodulated pulses of duration,  $t_0$ , and repetition period,  $T$ , are described by the time function<sup>(10)</sup>:

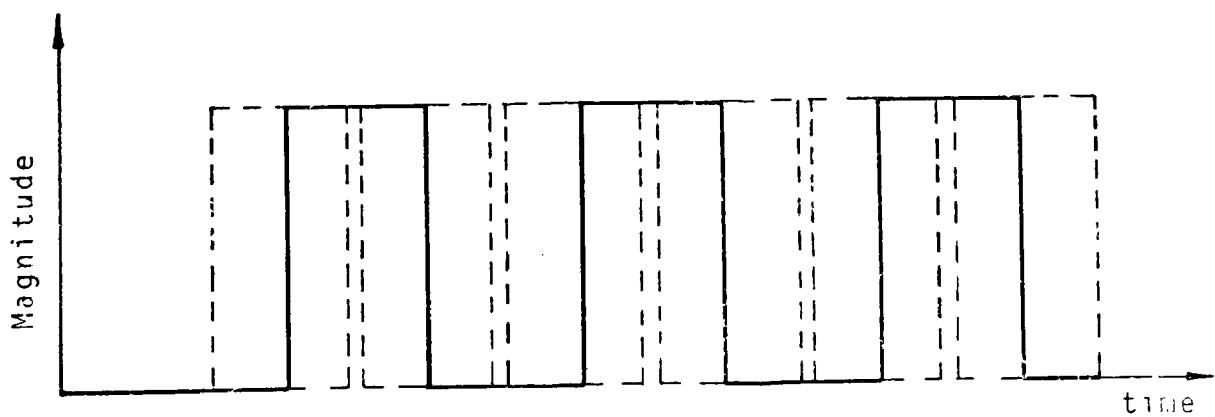
$$f(t) = k + k \sum_{m=1}^{m=\infty} \frac{\sin 2m k \pi}{m k \pi} \cos m\omega_c t + k \sum_{m=1}^{m=\infty} \frac{(1 - \cos 2 m k \pi)}{m k \pi} \sin m\omega_c t \quad \text{-----(2.6)}$$



(a) Trailing-Edge Modulation

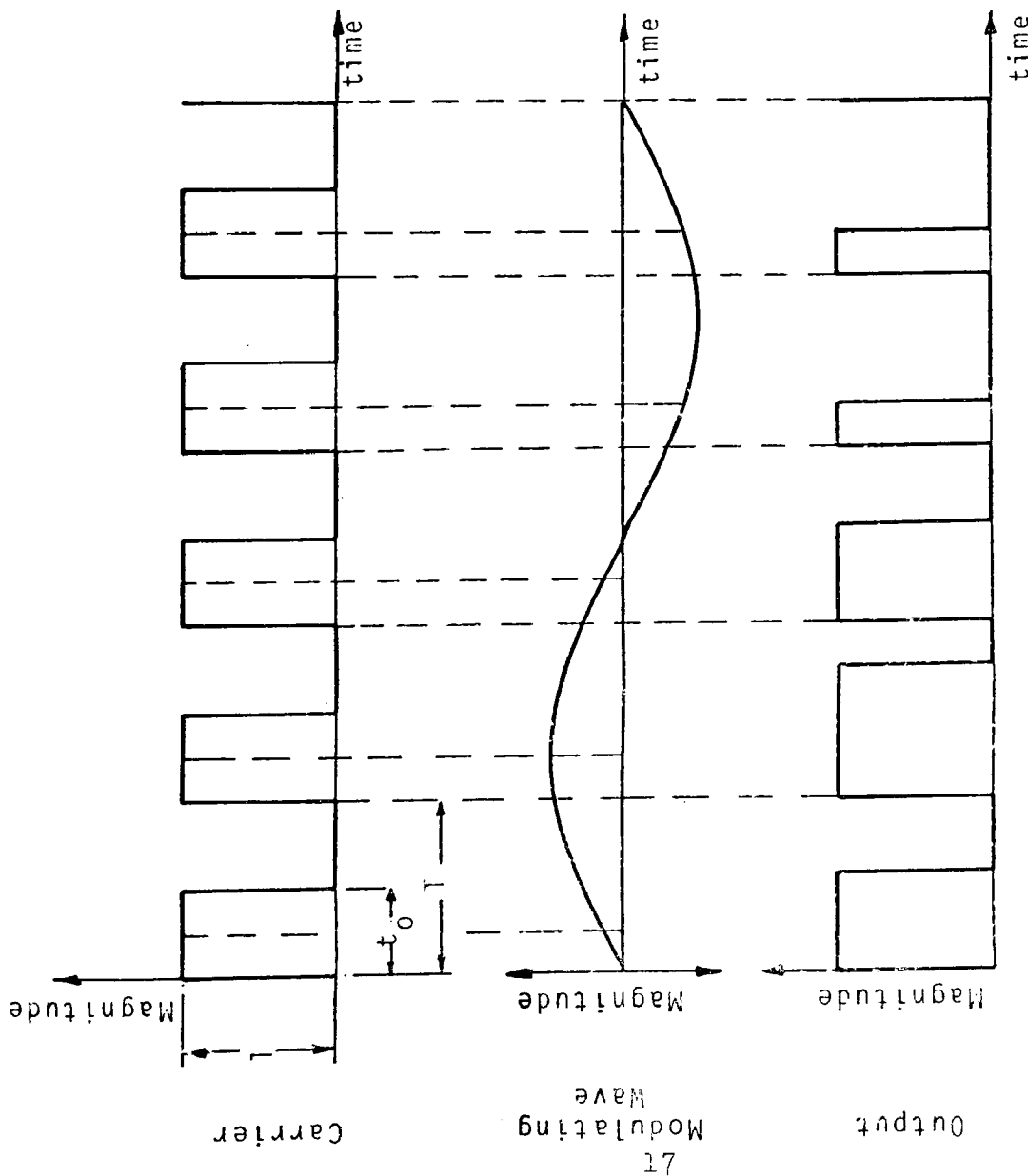


(b) Leading-Edge Modulation

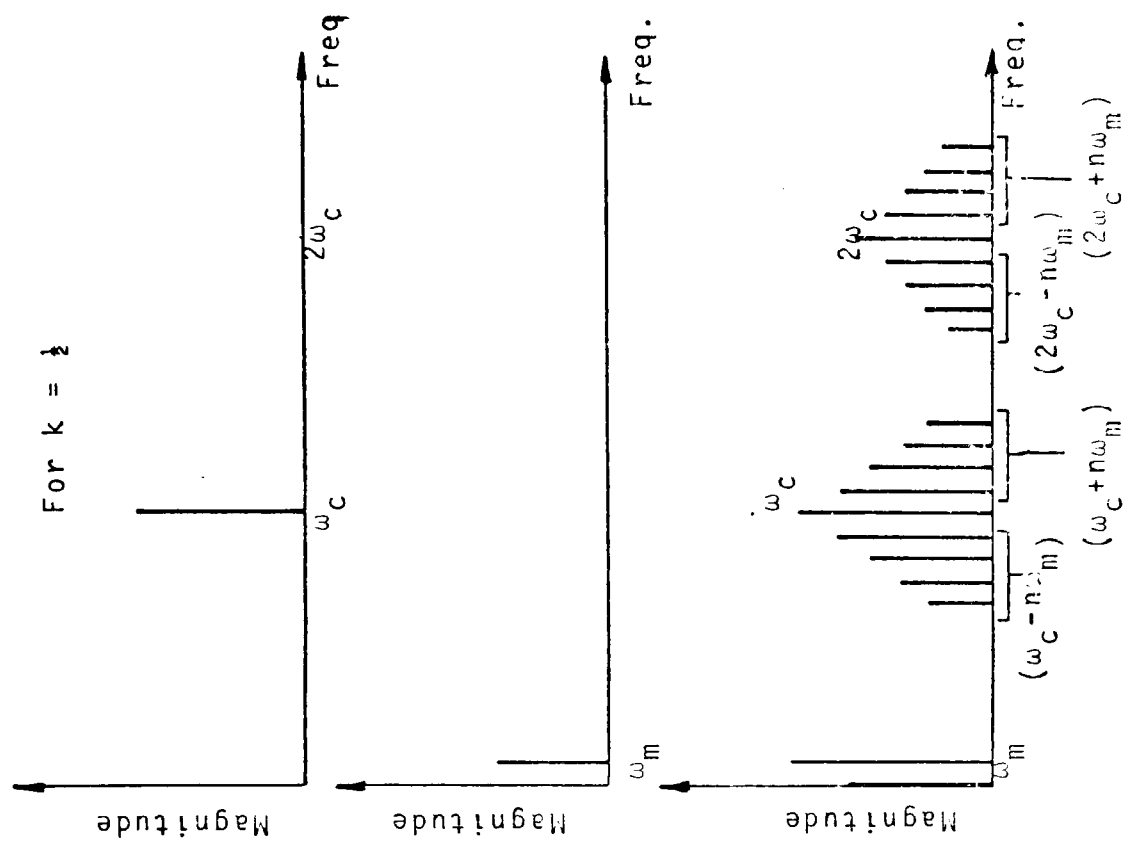


(c) Double-Edge Modulation

FIG.(2.5) TYPES OF PULSE WIDTH MODULATION



(a) TIME DOMAIN REPRESENTATION



(b) FREQUENCY DOMAIN REPRESENTATION

FIG. (2.6) TRAILING-EDGE PULSE WIDTH MODULATION



For this case one of the leading edges of the pulses, is chosen to coincide with zero time as illustrated in Fig. (2.6) If the duration of the pulses are varied according to the function:

$$T_0(1 + A_m \cos(\omega_m t + \phi_m)) \quad \text{-----(2.7)}$$

then the width modulated pulses are described by the function:

$$\begin{aligned} f(t) = & k(1 + A_m \cos(\omega_m t + \phi_m)) \\ & + \frac{1}{\pi} \sum_{m=1}^{m=\infty} \frac{1}{m} [\sin 2 m \pi k(1 + A_m \cos(\omega_m t + \phi_m))] \cos m \omega_c t \\ & + \frac{1}{\pi} \sum_{m=1}^{m=\infty} \frac{1}{m} [1 - \cos 2 \pi m k(1 + A_m \cos(\omega_m t + \phi_m))] \sin m \omega_c t \end{aligned} \quad \text{-----(2.8)}$$

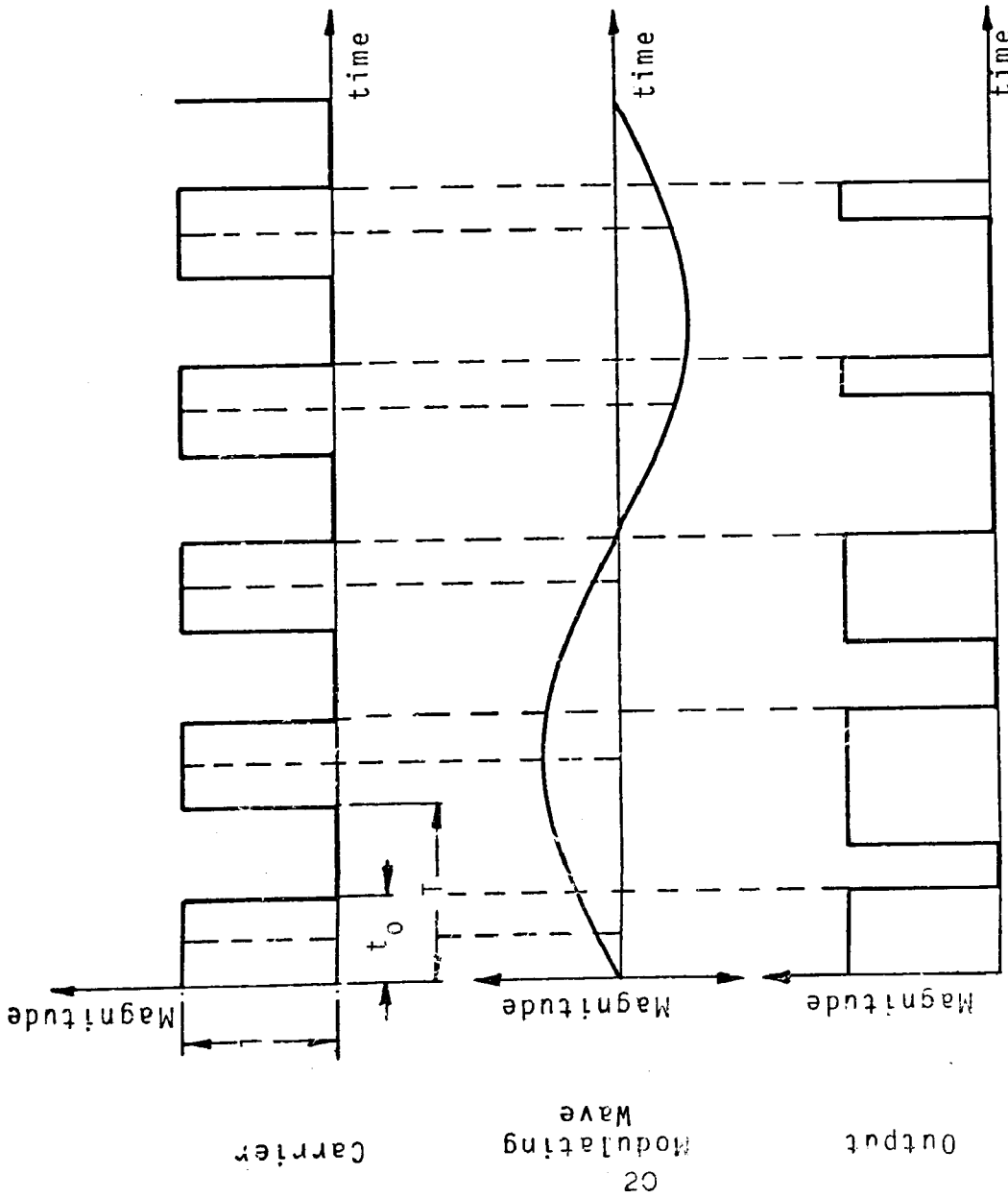
This function can also be described in terms of Bessel functions as follows:

$$\begin{aligned} f(t) = & k(1 + A_m \cos(\omega_m t + \phi_m)) + \frac{1}{\pi} \sum_{m=1}^{m=\infty} \frac{1}{m} (\sin m \omega_c t) \\ & + \frac{1}{\pi} \sum_{m=1}^{m=\infty} \sum_{n=1}^{n=\infty} \frac{1}{m} [J_n(2 m \pi k A_m) \sin(2 m \pi k + \frac{n \pi}{2})] \cos((m \omega_c \pm n \omega_m)t \pm n \phi) \\ & - \frac{1}{\pi} \sum_{m=1}^{m=\infty} \sum_{n=1}^{n=\infty} \frac{1}{m} [J_n(2 m \pi k A_m) \cos(2 m \pi k + \frac{n \pi}{2})] \sin((m \omega_c \\ & \pm n \omega_m)t \pm n \phi) \end{aligned} \quad \text{-----(2.9)}$$

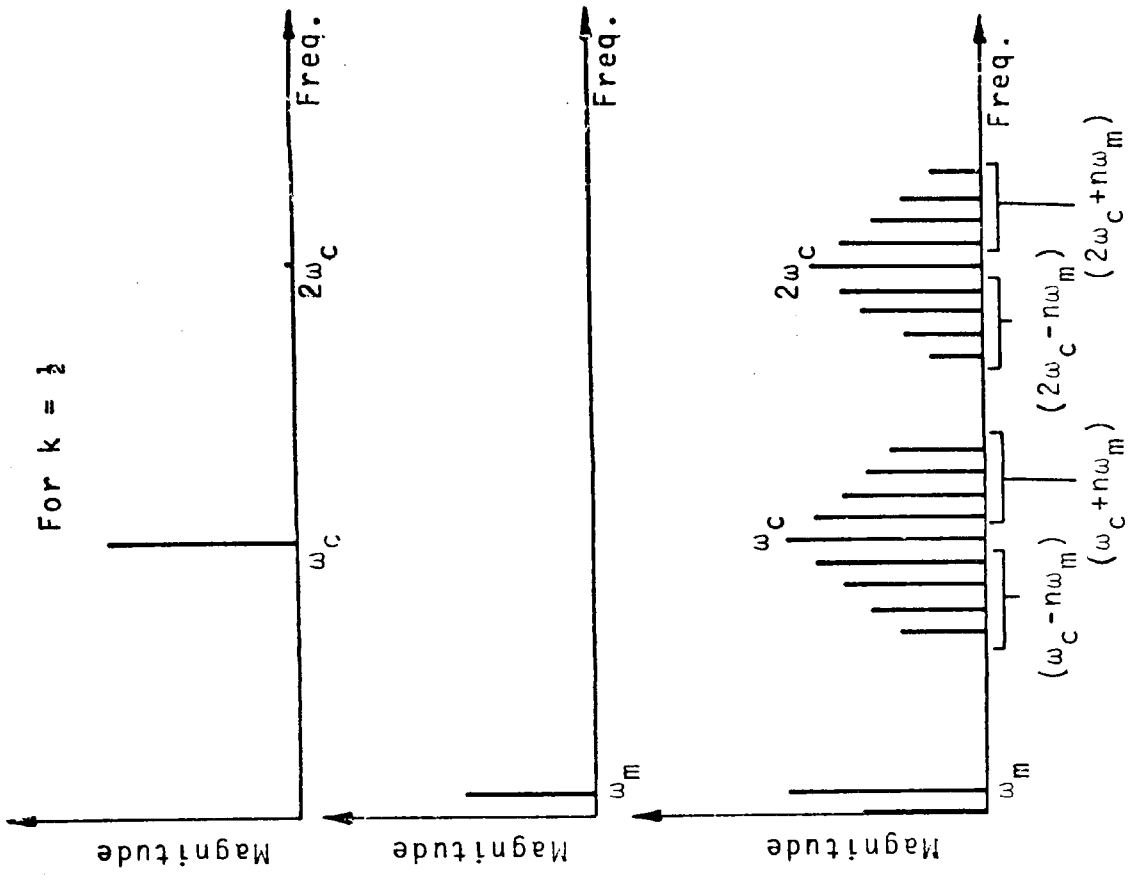
From equation (2.9), several interesting facts are apparent: the amplitude of the harmonic component of modulating frequency, is directly proportional to the amplitude of the modulating wave. No harmonics of the modulating wave are present. The amplitude of a harmonic of the carrier wave is inversely proportional to its order. It is of particular interest to note that if the mark/space ratio of the unmodulated pulse carrier-wave is made equal to 1:1, that is to say:  $k = \frac{1}{2}$ ; then only one of the two side-band terms exists for integer values of  $m$  and  $n$ . Therefore, for odd values of  $m$  and  $n$  the side-band components  $\text{Sin}((m\omega_c \pm n\omega_m)t \pm \phi_m)$  will exist with amplitudes of  $\frac{1}{m} J_n(2 m \pi k A_m)$ , whereas, for even values of  $m$  and  $n$  the side-band terms of  $\text{Cos}((m\omega_c \pm n\omega_m)t \pm \phi_m)$  will exist, their amplitudes being given by:  $\frac{1}{m} J_n(2 m \pi k A_m)$ . This means that for all integer values of  $m$  and  $n$ , side-band frequency components of frequencies:  $(m\omega_c + n\omega_m)$  and  $(m\omega_c - n\omega_m)$  will always occur for this particular form of P.W.M.

#### (2.2.7) Leading-Edge Pulse-Width-Modulation

For this p.w.m. process the trailing-edges of the pulses are fixed while the leading-edges are modulated. Fig.(2.7) illustrates this process in both the time and frequency domains. The time function which describes the modulation of the pulses can be determined from equation (2.9) by reversing the time scale; that is to say: substituting  $-t$  for  $t$ . This results in the following function:



(a) TIME DOMAIN REPRESENTATION



(b) FREQUENCY DOMAIN REPRESENTATION

FIG. (2.7) LEADING-EDGE PULSE WIDTH MODULATION

$$\begin{aligned}
f(t) = & k(1 + A_m \text{Cos}(\omega_m t + \phi_m)) - \frac{1}{\pi} \sum_{m=1}^{m=\infty} \frac{1}{m} \text{Sin } m\omega_c t \\
& + \frac{1}{\pi} \sum_{m=1}^{m=\infty} \sum_{n=1}^{n=\infty} \frac{1}{m} [J_n(2 m \pi k A_m) \text{Sin}(2 m \pi k + \frac{n \pi}{2})] \text{Cos}((m\omega_c \\
& \hspace{15em} + n\omega_m)t + n\phi_m) \\
& + \frac{1}{\pi} \sum_{m=1}^{m=\infty} \sum_{n=1}^{n=\infty} \frac{1}{m} [J_n(2 m \pi k A_m) \text{Cos}(2 m \pi k + \frac{n \pi}{2})] \text{Sin}((m\omega_c \\
& \hspace{15em} + n\omega_m)t - n\phi_m) \text{ ---(2.10)}
\end{aligned}$$

The amplitudes of the various components are the same as for trailing-edge modulation but the phase relationships are different.

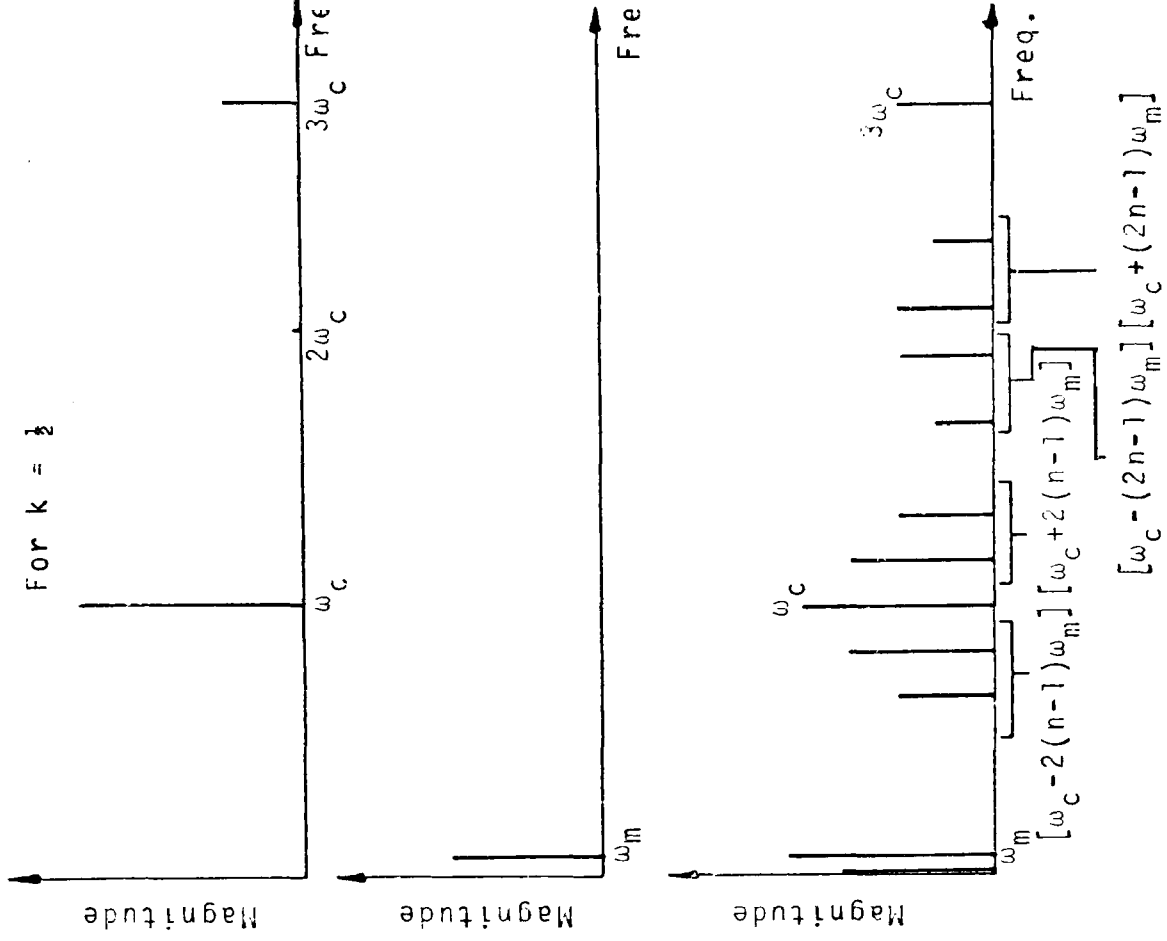
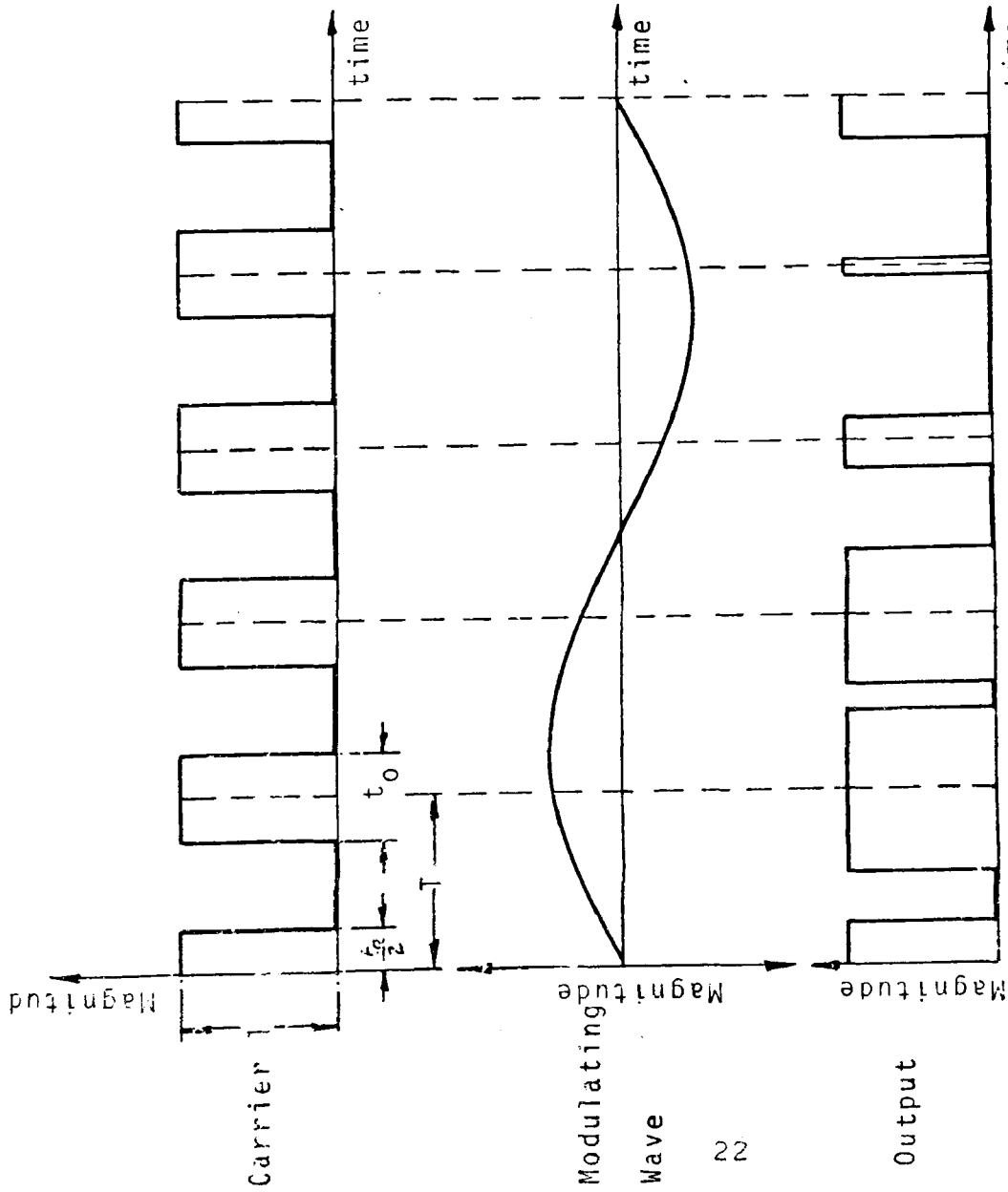
#### (2.2.8) Double-Edge Pulse-Width-Modulation

This form of modulation causes both edges of the pulses to be modulated. The instants in time at which the leading and trailing edges of each pulse occur, are dependent upon the respective instantaneous values of the modulating wave. This process is illustrated in Fig.(2.8). The unmodulated pulses of duration,  $t_o$ , with one pulse centred at  $t = 0$ , can be described by the time function:

$$f(t) = k + \frac{2}{\pi} \sum_{m=1}^{m=\infty} \left[ \frac{1}{m} \text{Sin } m \pi k \right] \text{Cos } m\omega_c t \text{ ----(2.11)}$$

If the duration of the pulses are varied according to the function:

$$t_o(1 + A_m \text{Cos}(\omega_m t + \phi_m)) \text{ ----(2.12)}$$



(a) TIME DOMAIN REPRESENTATION

(b) FREQUENCY DOMAIN REPRESENTATION

FIG.(2.8) DOUBLE-EDGE PULSE WIDTH MODULATION

then the width-modulated pulses are described by the function:

$$\begin{aligned}
 f(t) &= k(1 + A_m \cos(\omega_m t + \phi_m)) \\
 &+ \frac{2}{\pi} \sum_{m=1}^{m=\infty} \frac{1}{m} \{ \sin m \pi k \cos [m \pi k A_m \cos(\omega_m t + \phi_m)] \\
 &+ \cos m \pi k \sin [m \pi k A_m \cos(\omega_m t + \phi_m)] \} \cos m \omega_c t
 \end{aligned}
 \tag{2.13}$$

This function can also be described in its Bessel function form as follows:

$$\begin{aligned}
 f(t) &= k(1 + A_m \cos(\omega_m t + \phi_m)) \\
 &+ \frac{2}{\pi} \sum_{m=1}^{m=\infty} \frac{1}{m} \{ [J_0(m \pi k A_m) \sin m \pi k] \cos m \omega_c t \\
 &+ \sum_{n=1}^{n=\infty} J_n(m \pi k A_m) \sin(m \pi k + \frac{n \pi}{2}) [\cos((m \omega_c \\
 &+ n \omega_m)t + n \phi_m) \\
 &+ \cos((m \omega_c - n \omega_m)t - n \phi_m)] \}
 \end{aligned}
 \tag{2.14}$$

This function shows that, for this case also, the amplitude of the harmonic component of modulating frequency is proportional to the amplitude of the modulating wave.

The second term gives the carrier component and its harmonics of frequency,  $m \omega_c$ . The amplitude of the harmonics of the carrier wave are dependent upon the value of  $k$ .

If  $k = \frac{1}{2}$ , (that is to say: the mark/space ratio of the unmodulated pulses is 1:1) then only odd harmonics of the carrier will be present.

The third term gives the side-band about the carrier, whose frequencies are given by  $(m\omega_c + n\omega_m)$  and  $(m\omega_c - n\omega_m)$ . The amplitude of the side -bands are once again dependent upon the value of  $k$ . If  $k = \frac{1}{2}$  as before then for odd harmonics of the carrier only even order side-bands exist, and for even harmonics of the carrier only odd order side-bands exist.

(2.2.9) Amplitude Modulated P.P.M. (A.M.P.P.M)

This type of modulation employs a double modulation process. The p.p.m. wave is taken as the carrier, and is further amplitude modulated by a second modulating wave. It was shown in Section (2.2.4) that the p.p.m. output wave could be described by equation (2.4):

$$f(t) = k + 2k \sum_{m=1}^{m=\infty} \frac{\sin m k \pi}{m k \pi} \cos m\omega_c [t - T A_m \cos(\omega_m t + \phi_m)]$$

If this function is amplitude modulated by the time function:

$$V'(t) = A'_m \cos(\omega'_m t + \phi'_m)$$

the resulting modulated waveform is described by the time function:

CF	=	000000	XAR1	=	000400	XR	=	025052
CFTAB	=	000016R	XAR2	=	001000	XRET	=	077615
END	=	000240RG	XAR3	=	001400	XROVM	=	077612
GO	=	000060R	XAR4	=	002000	XS	=	025452
I	=	000022	XAR5	=	002400	XSACH	=	054000
M	=	000021	XAR6	=	003000	XSACL	=	050000
NEW0	=	177770	XAR7	=	003400	XSAR	=	030000
NEW1	=	177771	XB	=	174400	XSOVM	=	077613
NUM	=	000001	XBANZ	=	172000	XSPAC	=	077620
ONE	=	000144	XBGEZ	=	176400	XSST	=	076000
PA0	=	000000	XBGZ	=	176000	XSUB	=	010000
PA1	=	000400	XBIOZ	=	173000	XSUBC	=	062000
PA2	=	001000	XBLEZ	=	175400	XSUBH	=	061000
PA3	=	001400	XBLZ	=	175000	XSUBS	=	061400
PA4	=	002000	XBNZ	=	177000	XT	=	026452
PA5	=	002400	XBV	=	172400	XTBLR	=	063400
PA6	=	003000	XBZ	=	177400	XTBLW	=	076400
PA7	=	003400	XC	=	000003	XV	=	034530
RODEC	=	000230	XCALA	=	077614	XX	=	000004
ROINC	=	000250	XCALL	=	174000	XXOR	=	074000
RONOT	=	000210	XDINT	=	077601	XZAC	=	077611
R1DEC	=	000230	XDMOV	=	064400	XZALH	=	062400
R1INC	=	000250	XEINT	=	077602	XZALS	=	063000
R1NOT	=	000210	XI	=	000020	X0	=	000000
START	=	000006RG	XIN	=	040000	X1	=	000400
S0	=	000000	XLAC	=	020000	X10	=	*****
S1	=	000400	XLACK	=	077000	X11	=	*****
S10	=	005000	XLAR	=	034000	X12	=	*****
S11	=	005400	XLARK	=	070000	X13	=	*****
S12	=	006000	XLARF	=	064200	X14	=	*****
S13	=	006400	XLDF	=	067400	X15	=	*****
S14	=	007000	XLDFK	=	067000	X16	=	*****
S15	=	007400	XLST	=	075400	X17	=	*****
S2	=	001000	XLT	=	065000	X2	=	*****
S3	=	001400	XLTA	=	066000	X3	=	*****
S4	=	002000	XLTD	=	065400	X4	=	002000
S5	=	002400	XM	=	*****	X5	=	*****
S6	=	003000	XMAR	=	064000	X6	=	*****
S7	=	003400	XMASK	=	017777	X7	=	*****
S8	=	004000	XMPY	=	066400	X8	=	*****
S9	=	004400	XMPYK	=	100000	X9	=	*****
TI	=	*****						

6)

```
. ABS. 000000 000
      000240 001
ERRORS DETECTED: 46
```

```
VIRTUAL MEMORY USED: 4639 WORDS ( 19 PAGES)
DYNAMIC MEMORY AVAILABLE FOR 64 PAGES
FEB26,FEB26=TIMACN,FEB26
```

```
.TYPE TAUTO.MAC
;TESTED MAR 15 1983 (C) COPYRIGHT 1983, 1984 DSPS INC., OTTAWA
;ALL RIGHTS RESERVED
  .TITLE TAUTO
  .GLOBL START END
  .RADIX 10.
; **DEFINE CONSTANTS
XN=50. ;50 SAMPLES
INP=199. ;ALL SAMPLES SAME AMPLITUDE
M=10. ;10 LAGS
; **ASSIGN DATA STORAGE LOCATIONS
SCOUNT=123. ;STORE FOR SHIFT COUNT
TEMP=124. ;STORE FOR TEMP
```



$$\begin{aligned}
f'(t) &= k A'_m \text{Cos}(\omega'_m t + \phi'_m) \\
&+ 2 k A'_m \sum_{m=1}^{m=\infty} \frac{\text{Sin } m k \pi}{m k \pi} \text{Cos}(\omega'_m t + \phi'_m) \text{Cos } m\omega_c [t \\
&- T A'_m \text{Cos}(\omega'_m t + \phi'_m)] \quad \text{-----(2.15)}
\end{aligned}$$

This function can be described in terms of Bessel functions as follows:

$$\begin{aligned}
f'(t) &= k A'_m \text{Cos}(\omega'_m t + \phi'_m) \\
&+ k A'_m \sum_{m=1}^{m=\infty} \frac{\text{Sin } m k \pi}{m k \pi} \{ J_0(x) [\text{Cos}((m\omega_c + \omega'_m)t + \phi'_m) \\
&\quad + \text{Cos}((m\omega_c - \omega'_m)t - \phi'_m)] \\
&+ J_1(x) \text{Sin}[(m\omega_c \pm \omega'_m)t \pm \phi'_m] \\
&\quad - J_2(x) \text{Cos}[(m\omega_c \pm 2\omega'_m)t \pm 2\phi'_m] \\
&- J_3(x) \text{Sin}[(m\omega_c \pm 3\omega'_m)t \pm 3\phi'_m] + \dots \} \text{-----(2.16)}
\end{aligned}$$

where  $x = 2\pi A'_m$ .

Fig.(2.9) illustrates this form of modulation in the time domain only. Equation (2.16) illustrates that amplitude modulation of the time function describing p.p.m. introduces the following frequency components:

- (i) Harmonic of frequency,  $\omega'_m$ , and amplitude of,  $k A'_m$ .
- (ii) Side-band components of frequency,  $(m\omega_c \pm \omega'_m)$ , and amplitudes of,  $k A'_m \frac{\text{Sin } m k \pi}{m k \pi} J_0(x)$ , around the carrier and harmonics of the carrier.

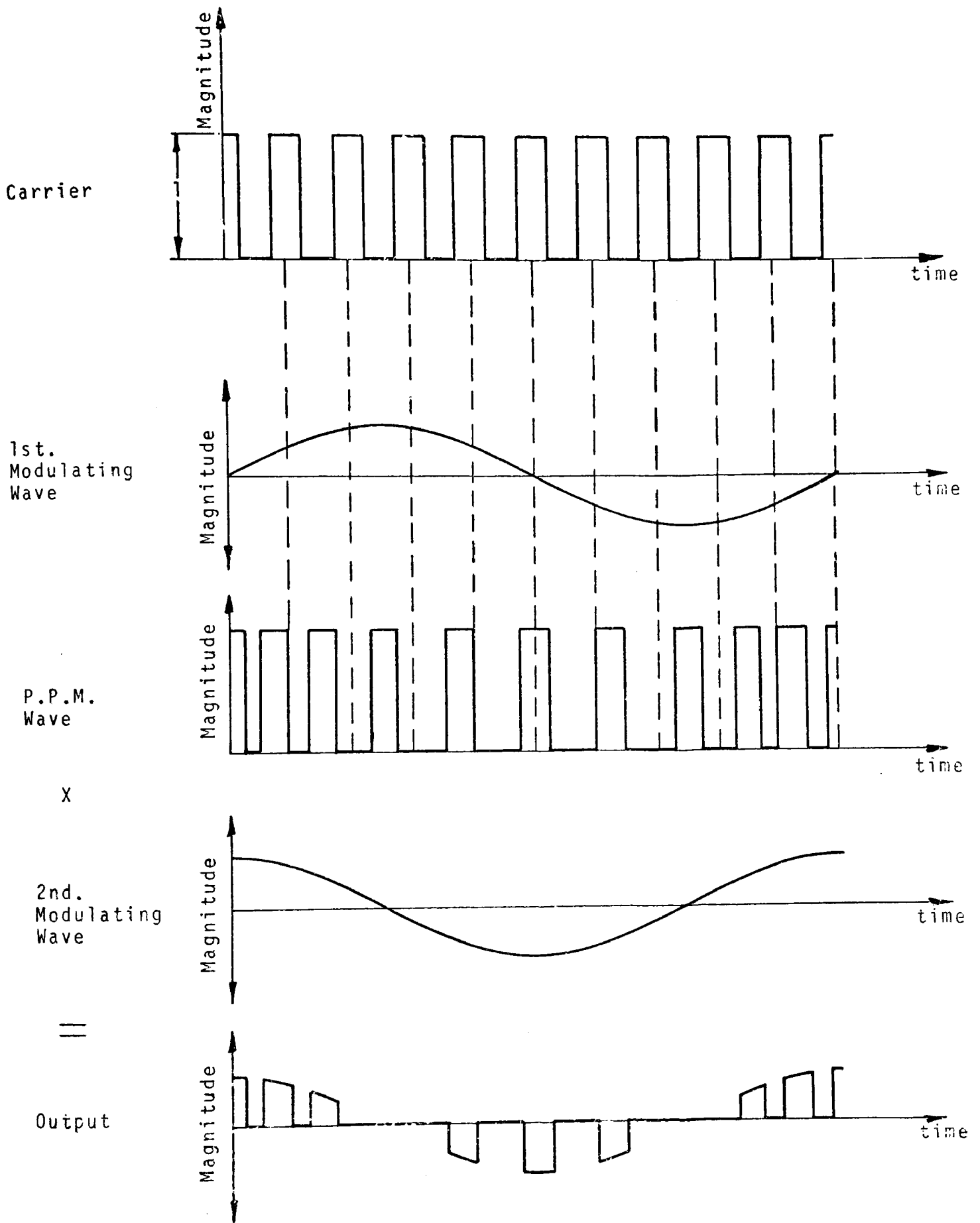


FIG.(2.9) AMPLITUDE MODULATION OF A P.P.M. WAVE

(iii) Double side-band components of frequency,  $[(m\omega_c \pm n\omega_m) \pm \omega'_m]$ , and amplitudes of  $k A'_m \frac{\text{Sin } m k \pi}{m k \pi} J_n(x)$  around the carrier and its harmonics.

By comparing equations (2.5) and (2.16) it becomes evident that the second modulation process considerably increases the harmonic content of the output modulated waveform. It may also be seen that no harmonic component exists, whose amplitude is proportional to the amplitude of the first modulating wave ( $A_m$ ). It is of particular interest to note that when the carrier frequency ( $\omega_c$ ) is commensurable with the modulating frequencies  $\omega_m$  and  $\omega'_m$ , harmonic component of frequency  $(\omega_c - \omega_m - \omega'_m)$  can exist. This component is of lower frequency than  $\omega_m$  or  $\omega'_m$ . Therefore, the amplitude modulation of p.p.m could not be considered for a practical system.

(2.2.10) Amplitude Modulated P.W.M. (A.M.P.W.M).

This particular type of double modulation basically entails the amplitude modulation of a p.w.m. carrier-wave. The double-edge pulse-width-modulated waveform was described in Section (2.2.8) by equation (2.13):

$$f(t) = k(1 + A_m \text{Cos}(\omega_m t + \phi_m)) + \frac{2}{\pi} \sum_{m=1}^{m=\infty} \frac{1}{m} \{ \text{Sin } m k \pi \text{Cos}[m k \pi A_m \text{Cos}(\omega_m t + \phi_m)] + \text{Cos } m k \pi \text{Sin}[m k \pi A_m \text{Cos}(\omega_m t + \phi_m)] \} \text{Cos } m\omega_c t$$

Amplitude modulation of this time function by  $A'_m \text{Cos}(\omega'_m t + \phi'_m)$  gives:

$$\begin{aligned}
f'(t) &= A'_m k \text{Cos}(\omega'_m t + \phi'_m) \cdot (1 + A_m \text{Cos}(\omega_m t + \phi_m)) \\
&+ \frac{2 A'_m}{\pi} \sum_{m=1}^{m=\infty} \frac{\text{Cos}(\omega'_m t + \phi'_m)}{m} \{ \text{Sin } m k \pi \text{ Cos}[m k \pi A_m \text{Cos}(\omega_m t + \phi_m)] \\
&+ \text{Cos } m k \pi \text{ Sin}[m k \pi A_m \text{Cos}(\omega_m t + \phi_m)] \} \text{Cos } m \omega_c t \quad \text{---(2.17)}
\end{aligned}$$

By means of trigonometric identities and Bessel functions this equation can be expressed in the following form:

$$\begin{aligned}
f'(t) &= k A'_m \text{Cos}(\omega'_m t + \phi'_m) + \frac{A_m A'_m}{2} \text{Cos}[(\omega_m \pm \omega'_m)t \\
&\quad + (\phi_m \pm \phi'_m)] \\
&+ \frac{A'_m}{\pi} \sum_{m=1}^{m=\infty} \frac{1}{m} [J_0(m \pi k A_m) \text{Sin } m k \pi] \text{Cos} [(m \omega_c \pm \omega'_m)t \pm \phi'_m] \\
&+ \frac{A'_m}{\pi} \sum_{m=1}^{m=\infty} \sum_{n=1}^{n=\infty} \frac{1}{m} J_n(m \pi k A_m) \text{Sin}(m k \pi \\
&+ \frac{n \pi}{2}) \text{Cos} [(m \omega_c \pm \omega'_m \pm n \omega_m)t \pm \phi'_m \pm n \phi_m] \quad \text{---(2.18)}
\end{aligned}$$

The modulation process in the time domain is illustrated in Fig.(2.10). Equation (2.18) illustrates a number of significant factors:

(i) A harmonic component corresponding to the second modulating wave of frequency  $(\omega'_m)$  and amplitude  $(k A'_m)$  is introduced.

(ii) Side-band frequency components around the first modulating frequency  $(\omega_m)$  of amplitude  $(\frac{A_m A'_m}{2})$  and of frequencies  $(\omega_m \pm \omega'_m)$  are introduced. It is of particular interest to note, for reasons which will be discussed later

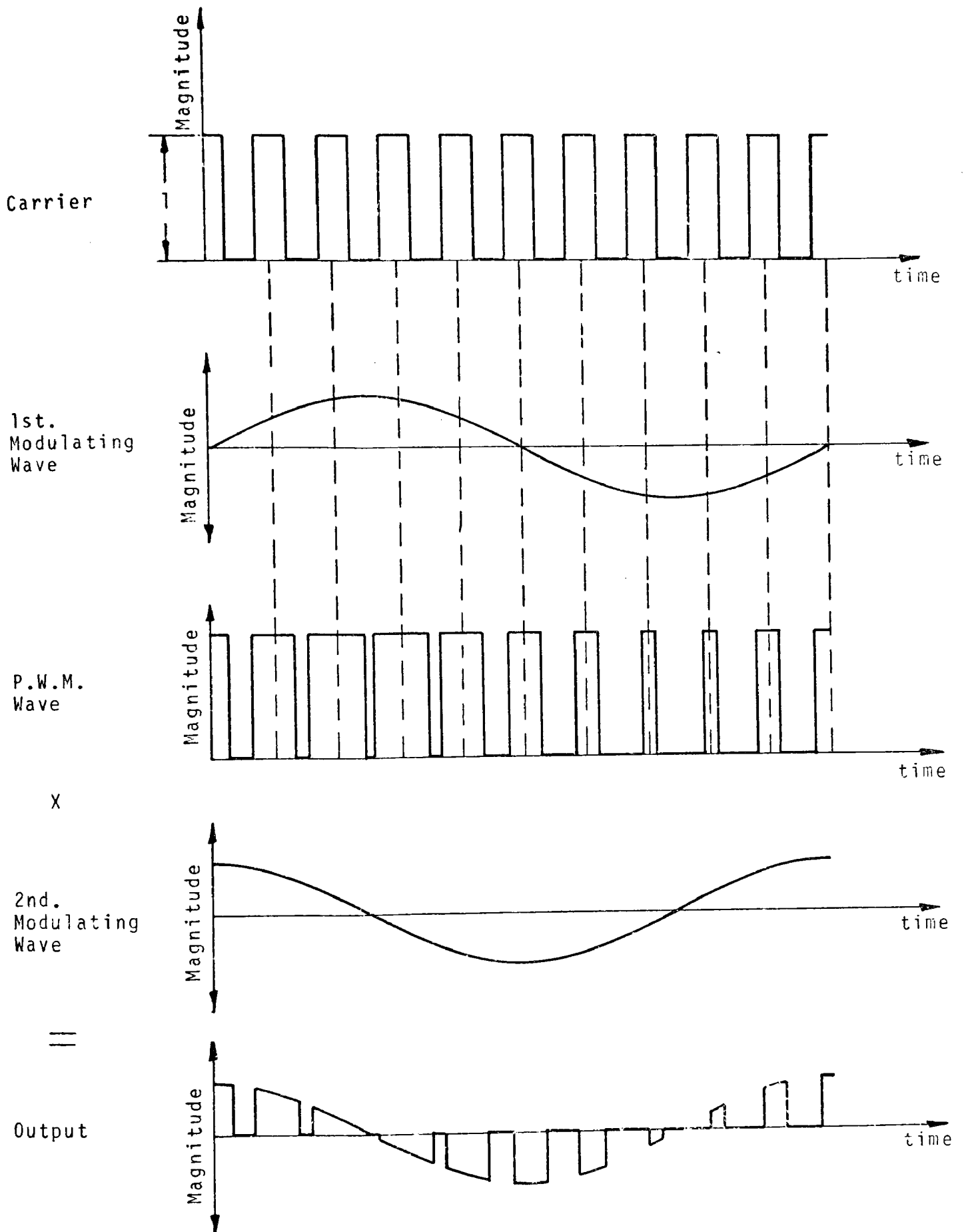


FIG.(2.10) AMPLITUDE MODULATION OF A P.W.M. WAVE

that the amplitude of the side-band components is proportional to the product of the amplitude of the first modulating wave and the amplitude of the second modulating wave. Therefore, if the amplitude ( $A'_m$ ) and frequency ( $\omega'_m$ ) of the second modulating wave are constant, the amplitude ( $\frac{A_m A'_m}{2}$ ) and frequency ( $\omega_m \pm \omega'_m$ ) can be directly controlled, by varying the amplitude ( $A_m$ ) and frequency ( $\omega_m$ ) of the first modulating wave.

(iii) The side-band frequency components of frequency, ( $m\omega_c \pm \omega'_m$ ), around the carrier and its harmonics are eliminated for odd values of  $m$  when  $k = \frac{1}{2}$ .

(iv) The carrier frequency ( $\omega_c$ ) and its harmonics of frequency, ( $m\omega_c$ ), are completely eliminated from the output.

(v) The amplitude of the double side-band harmonic components of frequencies, ( $m\omega_c \pm \omega'_m \pm n\omega_m$ ), is dependent upon the value of  $k$ . When  $k = \frac{1}{2}$ , the term:

$$\sin\left(mk\pi + \frac{n\pi}{2}\right) = 0,$$

when  $m$  and  $n$  both have odd integer values, or when  $m$  and  $n$  both have even integer values. Therefore, the double side-band harmonic components of frequencies ( $m\omega_c \pm \omega'_m \pm n\omega_m$ ) are eliminated for these values of  $m$  and  $n$ .

(vi) If the carrier frequency ( $\omega_c$ ) is of the same order as the modulating frequencies  $\omega_m$  and  $\omega'_m$ , a double side-band frequency component of frequency; ( $\omega_c - \omega'_m - \omega_m$ ), can exist which is of lower order than  $\omega_m$  or  $\omega'_m$ .

## (2.3) Requirements of a Practical Pulse-Modulated Power-Convertor.

### (2.3.1) Introduction

Because power frequency convertors handle large amounts of power, it is of prime importance that the modulation process be efficient. If the losses are excessive, large amounts of energy in the form of heat, are dissipated and can pose a considerable practical problem. In communication practice, modulation is normally performed by linear devices such as valves and transistors. However, the necessary power dissipation in linear devices rises to unmanageable proportions when they are required to handle large amounts of energy in the linear mode. Therefore, any practical power modulator must employ a non-linear device which incurs low power losses.

### (2.3.2) Choice of Modulation Device

Pulse-modulated power-convertors require a modulating device which performs the operation of a switch. The choice of device basically lies between the thyristor and the power transistor. The factors which have greatest influence when comparing these two devices are as follows:

- (i) The maximum reverse voltage that the device can block.
- (ii) The maximum forward voltage that the device can block.
- (iii) The forward current rating of the device.
- (iv) The forward voltage drop at rated current.
- (v) The characteristics of the device in regard to turn-on power, turn-off power, and switching speed.

A comparison made between the thyristor and power transistor based upon the above five factors, suggested that the thyristor is most suited to power switching applications.

### (2.3.3) The Use of Thyristors as Pulse Modulating Devices.

It is fundamental to the operation of pulse-modulated power convertors, that pulses of both positive and negative polarity be modulated. A single thyristor can only modulate pulses of one polarity. Therefore, two thyristors and two d.c. supplies or four thyristors and one d.c. supply are necessary. Fig.(2.11) and (2.12) illustrates both types of power-modulator.

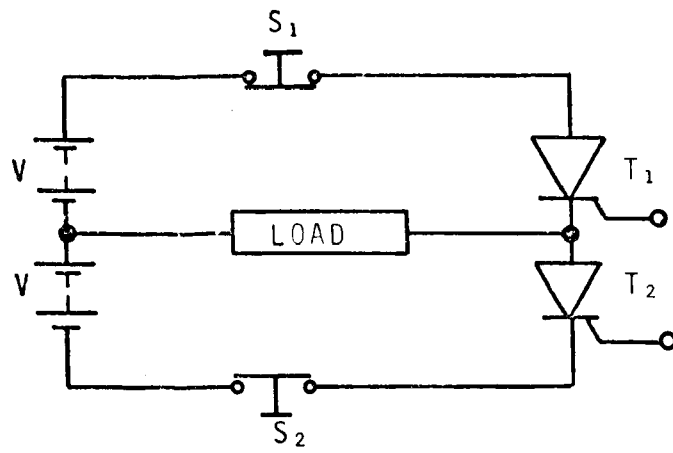
The two-thyristor and four-thyristor convertor configurations are a common requirement in d.c. to variable frequency a.c. power control. The commutation of current from thyristors passing current through the load in one direction to thyristors passing current through the load in the reverse direction is generally brought about by the use of auxiliary circuits consisting of capacitors and inductors.<sup>(5)</sup> The use of these auxiliary circuits is normally referred to in the literature as 'forced commutation'.

### (2.3.4) Forced Commutation.

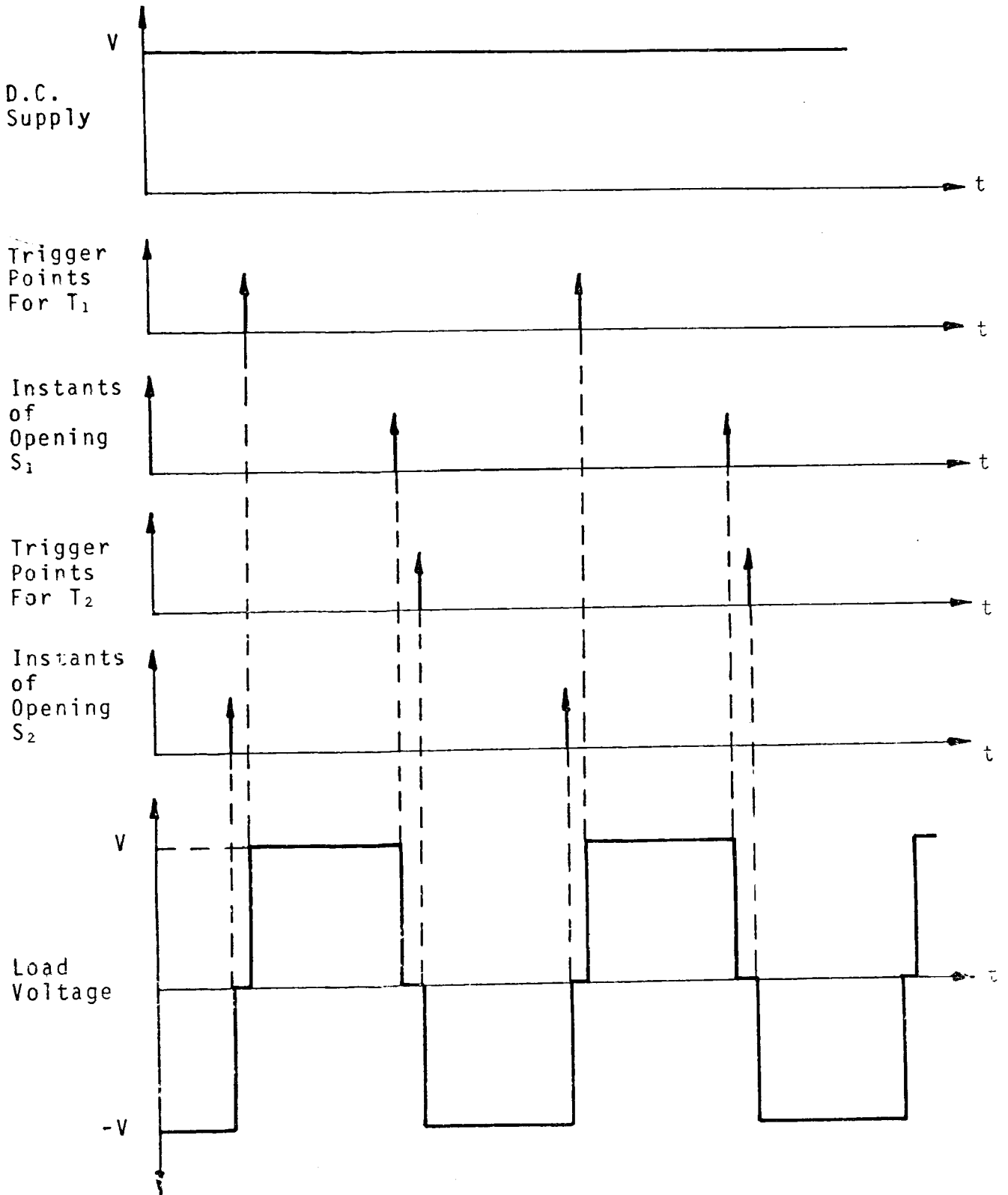
The prime objective of a commutating circuit is to reduce the current flowing through a thyristor to zero, and hold the thyristor in a reverse biased state for a period of time, sufficient to allow the thyristor to regain its forward blocking ability.

A circuit which has proved to provide reliable commutation



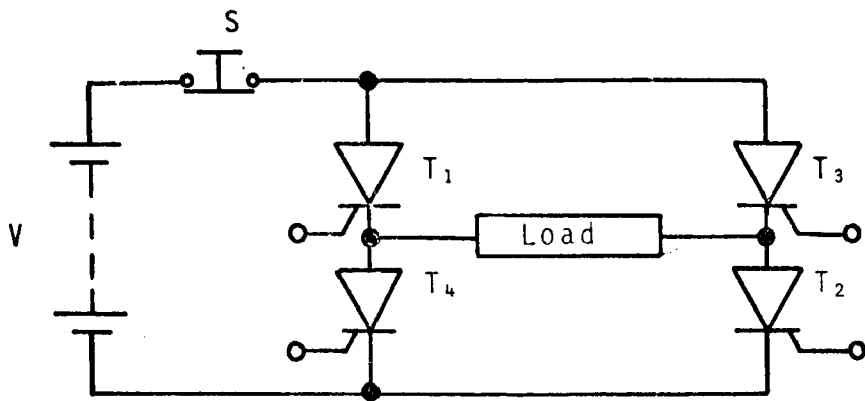


(a) Circuit Diagram

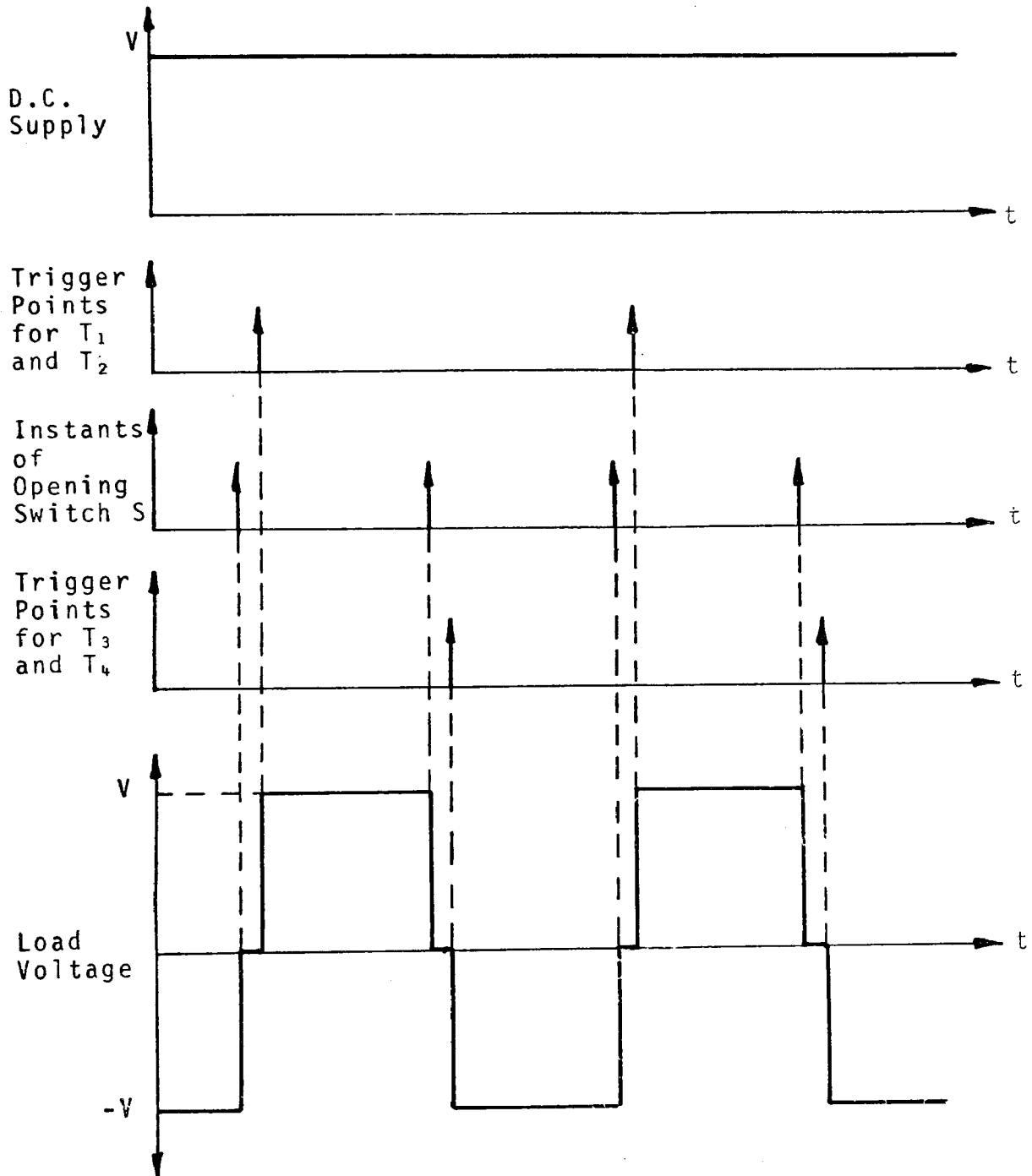


(b) Waveforms And Trigger Points

FIG.(2.11) TWO-THYRISTOR/TWO-D.C. SUPPLY PULSE CONVERTOR



(a) Circuit Diagram

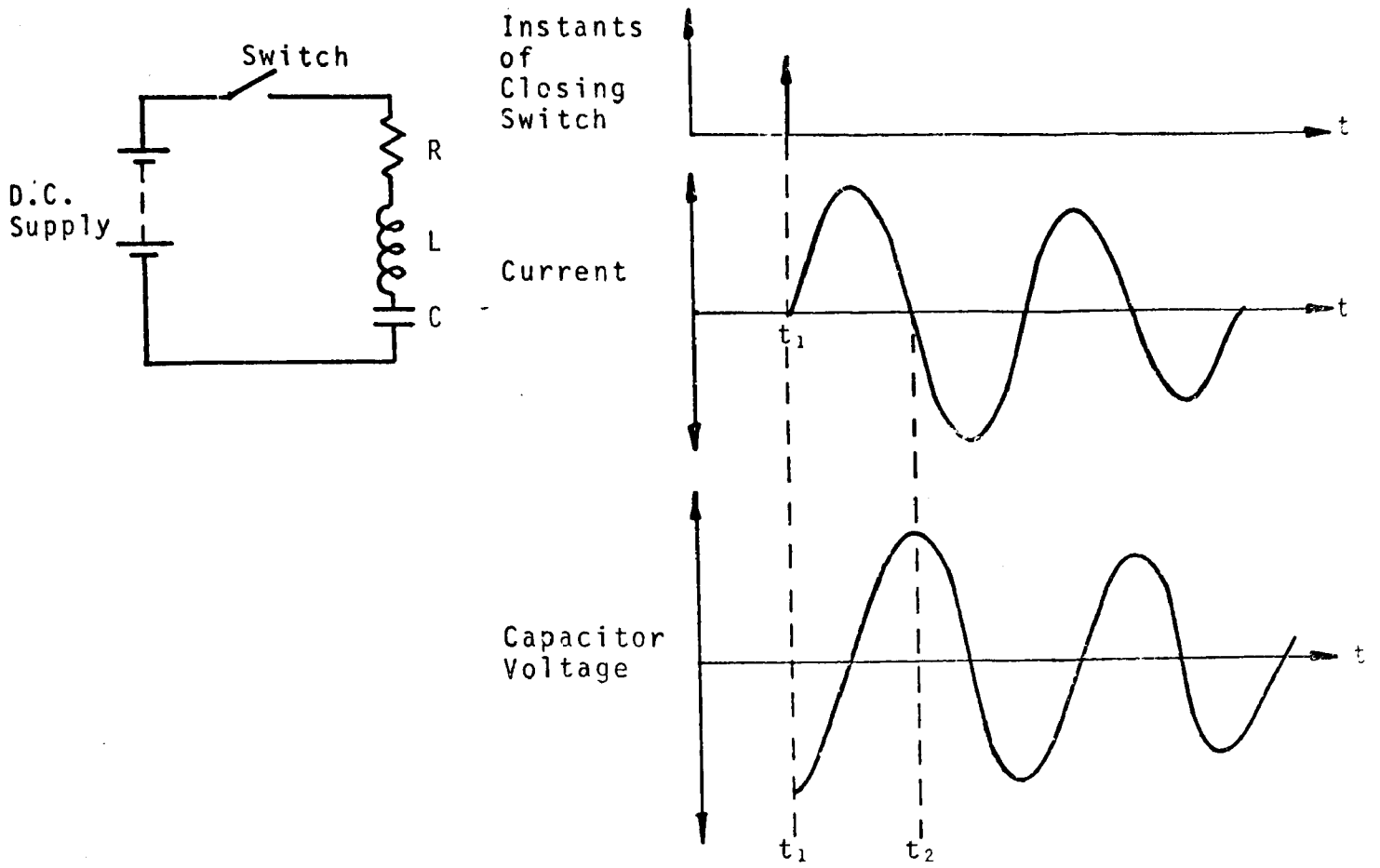


(b) Waveforms And Trigger Points

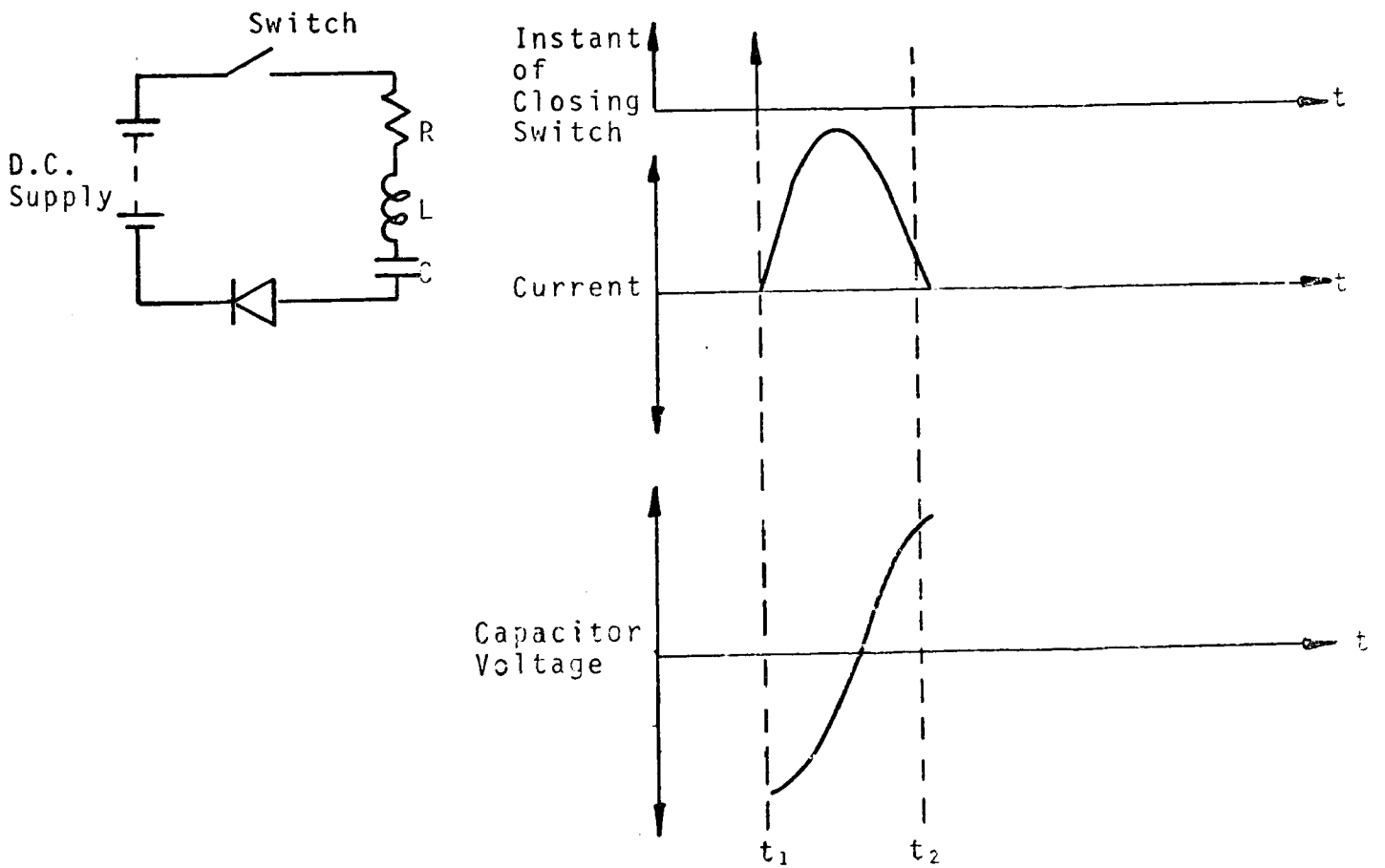
FIG. (2.12) FOUR-THYRISTOR/SINGLE-D.C. SUPPLY PULSE CONVERTOR

in forced commutated convertors is the series R.L.C circuit. (Fig.(2.13a)). If the circuit is underdamped, that is to say:  $\frac{1}{L.C.} > \frac{R^2}{4.L^2}$ , then the current flowing in the circuit is a damped sinusoid. This means that the voltage on the capacitor also has a damped sinusoidal waveform. If a diode or thyristor is connected in the circuit as shown in Fig. (2.13b), then the voltage on the capacitor at instant in time,  $t_2$ , is trapped. This voltage can be used to commutate a load-current-carrying thyristor, when used with auxiliary thyristors.

The normally closed switches shown in Fig.(2.11) can be replaced by a R.L.C. circuit and two thyristors. The modified circuit is known as a half-bridge circuit and is illustrated in Fig.(2.14). If thyristors  $T_1$  and  $T_{2a}$  are initially switched-on, the capacitor C charges to approximately 2V, (right hand plate + ve, left hand plate - ve) via:  $T_1$ , C, L and  $T_{2a}$ . Load current flows via:  $T_1$  and load. Thyristor  $T_{2a}$  is naturally commutated when the oscillatory current in the R.L.C. circuit tries to reverse, but thyristor  $T_1$  continues to conduct load-current. When  $T_{1a}$  is turned-on, thyristor  $T_1$  is reverse-biased by the voltage on the capacitor. After  $T_1$  has regained its forward blocking state, thyristor  $T_2$  is turned-on. The capacitor then continues to charge (left hand plate + ve, right hand plate - ve) via:  $T_{1a}$ , L, C and  $T_2$  to approximately 2V. The load current reverses direction and flows via:  $T_2$  and load. The thyristor  $T_{1a}$  ceases to conduct when the oscillatory current in the R.L.C. circuit tries to reverse.  $T_2$  continues to conduct load-current until  $T_{2a}$  is turned-on. The process is then repeated for each cycle of

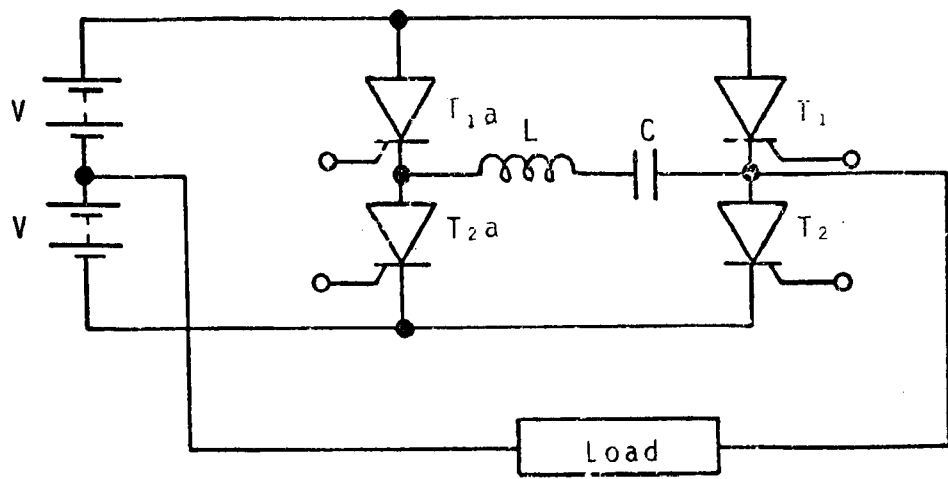


(a) Series R.L.C. Circuit and Waveforms

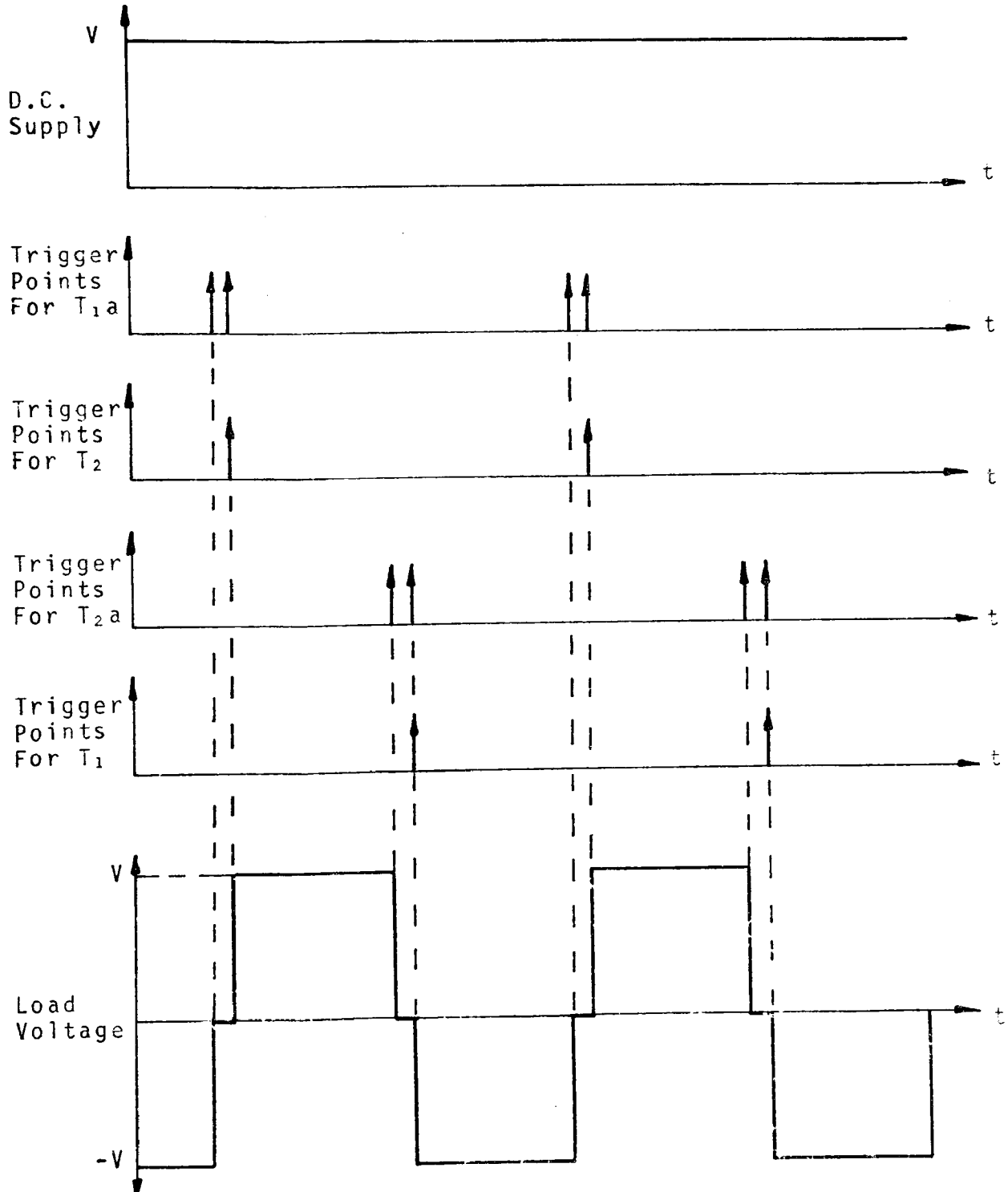


(b) Series R.L.C. Circuit With Diode and Waveforms

FIG.(2.13). R.L.C. COMMUTATION CIRCUIT



(a) Circuit Diagram



(b) Waveforms and Trigger Points

FIG.(2.14). AUXILIARY IMPULSE COMMUTATED HALF-BRIDGE CIRCUIT

output voltage. It is important to note that thyristors  $T_1$  and  $T_2$  or  $T_{1a}$  and  $T_{2a}$  must never conduct simultaneously, otherwise a short circuit will occur across the d.c. supply lines. This short circuit condition is prevented in practice by inhibiting the firing pulses to the gates of the on-coming thyristors until the out-going thyristors have regained their forward blocking ability. The necessary inhibition and steering circuits required to prevent short circuits in the power modulator described, are presented in Section (6.2.3) of this thesis.

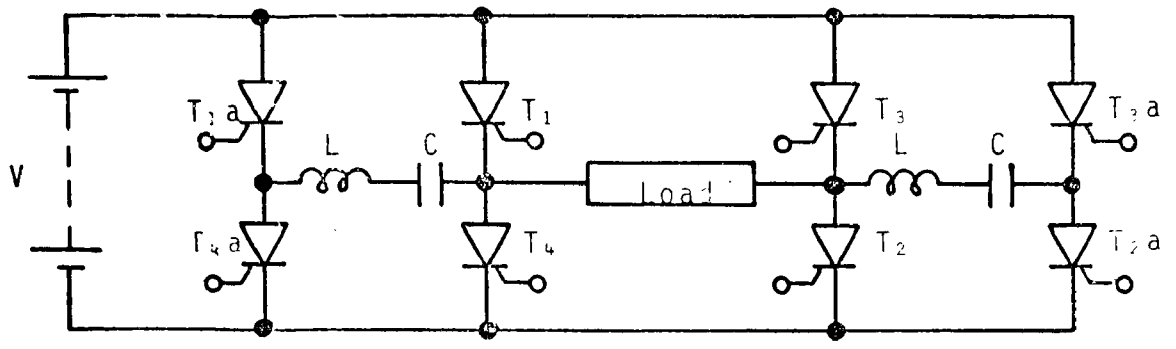
A combination of two half-bridge circuits of the type shown in Fig.(2.14), can be used to replace the normally closed switch shown in Fig.(2.12). This process is illustrated in Fig.(2.15). The resulting circuit is known as a full-bridge circuit. Polyphase circuits can similarly be built by using the half-bridge circuit as a building block.

#### (2.3.5) The Need for Feedback Diodes.

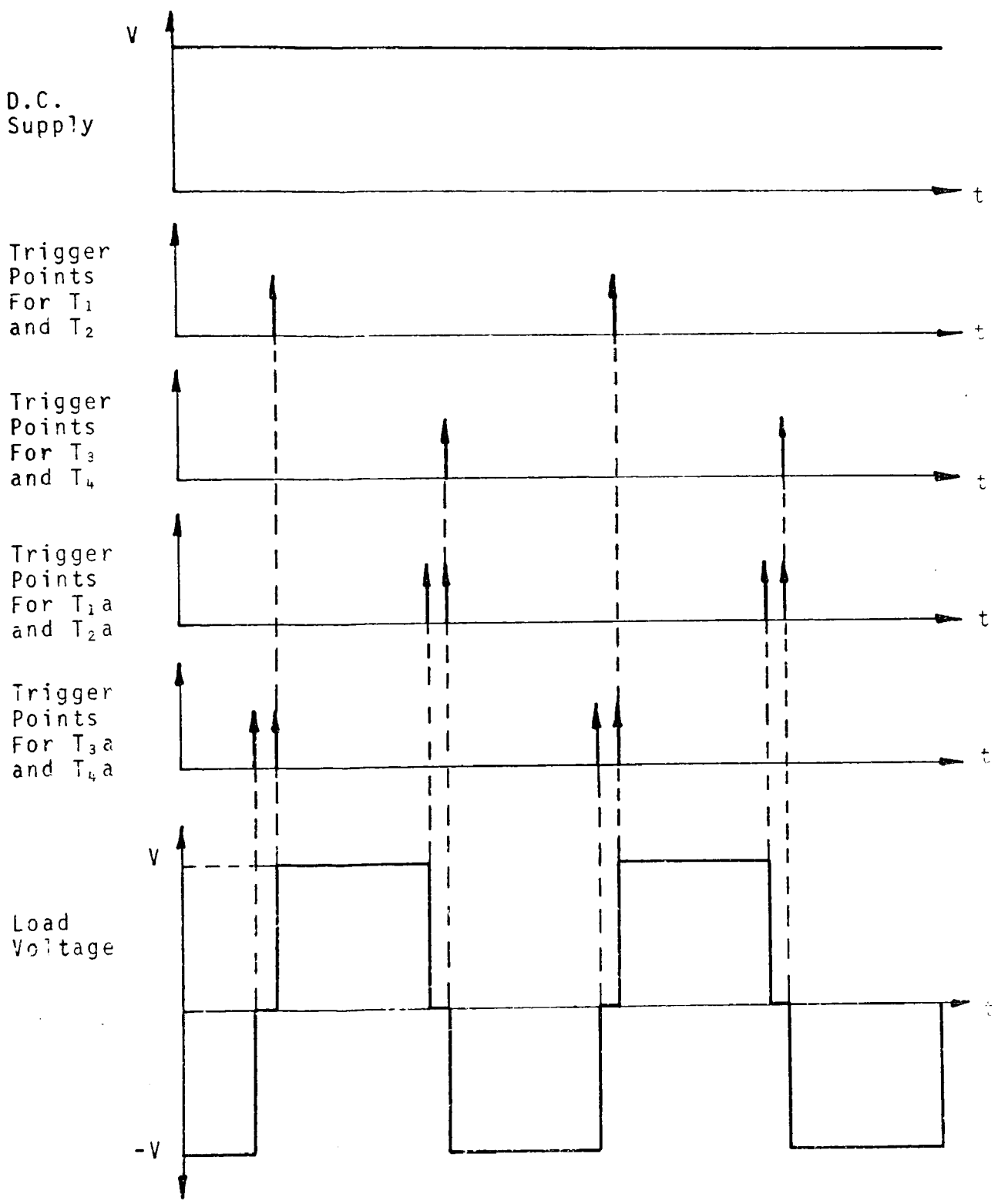
It is essential to the operation of all pulse-modulated power convertors when supplying an inductive load that an alternative path be provided for the load current during the commutation from the out-going thyristor to the on-coming thyristor. This is achieved by connecting feed-back diodes in inverse parallel with the load-current-carrying thyristors. The application of feed-back diodes to the half-bridge and full-bridge circuit is shown in Fig.(2.16)

Feed-back diodes offer the advantages of:

- (i) preventing excessive build-up of voltage on the

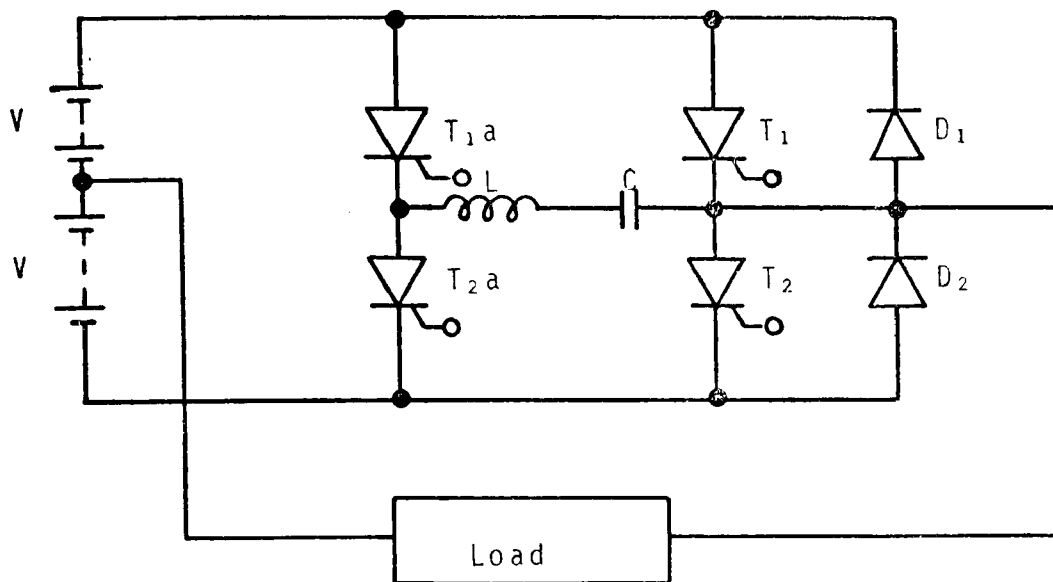


(a) Circuit Diagram

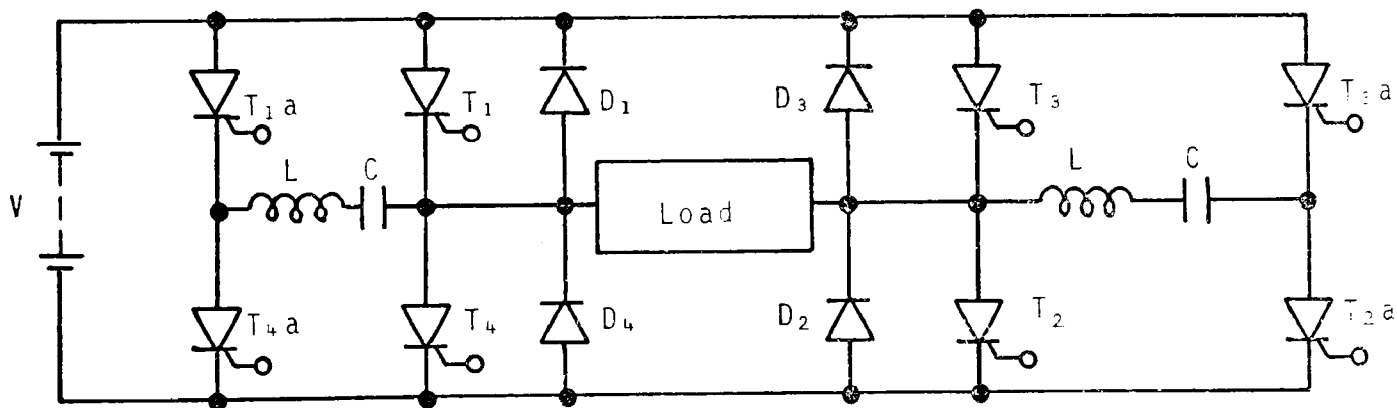


(b) Waveforms And Trigger Points

FIG.(2.15) AUXILIARY IMPULSE COMMUTATED FULL-BRIDGE CIRCUIT  
39



(a) Half-Bridge With Feedback Diodes



(b) Full-Bridge With Feedback Diodes

FIG. (2.16) AUXILIARY IMPULSE COMMUTATED BRIDGE CIRCUITS WITH FEEDBACK DIODES.



commutating capacitor,

(ii) providing reverse power flow when the load is reactive or when the load is an induction motor which is 'overhauling',

(iii) holding a.c. output voltage to an approximate rectangular waveform whose peak-value is equal to the d.c. input voltage and is independent of the load power factor.

(2.3.6) Requirement for Variation of Frequency and Magnitude of Output Voltage Waveform from Modulator.

For any induction motor to produce its full rated torque, it is necessary that the magnetic flux produced in the iron core be maintained at its designed level for all operating speeds. This entails maintaining the relationship between voltage and frequency approximately linear. It is important to note that it is the voltage integral over one half-cycle that must be maintained proportional to the stator supply frequency; the instantaneous voltage being of less consequence. This fact allows the design of pulse-modulated power-convertors which operate from either a constant d.c. supply voltage or from a variable source.

(2.3.7) Frequency Control.

A prime requirement of a practical pulse-modulated power-converter intended for an infinitely variable induction motor speed control system, is that the frequency of the output modulated waveform be infinitely variable; that is to say: the period over which the output waveform repeats itself

must be linearly variable between the limits of infinity and some value greater than zero. This requirement is satisfied by controlling the firing sequence of the thyristors by means of a 'switching function'. The waveform of the 'switching function' must be identical to the required output waveform from the pulse-modulated power-converter so far as the time-scale is concerned, whereas, the amplitude of the waveform is only of significance when the power-converter is of the amplitude modulated type. Therefore, the power-converter is basically a power amplifier, where the input signal is generated by a light current modulator circuit and is known as the 'switching function'. The 'switching function' control of the power-modulator for the p.w.m. and p.a.m. processes is illustrated in Fig.(2.17) and Fig.(2.18) respectively.

#### (2.3.8) Voltage Control.

If the frequency of the a.c. supply to the stator of an induction motor is varied, then it is necessary for the magnitude of the stator voltage to be varied in direct proportion, if the torque produced by the motor is to remain constant (Section(2.3.6)). Therefore, a practical pulse-modulated power-converter supplying an induction motor must provide a means of voltage control for variable speed applications. Basically there are three methods by which this required voltage control can be achieved:

- (i) control of voltage supplied to the power-converter,
- (ii) control of voltage supplied by power-converter,
- (iii) control of voltage within the power-converter.

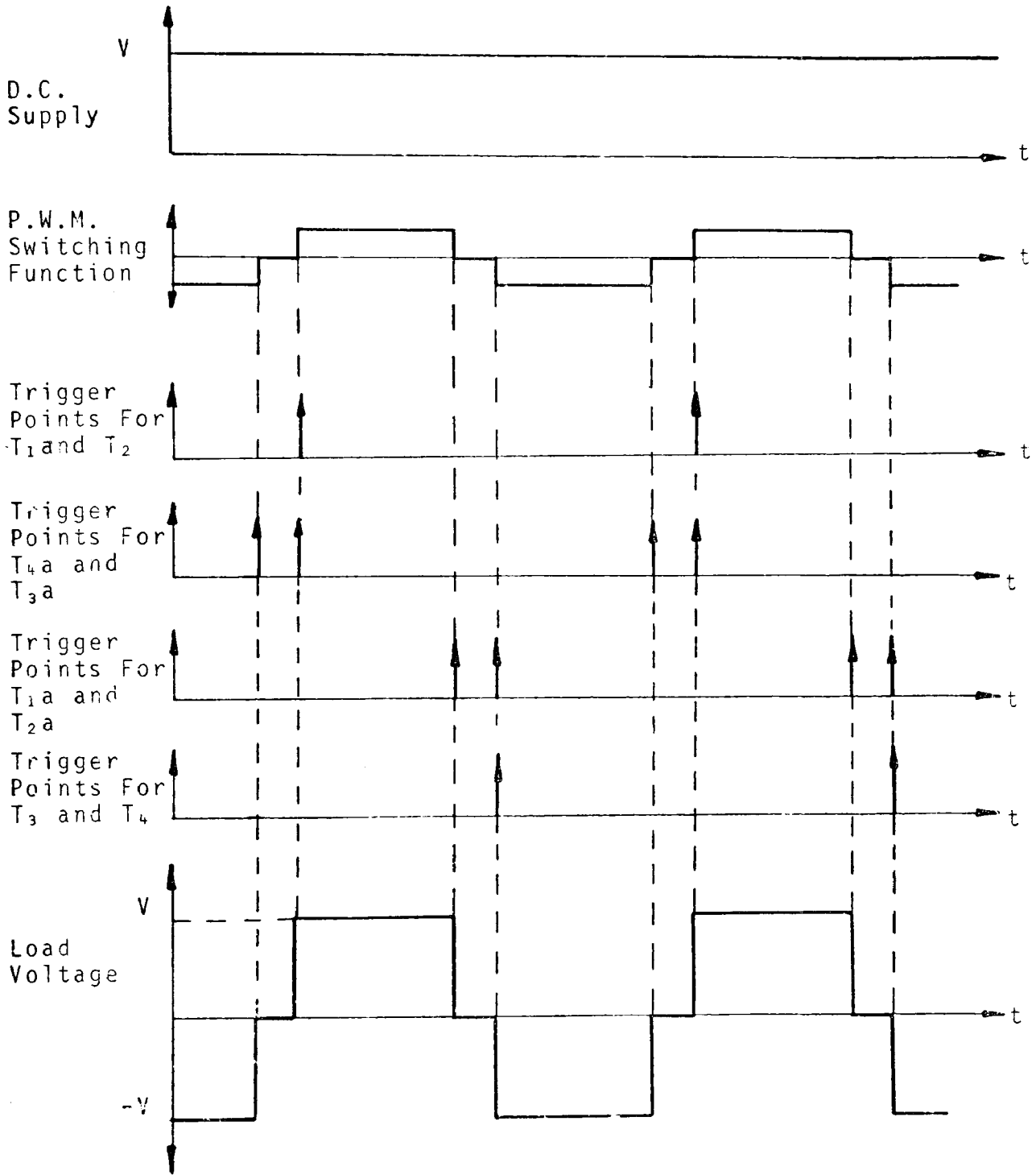
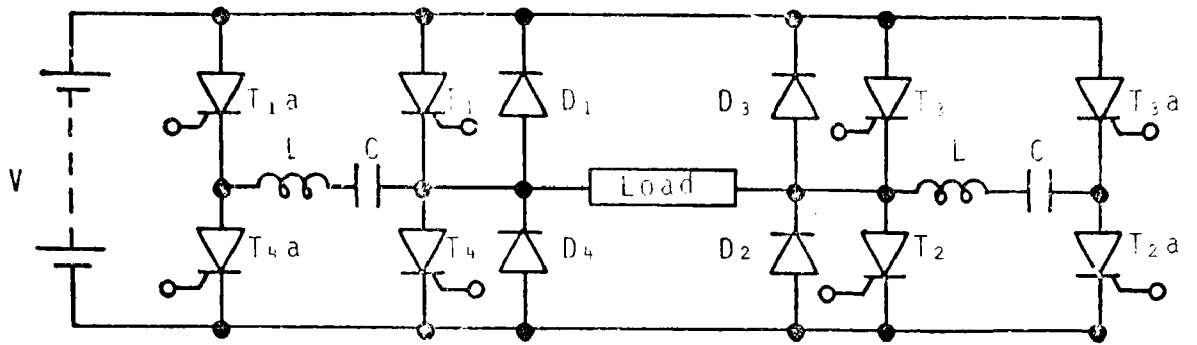


FIG.(2.17) SWITCHING FUNCTION CONTROL OF P.W.M. POWER CONVERTOR

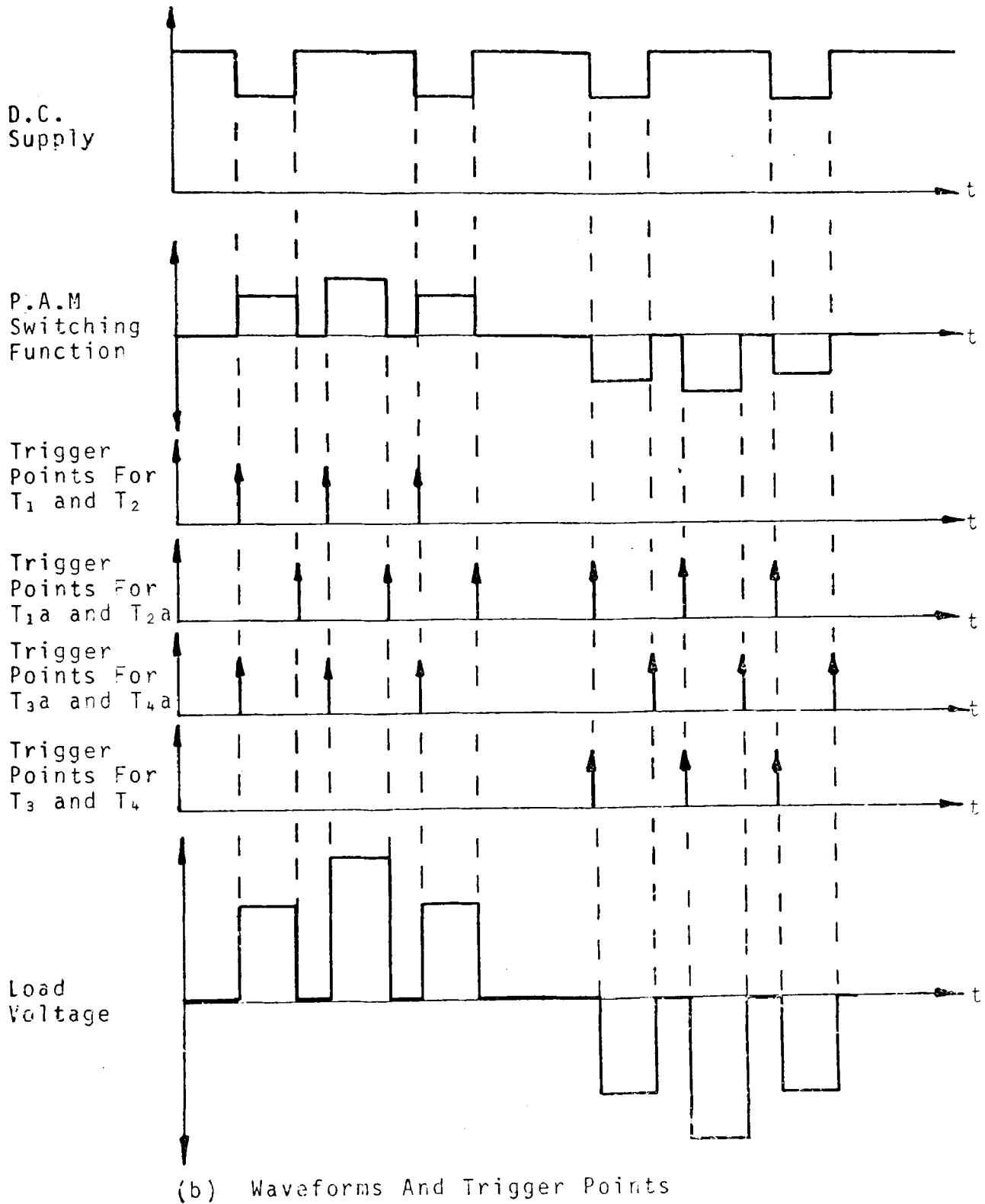
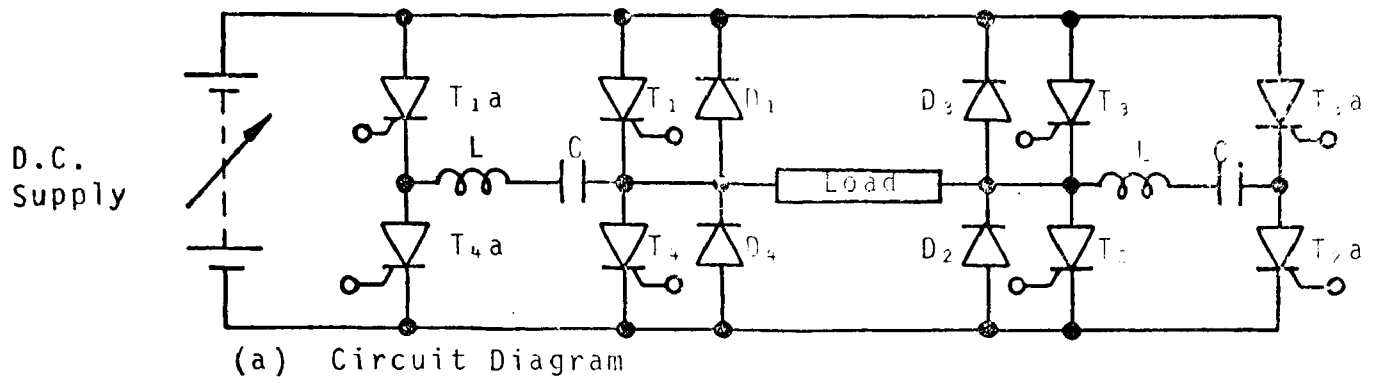
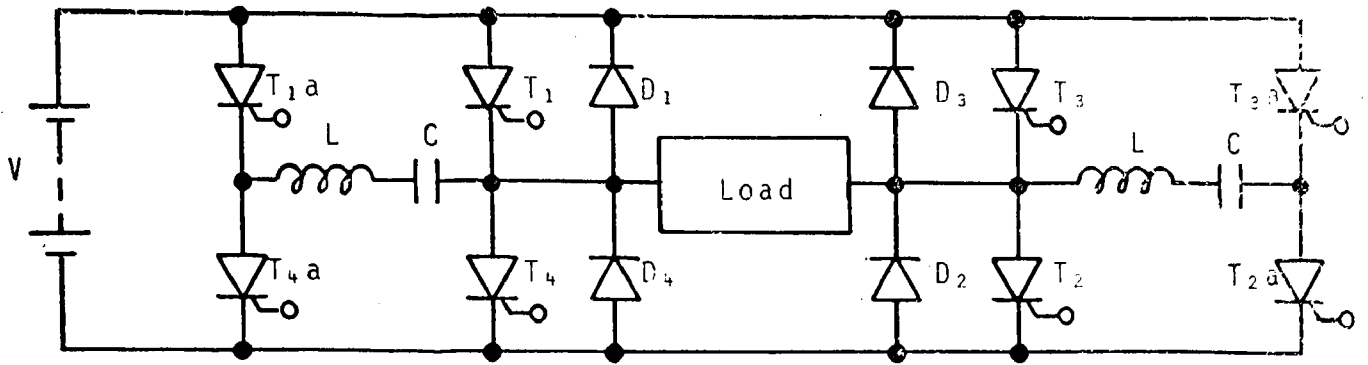


FIG.(2.18) SWITCHING FUNCTION CONTROL OF P.A.M. POWER CONVERTOR

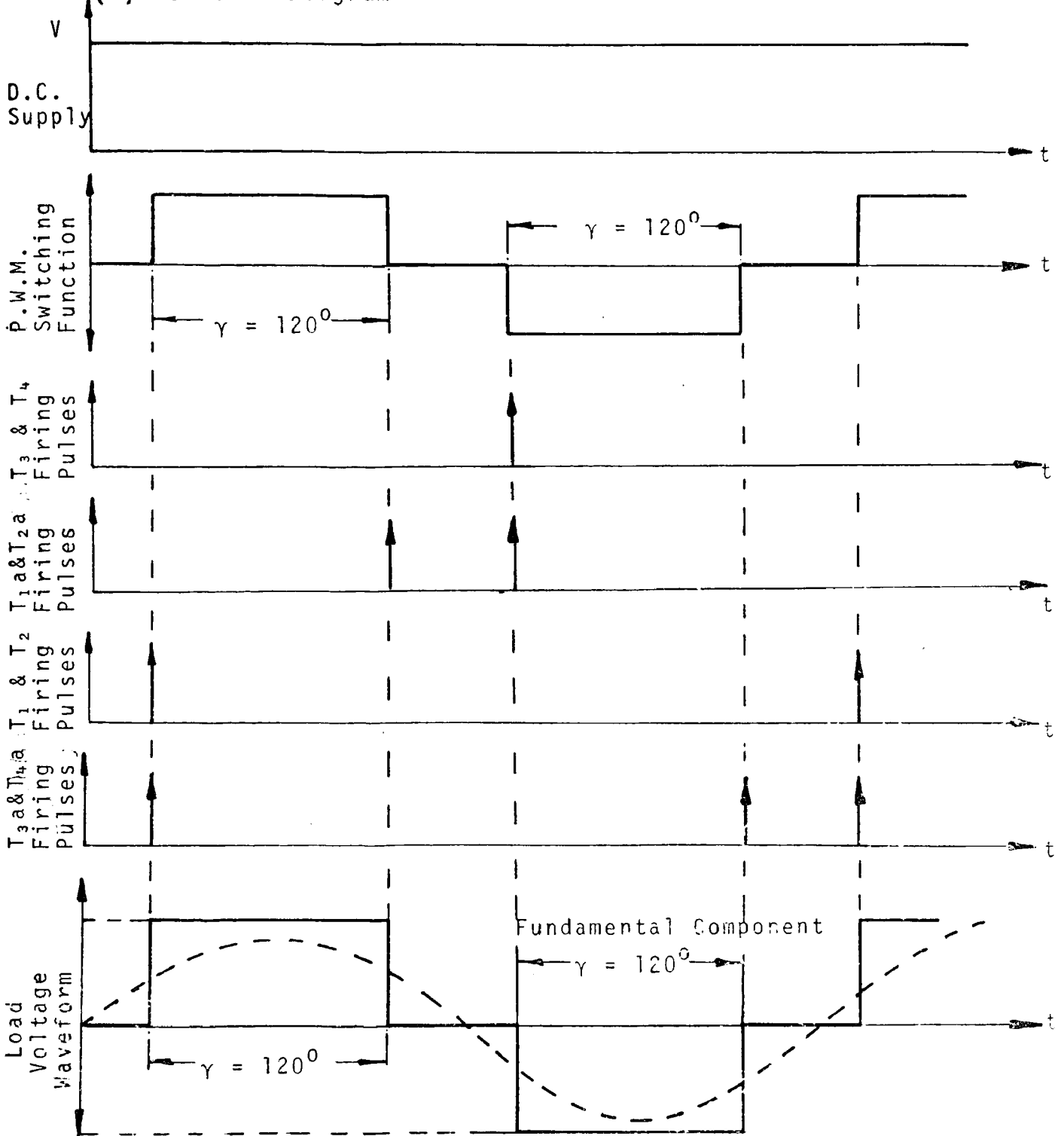
Method (i) entails the incorporation of either a phase controlled a.c. to d.c. convertor or a d.c. to d.c. time-ration controlled convertor in the supply to the pulse-modulated power-convertor. Both these systems involve: extra components, increased possibility of commutation failure and increased harmonic distortion of the output waveform.<sup>(5)</sup> Method (ii) is achieved by means of a.c. voltage regulation techniques which results in the use of extra components and transformers. This increases the cost and weight of the power-convertor.<sup>(5)</sup> Method (iii) can be realized without requiring any extra components provided the type of modulation used is a p.w.m. process and not a p.a.m. process. Because as with method (i) the p.a.m. process requires variation of the supply voltage to the pulse-modulated power-convertor. By means of the p.w.m. process the half-cycle mean-value of voltage can be controlled by varying the area under the output voltage waveform. This is achieved by maintaining the supply voltage constant and varying the instants of conduction and commutation of the relevant thyristors in the power-convertor. Fig.(2.19) and (2.20) illustrates this process for conduction angles,  $\gamma$ , of  $120^\circ$  and  $160^\circ$  respectively. The half-cycle mean-value of the load voltage illustrated in Figures (2.19) and (2.20), in terms of the conduction angle,  $\gamma$ , is given by:

$$V_{\text{mean}} = \frac{1}{\pi} \int_{\frac{\pi+\gamma}{2}}^{\frac{\pi+\gamma}{2}} V \cdot d(\omega t) = \frac{V \gamma}{\pi} \quad \text{-----(2.19)}$$

whereas, the peak-value of the fundamental component of the load voltage is given by:

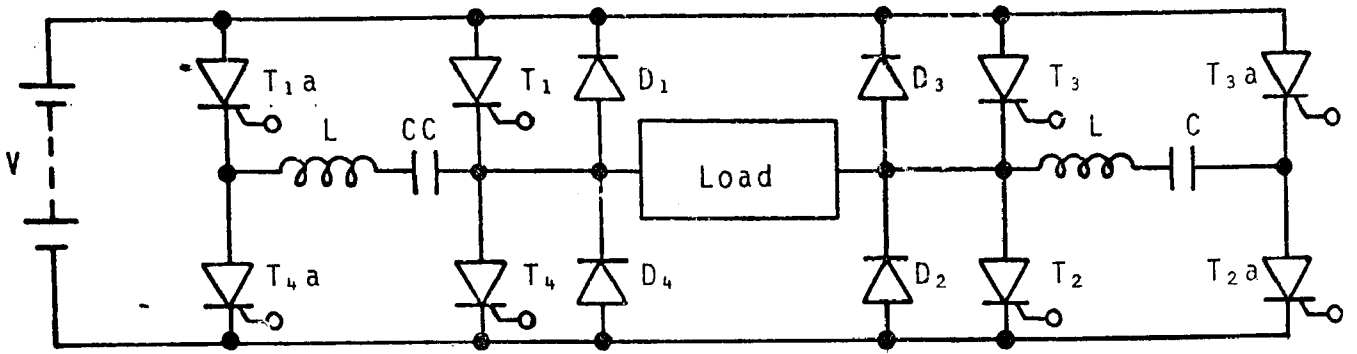


(a) Circuit Diagram

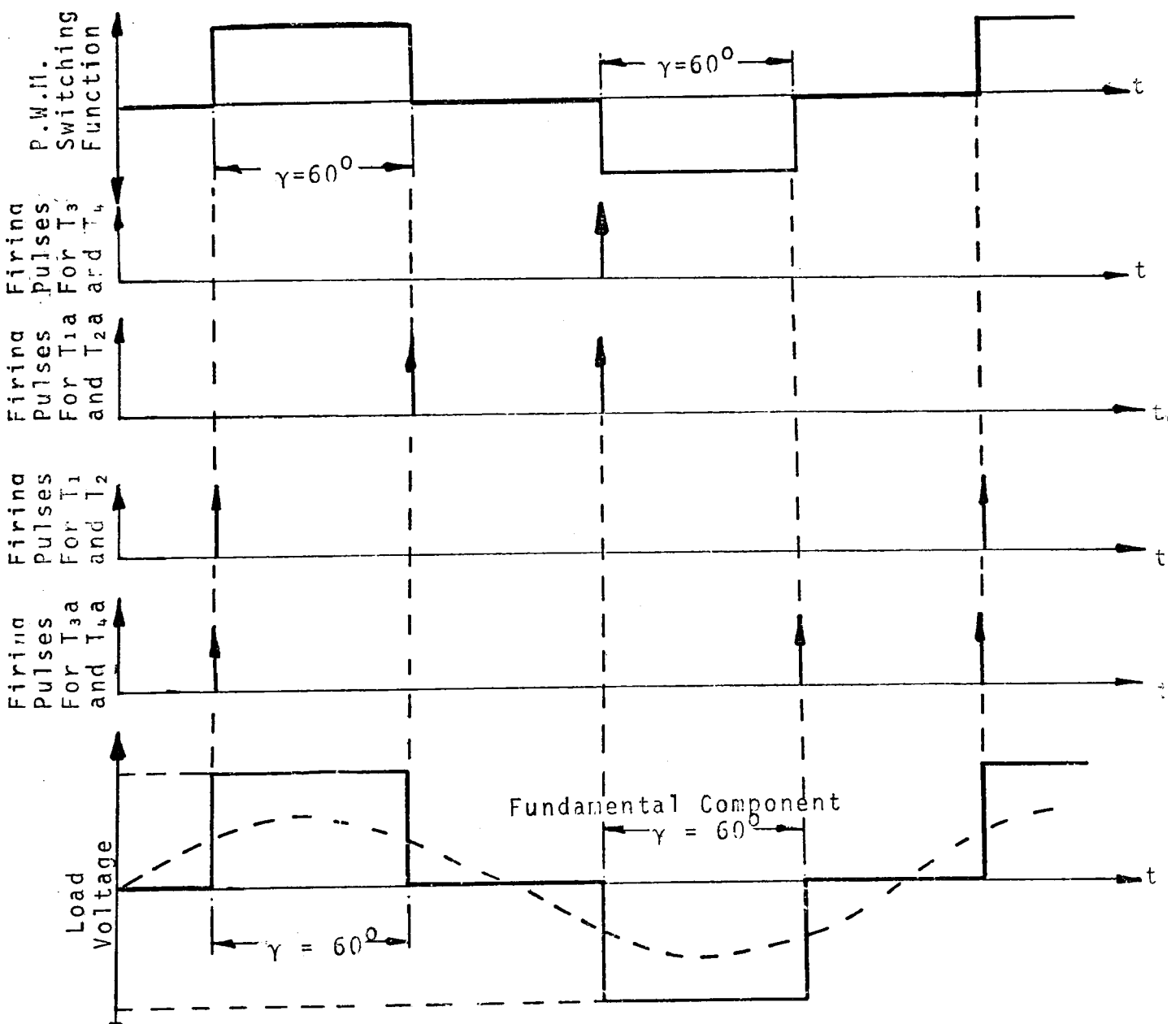
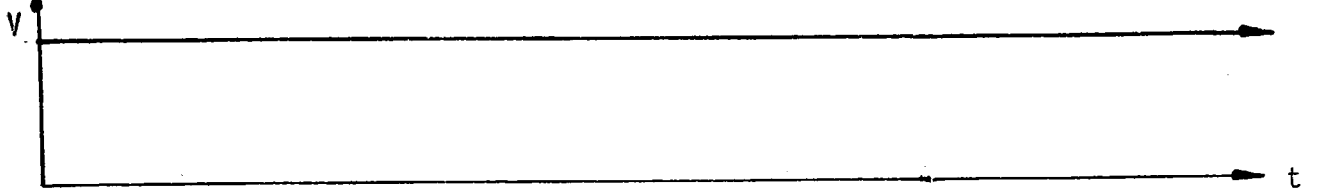


(b) Waveforms And Trigger Points

FIG.(2.19) P.W.M. CONTROL FOR CONDUCTION ANGLE ( $\gamma$ ) OF  $120^\circ$



(a) Circuit Diagram



(b) Waveforms And Trigger Points

FIG.(2.20) P.W.M. CONTROL FOR CONDUCTION ANGLE ( $\gamma$ ) OF  $60^\circ$

$$V_{\text{peak}} = \frac{4}{\pi} \int_0^{\frac{\gamma}{2}} V \cos \omega t \, d(\omega t) = \frac{4V}{\pi} \sin \frac{\gamma}{2} \quad \text{-----(2.20)}$$

Therefore, it can be seen that the half-cycle mean-value and the peak-value of the fundamental component of the load voltage can both be varied by controlling the conduction angle,  $\gamma$ . The method by which voltage control is incorporated in the p.w.m. control circuit will be fully discussed in Chapter (6) of this thesis.

## (2.4) Elimination of Unwanted Frequency Components.

### (2.4.1) Introduction.

In general, the output waveform from all pulse-modulators will contain unwanted frequency components which must be removed or suppressed. In telecommunications practice this is generally achieved by filtering. Standard methods involving L.C. tuned circuits are not only impractical in power applications, because of the cost and size of the components, but also because they could not adequately discriminate between wanted and unwanted frequency components. When the modulating frequency and carrier frequency are commensurable, lower and upper side-band frequency components are very close and the filter would be required to have an unrealistically sharp cut-off to satisfactorily block the unwanted frequency components without seriously attenuating the wanted frequency component.

There are many possible ways by which unwanted frequency components may be eliminated from the output waveform from a pulse-modulator. These methods may be generalized under the following:



- (i) Control of the modulation process.
- (ii) Modulation and summation by means of a transformer.
- (iii) Modulation and cancellation by supplying a 3-phase, 3-wire load.

(2.4.2) Control of the Modulation Process.

The modulation process can be controlled by numerous methods, some of which will be discussed in this Section while more sophisticated methods will be discussed in Chapter (3) of this thesis.

(2.4.2.1) Use of a Bipolar Carrier Wave.

It was shown in Section (2.2.2) that the unmodulated carrier wave consisted of a uniform train of unipolar pulses. If the carrier waveform is considered to be a uniform train of bipolar pulses as shown in Fig.(2.2 1), then the harmonic content of the output modulated waveforms from the various modulation processes is significantly changed. The d.c. term in equation (2.1) reduces to zero when  $\frac{t_o}{T} = \frac{1}{2}$ , therefore, the time function describing the unmodulated bipolar carrier wave is reduced to:

$$U'(t) = \frac{1}{\pi} \sum_{m=1}^{m=\infty} \frac{1}{m} \sin \frac{m\pi}{2} \cos m \omega_c t \quad \text{---- (2.21)}$$

The equation (2.3) describing the amplitude modulation process (P.A.M) is modified as follows:

$$V(t) U'(t) = \frac{A_m}{2\pi} \sum_{m=1}^{m=\infty} \frac{1}{m} \sin \frac{m\pi}{2} \cos [(m \omega_c \pm \omega_m)t \pm \phi_m] \quad \text{--(2.22)}$$

It is immediately apparent that the harmonic component of frequency ( $\omega_m$ ) is eliminated. It may also be seen that the

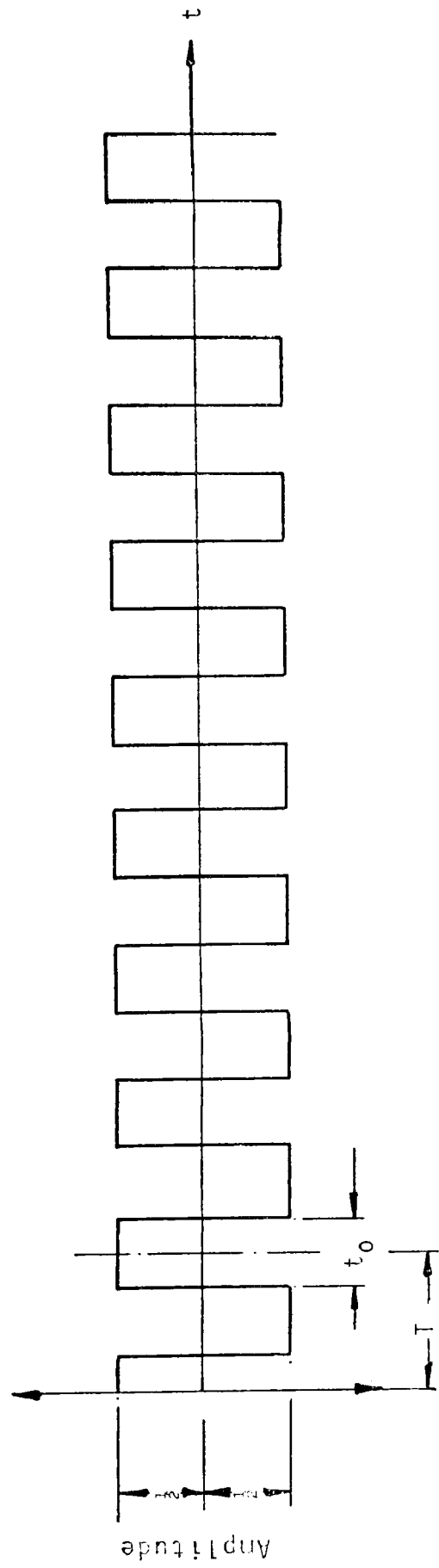


FIG.(2.21) UNMODULATED BIPOLAR CARRIER WAVE

components of frequency,  $(m\omega_c \pm \omega_m)$ , are also eliminated for all even values of  $m$ . Therefore, if the wanted frequency component from the pulse modulator is of frequency,  $(\omega_c - \omega_m)$ , the harmonic distortion of the output waveform is considerably reduced.

The pulse-position-modulation (P.P.M.) process described by equation (2.5) is also considerably improved. This can be seen from the following equation:

$$\begin{aligned}
 f'(t) = & \frac{2}{\pi} \sum_{m=1}^{m=\infty} \frac{1}{m} \sin \frac{m\pi}{2} \{ J_0(x) \cos m\omega_c t \\
 & + J_1(x) [\sin [(m\omega_c - \omega_m)t - \phi_m] - \sin [(m\omega_c + \omega_m)t + \phi_m]] \\
 & - J_2(x) [\cos [(m\omega_c - 2\omega_m)t - 2\phi_m] + \cos [(m\omega_c + 2\omega_m)t + 2\phi_m]] \\
 & - J_3(x) [\sin [(m\omega_c - 3\omega_m)t - 3\phi_m] - \sin [(m\omega_c + 3\omega_m)t + 3\phi_m]] \\
 & + \dots \dots \dots \} \dots \dots \dots (2.23)
 \end{aligned}$$

where again  $x = 2\pi A_m$ . Once again it may be seen that for all even values of  $m$ , all side-band frequency components of frequency;  $(m\omega_c \pm n\omega_m)$ , are eliminated. It may also be observed that the most dominant component of frequency,  $\omega_c$ , still exists. Since no harmonic component exists whose amplitude is directly proportional to the amplitude of the modulating wave ( $A_m$ ), this type of modulation could still not be considered for a practical pulse-modulation system.

The d.c. component in the output waveform from the leading-

edge, trailing-edge and double-edge p.w.m. process can be reduced and in some cases completely eradicated by the use of a bipolar carrier-wave. It is of particular interest to note that the harmonic components remain unchanged. The elimination of the d.c. component from the output wave will be discussed at greater length in Chapters (4), (5) and (6) of this thesis.

Significant improvement in the output waveform of the amplitude modulated p.p.m. wave described by equation (2.16) is achieved by means of a bipolar carrier wave. The term corresponding to the second modulating wave of frequency,  $\omega'_m$ , is eliminated. The harmonic terms of frequency,  $(m\omega_c \pm \omega'_m)$  and  $(m\omega_c \pm n\omega_m \pm \omega'_m)$ , are completely removed for even values of m. It is again of particular interest to note that no harmonic component of modulating frequency,  $\omega_m$ , exists whose amplitude is proportional to  $A_m$ . This makes this particular form of modulation impractical for variable speed induction motor drives.

The process of amplitude modulating a p.w.m. wave is considerably improved by the use of a bipolar carrier wave. It may be seen from equation (2.18) that the term of frequency,  $\omega'_m$ , corresponding to the second modulating wave is completely eradicated. For  $k = \frac{1}{2}$  the components of frequency,  $(m\omega_c \pm \omega'_m)$ , are also eliminated. Similarly for even values of m and n the terms of frequency,  $(m\omega_c \pm \omega'_m \pm n\omega_m)$ , are again removed. It may therefore be seen that when the term given by:

$$\frac{A_m A'_m}{2} \cos [(\omega_m \pm \omega'_m)t + (\omega_m \pm \phi'_m)]$$

is considered to be the wanted term, its frequency is given

by:  $(\omega_m + \omega'_m)$ , or  $(\omega_m - \omega'_m)$ , and its amplitude by  $\frac{A_m A'_m}{2}$ .

This term could provide the basis of a practical a.c. to a.c. speed control system, where the output frequency is controlled by varying  $\omega_m$  and the amplitude by varying  $A_m$ .  $A'_m$  and  $\omega'_m$  would be the amplitude and frequency of the mains supply which would be constant.

#### (2.4.2.2) Width Control of the Output Waveform

It was shown in Section (2.3.8) of this thesis that by controlling the conduction angle of the pulse-modulated power-converter illustrated in Figures (2.19) and (2.20), the half-cycle mean-value and peak-value of the fundamental component of the output voltage waveform could be controlled. It will now be shown that this process also provides a means of controlling the harmonic content of the output waveform.

Consider the output voltage waveform illustrated in Fig. (2.22). By means of Fourier analysis it can be shown that the load voltage waveform is described by:

$$f(t) = \sum_{m=1}^{\infty} \frac{4V}{m\pi} \sin m \frac{\gamma}{2} \cos m\omega t \quad \text{----(2.24)}$$

where it may be seen that the amplitude of the frequency components is a function of the conduction angle  $\gamma$ . This provides a means of controlling the harmonic distortion of the load voltage waveform. Firstly, it may be seen that for all even values of  $m$ , all even order harmonics are eliminated. Therefore, the load voltage waveform only contains odd order harmonic components. Secondly, it may be seen that when  $\gamma$  is made equal to  $\frac{2\pi}{3}$  radians, the third harmonic component of

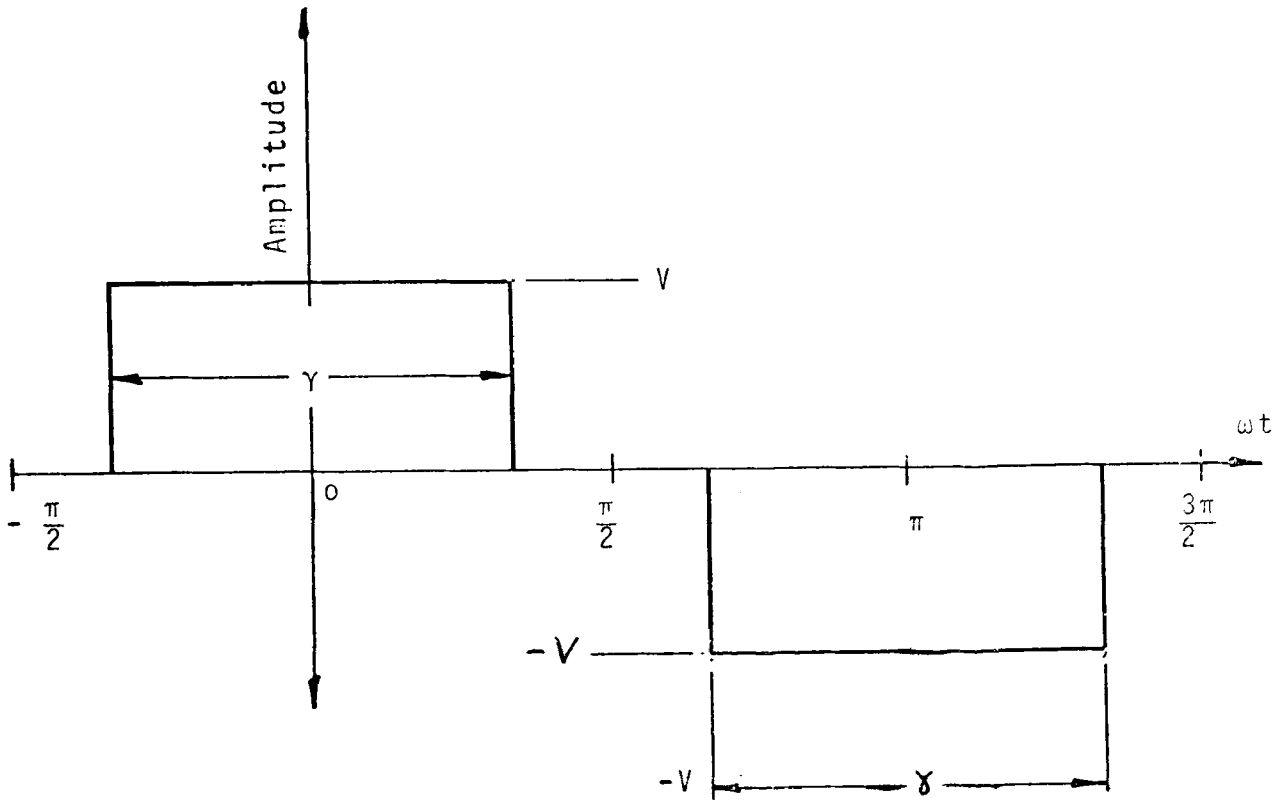


FIG.(2.22) WIDTH CONTROL OF THE LOAD VOLTAGE WAVEFORM

frequency,  $3\omega$ , is eliminated. Similarly, it may be seen that when  $\gamma$  equals  $\frac{2\pi}{5}$  radians the fifth harmonic component of frequency,  $5\omega$ , is eradicated. In general, the  $m$ th harmonic can be eliminated from the output waveform by making  $\gamma = \frac{2\pi}{m}$  radians. The main disadvantage of this system of harmonic elimination is that it is only suitable for applications where the magnitude of the output voltage from the pulse-modulated power convertor is required to be constant. Otherwise voltage regulation techniques on the input or output side of the power-convertor would be required.

(2.4.2.3) Width Control of Multiple Pulse Output Waveform

Selected harmonics can be eliminated from the output voltage waveform of a pulse-modulator by increasing the number of pulses per cycle of output.<sup>(11)</sup> This method of harmonic elimination does not require any increase in the number of power components. Consider the waveform illustrated in Fig.(2.23). This waveform can be described by the following time function:<sup>(11)</sup>

$$f(t) = \frac{4V}{\pi} \sum_{m=1}^{\infty} \frac{1}{m} \sin \frac{m\pi}{2} \left[ \frac{1 - 2 \cos m\alpha_1 + 2 \cos m\alpha_2}{m} \right] \cos \frac{m\phi}{2} \cos m\omega t$$

---- (2.25)

Once again it may be seen that odd harmonics only are present in the output waveform, because for even values of  $m$ , the term:  $\sin \frac{m\pi}{2} = 0$ . It may also be seen that harmonics can be eliminated by determining values for  $m\alpha_1$  and  $m\alpha_2$  which makes the term:

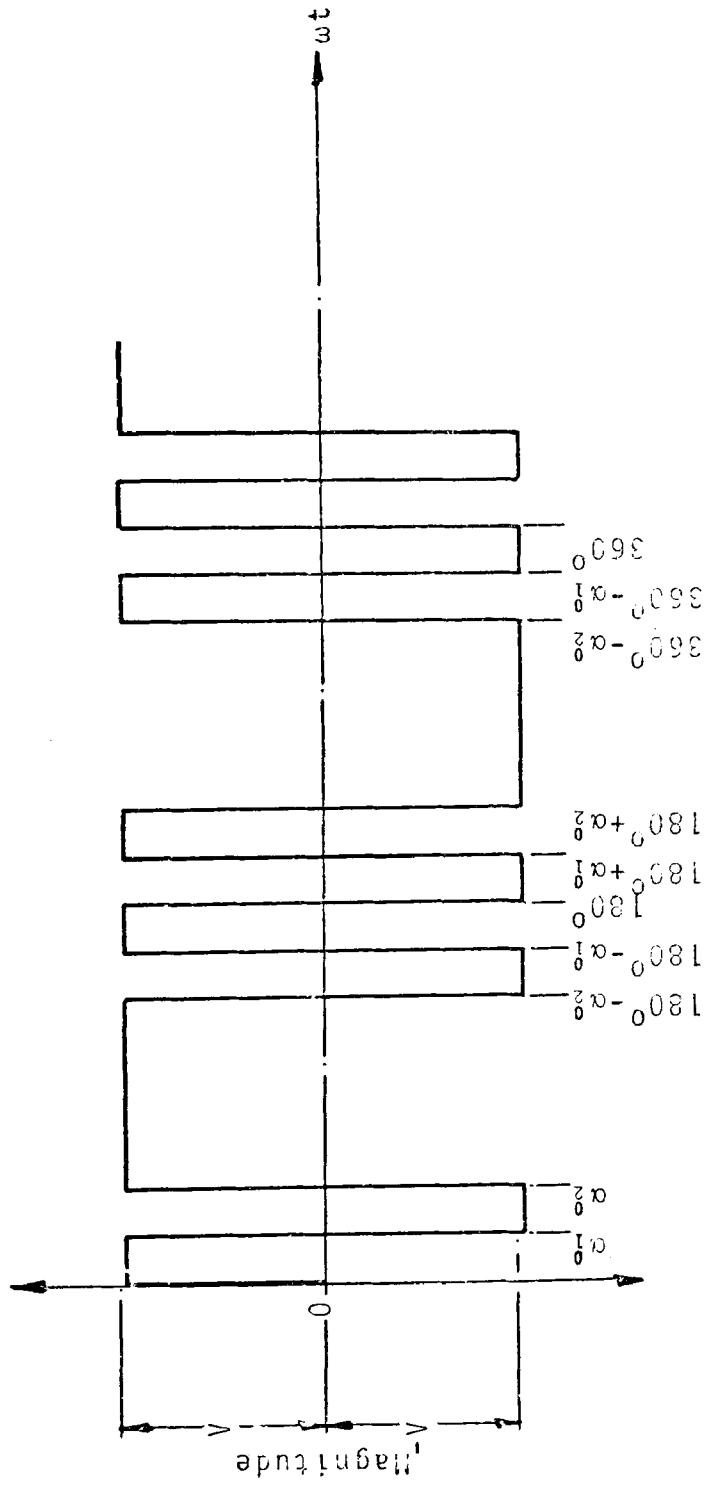


FIG. (2.23) MULTIPLE PULSE OUTPUT WAVEFORM



$$1 - 2 \cos m\alpha_1 + 2 \cos m\alpha_2 = 0.$$

when  $\alpha_1 = 23.62^\circ$  and  $\alpha_2 = 33.30^\circ$  the 3rd and 5th harmonic terms are eliminated, whereas, when  $\alpha_1 = 16.25^\circ$  and  $\alpha_2 = 22.07^\circ$  the 5th and 7th harmonics are eliminated. Control of the magnitude of the output voltage is achieved by varying the phase angle,  $\phi$ . (Equation (2.2.5)).

Further development of this method of harmonic elimination has resulted in a system, which eradicates as many harmonic components from the output waveform as there are pulses per half cycle of the output waveform. (12)

The main disadvantages of this form of harmonic elimination are as follows:

(i) The modulation process employed is not a true continuous pulse-width-modulation process. In fact it could be argued on a theoretical basis that the edges of the pulses in the output waveform are determined by a pulse-position process. This makes the control system for the thyristors in the pulse-modulated power-converter very complex and rather costly.

(ii) The angles at which the leading and trailing edges of each pulse occur must be maintained for each cycle of the output waveform if the elimination of the selected harmonics is to be retained. This essentially restricts the application of such systems to constant-voltage constant-frequency applications.

(iii) It must not be forgotten (Section(2.3)) that the occurrence of every pulse in one cycle of output waveform from the pulse-modulated power-converter, requires two commutations.

Therefore, the larger the number of pulses per cycle of output waveform, the greater is the commutation losses and the lower is the efficiency of the frequency conversion process.

(iv) When considering the harmonic distortion of a modulated waveform the complete elimination of say two selected harmonics can prove to be less beneficial than say the reduction of four harmonics for the same number of commutations in the power-converter. This will be enlarged upon later in the thesis.

#### (2.4.2.4) Changing the Waveform of the Modulating Wave.

Harmonic elimination in pulse modulated power converters has been successfully achieved by using modulating waves which do not have a sinusoidal waveform. One such scheme employed a trapezoidal modulating waveform which is said to have reduced certain significant harmonic components.<sup>(14)</sup> Although many schemes exist which use non-sinusoidal modulating waves, the main objective of these schemes has been to use a modulating wave which is easily generated by electronic means.

A novel technique which uses non-sinusoidal modulating waves for generating p.w.m. waveforms is discussed at length in Chapter (3) of this thesis. These new schemes have a very significant effect on the reducing of unwanted harmonic components.<sup>(13)</sup>

#### (2.4.2.5) Increasing the Ratio of Carrier-Frequency to Modulating Frequency.

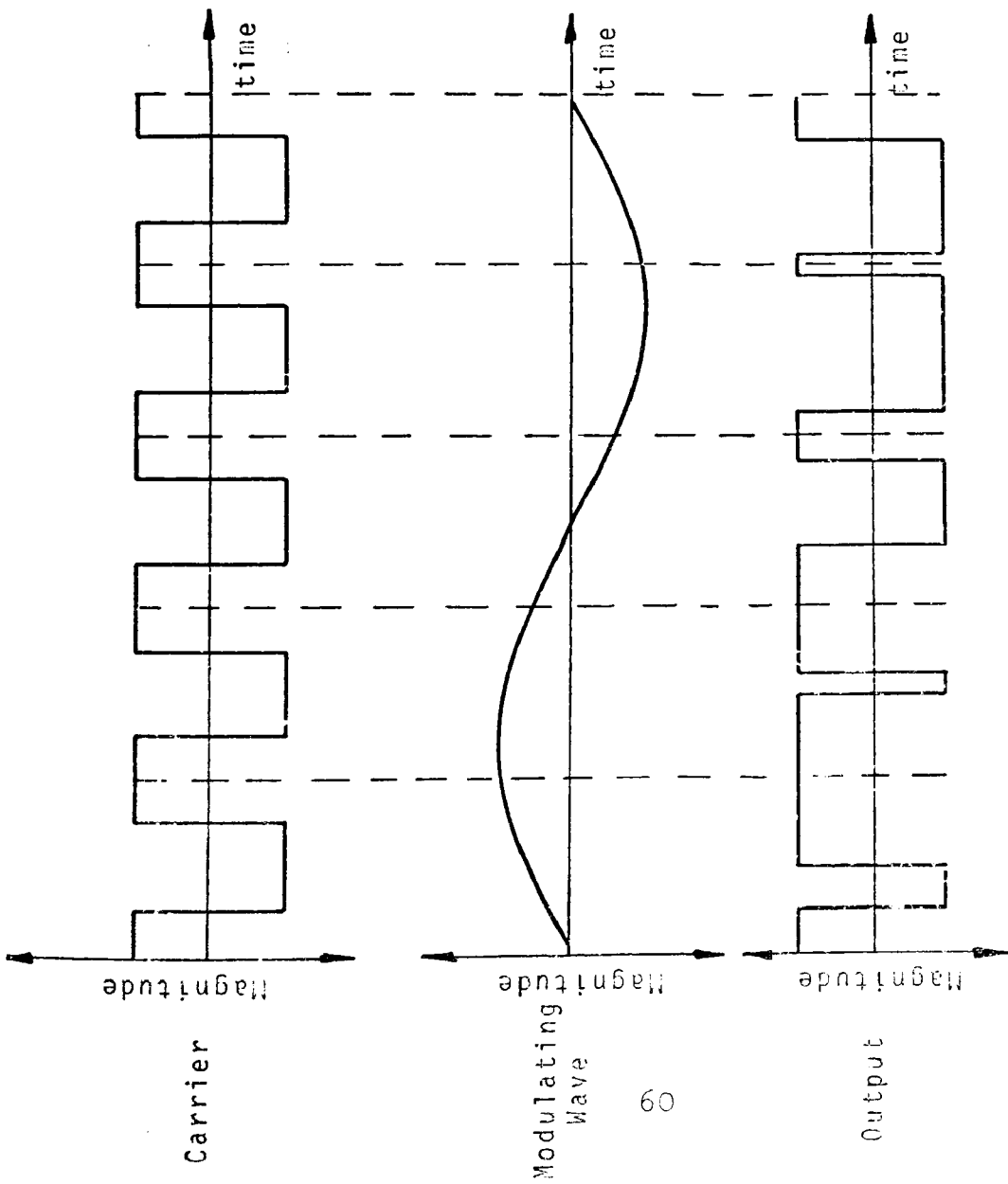
The most significant unwanted harmonic components are the

components nearest the wanted component in the frequency domain. The difference in frequency between the wanted component (of frequency  $\omega_m$ ) and the nearest unwanted component (of frequency  $(\omega_c - \omega_m)$ ) described by the equations: (2.3), (2.9), (2.10) and (2.14) can be increased by increasing the frequency ratio. This is also true for the double modulation process described by equation (2.18) where the unwanted component is of frequency,  $(\omega_c - \omega'_m - \omega_m)$ , and the wanted component is of frequency,  $(\omega_m - \omega'_m)$ . Therefore, if the stator leakage impedance of an induction motor (15) is considered as a low-pass filter, its ability to block the unwanted component is enhanced by increasing the carrier to modulating frequency ratio. Although this technique has been used in a number of systems, (16), (17) its major disadvantage is that it increases the number of commutations per cycle of output voltage as illustrated in Fig.(2.24). This reduces the efficiency of the frequency conversion process.

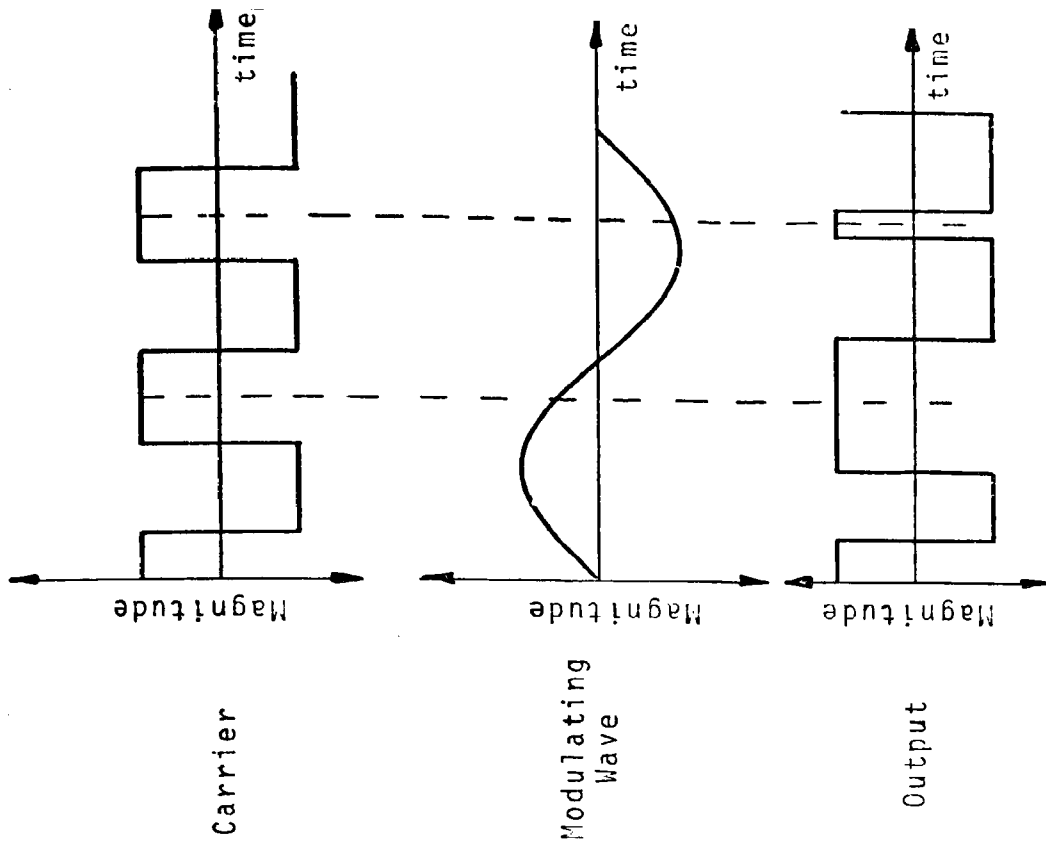
It is of particular interest to note at this point that the novel technique mentioned in Section (2.4.2.3)<sup>(13)</sup> of this thesis which will be fully described in Chapter (3) has a similar reduction effect on the magnitude of the most significant unwanted harmonic components without increasing the frequency ratio.

#### (2.4.3) Modulation and Summation by means of a Transformer

The harmonic distortion of p.w.m. waveforms can be considerably reduced by combining the output modulated waveforms from two or more modulators where either the



(a) Carrier To Modulating Frequency Ratio of 5:1



(b) Carrier To Modulating Frequency Ratio Of 2.5:1

FIG. (2.24) INCREASE IN THE NUMBER OF COMMUTATIONS WITH INCREASE IN FREQUENCY RATIO

phases of the modulating waves are displaced or the phases of the carrier waves are displaced. The combining of the two or more waveforms is achieved by means of a transformer as shown in Fig.(2.25)

It was shown in Section (2.2.8) that the double-edge p.w.m. process could be described by equation (2.14). Therefore, the equations describing the output waveforms from two such modulators, where the modulating waves are in phase but the carrier waves are displaced by  $180^\circ$  are as follows:

$$\begin{aligned}
 f(t)_1 = & k + k A_m \cos \omega_m t + \frac{2}{\pi} \sum_{m=1}^{m=\infty} \frac{1}{m} \{ [J_0(m \pi k A_m) \sin m \pi k] \cos m \omega_c t \\
 & + \sum_{n=1}^{n=\infty} J_n(m \pi k A_m) \sin(m \pi k + \frac{n\pi}{2}) [\cos(m \omega_c + n \omega_m)t \\
 & + \cos(m \omega_c - n \omega_m)t] \} \quad \text{-----(2.26)}
 \end{aligned}$$

$$\begin{aligned}
 \text{and } f(t)_2 = & k + k A_m \cos \omega_m t \\
 & + \frac{2}{\pi} \sum_{m=1}^{m=\infty} \frac{1}{m} \{ [J_0(m \pi k A_m) \sin m \pi k] \cos(m \omega_c t - m \pi) \\
 & + \sum_{n=1}^{n=\infty} J_n(m \pi k A_m) \sin(m \pi k + \frac{n\pi}{2}) [\cos((m \omega_c \\
 & + n \omega_m)t - m \pi) + \cos((m \omega_c - n \omega_m)t - n \pi)] \} \quad \text{-----(2.27)}
 \end{aligned}$$

The summation of the two time functions  $f(t)_1$  and  $f(t)_2$  gives the following time function:

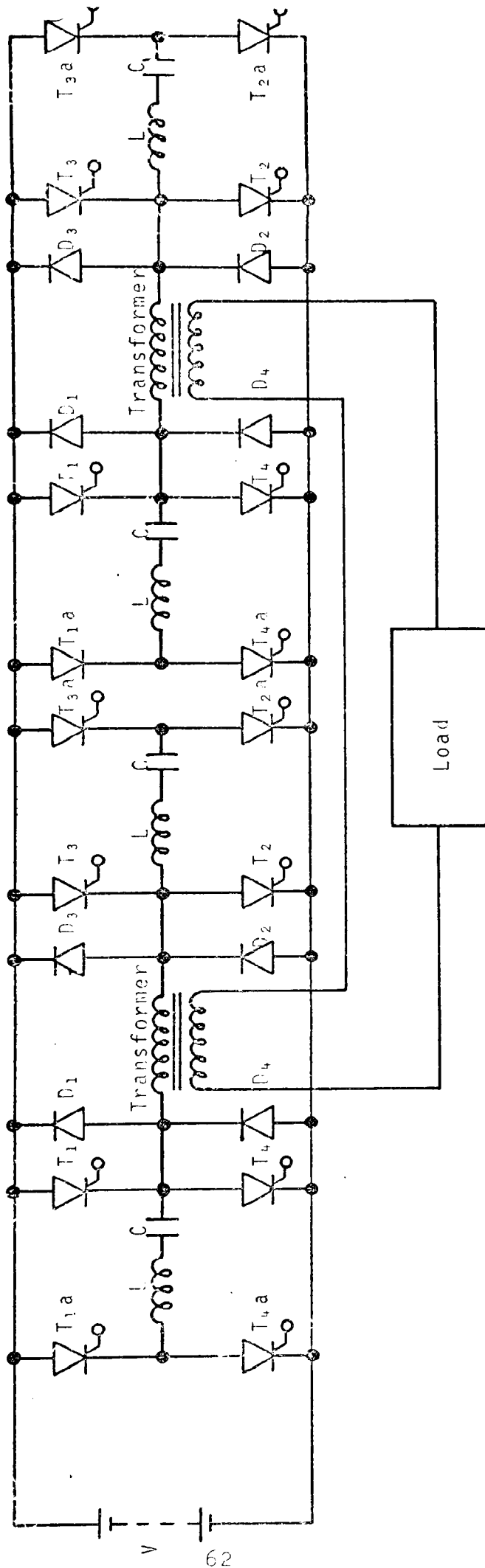


FIG. (2.25a) COMBINING OF TWO MODULATING WAVEFORMS BY MEANS OF A TRANSFORMER

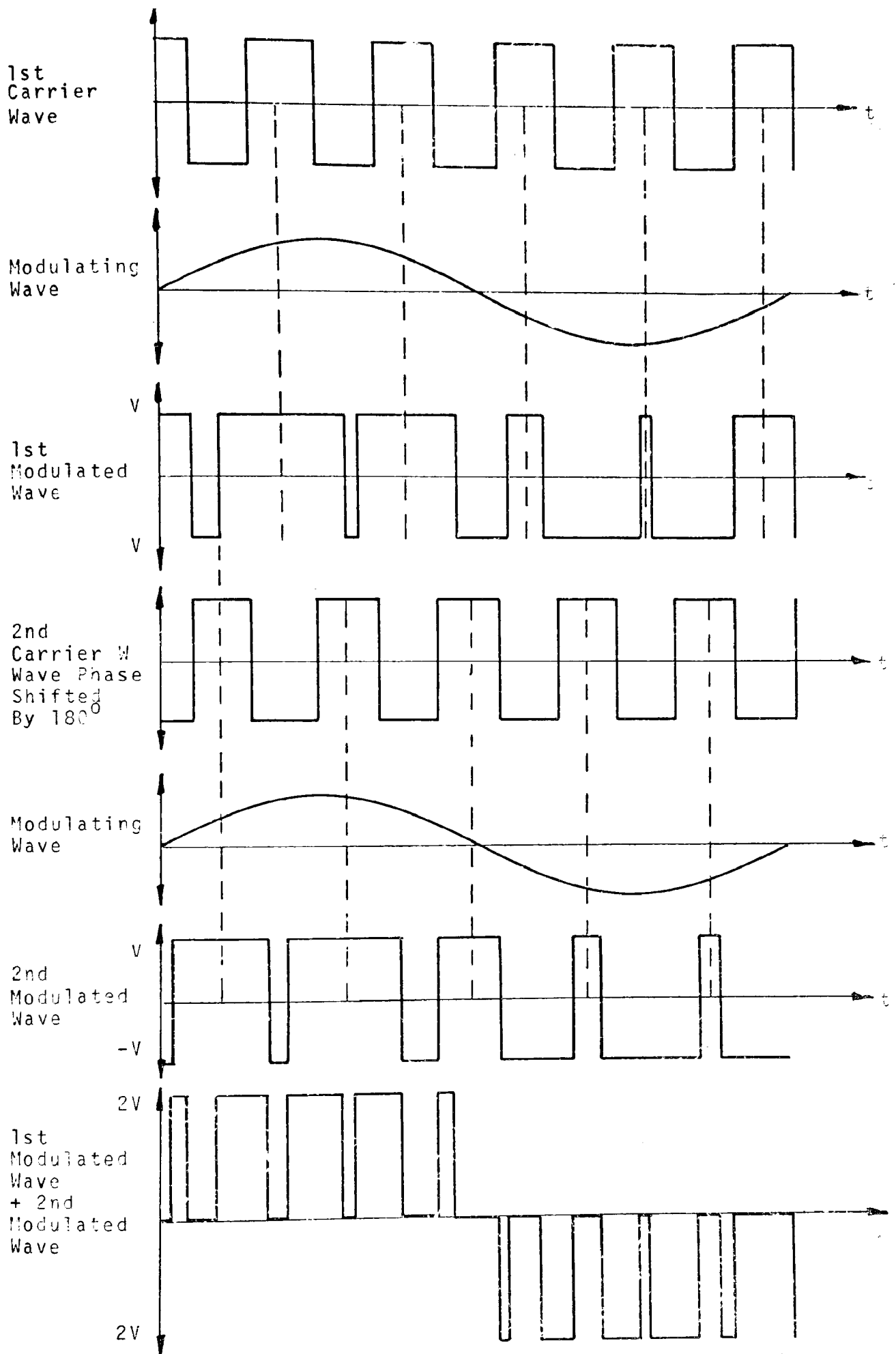


FIG. (2.25b) THE COMBINING OF TWO P.W.M. WAVEFORMS BY MEANS OF A TRANSFORMER IN THE TIME DOMAIN

$$\begin{aligned}
f(t)_1 + f(t)_2 &= 2k + 2k A_m \cos \omega_m t \\
&+ \sum_{m=1}^{m=\infty} \frac{1}{m} \{ [J_0(m \pi k A_m) \sin m \pi k] [\cos m \omega_c t + \cos(m \omega_c t - m\pi)] \\
&+ \sum_{n=1}^{n=\infty} J_n(m \pi k A_m) \sin(m \pi k + \frac{n\pi}{2}) [\cos(m \omega_c t + n \omega_m)t \\
&+ \cos((m \omega_c + n \omega_m)t - m\pi)] \\
&+ \sum_{n=1}^{n=\infty} J_n(m \pi k A_m) \sin(m \pi k + \frac{n\pi}{2}) [\cos(m \omega_c - n \omega_m)t \\
&+ \cos((m \omega_c - n \omega_m)t - m\pi)] \} \quad \text{-----(2.28)}
\end{aligned}$$

Now for odd values of m the term:

$$[\cos m \omega_c t + \cos(m \omega_c t - m\pi)] = 0$$

whereas for even values of m the term:

$$\sin m \pi k = 0$$

Therefore, the carrier of frequency,  $(\omega_c)$ , and all its harmonics of frequency,  $(m \omega_c)$ , cancel.

Similarly for odd values of m the term:

$$[\cos(m \omega_c + n \omega_m)t + \cos((m \omega_c + n \omega_m)t - m\pi)] = 0$$

and

$$[\cos(m \omega_c - n \omega_m)t + \cos((m \omega_c - n \omega_m)t - m\pi)] = 0$$

For even values of m and even values of n the term:

$$\sin(m \pi k + \frac{n\pi}{2}) = 0$$

Hence it can be seen that the terms:



$$[\cos(m\omega_c + n\omega_m)t + \cos((m\omega_c + n\omega_m)t - n\pi)]$$

$$\text{and } [\cos(m\omega_c - n\omega_m)t + \cos((m\omega_c - n\omega_m)t - m\pi)]$$

only exist for even values  $m$  and odd values of  $n$ .

Therefore, the time function described by equation (2.28) can be reduced to:

$$f(t)_1 + f(t)_2 = 2k + 2k A_m \cos \omega_m t$$

$$+ \sum_{m=1}^{m=\infty} \frac{1}{m} \left\{ \sum_{n=1}^{n=\infty} J_n(m\pi k A_m) \sin\left(m\pi k + \frac{n\pi}{2}\right) [\cos(m\omega_c + n\omega_m)t$$

$$+ \cos((m\omega_c + n\omega_m)t - m\pi)]$$

$$+ \sum_{n=1}^{n=\infty} J_n(m\pi k A_m) \sin\left(m\pi k + \frac{n\pi}{2}\right) [\cos(m\omega_c - n\omega_m)t$$

$$+ \cos((m\omega_c - n\omega_m)t - m\pi)] \} \quad \text{-----(2.29)}$$

It may therefore be seen that the displacing of the two carrier waves by  $180^\circ$  increases the magnitude of the component of frequency,  $\omega_m$ , by a factor of 2 and considerably decreases the harmonic distortion of the output waveform. The main disadvantage of this method of harmonic elimination is that it requires two modulators and one transformer per phase. This increases the number of components, weight and cost of the system which restricts its application to large capacity speed control systems which can justify the increase in cost of the added components and weight.

It can similarly be shown that if the two modulating waves are displaced in time phase by  $180^\circ$ , and the modulated waves subtracted, then the resulting modulated waveform can be described by the following time function:

$$\begin{aligned}
 f(t)_3 - f(t)_4 &= k + k A_m \cos \omega_m t \\
 &+ \frac{2}{\pi} \sum_{m=1}^{m=\infty} \frac{1}{m} \{ [J_0(m \pi k A_m) \sin m \pi k] \cos m \omega_c t \\
 &+ \sum_{n=1}^{n=\infty} J_n(m \pi k A_m) \sin(m \pi k + \frac{n\pi}{2}) [\cos(m \omega_c \\
 &+ n \omega_m)t + \cos(m \omega_c - n \omega_m)t] \} \\
 &- k - k A_m \cos(\omega_m t - \pi) \\
 &- \frac{2}{\pi} \sum_{m=1}^{m=\infty} \frac{1}{m} \{ [J_0(m \pi k A_m) \sin m \pi k] \cos m \omega_c t \\
 &- \sum_{n=1}^{n=\infty} J_n(m \pi k A_m) \sin(m \pi k + \frac{n\pi}{2}) [\cos((m \omega_c \\
 &+ n \omega_m)t + n\pi) + \cos((m \omega_c - n \omega_m)t - n\pi)] \} \quad \text{-----(2.30)}
 \end{aligned}$$

By the use of trigonometric identities this reduces to:

$$\begin{aligned}
 f(t)_3 - f(t)_4 &= 2k A_m \cos \omega_m t \\
 &+ \frac{2}{\pi} \sum_{m=1}^{m=\infty} \frac{1}{m} \sum_{n=1}^{n=\infty} \{ J_n(m \pi k A_m) \sin(m \pi k + \frac{n\pi}{2}) [\cos(m \omega_c + n \omega_m)t \\
 &- \cos n \pi \cos(m \omega_c + n \omega_m)t + \cos(m \omega_c \\
 &- n \omega_m)t - \cos n \pi \cos(m \omega_c - n \omega_m)t] \}
 \end{aligned}$$

$$- n\omega_m)t - \text{Cos } n \pi \text{ Cos}(m\omega_c - n\omega_m)t] \} \quad \text{----(2.31)}$$

It can be seen from equation (2.31) that for this case the terms of frequency,  $(m\omega_c + n\omega_m)$  and  $(m\omega_c - n\omega_m)$ , all cancel for even values of  $n$ .

It may also be seen that these terms cancel when both  $m$  and  $n$  have odd values. Therefore, harmonics of frequency,  $(m\omega_c + n\omega_m)$  and  $(m\omega_c - n\omega_m)$ , only exist for even values of  $m$  and odd values of  $n$  as in the previous case. Similarly this system has the same disadvantages as the previous case.

(2.4.4) Modulation and Cancellation by  
Supplying a 3-Wire, 3-Phase Load.

The pulse-width modulation of the bi-polar carrier wave described by equation(2.21) in Section (2.4.2.1) by three sinusoidal modulating waves of equal amplitude and frequency but displaced in time-phase by  $120^\circ$ , provides the following three equations for the output modulated waveforms:

$$f_1(t) = k A_m \text{Cos } \omega_m t + \frac{2}{\pi} \sum_{m=1}^{\infty} \frac{1}{m} \{ [J_0(m \pi k A_m) \text{Sin } m \pi k] \text{Cos } \omega_c t$$

$$+ \sum_{n=1}^{\infty} J_n(m \pi k A_m) \text{Sin}(m \pi k + \frac{n\pi}{2}) [\text{Cos}(m\omega_c$$

$$+ n\omega_m)t + \text{Cos}(m\omega_c - n\omega_m)t] \} \quad \text{----(2.32)}$$

$$f_2(t) = k A_m \text{Cos}(\omega_m t + \frac{4\pi}{3})$$

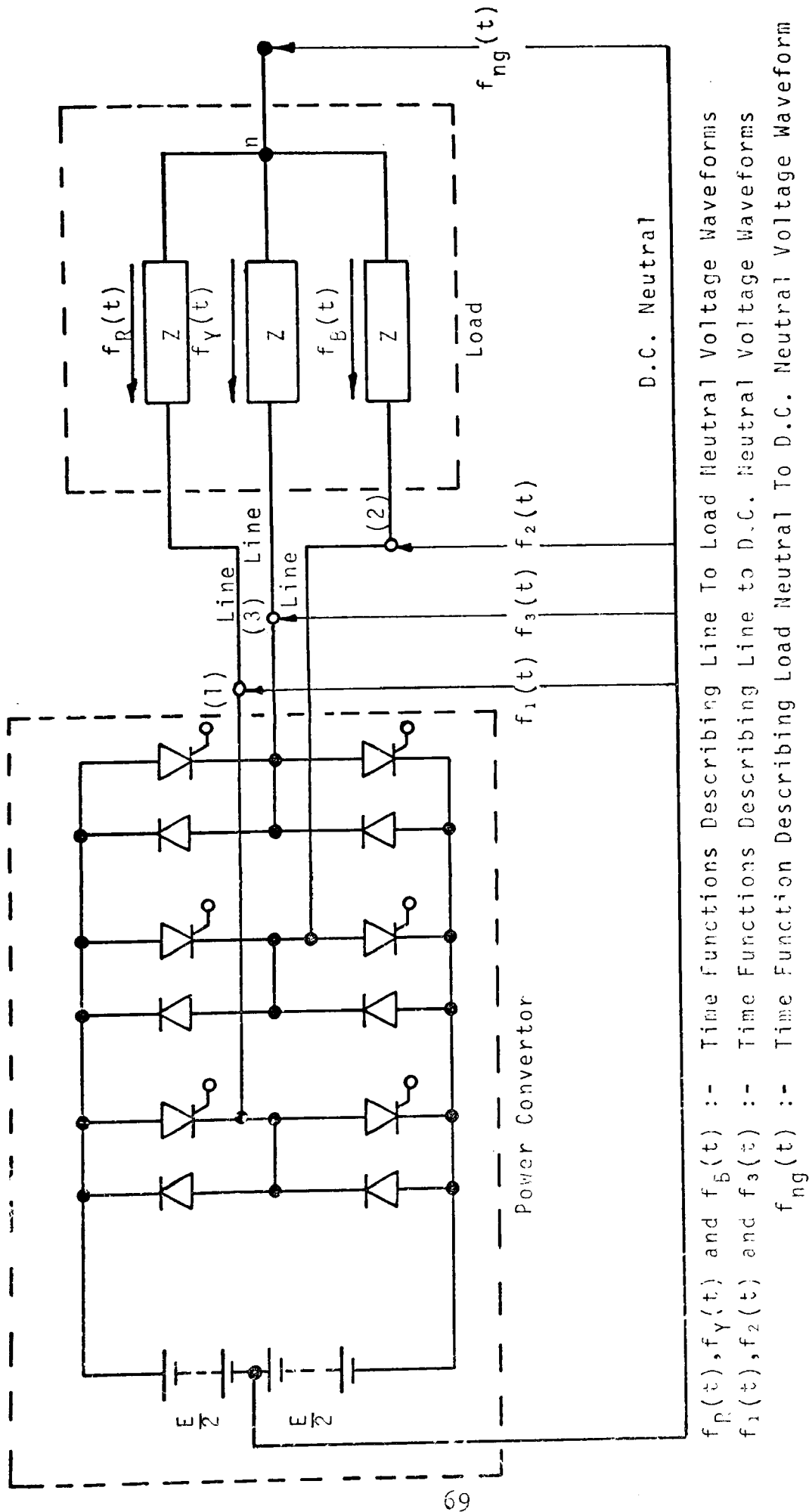
$$+ \frac{2}{\pi} \sum_{m=1}^{\infty} \frac{1}{m} \{ [J_0(m \pi k A_m) \text{Sin } m \pi k] \text{Cos } m\omega_c t$$

$$\begin{aligned}
& + \sum_{n=1}^{\infty} J_n(m \pi k A_m) \text{Sin}(m \pi k + \frac{n\pi}{2}) [\text{Cos}((m\omega_c + n\omega_m)t \\
& + \frac{4\pi n}{3} + \text{Cos}((m\omega_c - n\omega_m)t - \frac{4\pi n}{3})] \} \quad \text{-----(2.33)}
\end{aligned}$$

$$\begin{aligned}
f_3(t) & = k A_m \text{Cos}(\omega_m t + \frac{2\pi}{3}) \\
& + \frac{2}{\pi} \sum_{m=1}^{\infty} \frac{1}{m} \{ [J_0(m \pi k A_m) \text{Sin } m \pi k] \text{Cos } m\omega_c t \\
& + \sum_{n=1}^{\infty} J_n(m \pi k A_m) \text{Sin}(m \pi k + \frac{n\pi}{2}) [\text{Cos}((m\omega_c \\
& + n\omega_m)t + \frac{2\pi n}{3}) + \text{Cos}((m\omega_c - n\omega_m)t - \frac{2\pi n}{3})] \} \quad \text{-----(2.34)}
\end{aligned}$$

These three time functions are representative of the output voltage between the points: (1), (2) and (3) and the neutral of the d.c. supply as shown in Fig.(2.26). The phase voltage across the load can be determined in terms of the functions  $f_1(t)$ ,  $f_2(t)$  and  $f_3(t)$  by means of Millmans Theory:

$$\begin{aligned}
f_R(t) & = \frac{2f_1(t) - f_2(t) - f_3(t)}{3} \\
& = \frac{A_m}{2} \text{Cos } \omega_m t + \frac{4}{3\pi} \sum_{n=1}^{\infty} \sum_{m=1}^{\infty} \frac{1}{m} [J_n(\frac{m \pi A_m}{2}) \text{Sin}(\frac{m\pi}{2} \\
& + \frac{n\pi}{2})] \{ [1 - \frac{1}{2} \text{Cos } \frac{4\pi n}{3} - \frac{1}{2} \text{Cos } \frac{2\pi n}{3}] \\
& [\text{Cos}(m\omega_c + n\omega_m)t + \text{Cos}(m\omega_c - n\omega_m)t] \\
& + [\frac{1}{2} \text{Sin } \frac{4\pi n}{3} + \frac{1}{2} \text{Sin } \frac{2\pi n}{3}] [\text{Sin}(m\omega_c
\end{aligned}$$



$f_R(t), f_Y(t)$  and  $f_B(t)$  :- Time Functions Describing Line To Load Neutral Voltage Waveforms  
 $f_1(t), f_2(t)$  and  $f_3(t)$  :- Time Functions Describing Line to D.C. Neutral Voltage Waveforms  
 $f_{ng}(t)$  :- Time Function Describing Load Neutral To D.C. Neutral Voltage Waveform

FIG. (2.26) 3-PHASE MODULATOR EXCLUDING AUXILIARY COMMUTATING COMPONENTS

$$+ n\omega_m)t - \text{Sin}(m\omega_c - n\omega_m)t] \} \quad \text{-----(2.35)}$$

$$f_Y(t) = \frac{2f_2(t) - f_1(t) - f_3(t)}{3}$$

$$\equiv \frac{A_m}{2} \text{Cos}(\omega_m t + \frac{4\pi}{3}) + \frac{4}{3\pi} \sum_{n=1}^{\infty} \sum_{m=1}^{\infty} \frac{1}{m} [J_n(\frac{m\pi A_m}{2}) \text{Sin}(\frac{m\pi}{2} + \frac{n\pi}{2})] \{ [\text{Cos} \frac{4\pi n}{3} - \frac{1}{2} - \frac{1}{2} \text{Cos} \frac{2\pi n}{3}] \times$$

$$[\text{Cos}(m\omega_c + n\omega_m)t + \text{Cos}(m\omega_c - n\omega_m)t]$$

$$+ [\text{Sin} \frac{4\pi n}{3} - \frac{1}{2} \text{Sin} \frac{2\pi n}{3}] [\text{Sin}(m\omega_c - n\omega_m)t - \text{Sin}(m\omega_c + n\omega_m)t] \} \quad \text{-----(2.36)}$$

$$f_B(t) = \frac{2f_3(t) - f_1(t) - f_2(t)}{3}$$

$$= \frac{A_m}{2} \text{Cos}(\omega_m t + \frac{2\pi}{3}) + \frac{4}{3\pi} \sum_{n=1}^{\infty} \sum_{m=1}^{\infty} \frac{1}{m} [J_n(\frac{m\pi A_m}{2}) \text{Sin}(\frac{m\pi}{2} + \frac{n\pi}{2})] \{ [\text{Cos} \frac{2\pi n}{3} - \frac{1}{2} \text{Cos} \frac{4\pi n}{3}] [\text{Cos}(m\omega_c + n\omega_m)t + \text{Cos}(m\omega_c - n\omega_m)t] + [\text{Sin} \frac{2\pi n}{3} - \frac{1}{2} \text{Sin} \frac{4\pi n}{3}] \times$$

$$[\text{Sin}(m\omega_c - n\omega_m)t - \text{Sin}(m\omega_c + n\omega_m)t] \} \quad \text{-----(2.37)}$$

From equations (2.35), (2.36) and (2.37) it may be seen that the voltage waveforms across each phase of the load does not contain harmonic components of carrier frequency ( $\omega_c$ ). It may also be seen that for triple integer values of  $n$  (3,6,9,12, etc.), side-band components of frequency ( $m\omega_c + n\omega_m$ ) and ( $m\omega_c - n\omega_m$ ) cancel, because the terms:

$$\begin{aligned} & (1 - \frac{1}{2} \cos \frac{4\pi n}{3} - \frac{1}{2} \cos \frac{2\pi n}{3}), (\frac{1}{2} \sin \frac{4\pi n}{3} + \frac{1}{2} \sin \frac{2\pi n}{3}), \\ & (\cos \frac{4\pi n}{3} - \frac{1}{2} - \frac{1}{2} \cos \frac{2\pi n}{3}), (\sin \frac{4\pi n}{3} - \frac{1}{2} \sin \frac{2\pi n}{3}), \\ & (\cos \frac{2\pi n}{3} - \frac{1}{2} - \frac{1}{2} \cos \frac{4\pi n}{3}), \text{ and } (\sin \frac{2\pi n}{3} - \frac{1}{2} \sin \frac{4\pi n}{3}) \end{aligned}$$

equate to zero. Similarly the side-band components also cancel when  $m$  and  $n$  are both even and when  $m$  and  $n$  are both odd, because the term:  $\sin \left( \frac{m\pi}{2} + \frac{n\pi}{2} \right) = 0$ .

Therefore it is clear that the harmonic content of the voltage waveforms across each phase of the load, is considerably less than the harmonic content of the voltage waveforms which occur between the neutral of the d.c. supply and the output points (1), (2) and (3) of the convertor shown in Fig.(2.26). It is also of particular interest to note that the wanted harmonic components of frequency,  $\omega_m$ , form a balanced three-phase set. This is of particular importance when the load is a 3-phase induction motor, because such motors requires a balanced 3-phase supply for stable operation.

#### (2.5) Interim Conclusions.

The fundamental rules of frequency changing have been established, and it has been shown that all power inverters are basically pulse modulators. The requirements of a

practical power modulator have been outlined, and a circuit configuration which satisfies many of these requirements has been presented. The various pulse modulation processes have been analysed, and it has been shown that the p.w.m. process is most suited to power modulators. A novel double modulation process has been presented and analysed (A.M.P.W.M) which could be of significant importance in the development of force commutated a.c to a.c power modulators. Existing harmonic elimination techniques have been analysed, and the disadvantages and implications of such systems have been exposed.

Since it has been shown that the p.w.m process is most suited to power modulators it is valuable to consider how the application of sophisticated telecommunication techniques, which have not previously been applied to p.w.m power convertors, may be used to provide a viable system of infinitely variable speed control.



### (3) THE GENERATION AND REALISATION OF P.W.M. WAVEFORMS

#### (3.1) Introduction

It is important to note that the time functions used to describe the single-edge and double-edge p.w.m. processes in Sections (2.2.6), (2.2.7) and (2.2.8) are only applicable to the modulation processes which occur in existing p.w.m. power convertors. In fact the treatment of p.w.m. in Chapter (2) is general and does not entail a deep study of the continuous p.w.m. processes, nor does it identify concepts and phenomena which are common to communications practice, but which have not previously been identified in or applied to p.w.m. power convertors.

Basically, p.w.m. can be realised by analogue<sup>(17)</sup> or digital<sup>(18)</sup> means. The analogue method has proved to be more acceptable than the digital method mainly because it requires less electronic components and circuit complexity. However, it is probable that in the future digital techniques will become more acceptable due to the introduction of micro electronic circuits and techniques. So far as this thesis is concerned it is the analogue method only which will be considered.

The generation of p.w.m. waveforms by analogue means basically entails the comparing of a modulating wave with a sweep-wave or carrier wave. In prior-art p.w.m. power convertor techniques, the carrier signal has mainly been of triangular waveform whereas the waveform of the modulating signal has taken many forms, some of which are as follows: triangular, sinusoidal, square and trapezoidal.<sup>(14), (19)</sup> Where quantized approximate

sinewaves have been generated by digital means, they have been filtered to convert them to smooth sinewaves. The choice of carrier wave and modulating wave which in turn determines the p.w.m. process, does not appear to be based on any underlying fundamental basis or theory. In fact the fundamental theory and practice which has been applied in communication systems has not been applied or referred to in existing p.w.m. power convertor systems. Therefore, it was thought that the application of established communications concepts to p.w.m. power convertors could provide a basis for their design and possible improvement.

### (3.2) The Choice of Carrier Waveform.

The choice of carrier waveform in communications practice has been based upon the requirement for linear modulation, that is to say: the width of the modulated pulses must be directly proportional to respective instantaneous values of the modulating wave. This process is demonstrated graphically in Fig.(3.1) and may be proved mathematically as follows:

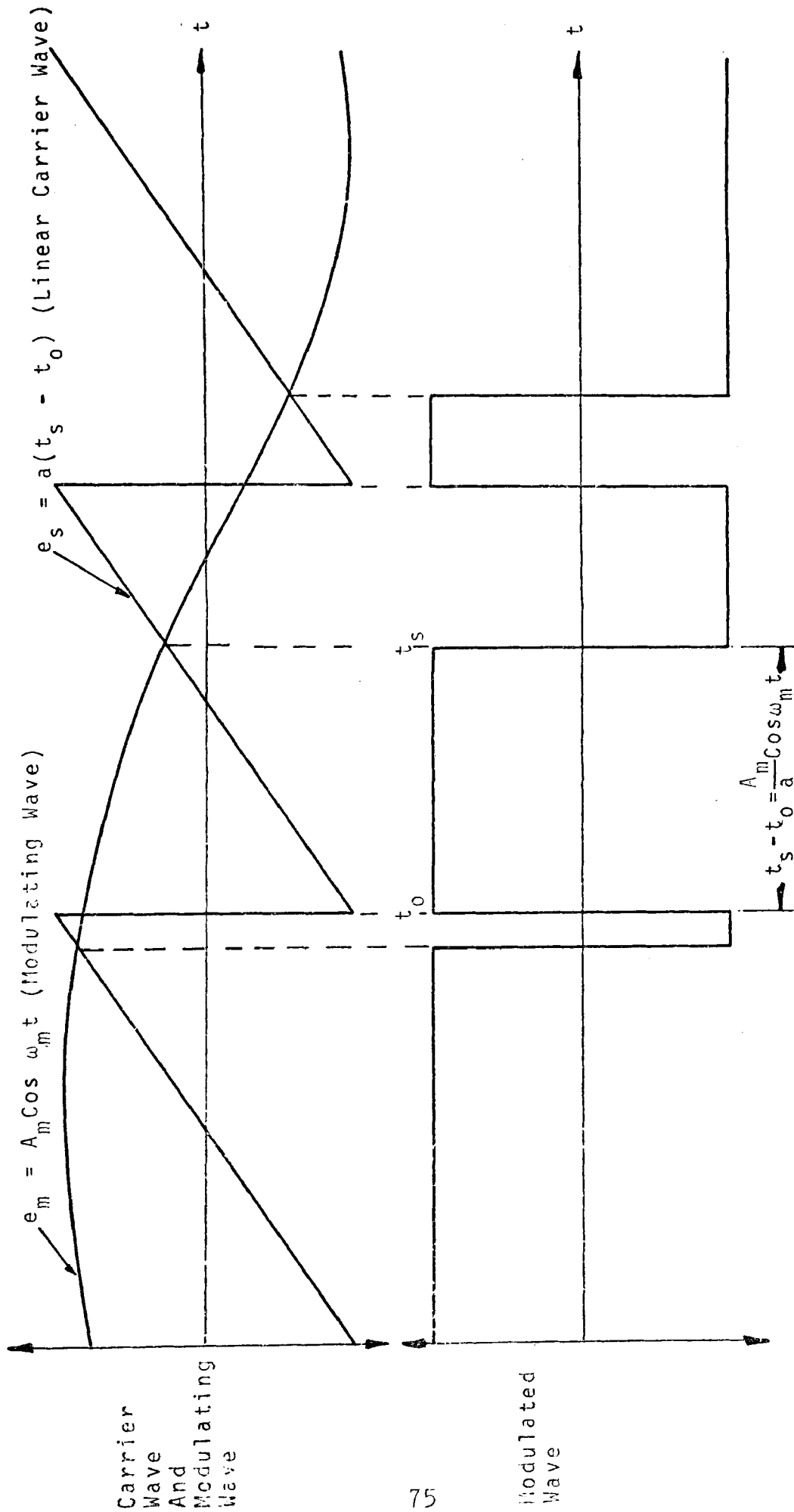
Let the linear sweep-wave or carrier wave be represented by:  $e_s = a(t_s - t_o)$ , and the modulating waveform by:  $e_m = A_m \cos \omega_m t$ .

The instant of intersection of the two waveforms is then defined by:  $e_m = e_s$ ,

therefore,  $A_m \cos \omega_m t = a(t_s - t_o)$

and  $t_s - t_o = \frac{A_m}{a} \cos \omega_m t_s$  -----(3.1)

Therefore, the time shift  $(t_s - t_o)$  of a given pulse edge is proportional to the instantaneous value of the modulating wave at instant,  $t_s$ , which means that the width



$t_0$  :- Reference Time  
 $t_s$  :- Switching Time

FIG.(3.1) LINEAR TIME - POSITION MODULATION PROCESS

of the modulated pulse is directly proportional to  $A_m \cos \omega_m t$  at the instant of intersection of the two waves. It may therefore be seen that the law of linear pulse-width-modulation is satisfied when the carrier wave has a waveform which is a linear function of time. It is for this reason that the carrier wave (or sweep wave) chosen for the systems to be described in succeeding sections of this thesis will be linear functions of time. It is probably for this same reason that prior-art p.w.m power convertor techniques have mainly used carrier waves which are linear functions of time.

### (3.3) Modulation Depth or Modulation Index

This is defined as the ratio of the peak-value of the modulation wave to the peak-value of the carrier wave. It may be seen from the waveforms illustrated in Fig.(3.2) that when the modulation index is zero, the unmodulated output waveform consists of a uniform train of bi-polar pulses of the same frequency as the carrier wave (or sweep wave). It is important to note that it was this unmodulated bi-polar waveform which was taken as the carrier wave in the analysis presented in Section (2.4.2.1). It may also be seen that the modulation index defines the voltage-time area and its distortion over one cycle of the output modulated waveform. The greater the modulation index the larger is the effective amplitude of the wanted component of the output modulated

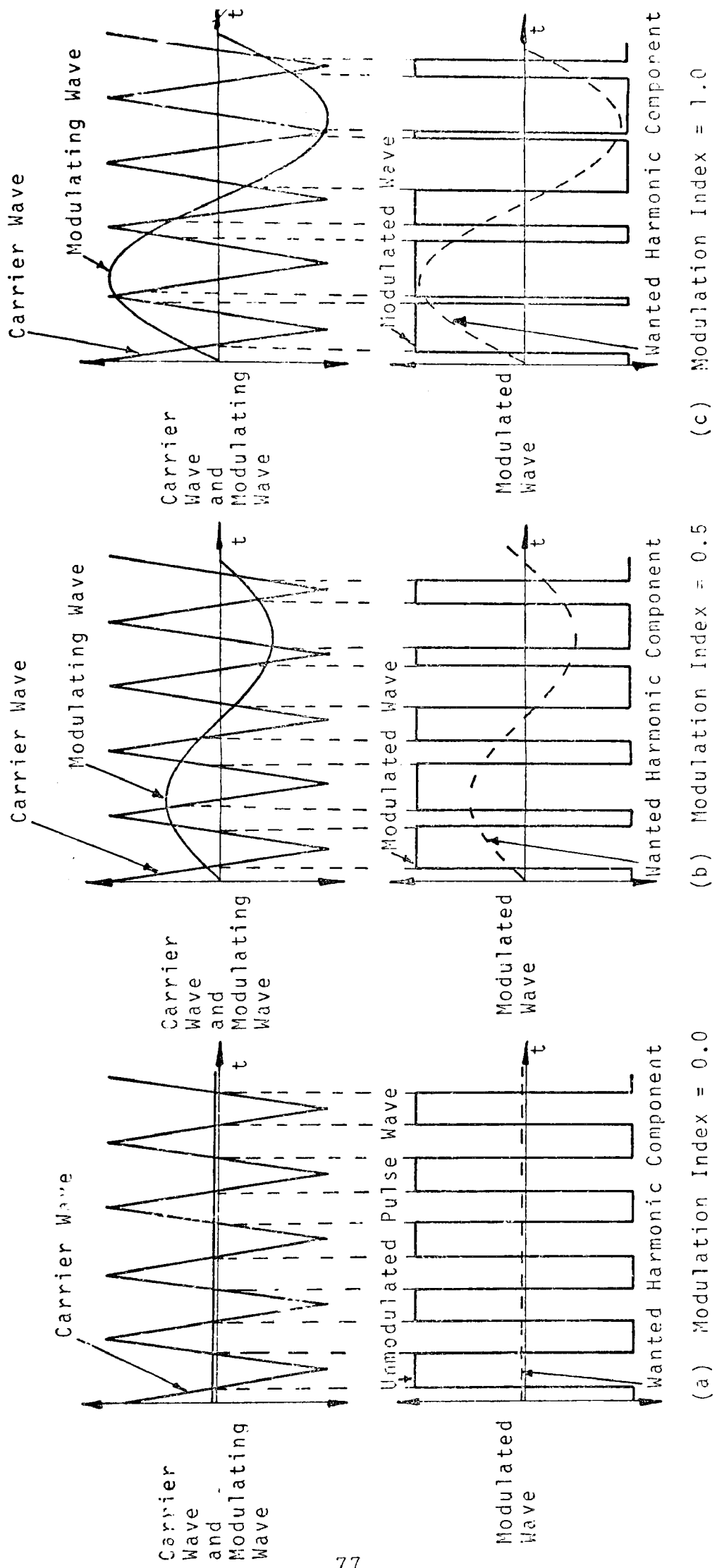


FIG.(3.2) OUTPUT MODULATED WAVEFORMS FOR MODULATION INDICES OF: 0.0, 0.5 AND 1.0

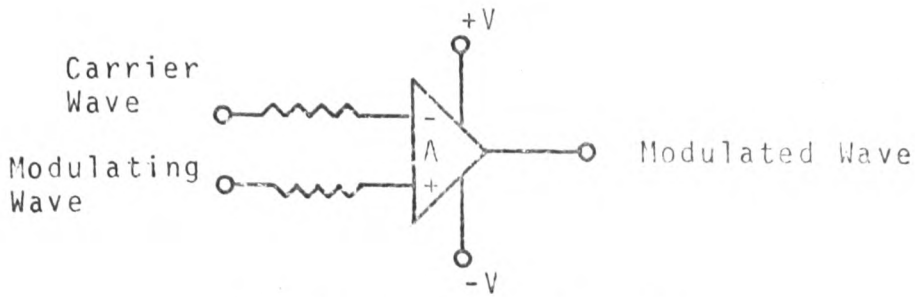
waveform. Therefore, the variation of the modulating index provides a means of controlling the wanted component of the output waveform from the power modulator. Although the variation of the modulation index provides an ideal means of controlling the amplitude of the wanted component of the output waveform, it also changes the amount of harmonic distortion. Decreasing the modulation index can increase the percentage amplitude of harmonics of carrier frequency and multiples of the carrier frequency. This will be enlarged upon later in the thesis and it will be shown that a fixed carrier frequency p.w.m. power modulator does not suffer from this increase in harmonic distortion with decrease in modulation index when used for constant torque, cage rotor, induction motor drives.

#### (3.4) The Generation of Leading-Edge P.W.M. Waveforms

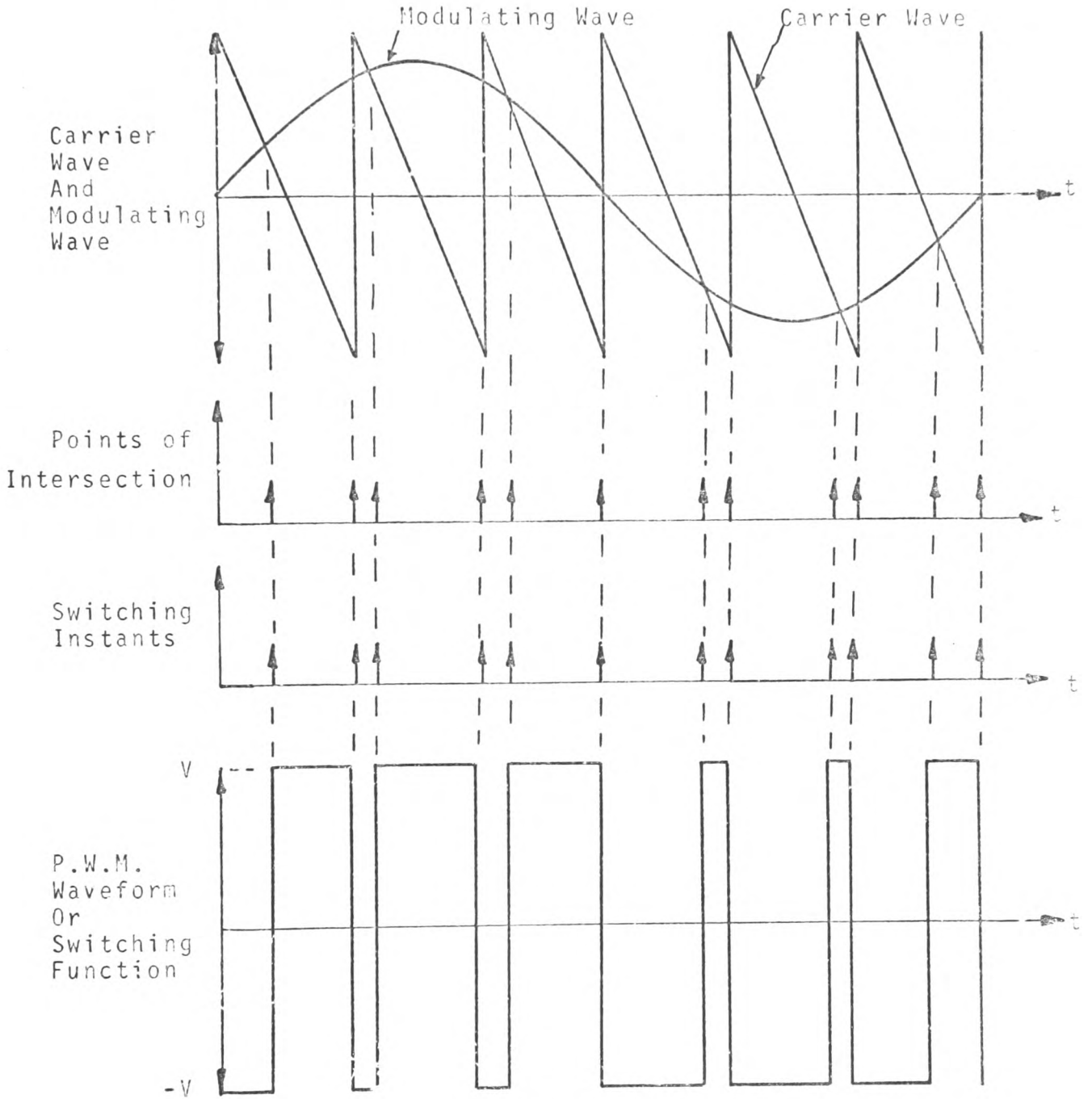
The prior-art<sup>(17)</sup> analogue technique of realising this type of waveform, has mainly consisted of a direct comparison made between the carrier wave and modulating wave as illustrated in Fig.(3.3). It is immediately apparent that the trailing-edges of the pulses occur at discreet uniform intervals, whereas, the leading-edges are modulated, the amount of modulation being dependent upon respective instantaneous values of the modulating wave at the points of intersection between the carrier wave and modulating wave. It is important to note that points of intersection and switching instants are coincident.

#### (3.5) The Generation of Trailing-Edge P.W.M. Waveforms

The existing<sup>(17)</sup> method of generating trailing-edge p.w.m. waveforms in power convertors is illustrated in Fig.(3.4).

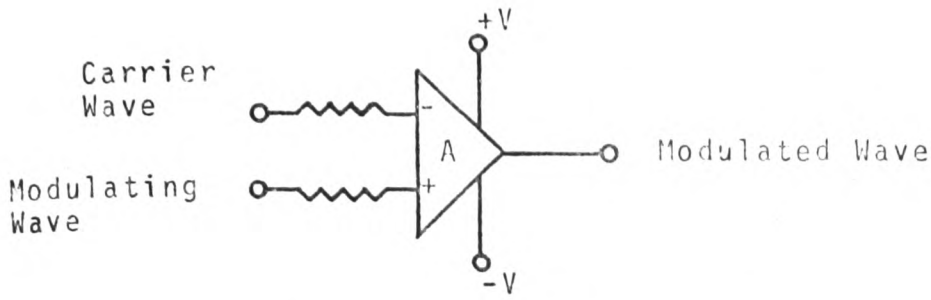


(a) Comparator Circuit

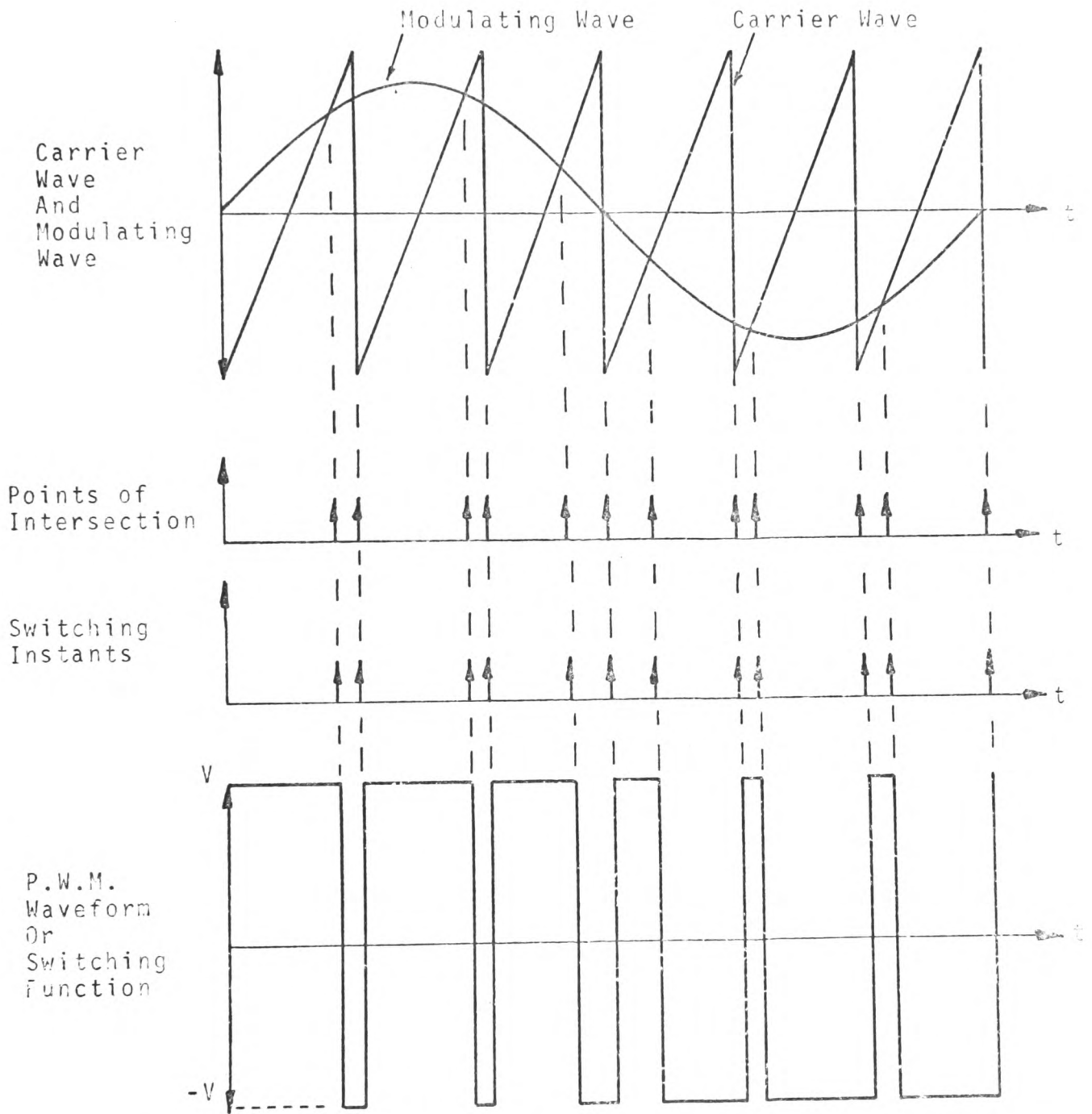


(b) Modulation Process

FIG.(3.3) LEADING-EDGE P.W.M.



(a) Comparator Circuit



(b) Modulation Process

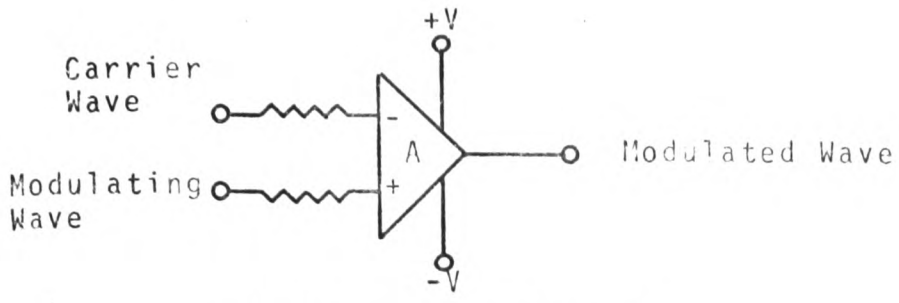
FIG.(3.4) TRAILING-EDGE P.W.M.



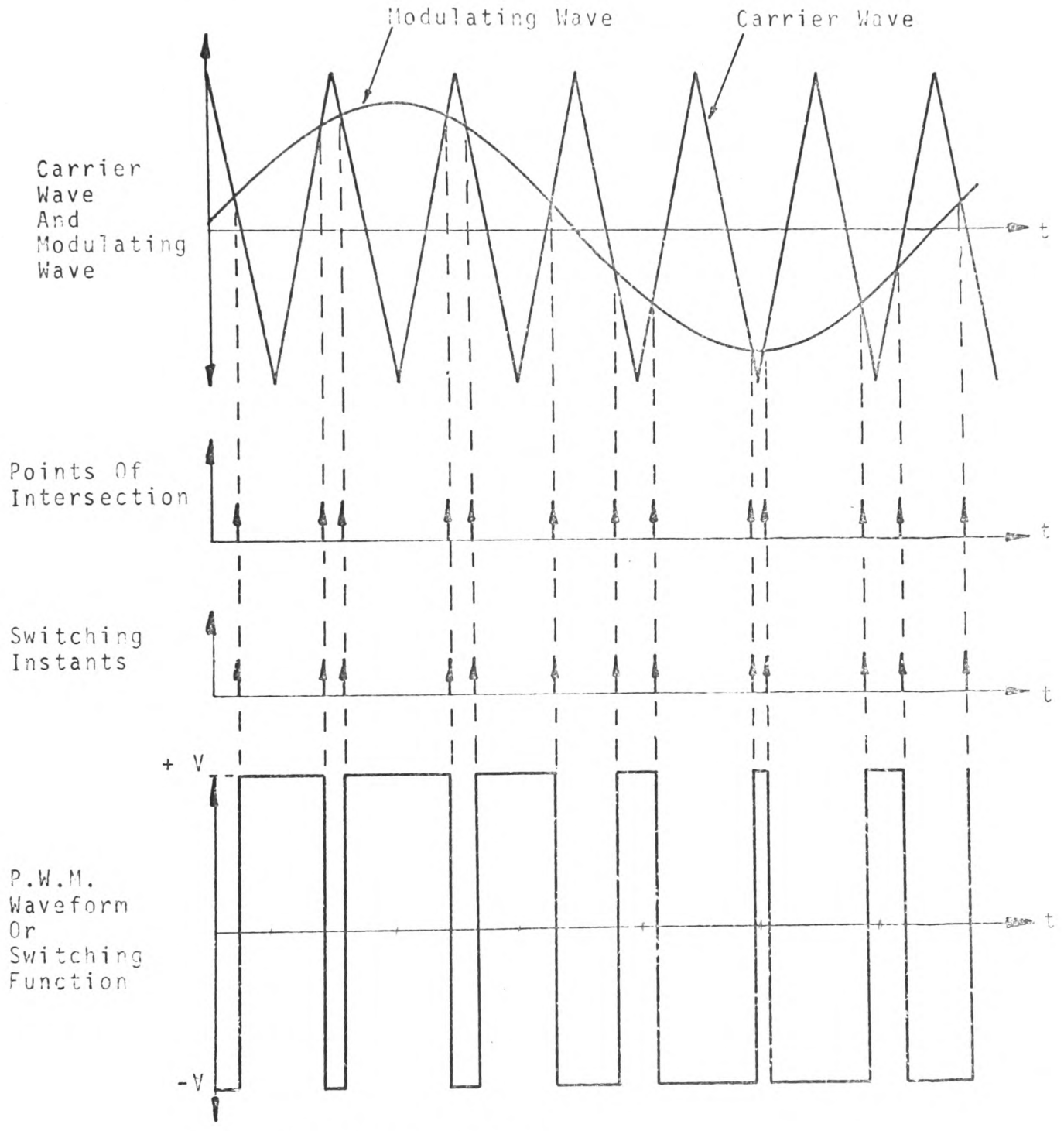
It may be seen that the trailing-edges of the pulses are modulated by an amount, which is proportional to instantaneous values of the modulating wave, at respective points of intersection. Once again it may be seen that respective points of intersection and switching instants are again coincident. The unmodulated leading-edges of the pulses occur at uniformly spaced intervals which coincide with the respective vertical sides of the triangular carrier wave.

### (3.6) The Generation of Double-Edge P.W.M. Waveform

This form of modulation has been achieved in prior-art<sup>(17)</sup> p.w.m. power convertors by comparing the modulating wave with a carrier wave having two slopes. This process is illustrated in Fig.(3.5). It can be seen that both edges of the pulses are modulated about their mean positions (the positions corresponding to the negative apices of the carrier wave) by different amounts; the amount of modulation being dependent upon the respective instantaneous values of the modulating wave at the points of intersection. The degree of asymmetry of modulation is dependent upon the ratio of carrier frequency to modulating frequency. For very large frequency ratio's, the modulation of both edges of pulses about their mean positions becomes symmetrical;<sup>(20)</sup> whereas, for low frequency ratio's the amount of modulation of both edges of each pulse becomes asymmetrical. The switching instants and points of intersection for the leading-edges and trailing-edges of respective pulses do not occur at uniform instants, but the switching instant and the point of intersection between the carrier wave and modulating wave for each pulse-edge still remain coincident. The fact that respective switching instants



(a) Comparator Circuit



(b) Modulation Process

FIG.(3.5) DOUBLE-EDGE P.W.M.

and points of intersection have always been coincident in existing p.w.m power convertors is of considerable significance, and will be enlarged upon in Section (3.7).

(3.7) Identification of the Sampling Process in Existing P.W.M. Power Convertors.

In Sections (3.6), (3.5) and (3.4) of this thesis it has been shown that in all existing p.w.m. power convertors which employ the analogue method of generating p.w.m. waveforms or switching functions, the points of intersection between the carrier wave and modulating wave and respective switching instants of the p.w.m. waveform or switching waveform are always coincident. It was also shown in Section (3.2) that the width of the modulated pulses is directly proportional to the corresponding instantaneous values of the modulating wave at the points of intersection. It may therefore be said that the p.w.m. wave has been modulated according to discrete 'samples' of the modulating wave, such that the width of the pulses reflect the information contained in respective 'samples'.

Although the concept of 'sampling' is well established in communications practice, it does not appear to have been identified in or applied to existing p.w.m. power convertors. It may be seen from Figures (3.5), (3.4) and (3.3) that 'samples' (instantaneous values) of the modulating wave which occur at the instants of the natural intersection of the modulating wave and carrier wave coincide with the switching instants of the p.w.m waveform. This process constitutes 'natural sampling', which is a well known concept in communication theory and practice. Therefore, the sampling

process in all existing p.w.m power convertors can be identified as 'natural sampling'. It is also of particular interest to note: that in Figures (3.5), (3.4) and (3.3) the sampling instants (points of intersection) do not occur at regular intervals. It will be shown later that a form of sampling exists in which the sampling instants do occur at regular intervals, and is known as 'regular sampling'. The 'regular sampling' process is also well known in telecommunications practice, <sup>(8)</sup> but its application to p.w.m. power convertors is entirely novel. The application of 'regular sampling' techniques to p.w.m. power convertors and the numerous advantages it has to offer, will be greatly enlarged upon in succeeding chapters of this thesis.

### (3.8) The Generalised Sampling Theorem.

Any sampling process must lie within the limitations of the 'generalised sampling theorem'. Before discussing the basic sampling theorem and one of its generalised versions, it is important that the concept of a 'sample' be clearly defined: "A sample is a measure of the amplitude of a signal, evaluated over a short period of time during which the signal changes by only a negligible amount". <sup>(8)</sup>

The basic sampling theorem stems from the work of Nyquist on telegraph theory and can be stated as follows: "If a signal that is a magnitude-time function is sampled instantaneously at regular intervals and at a rate slightly higher than twice the highest significant signal frequency, the samples contain all of the information of the original signal". <sup>(21)</sup> This statement implies that the signal must be sampled at regular

or uniform instants and therefore, does not apply to the natural sampling process. The basic sampling theory was extended by Counchy, Yen, Yao and Thomas to include uniform and non-uniform sampling and is now known as the generalised sampling theorem.<sup>(8)</sup> This theorem states that: "If a signal is band limited and if the time interval is divided into equal parts forming sub-intervals ( $T_c$ ) such that  $T_c$  is less than half the period ( $T_m$ ) of the highest significant frequency ( $f_m = \frac{1}{T_m}$ ) component of the signal; and if one instantaneous sample is taken from each sub-interval in any manner; then a knowledge of the instantaneous magnitude of each sampled plus a knowledge of the time within each sub-interval at which a sample is taken contains all the information of the original signal".<sup>(21)</sup>

In the case of p.w.m the signal referred to in the generalised sampling theorem would be the modulating wave and the sample taken in the sampling interval,  $T_c$ , would modulate the pulse occurring in the same sampling interval. Although the generalised sampling theorem has been applied extensively to communication systems it does not appear to have been applied to p.w.m. power convertors. This point is of particular interest since the limitations of the sampling theorem, which will be discussed fully in the next Section, are of more relevance to p.w.m. power convertors than communication systems. This is because the ratio of carrier frequency to modulating frequency is generally much lower in power convertor techniques than in communication techniques.

(3.8.1) Limitations of the Generalised Sampling Theorem When Applied to the Natural Sampled P.W.M. Process

It is essential to the natural sampling process in p.w.m. power convertors that only one intersection between the carrier wave and modulating wave occurs during the sampling period,  $T_c$ , referred to in the generalised sampling theorem and illustrated in Fig.(3.6). Otherwise the frequency of the pulses in the modulated wave will be greater than the carrier frequency. Such a condition would pose considerable practical problems to the design of the power convertor, because the upper limit of frequency operation of the power convertor (so far as the commutating circuit is concerned) is nearly always chosen according to the lowest value of frequency ratio and the highest value of wanted output frequency. For the single-edge p.w.m. process illustrated in Fig.(3.6) the condition for one intersection between the carrier wave and modulating wave in one sampling period,  $T_c$ , is that the slope of the carrier wave must be greater than the maximum slope of the modulating wave, which means:

$$\frac{V}{2} \omega_m < \frac{\omega_c}{2\pi} \quad \text{or} \quad \frac{\omega_m}{\omega_c} < \frac{1}{\pi V} \quad \text{----(3.2)}$$

Now the condition imposed by the sampling theorem is given by:

$$\frac{1}{2 \cdot T_m} < \frac{1}{T_c} \quad \text{or} \quad \omega_m < 2\omega_c \quad \text{----(3.3)}$$

Therefore, the question arises as to how must  $\frac{1}{2T_m}$  must be less than  $\frac{1}{T_c}$ , for it can be seen from equation (3.2) that when the modulation index is unity (that is to say:

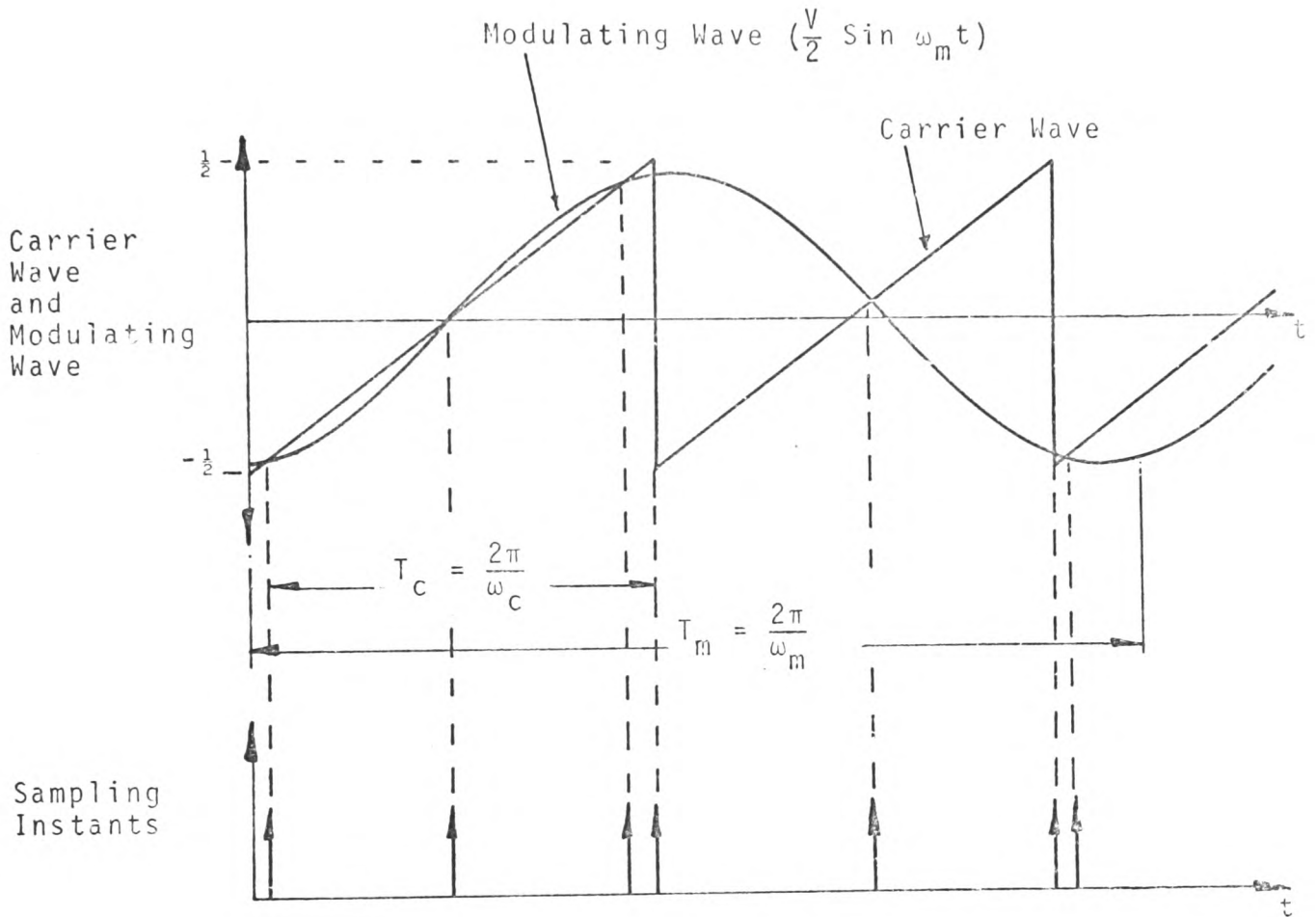


FIG.(3.6) LIMITATION OF THE GENERALISED SAMPLING THEOREM APPLIED TO THE NATURAL SAMPLED SINGLE-EDGE P.W.M. PROCESS.

( $\frac{\text{Peak-value of carrier wave}}{\text{Peak-value of modulating wave}} = 1$ ) the required sampling rate rises to  $\pi$  per cycle of the modulating wave which is greater than the Nyquist rate of 2. It may also be seen from equation (3.2) that for values of  $V < \frac{2}{\pi}$ , a sampling rate lower than the Nyquist rate is implied. Therefore, for the single-edge natural sampled p.w.m process it can be concluded that the required sampling rate is dependent upon the modulation index, and the sampling theorem only applies for the condition  $V = \frac{2}{\pi}$ .

With the aid of Fig.(3.7) it can similarly be proved that for natural sampled double-edge p.w.m.the condition for one intersection between the carrier wave and modulating wave per sampling period,  $T_s$ , is:

$$\frac{\omega_m}{\omega_c} < \frac{2}{\pi V} \quad \text{or} \quad \frac{\omega_m}{\omega_s} < \frac{4}{\pi V} \quad \text{-----(3.4)}$$

where  $\omega_s = 2\omega_c$

Therefore, for a modulation index of unity the sampling rate must be greater than  $\frac{\pi}{4}$  per cycle of the modulating wave. In fact for all values of  $V$  less than  $\frac{8}{\pi}$ , a lower sampling rate than the Nyquist rate is implied.

From the above discussion it can be concluded that the double-edge natural sampled p.w.m.process requires a lower sampling rate than the single-edge natural sampled p.w.m. method for all values of modulation index. This allows the double-edge p.w.m.process to operate at lower frequency ratio's than the single-edge system without contravening the condition for intersection of the modulating wave and carrier wave. It is appropriate at this point to note that the limitations of



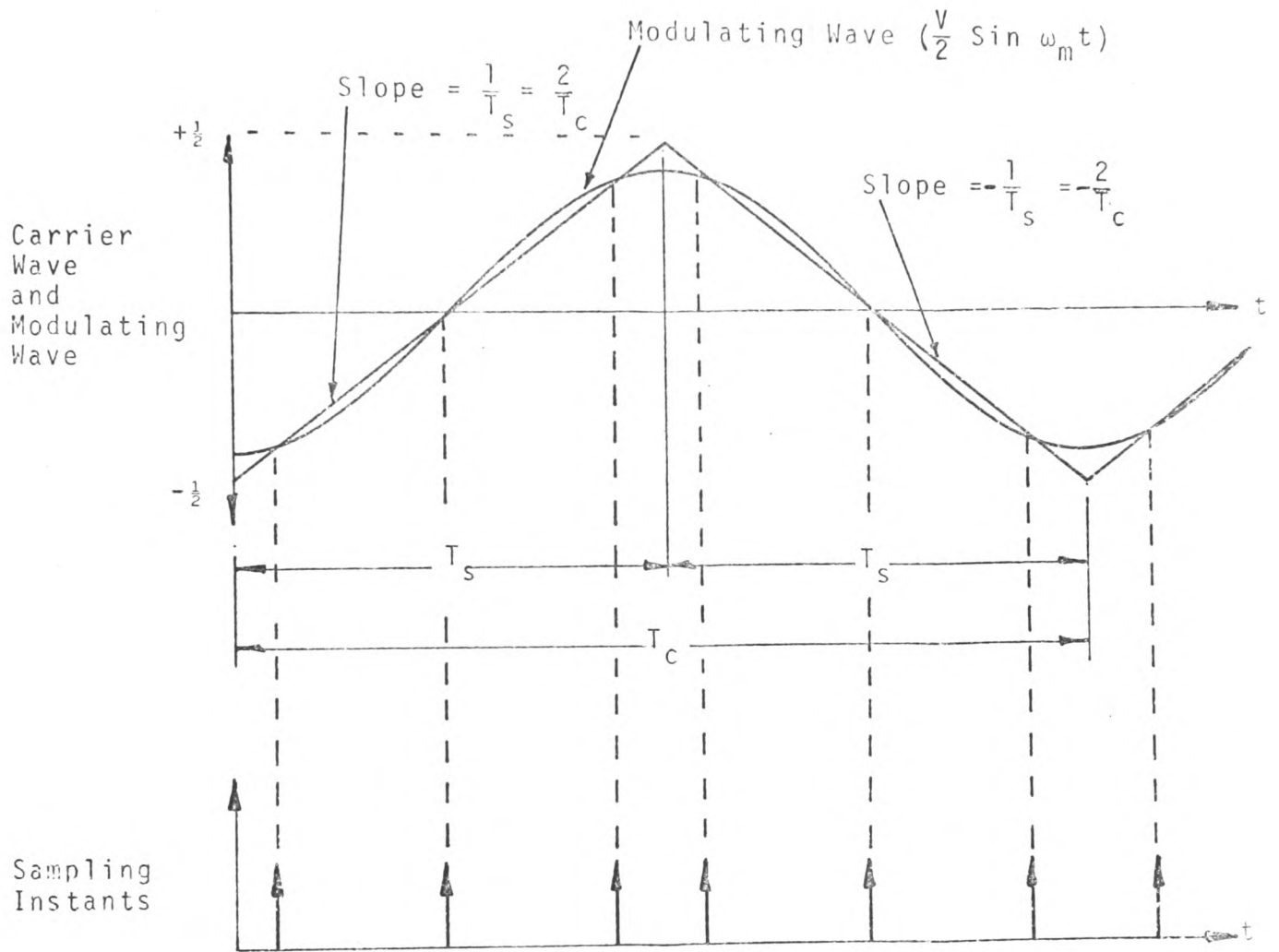


FIG.(3.7) LIMITATION OF THE GENERALISED SAMPLING THEOREM APPLIED TO THE NATURAL SAMPLED DOUBLE-EDGE P.W.M. PROCESS

the sampling theorem and the conditions for intersection of the two waveforms have not been applied to existing p.w.m. power convertors, nor referred to in the literature available on such convertors.

### (3.9) Regular Sampling.

This particular type of sampling has been widely used in communication systems but has not previously been applied to p.w.m. power convertors. The reasons for its wide acceptance in communications are not clearly defined, the literature available suggest that its acceptance might have been influenced by two factors: (i) it satisfies the basic sampling theorem and (ii) it is argued that it provides an improved signal to noise ratio when compared with natural sampling. Therefore, it was thought that the application of regular sampling techniques to p.w.m. power convertors might provide a means of improving the harmonic spectra. The application of the regular sampling process to the generation of p.w.m. waveforms, basically entails the sampling of the modulating wave prior to comparison with the carrier wave (Fig.(3.8)). Samples of the modulating wave are taken at regular intervals by means of the sampling switch, and are then held constant over the sampling period by storing the samples on a capacitor. This converts the modulating wave to its regular sampled version which is then compared with the carrier wave to produce the switching instants of the width modulated pulses. It may be seen from Fig.(3.8a) that the generation of the regular sampled modulating wave is achieved at a cost of only four extra components. This point is of

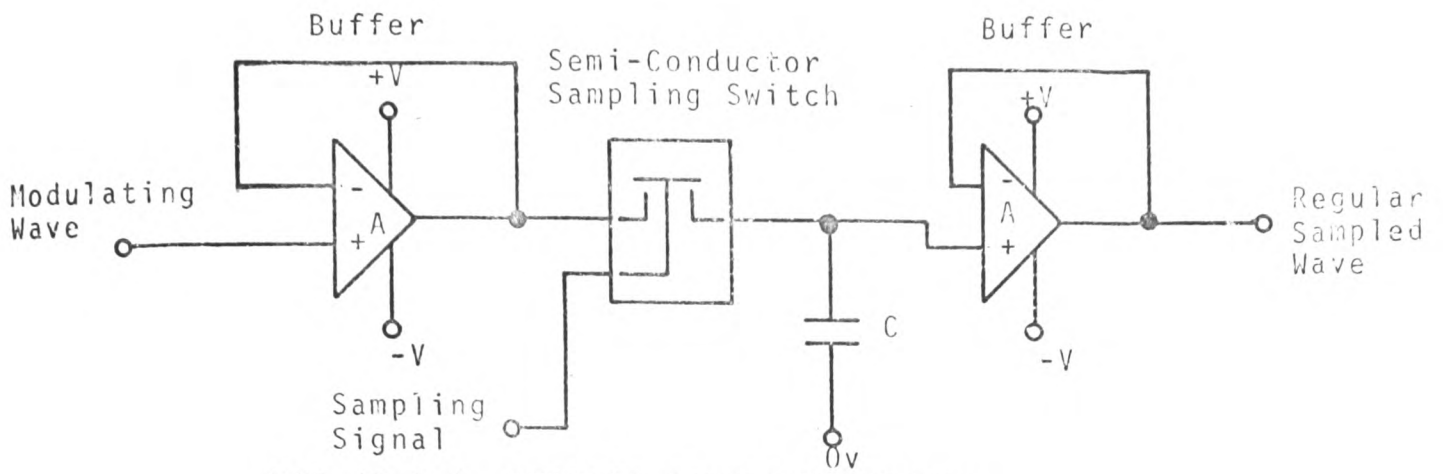


FIG.(3.8a) REGULAR SAMPLING CIRCUIT

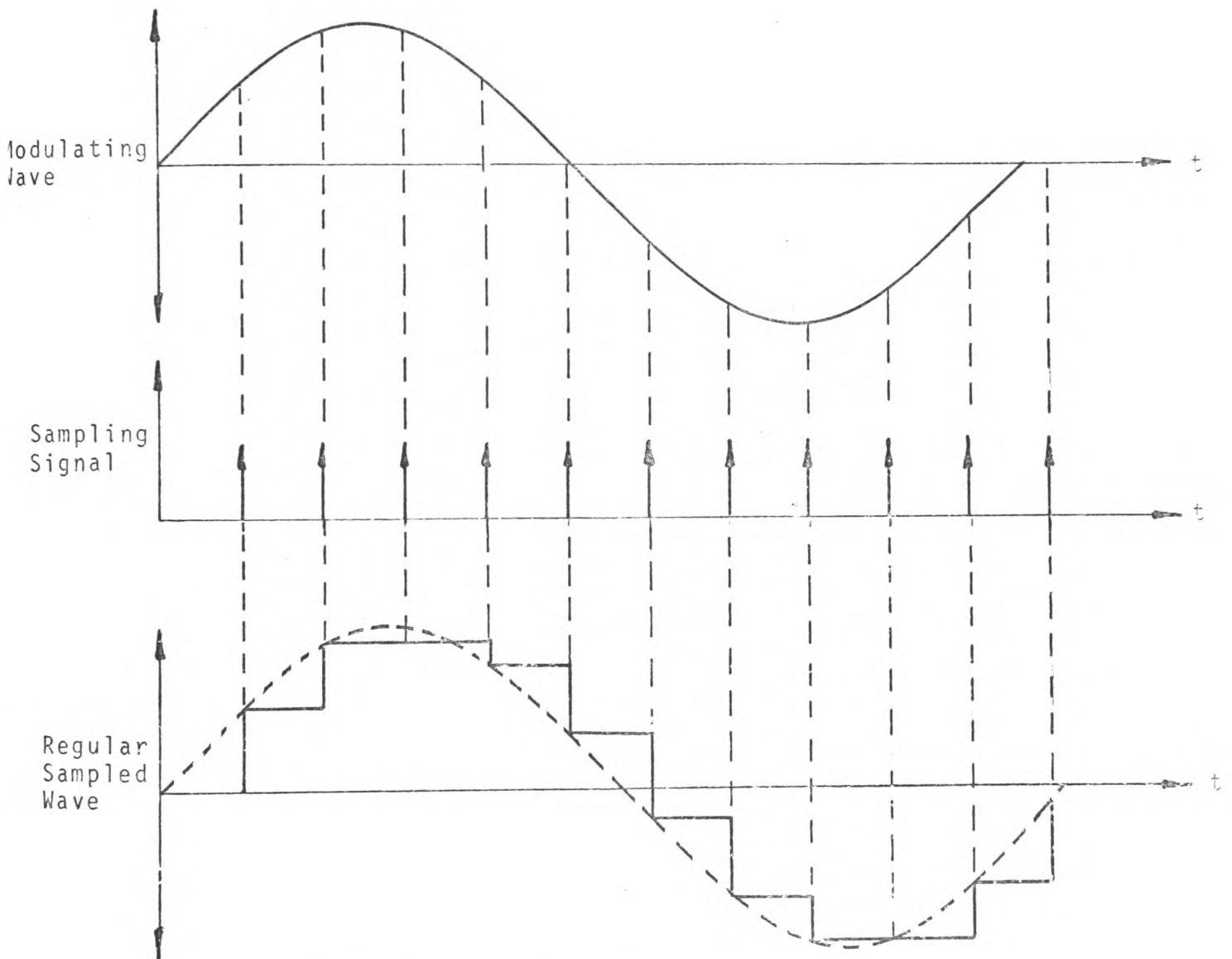


FIG.(3.8b) WAVEFORMS

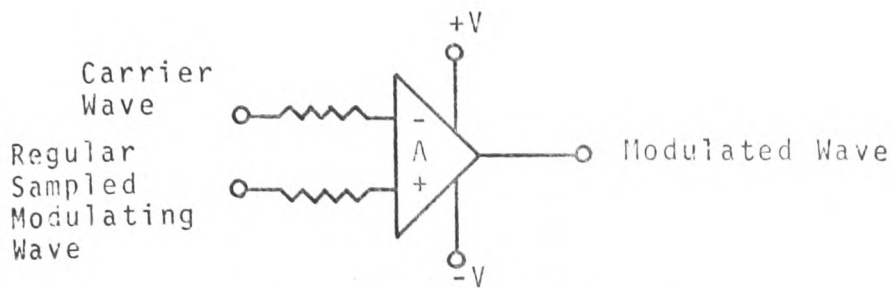
FIG(3.8) GENERATION OF REGULAR SAMPLED MODULATING WAVE

considerable significance since the capital cost of the p.w.m. convertor must be kept to a minimum if it is to compete with prior-art systems.

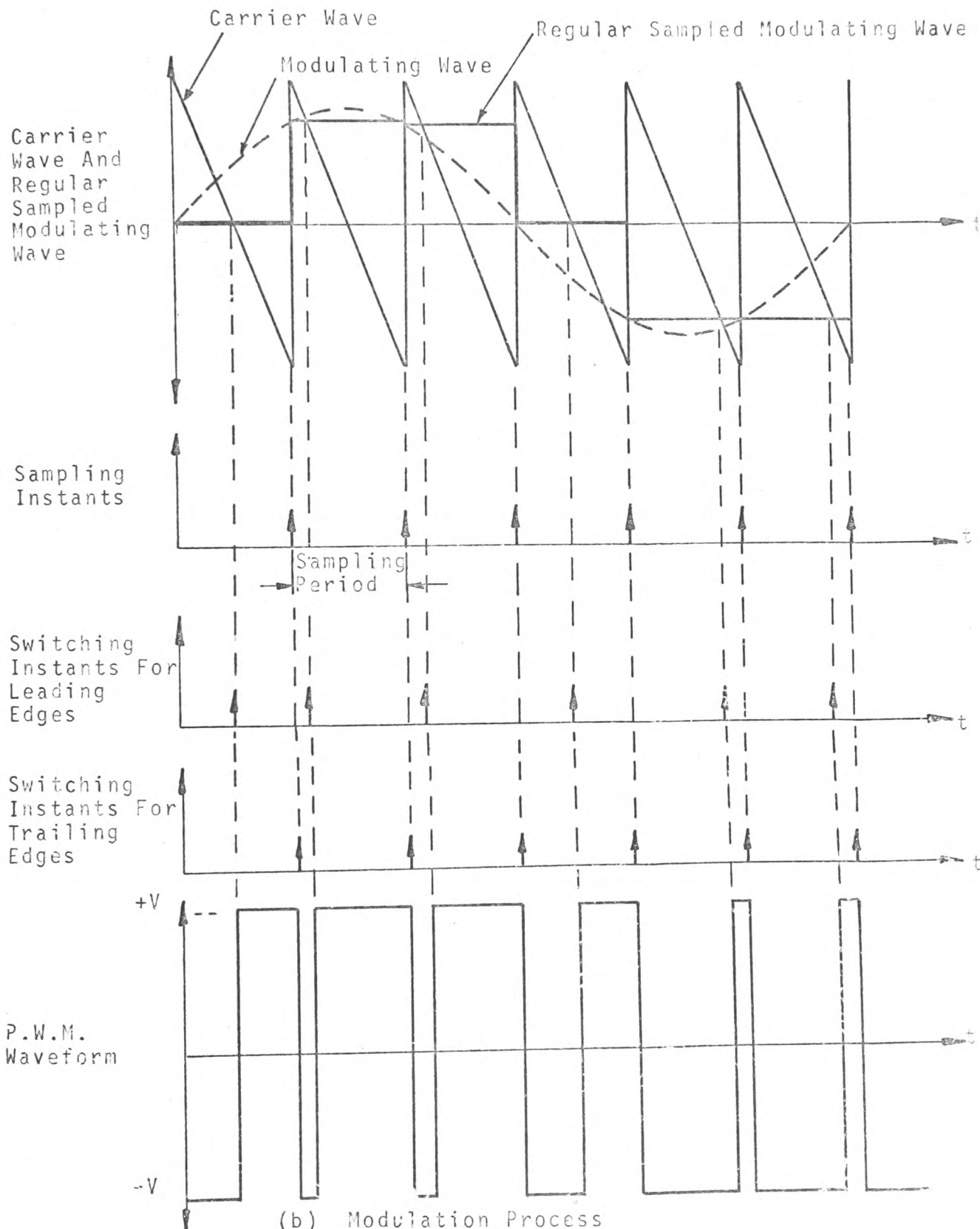
It was therefore felt to be appropriate at this point to demonstrate the various methods by which p.w.m. could be achieved by means of the regular sampling process, and to consider the limitations of this process at low values of frequency ratio.

#### (3.9.1) Regular Sampled Leading-Edge P.W.M.

The analogue method of generating leading-edge p.w.m. waveforms is illustrated graphically in Fig.(3.9). The sinusoidal modulating wave is sampled at regular intervals corresponding with the vertical sides of each cycle of the triangular carrier wave. It may also be seen that the trailing-edges of the pulses occur at these same regular instants. The samples of the modulating wave are held constant over their respective sampling periods, the sampling period in each case being constant. The switching instants for the leading-edges of the modulated pulses, are defined by the points of intersection between the carrier wave and regular sampled modulating wave. It is of particular interest to notice that the respective sampling instants and switching instants for the leading-edges of the pulses are displaced in time-phase. In fact the switching instants lag the corresponding sampling instants. When the leading-edge regular sampled p.w.m. waveform illustrated in Fig.(3.9) is compared with the leading-edge, natural sampled p.w.m. waveform illustrated in Fig.(3.3) it is immediately apparent



(a) Comparator Circuit



(b) Modulation Process

FIG.(3.9) REGULAR SAMPLED LEADING-EDGE P.W.M.

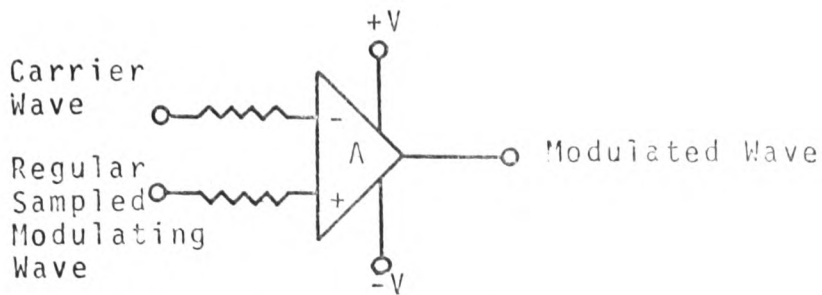
that the waveforms are different. Therefore, the harmonic spectra for the two waveforms must also be different. It will be shown in Chapters (4) and (5) that the harmonic spectra for the regular sampled wave is greatly superior to that for the natural sampled wave so far as induction motor drives operating at low frequency ratio's are concerned.

### (3.9.2) Regular Sampled Trailing-Edge P.W.M

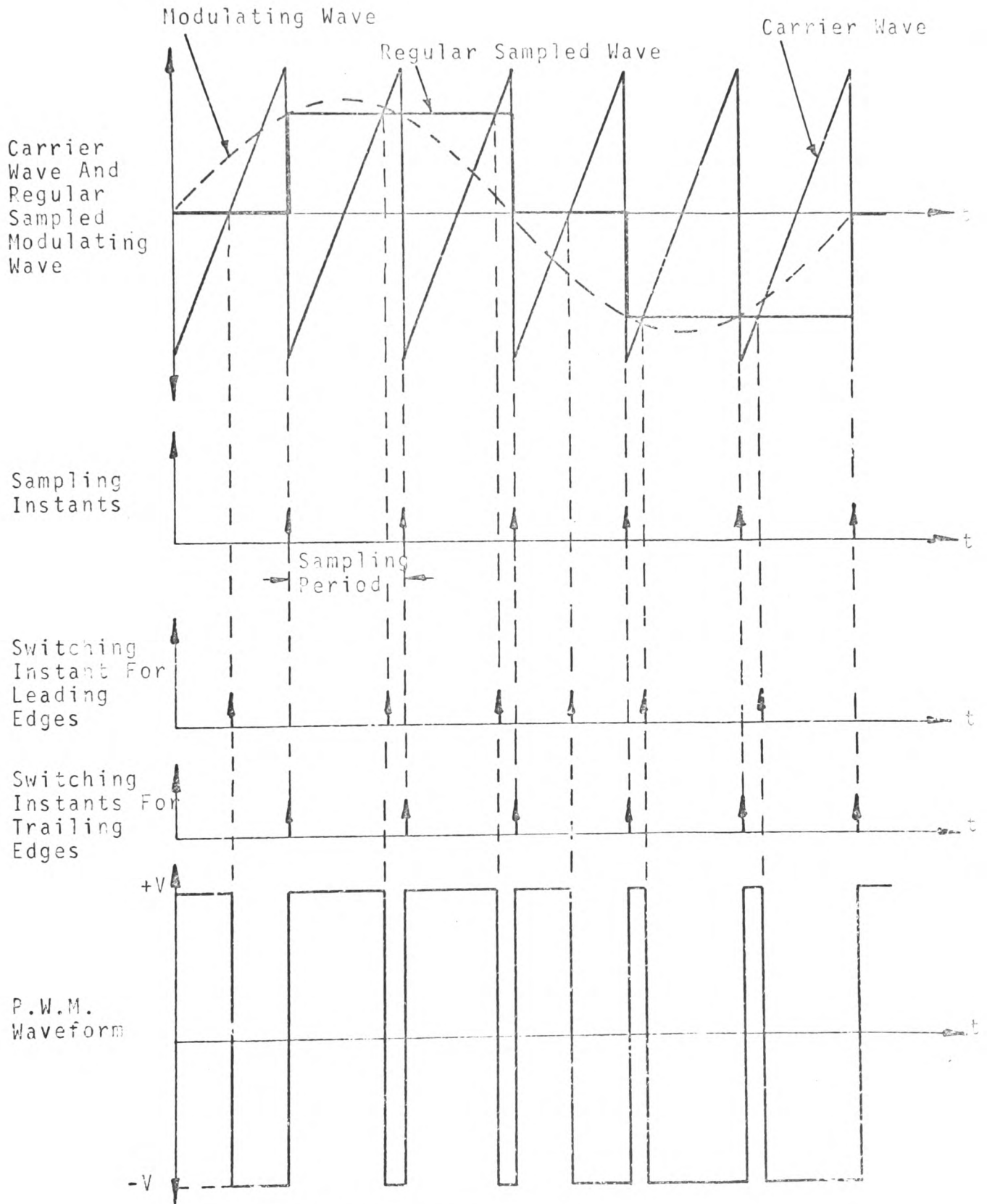
It can be seen from Fig.(3.10) that the respective sampling instants and switching instants for the trailing-edges of the pulses are again displaced in time phase, whereas, for all the natural sampled p.w.m processes they were coincident. The leading-edges of the width modulated pulses occur at uniform intervals fixed by the carrier wave frequency. By comparing the p.w.m. waveform illustrated in Fig.(3.10) with the natural sampled waveform illustrated in Fig.(3.4) it can again be seen that the waveforms are different. The degree of superiority of the regular sampled system over the natural sampled system will be fully described in Chapters (4) and (5).

### (3.9.3) Regular Sampled Symmetrical-Double-Edge Modulation

With this form of modulation both edges of the width modulated pulses are modulated by the same amount about their mean-positions. In Fig.(3.11) the mean-positions of the pulses coincide with the negative peaks of the triangular carrier wave. It may also be seen that for this method of modulation, the modulating wave is sampled once per cycle of the carrier wave at instants corresponding to the positive



(a) Comparator Circuit



(b) Modulation Process

FIG.(3.10) REGULAR SAMPLED TRAILING-EDGE MODULATION

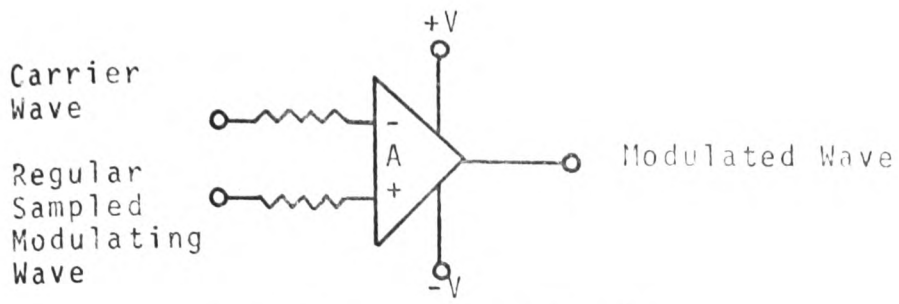
apices of the isocetes-triangular carrier wave, each sample again being held constant over its respective sampling period. The intersections between each sample and the positive and negative slopes of respective cycles of the carrier wave provide the switching instants for both edges of the width-modulated-pulses. By comparing the p.w.m. waveform illustrated in Fig.(3.11) with the natural sampled double-edge waveform illustrated in Fig.(3.5), it can again be seen that the waveforms are different. It will be shown in Chapter (5) that this particular type of modulation is very superior in reducing the amplitude of unwanted low frequency harmonic components when the ratio of carrier frequency to modulating frequency is also low. It will similarly be shown that this type of modulation increases the amplitude of unwanted high frequency harmonic components and may also introduce unbalance problems. This will be discussed at length in Chapters (4) and (5).

It is important to note at this point that should the symmetry of the carrier wave be changed such that its waveform ceases to be an isocetes triangle, the sampling process still remains regular, although the modulation becomes asymmetrical. Therefore, varying the symmetry of the carrier wave, provides an extra degree of control over the pulse-width-modulation process, and yet maintains the regular sampling.

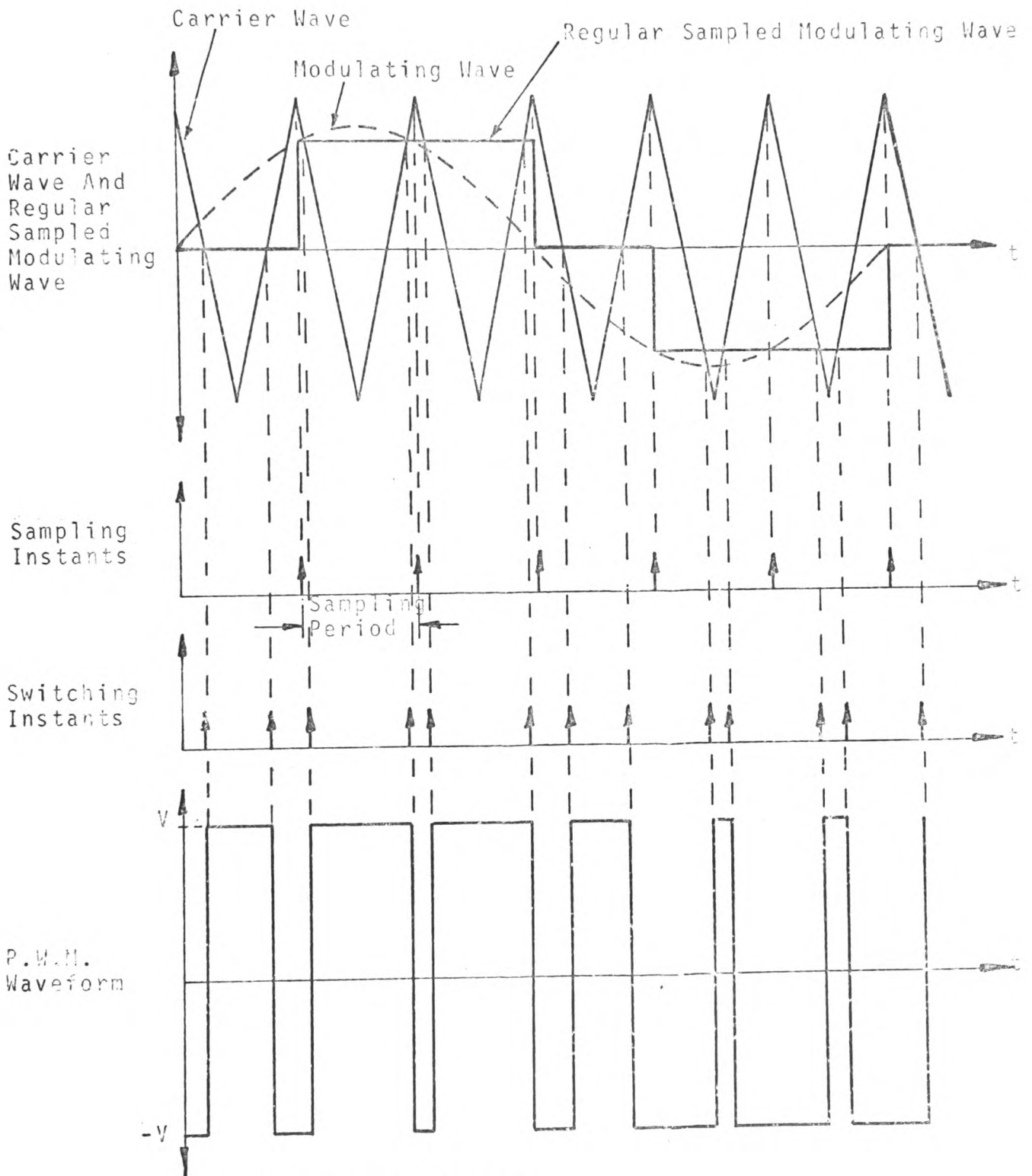
#### (3.9.4) Regular Sampled Asymmetrical-Double-Edge Modulation

Although there are numerous forms of asymmetrical double-edge modulation, many of which have been described in Sections (3.9.3) and (3.6) of this thesis, the form referred to





(a) Comparator Circuit



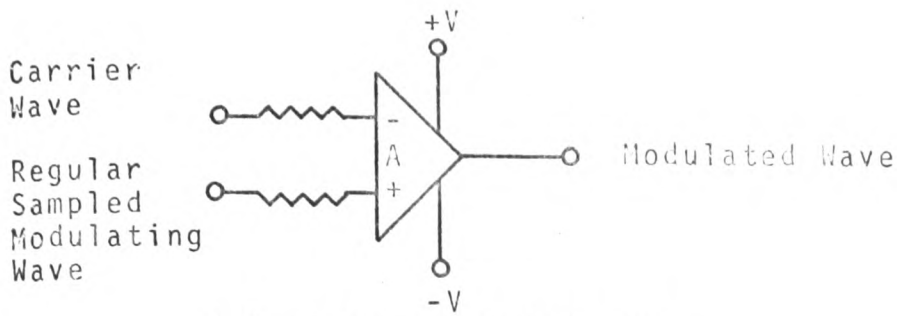
(b) Modulation Process

FIG.(3.11) REGULAR SAMPLING SYMMETRICAL DOUBLE-EDGE P.W.M.

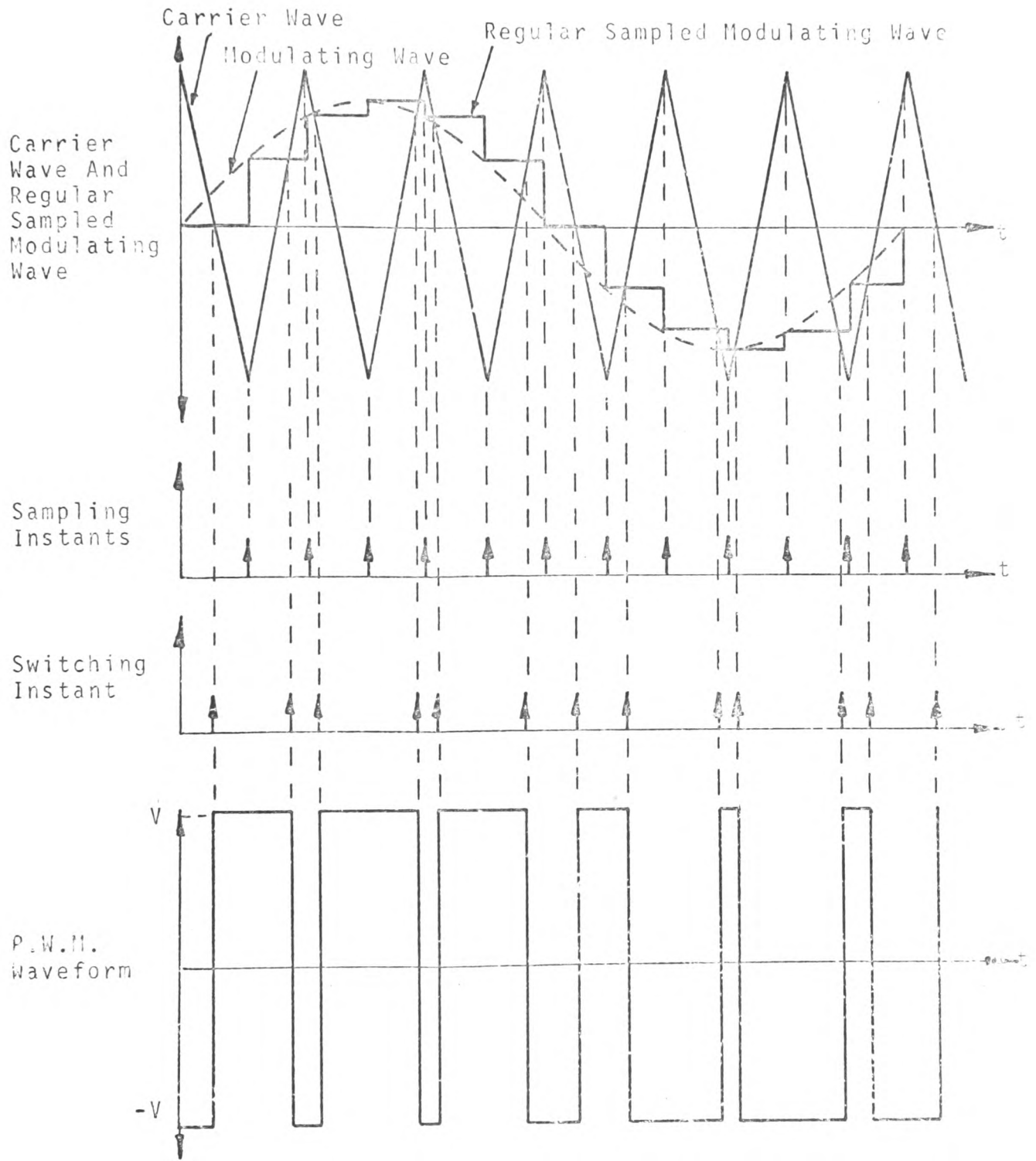
throughout this thesis as 'asymmetrical' is dependent upon regular sampling at twice the carrier frequency and the comparison of the regular sampled modulating wave with an isosceles triangular carrier wave. This type of pulse-width-modulation is illustrated in Fig.(3.12), and it is immediately apparent that both edges of the width-modulated-pulses are modulated by different amount. The amount of modulation of both edges of each pulse is dependent upon the magnitude of the respective adjacent samples taken at regular intervals corresponding to the positive and negative apices of the isosceles-triangular carrier wave. It may also be seen that a time-phase displacement again exists between the sampling instants and switching instants. When the p.w.m waveform illustrated in Fig.(3.12) is compared with the double-edge modulated waveforms illustrated in Figures (3.11) and (3.5) it is apparent that the waveforms are again different. It will be shown in Chapters (4) and (5) of this thesis that this regular sampled asymmetrical-double-edge p.w.m.process which is entirely novel, is far superior to existing p.w.m. processes in power convertors.

#### (3.9.5) Limitations of the Regular Sampling Process in P.W.M. Systems

It is essential to the analogue method of generating pulse-width-modulated waveforms, that only one pulse per cycle of the carrier wave occurs (for the reasons described in Section (3.8.1.) of this thesis). For this condition to be satisfied two requirements must be met: (i) each slope of the carrier wave must not be intersected by more than one held sample



(a) Comparator Circuit



(b) Modulation Process

FIG.(3.12) REGULAR SAMPLING ASYMMETRICAL DOUBLE EDGE MODULATION

of the modulating wave and (ii) the modulating wave must be sampled at a rate greater than twice the frequency of the modulating wave when the wave is a sinusoid. Therefore, when the modulating wave is sampled at the carrier frequency or at a multiple of the carrier frequency the above requirements impose limitations on the minimum value of the ratio of carrier frequency to modulating frequency. It may be seen from Figures (3.9), (3.10) and (3.11) that for regular sampled single-edge modulation and symmetrical-double-edge modulation, the minimum value of frequency ratio must be greater than 'two' ( $\frac{f_c}{f_m} > 2$ ), whereas for asymmetrical-double-edge modulation, the minimum value of frequency ratio must be greater than 'one' ( $\frac{f_c}{f_m} > 1$ ). Therefore, on account of the requirements of the regular sampled p.w.m. process alone, it is apparent that the asymmetrical -double-edge system is superior when the main objective is to operate with a frequency ratio as low as possible. It will also be shown later that the asymmetrical-double-edge system provides a means of cancelling significant unwanted harmonic and d.c. components in the spectra of the output modulated waveforms.

### (3.10) Interim Conclusions

The realisation of p.w.m. waveforms by analogue means has been presented. The concept of sampling has been introduced and the sampling process in all prior-art p.w.m. power convertors has been identified as 'natural sampling' which is a well known process in communications practice. The generalised sampling theorem was discussed and its limitations when applied to the natural sampled p.w.m process were exposed.

It was shown that the voltage-time-integral of the output modulated voltage from the power modulator could be controlled by varying the modulation index (or amplitude of the modulating wave in the control circuit), which is an essential requirement for infinitely variable induction motor speed control systems. 'Regular sampling' was introduced and it was shown that regular sampled p.w.m. can be achieved at an added cost of only four components. It was also shown that the regular sampled, asymmetrical-double-edge system allows the ratio of carrier frequency to modulating frequency to approach unity, whereas, for the regular sampled single-edge and symmetrical-double-edge systems the frequency ratio can only theoretically approach 'two'.

The use of the regular sampling process for reducing and eliminating significant unwanted harmonic components will be enlarged upon in the succeeding two chapters of this thesis.

(4) IMPROVEMENTS IN THE P.W.M. POWER CONVERTOR WHEN OPERATING IN THE SYNCHRONISED MODE.

(4.1) Introduction

Although p.w.m. can be achieved by numerous methods, seven of which have been described in Chapter (3) of this thesis, there are only two possible modes of operation so far as the comparison of the carrier wave with the modulating wave is concerned. The carrier wave and modulating wave are either 'synchronous' or 'asynchronous'. Synchronous operation allows the ratio of carrier frequency to modulating frequency to take integer values only, whereas, asynchronous operation allows the frequency ratio to be infinitely variable. The choice of mode has a significant bearing on the frequency spectrum of the output p.w.m. waveform. This chapter will deal with the synchronous-mode only, whereas, Chapter (5) will be entirely devoted to the asynchronous-mode of operation.

(4.2) Prior-art P.W.M Systems

Almost all prior-art p.w.m. power inverter systems have operated on integer ratio's only.<sup>(21)</sup> Since integer ratio operation can only be achieved by synchronising the carrier wave with the modulating wave or by synchronising the 'chops' or 'pulses' in the p.w.m. output waveform with some reference wave,<sup>(22)</sup> such systems fall into the synchronised-mode of operation.

It was shown in Chapter (3), Section (3.7), that the sampling process in existing analogue p.w.m. control schemes is natural sampling. It is said in the literature<sup>(21)</sup> that such systems of control have many disadvantages:

(i) Considerable harmonic distortion occurs in the output p.w.m.voltage waveform when the ratio of carrier frequency to modulating frequency is low.

(ii) Amplitude and phase unbalance of the fundamental components of the output p.w.m.waveforms in a three-phase system can occur.

(iii) D.C. components can exist in the harmonic spectra of the output p.w.m.voltage waveform.

It was therefore decided to investigate the operation of the three natural sampled prior-art control schemes presented in Sections: (3.4), (3.5) and (3.6) of Chapter (3), with the aim of establishing relationships between the above disadvantages and the ratio of carrier frequency to modulating frequency.

#### (4.2.1) Analytical Investigation Into Natural Sampled P.W.M Systems

The three natural sampled systems described in Chapter (3) were numerically synthesised by means of a digital computer. The details of the computer programs developed for this purpose, are described in Appendix(1 ) of this thesis. The reason for the choice of numerical synthesis rather than time-domain analysis is basically because the production of time-functions which describe harmonic spectra for p.w.m.waveforms, becomes very tedious and time consuming. However, it may be of interest to note that time-functions can be produced for all of the p.w.m.process described in Chapter (3) by means of a Double-Fourier-Series technique.<sup>(8)</sup>

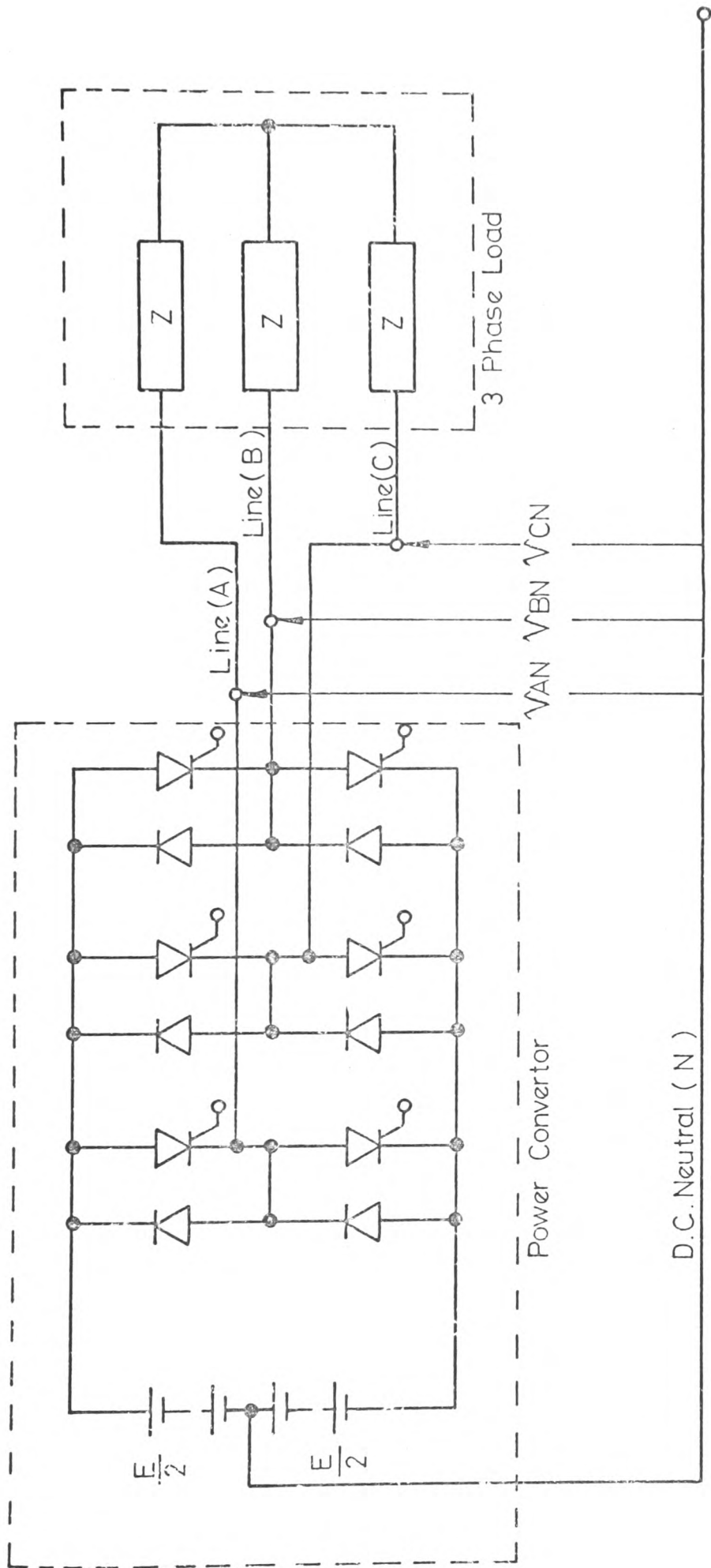
It is important to note at this point that the three natural

sampled p.w.m. waveforms described in Chapter (3) are for single-phase operation only. Three phase operation is achieved by comparing three sinusoidal modulating waves of equal amplitude but displaced in time-phase by  $120^\circ$  and  $-120^\circ$  respectively, with a single-phase carrier wave, where the carrier wave and modulating waves are synchronised in time-phase. The reason for comparing the three-phase modulating waves with a single-phase carrier wave rather than with three-phase carrier waves is that harmonic components of carrier frequency and multiples of the carrier frequency are said to cancel in three-phase, three-wire systems.<sup>(21)</sup> This will become more apparent in the succeeding sections of this chapter.

#### (4.2.1.1) Details of Computed Harmonic Spectra

The switching instants of the natural sampled p.w.m. control waveforms coincide with the instantaneous points of intersection between the carrier wave and respective modulating waves as described in Chapter (3). The switching instants of the three-phase p.w.m. control waveforms resulting from the natural sampled trailing-edge, leading-edge and double-edge p.w.m. processes are also representative of the output voltage waveforms between each LINE and D.C. NEUTRAL of the power convertor shown in Fig.(4.1) when the power convertor is controlled by each of the three p.w.m. control schemes. The method by which a p.w.m. control signal is made to drive the power convertor will be fully described in Chapter (6), however, at this point in the analysis it was thought sufficient to state: that the p.w.m. output waveforms from the power convertor





$V_{AN}$  :- Line (A) to D.C. Neutral Voltage Waveform.  
 $V_{BN}$  :- Line (B) " " " "  
 $V_{CN}$  :- Line (C) " " " "

FIG.(4.1) 3-PHASE MODULATOR (EXCLUDING AUXILIARY COMMUTATING COMPONENTS)

are identical to the respective p.w.m. control signals so far as the switching instants are concerned. Therefore, the computed harmonic spectra are directly related to the output voltage waveforms of the convertor shown in Fig.(4.1).

The LINE (A) to D.C. NEUTRAL voltage illustrated in Fig. (4.1) is taken as the reference so far as the computation of harmonic spectra for each LINE((A),(B) and (C)), to D.C.NEUTRAL voltage is concerned. This means that every harmonic component for each of the above mentioned waveforms, is divided by the wanted component of the LINE (A) to D.C. NEUTRAL voltage waveform and expressed as a percentage. Similarly the LINE (A) to LINE (B) voltage waveform is also taken as reference for the harmonic spectra of the three LINE to LINE voltage waveforms. This means the harmonic components for each LINE to LINE voltage waveform is divided by the wanted component of the LINE (A) to LINE (B) voltage waveform and expressed as a percentage. This procedure allows an immediate check to be made on the degree of amplitude unbalance between any three respective components of the three modulated waveforms concerned.

The phase of every harmonic component is expressed as an angle between 0 and  $+\pi$  or 0 and  $-\pi$ . This allows a check on the phase unbalance between respective harmonics to be made, and also provides a facility for determining the phase-sequence of any three harmonics of the same order for any three respective voltage waveforms.

#### (4.2.1.2) Leading-Edge\_P.W.M.

It may be seen from the computed results presented in Fig. (4.2) that d.c. components of different magnitude exist in the

Harmonic Order	Line To D.C. Neutral Components			Line to Line Components			Frequency Ratio $\frac{f_c}{f_m}$	Mod. Index.
	$V_{AB}(\%)$	$V_{BN}(\%)$	$V_{CN}(\%)$	$V_{AB}(\%)$	$V_{BC}(\%)$	$V_{CA}(\%)$		
D.C.	0.0	- 36	0.0	21	- 21	0.0		
1	100/0°	137/-90°	137/150°	100/54°	140/-60°	135/-163°		
2	137/0°	118/90°	118/-150°	107/-41°	121/60°	146/-163°		
3	182/-180°	144/161°	144/162°	38/-135°	0.0	38/45°	3.0	1.0
4	0.0	59/90°	59/-30°	35/- 90°	61/120°	35/-30°		
5	75/-180°	27/-90°	27/30°	47/160°	28/-120°	59/8°		
6	91/-180°	137/-180°	137/-180°	27/0°	0.0	27/-180°		
7	53/-180°	20/90°	20/-30°	34/-160°	20/120°	42/-8°		
8	0.0	30/-90°	20/30°	18/90°	30/-120°	18/30°		
9	61/-180°	48/-161°	48/-162°	13/135°	0.0	13/-45°		

FIG(4.2) AMPLITUDE AND PHASE OF HARMONIC COMPONENTS OF LINE TO D.C. NEUTRAL VOLTAGE WAVEFORMS AND LINE TO LINE VOLTAGE WAVEFORMS FOR NATURAL SAMPLED, LEADING-EDGE P.W.M.

the LINE to D.C. NEUTRAL voltage waveforms. This leads to the existence of d.c. components in the LINE to LINE voltage waveforms. It may also be seen from Fig.(4.2) and Fig.(4.3) that any three harmonics of the same order in both the LINE to D.C. NEUTRAL voltage waveforms and LINE to LINE voltage waveforms do not form balanced sequence sets. Further computed results illustrated that the reason for the existence of d.c components in the LINE to LINE voltage, and amplitude and phase unbalance between any three harmonic components of the same order, in both the LINE to D.C. NEUTRAL voltages and LINE to LINE voltages, for a frequency ratio of 'three' and modulation index of 'unity'; was entirely due to the natural sampling process lying outside the limitations presented in Section (3.8.1) of Chapter (3). It was shown in Section (3.8.1) of Chapter (3) that for leading-edge p.w.m. and a modulation index of 'unity'  $\left[ \frac{\text{Peak value of Carrier Wave}}{\text{Peak value of Modulating Wave}} = 1 \right]$  the minimum value of frequency ratio was,  $\frac{f_c}{f_m} = \pi$ . However, when the modulation index was reduced to 0.5 and the frequency ratio,  $\frac{f_c}{f_m}$ , held constant at 'three' such that the sampling process lay within the limitation presented in Chapter (3), it became evident from the computed results that the d.c. components and amplitude and phase unbalance of harmonics of the same order were completely eradicated. It was also found that the triplen harmonics in the LINE to D.C. NEUTRAL voltages formed balanced zero-sequence sets, which resulted in complete cancellation of these harmonics in the LINE to LINE voltage waveforms.

From the computed results illustrated in Figures: (4.2) and (4.3) and further computed results the following relationships

Voltage Waveforms	Sampling Process	Phase Sequence	Harmonic Order											
			1	2	3	4	5	6	7	8	9			
Line to D.C. Neutral	Natural	Reference	Xu											
		Reverse		Xu	Xu		Xu							Xu
		In Phase								Xu				
Line to Line	Natural	Reference	Xu				Xu							
		Reverse		Xu					Xu				Xu	
		In Phase												

$X_B$  - Balanced Sequence Components

$X_u$  - Unbalanced Sequence Components

FIG. (4.3) PHASE-SEQUENCE CHART FOR RESPECTIVE HARMONICS OF LINE TO D.C. NEUTRAL VOLTAGE WAVEFORM AND LINE TO LINE VOLTAGE WAVEFORM.

became apparent for leading-edge p.w.m., provided the natural sampling process lay within the limitation described in Section (3.8.1) of Chapter (3):

(1) For all values of integer frequency ratio given by:

$$\frac{f_c}{f_m} = n,$$

even order and odd order harmonics are present in both the LINE to D.C. NEUTRAL voltage waveforms and in the LINE to LINE voltage waveforms.

(2) For all triple-integer values of frequency ratio given by:

$$\frac{f_c}{f_m} = 3n,$$

harmonics of order,  $3n$ , which are present in the LINE to D.C. NEUTRAL voltage waveforms, form balanced zero-sequence sets. This means that such harmonics completely cancel in the LINE to LINE voltage waveforms. D.C. voltage components are also eliminated from the LINE to D.C. NEUTRAL voltage waveforms which means that such components of voltage are also eliminated from the LINE to LINE voltage waveforms. It was also found that for these values of frequency ratio, respective harmonics of orders:

$$(3n - 2),$$

form balanced positive-sequence sets, whereas, respective harmonics of order:

$$(3n - 1),$$

form balanced negative-sequence sets.

(4) For odd and even non-triple-integer values of frequency ratio given by:

$$\frac{f_c}{f_m} = 3n + \frac{1}{2} [3 - (-1)^n]$$

and

$$\frac{f_c}{f_m} = 3n - \frac{1}{2} [3 + (-1)^n]$$

respectively, respective harmonics of order, n, in the LINE to D.C. NEUTRAL voltage waveform, did not form balanced sequence sets. It was also found that a relationship between phase-sequence and harmonic order for any three respective harmonics did not exist. D.C. components of voltage were also found to occur in the LINE to LINE voltage waveforms.

#### (4.2.1.3) Trailing-Edge P.W.M.

From the computed results for this particular modulation process, it was found that the amplitudes of harmonic components and d.c. components were the same as for the leading-edge p.w.m. process, for all values of frequency ratio. Harmonic order and phase-sequence were also found to be the same as for the leading-edge p.w.m. process.

#### (4.2.1.4) Double-Edge P.W.M.

From the computed results illustrated in Figures (4.4) and (4.5) and from further computed results the following relationships became apparent:

(1) For odd values of triple-integer frequency ratio given by:

$$\frac{f_c}{f_m} = 3(2n - 1),$$

d.c. components did not exist in the LINE to D.C. NEUTRAL voltage waveform nor in the LINE to LINE voltage waveforms. Harmonic components of order, 2n, were eliminated from the LINE to D.C. NEUTRAL voltage waveform and therefore, from the

Harmonic Order	Line To D.C. Neutral Components				Line to Line Components				Frequency Ratio $\frac{f_c}{f_m}$	Mod. Index.
	V <sub>/AN</sub>	V <sub>/BN</sub>	V <sub>/CN</sub>	V <sub>/AB</sub>	V <sub>/BC</sub>	V <sub>/CA</sub>				
D.C.	0.0	0.0	0.0	0.0	0.0	0.0	0.0			
1	100 / -180°	100 / -138°	100 / 102°	100 / 12°	100 / -108°	100 / 132°				
2	0.0	0.0	0.0	0.0	0.0	0.0				
3	54 / -70°	54 / -70°	54 / -70°	0.0	0.0	0.0		3	1.0	
4	0.0	0.0	0.0	0.0	0.0	0.0				
5	20 / -54°	20 / 66°	20 / -174°	20 / -84°	20 / 36°	20 / 156°				
6	0.0	0.0	0.0	0.0	0.0	0.0				
7	25 / -178°	25 / 62°	25 / -58°	25 / -148°	25 / 92°	25 / -28°				
8	0.0	0.0	0.0	0.0	0.0	0.0				
9	23 / -135°	23 / -135°	23 / -135°	0.0	0.0	0.0				

FIG. (4.4) AMPLITUDE AND PHASE OF HARMONIC COMPONENTS OF LINE TO D.C. NEUTRAL VOLTAGE WAVEFORMS AND LINE TO LINE VOLTAGE WAVEFORMS FOR NATURAL SAMPLED DOUBLE-EDGE P.W.M



Voltage Waveforms	Sampling Process	Phase Sequence	Harmonic Order																
			1	2	3	4	5	6	7	8	9								
Line to D.C. Neutral	Natural	Reference	$X_B$																
		Reverse					$X_B$												
		In Phase			$X_B$														
Line to Line	Natural	Reference	$X_B$																
		Reverse								$X_B$									
		In Phase																	

$X_B$  - Balanced Sequence Components

$X_u$  - Unbalanced Sequence Components

FIG. (4.5) PHASE-SEQUENCE CHART FOR RESPECTIVE HARMONICS OF LINE TO D.C. NEUTRAL VOLTAGE WAVEFORM AND LINE TO LINE VOLTAGE WAVEFORM.

LINE to LINE Voltage waveform. Respective harmonic components in the LINE to D.C. NEUTRAL voltage waveform of order,  $3n$ , formed balanced zero-sequence sets, which therefore completely cancelled in the three LINE to LINE voltage waveforms.

Respective harmonic components in the LINE to D.C. NEUTRAL voltage waveforms and in the LINE to LINE voltage waveforms of order,  $(3n - 2)$ , formed balanced positive-sequence sets, whereas; respective harmonics of order,  $(3n - 1)$  formed balanced negative-sequence sets.

(2) For even triple-integer values of frequency ratio given by:

$$\frac{f_c}{f_m} = 3(2n),$$

d.c. components were eliminated from the LINE to D.C. NEUTRAL voltage waveforms and therefore from the LINE to LINE voltage waveforms. Respective harmonic components of order,  $3n$ , in the LINE to D.C. NEUTRAL voltage waveforms again formed balanced zero-sequence sets which resulted in complete cancellation of these components in the three LINE to LINE voltage waveforms. The phase-sequence of respective harmonic components in the LINE to D.C. NEUTRAL voltage waveforms and in the LINE to LINE voltage waveforms were the same as for the odd triple-integer values of frequency ratio, that is to say:

(i) respective harmonic components of order,  $3n$ , in the LINE to D.C. NEUTRAL voltage waveform formed balanced zero-sequence sets,

(ii) respective harmonic components of order,  $(3n - 2)$ , in the LINE to D.C. NEUTRAL voltage waveform and in the LINE to LINE voltage waveforms formed balanced positive-sequence

sets.

(iii) respective harmonic components of order,  $(3n - 1)$ , in both the LINE to D.C. NEUTRAL voltage waveforms and LINE to LINE voltage waveforms formed balanced negative-sequence sets.

(3) For odd non-triple-integer values of frequency ratio given by:

$$\frac{f_c}{f_m} = 3n + \frac{1}{2} [3 - (-1)^n]$$

d.c. components of voltage did not occur in the LINE to D.C. NEUTRAL voltage waveforms nor in the LINE to LINE voltage waveforms. Harmonics of order,  $(2n)$ , were also eliminated from the LINE to D.C. NEUTRAL voltage waveforms and LINE to LINE voltage waveforms. It is of particular interest to note that considerable 'amplitude' and 'phase' unbalance of the respective wanted harmonic components in both the LINE to D.C. NEUTRAL voltage waveforms and in the LINE to LINE voltage waveforms occurred for non-triple-integer frequency ratio values of 'five' and 'seven'. However for odd non-triple-integer values of frequency ratio of 'eleven' and above, the degree of 'amplitude' and 'phase' unbalance of respective wanted harmonic components became insignificant (less than 1%). Respective harmonic components corresponding to the carrier frequency and integer multiples of the carrier frequency of order,  $n \frac{f_c}{f_m}$ , which existed in the LINE to D.C. NEUTRAL voltage waveforms formed balanced zero-sequence sets which therefore cancelled in the LINE to LINE voltage waveforms.

However, respective harmonic components in the LINE to D.C. NEUTRAL voltage waveforms and LINE to LINE voltage waveforms

whose order was not equal to the carrier frequency or integer multiples of the carrier frequency, did not form balanced sequence sets. The phase-sequence of these components was also quite random.

(4) For even non-triple-integer values of frequency ratio given by:

$$\frac{f_c}{f_m} = 3n - \frac{1}{2} [3 + (-1)^n],$$

d.c. components of voltage of considerable magnitude existed in the LINE to LINE voltage waveforms for all values of modulation index. However, for non-triple-integer values of frequency ratio above 'ten' the d.c. components of voltage became insignificant (less than 1% of the fundamental component). Respective fundamental harmonic components of both the LINE to D.C. NEUTRAL voltage waveforms and LINE to LINE voltage waveforms were unbalanced in both 'magnitude' and 'phase', for non-triple-integer values of frequency ratio below 'eight'. Above 'eight' the degree of unbalance was less than 1%. Respective harmonic components in the LINE to D.C. NEUTRAL voltage waveforms of order,  $n \frac{f_c}{f_m}$ , formed balanced zero-sequence sets, which resulted in the cancellation of these components in the LINE to LINE voltage waveforms. Respective harmonic components in both the LINE to D.C. NEUTRAL voltage waveforms and in the LINE to LINE voltage waveforms of harmonic order other than ' $n \frac{f_c}{f_m}$ ' formed unbalanced sequence sets. A relationship between the phase sequence of these components and harmonic order was also not apparent.

#### (4.2.1.5) Choice of Natural Sampled

##### P.W.M. System

The computer analysis of the three natural sampled p.w.m. systems has shown, that natural sampled double-edge p.w.m. is superior to natural sampled single-edge p.w.m. for mainly two reasons:

(i) For single-edge p.w.m. operating with a modulation index of 'unity', the minimum value of frequency ratio is given by:

$$\frac{f_c}{f_m} > \pi, \text{ ((Section (3.8.1) of Chapter (3))}$$

Therefore, for integer-frequency-ratio operation, the minimum value of frequency ratio for a modulation index of 'unity' is  $\frac{f_c}{f_m} = 4$ , because,  $\pi$ , is not an integer value. However, for double-edge p.w.m. and a modulation index of 'unity' the minimum value of frequency ratio is given by:

$$\frac{f_c}{f_m} > \frac{\pi}{2}, \text{ ((Section (3.8.1.) of Chapter (3)).}$$

This means that for integer frequency ratio operation at a modulation index of 'unity', the minimum value of frequency ratio is given by:  $\frac{f_c}{f_m} = 2$ . When a natural sampled p.w.m. process is made to operate outside the above limitations of frequency ratio for a modulation index of unity, a very considerable increase in harmonic distortion of the output p.w.m. voltage waveforms will occur, as was discussed in Section (4.2.1.2) for natural sampled lead-edge p.w.m.

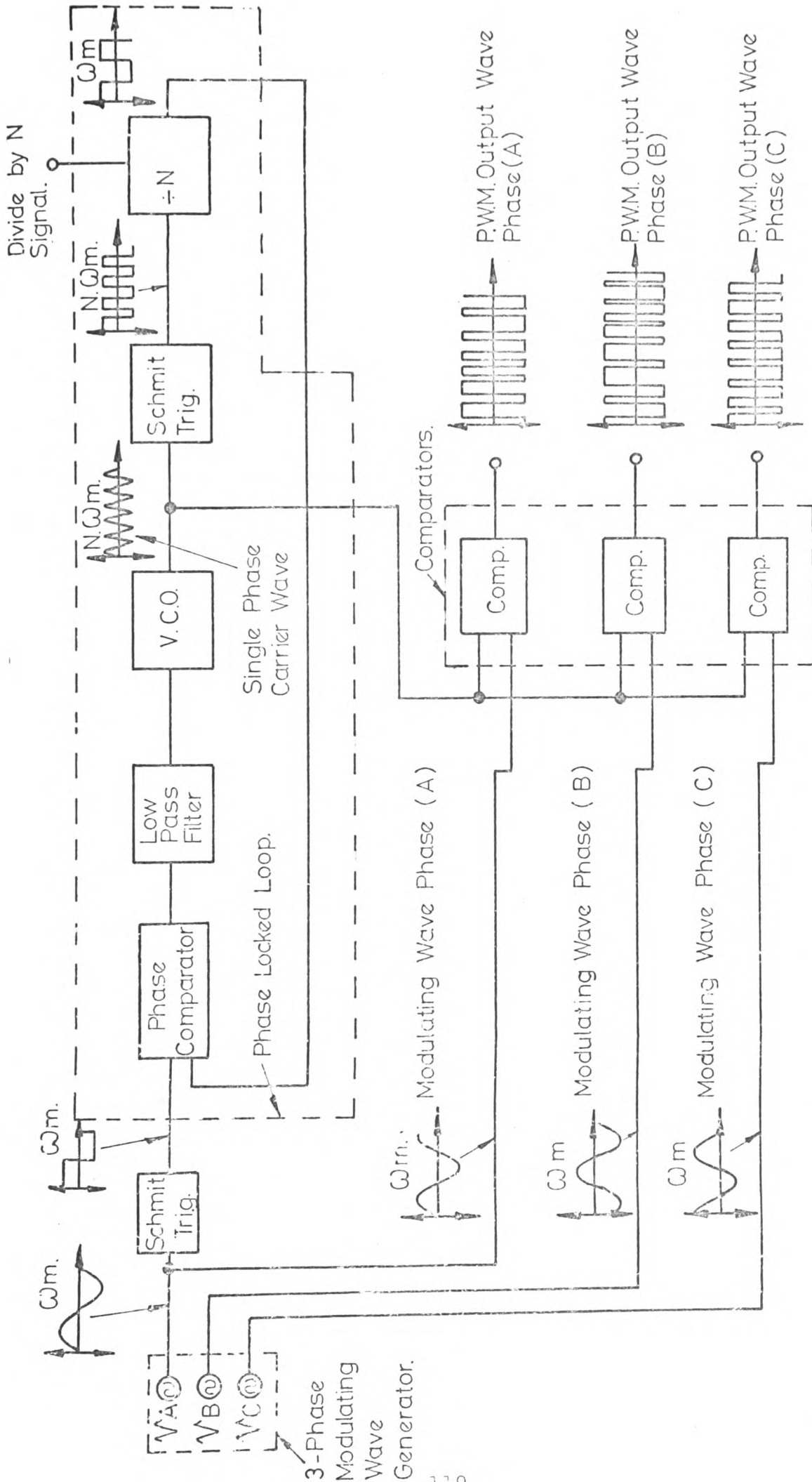
(ii) For all integer values of frequency ratio which lie within the limitation of the natural sampling process (as described in Section (3.8.1.) of Chapter (3)), the voltage

harmonic spectra of the natural sampled double-edge p.w.m. process is superior to the voltage harmonic spectra for the single-edge p.w.m. processes for two reasons: (a) for single-edge p.w.m. even order and odd order harmonics are always present in the LINE to LINE voltage spectra and (b) less harmonic cancellation takes place for single-edge p.w.m. than for double-edge p.w.m.

Because natural sampled double-edge p.w.m. has proved to be superior to natural sampled single-edge p.w.m. for all integer values of frequency ratio, it was decided to investigate the natural sampled double-edge p.w.m. process experimentally,

#### (4.2.2) Experimental Investigation Into Natural Sampled Double-Edge P.W.M.

A light-current three-phase, natural sampled double-edge p.w.m. control circuit was designed and constructed to check the authenticity of the computed harmonic spectra. A block diagram of the system is illustrated in Fig.(4.6) and a schematic diagram of the control circuit is included in Appendix (2). It may be seen from Fig.(4.6) that the control circuit mainly consists of: a three-phase signal generator, a phase-locked-loop and three voltage *comparator* circuits. The three-phase modulating wave generator supplies three output sinusoidal waveforms displaced in time-phase by  $-120^\circ$  and  $120^\circ$  respectively, where both the amplitude and frequency of the output waveforms can be varied. The phase-locked-loop generates a triangular carrier wave which is synchronised with the PHASE (A) output-wave of the modulating



FIG(4. 6) BLOCK DIAGRAM OF CONTROL CIRCUIT FOR NATURAL SAMPLED DOUBLE-EDGE P.W.M.

wave generator and is at "N" times its frequency (N.Wm). The three sinusoidal modulating waves are then compared with the single-phase triangular carrier wave in the three comparator circuits. The three output pulse-width-modulated waveforms from the three comparators are then made to supply three 1 K $\Omega$  resistors connected in star as shown in Fig.(4.7).

#### (4.2.2.1) Measurements Technique.

The d.c. components of voltage in the LINE to LINE voltage waveforms, were measured by connecting a moving-coil voltmeter between respective pairs of LINES in the circuit shown in Fig.(4.7).

The harmonic voltage components of the LINE to D.C. NEUTRAL voltage waveforms were measured by means of a low frequency wave analyser (Muirhead D-788A) connected between the D.C. NEUTRAL and respective LINES. Similarly, the LINE to LINE voltage harmonic components were measured by connecting the low frequency wave analyser between respective pairs of LINES.

The phase angle between any three harmonic components of the same order, were measured by means of two identical low frequency wave analysers and one phase-meter (Dawe, Type 630). Consider two identical wave analysers connected between LINE (A) and the D.C. NEUTRAL and LINE (B) and the D.C. NEUTRAL, where both wave analysers are tuned to harmonic components of the same frequency. By connecting a phase-meter between the two pairs of output terminals of the wave analysers such that the harmonic component of the LINE (A) to D.C. NEUTRAL voltage waveform is taken as reference, a phase angle, AB, can be measured. If the wave analyser between the LINE (B) and D.C.



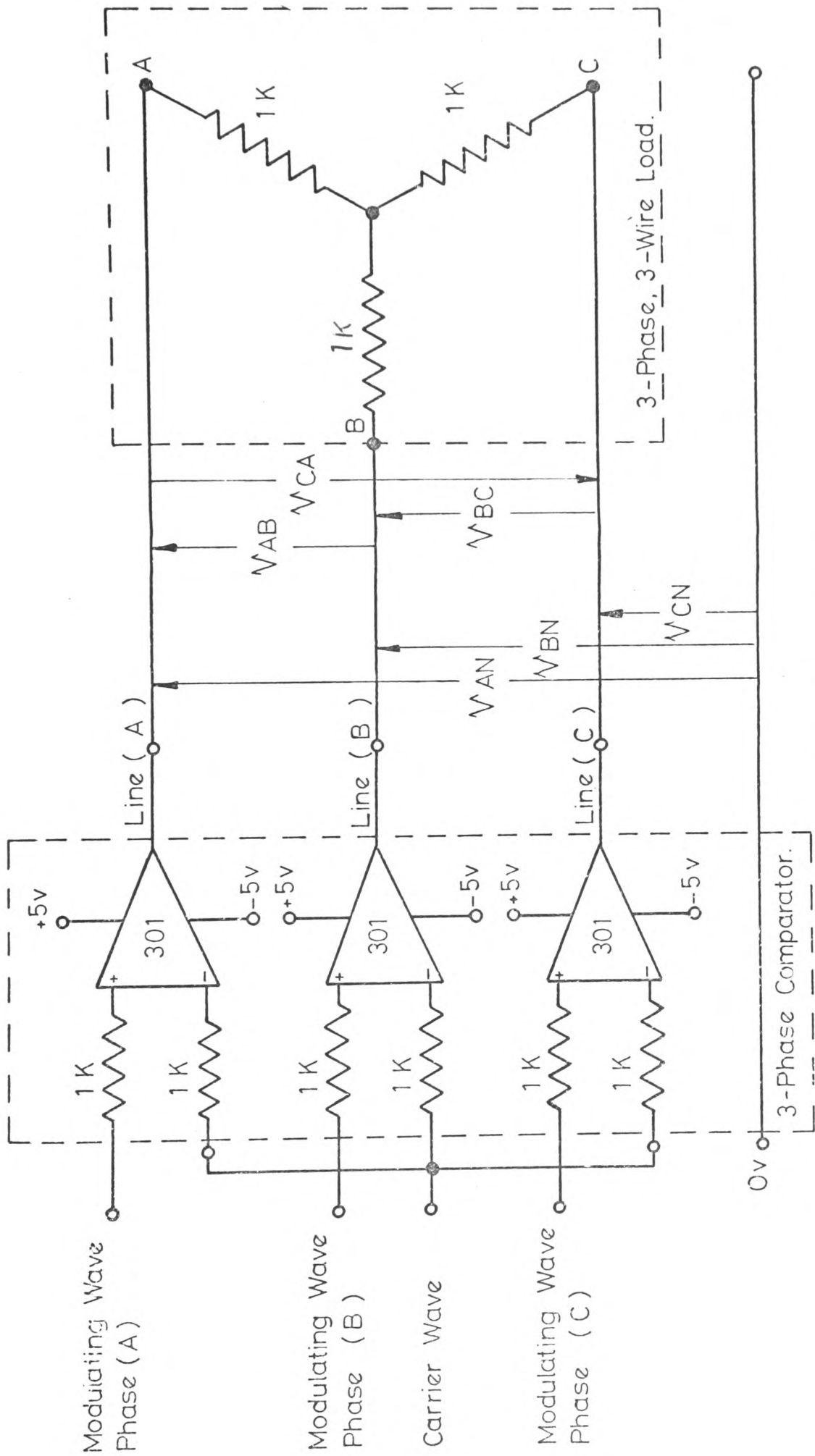


Fig (4.7) NATURAL SAMPLED DOUBLE-EDGE PWM CONTROL CIRCUIT SUPPLYING 3-PHASE 3-WIRE LOAD.

NEUTRAL is then transferred to the LINE (C) to D.C. NEUTRAL and again tuned to the harmonic component of the same frequency as in the previous case a phase angle,  $\theta_{AC}$ , can be measured by means of the phase-meter. The phase angle given by:  $\theta_{AC} - \theta_{AB}$ , is then the phase angle between respective harmonic components in the LINE (B) to D.C. NEUTRAL voltage waveform and LINE (C) to D.C. NEUTRAL voltage waveform. By repeating this process the phase angles between any three respective harmonic components can be measured.

#### (4.2.2.2) Experimental Results

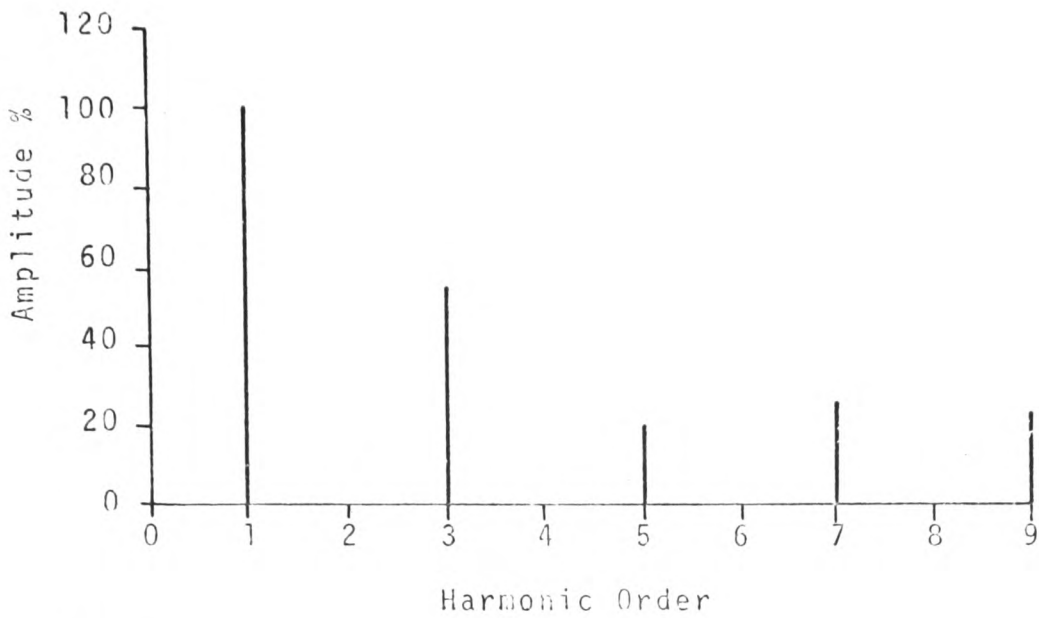
The 'amplitude' and 'phase' of respective harmonic components in the three LINE to D.C. NEUTRAL voltage waveforms and in the three LINE to LINE voltage waveforms were measured by the technique described in Section (4.2.2.1), for various values of frequency ratio and modulation index, the magnitude of the fundamental component of the LINE (A) to D.C. NEUTRAL voltage waveform was taken as reference for the LINE to D.C. NEUTRAL voltage harmonics, while the magnitude of the fundamental component of the LINE (A) to LINE (B) voltage waveform was taken as reference for the LINE to LINE voltage harmonics.

Experimental and theoretical LINE to D.C. NEUTRAL and LINE to LINE voltage harmonic spectra for a modulation index of unity and frequency ratio's of :  $\frac{f_c}{f_m} = 3, 6, 5$  and 2 are illustrated in Figures: (4.8), (4.9), (4.10) and (4.11) respectively.

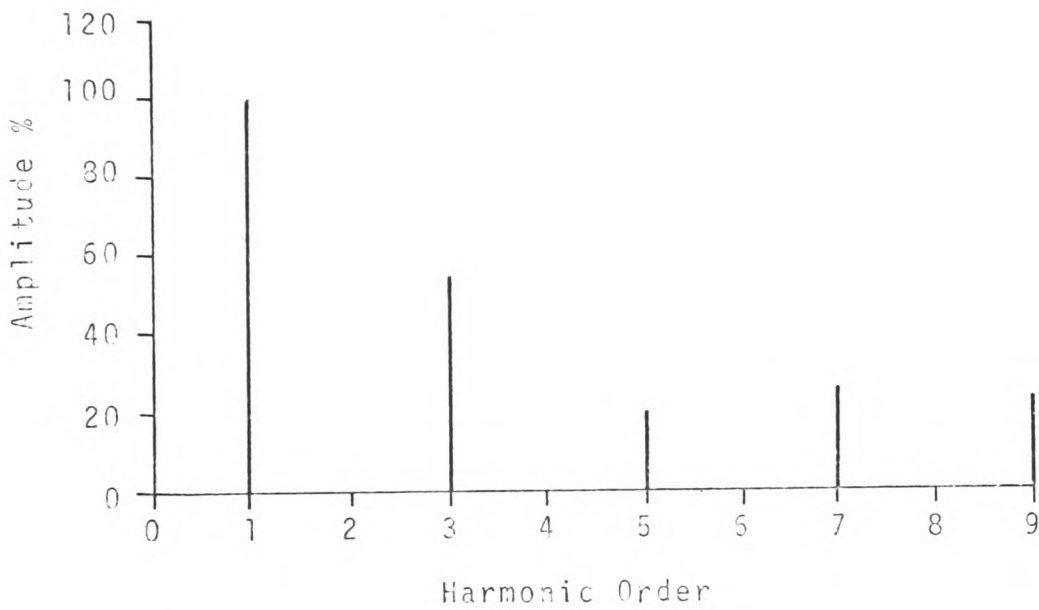
#### (4.2.2.3) Discussion of Results and Interim Conclusions

The result obtained from the analytical investigation into

Line (A) To Neutral Voltage  
(Reference)



Line (B) To Neutral Voltage



Line (C) To Neutral Voltage

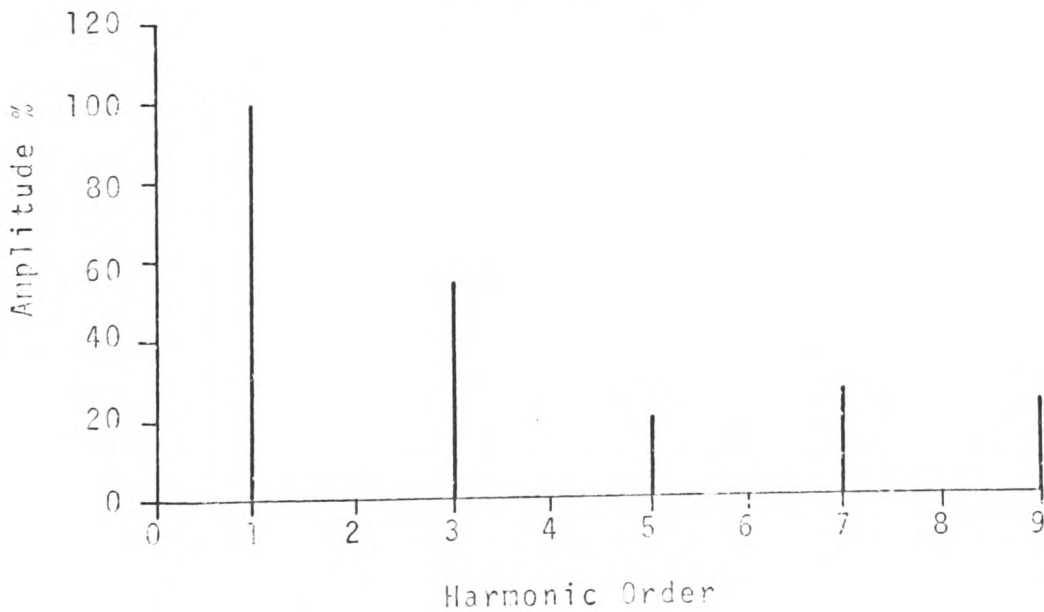


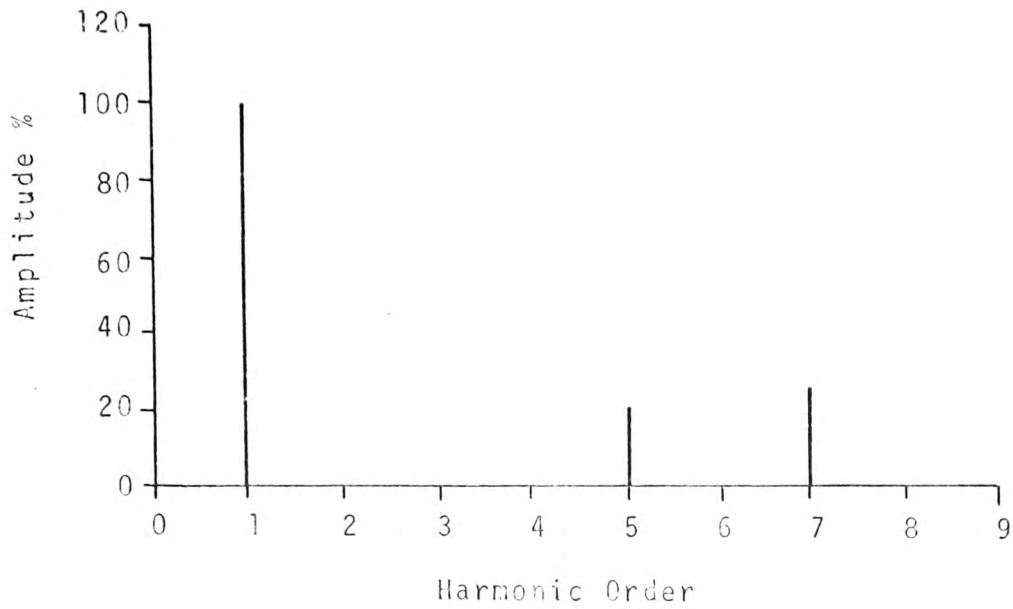
FIG.(4.8a) HARMONIC SPECTRA FOR LINE TO D.C. NEUTRAL VOLTAGE WAVEFORM FOR FREQUENCY RATIO OF 3 AND MODULATION INDEX OF 1.0 FOR NATURAL SAMPLED DOUBLE-EDGE P.W.M.

Voltage Waveforms	Sampling Process	Phase Sequence	Harmonic Order																
			1	2	3	4	5	6	7	8	9								
Line to D.C. Neutral	Natural	Reference	$X_B$																
		Reverse					$X_B$												
		In Phase								$X_B$									

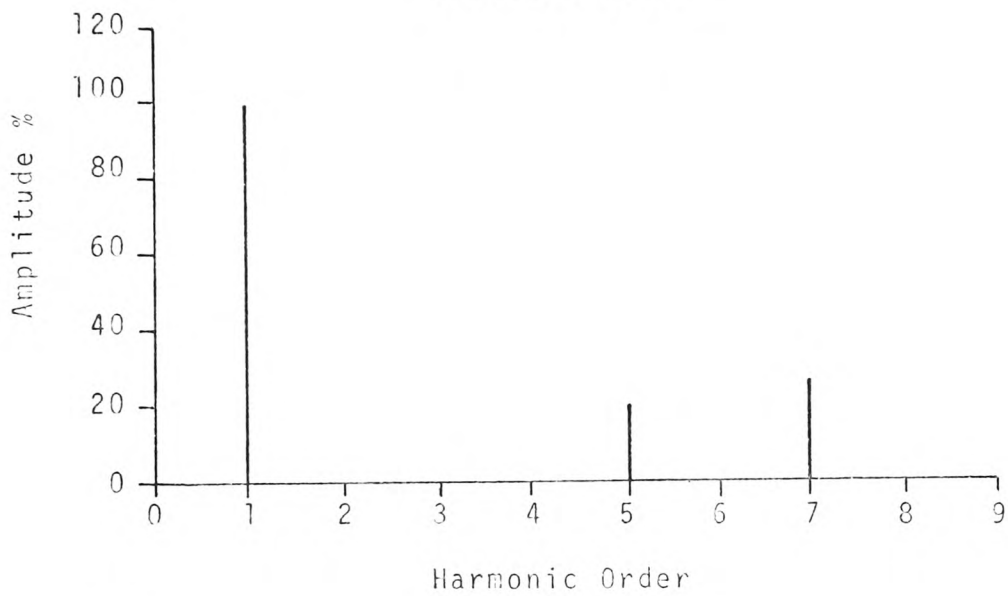
$X_B$  - Respective Harmonic Components Form Balanced Sequence Sets  
 $X_u$  - " " " Unbalanced " "

FIG. (4.8b) PHASE SEQUENCE OF RESPECTIVE LINE TO D.C. NEUTRAL VOLTAGE WAVEFORM HARMONICS FOR FREQUENCY RATIO OF 3, AND MODULATION INDEX OF 1.0 FOR NATURAL SAMPLED DOUBLE-EDGE P.W.M.

Line (A) To Line (B) Voltage  
(Reference)



Line (B) To Line (C) Voltage



Line (C) To Line (A) Voltage

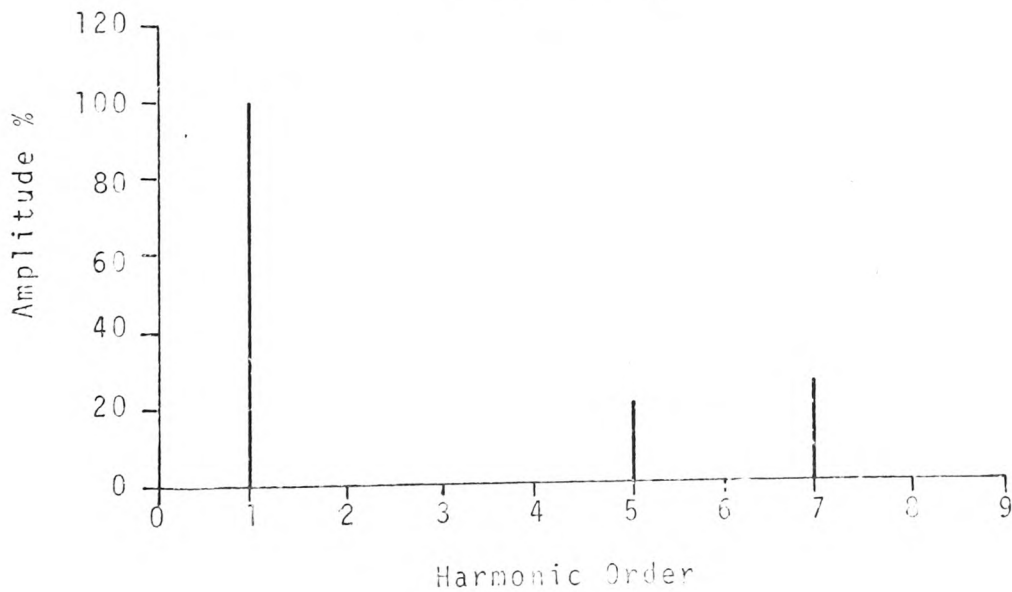
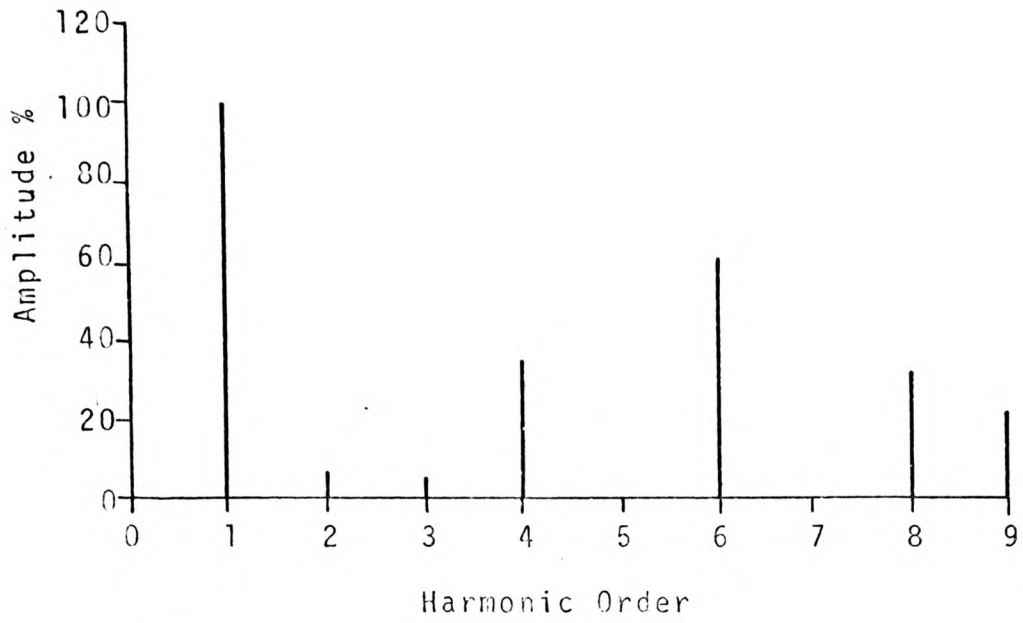
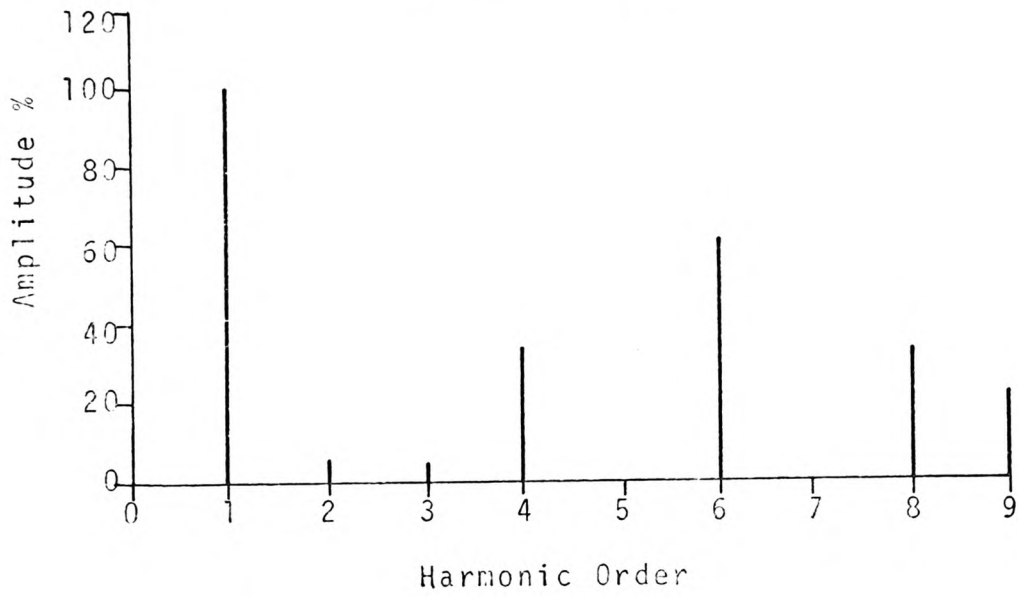


FIG. (4.8c) HARMONIC SPECTRA FOR LINE TO LINE VOLTAGE WAVEFORM FOR A FREQUENCY RATIO OF 3 AND MODULATION INDEX OF 1.0, FOR NATURAL SAMPLED DOUBLE-EDGE P.W.M.

Line (A) To Neutral Voltage  
(Reference)



Line (B) To Neutral Voltage



Line (C) To Neutral Voltage

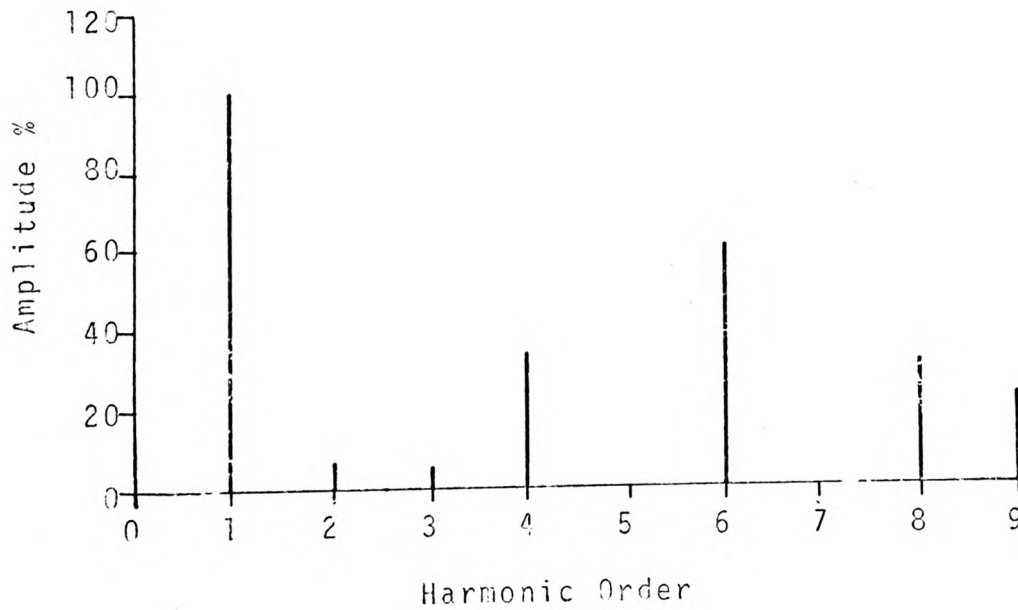


FIG.(4.9a) HARMONIC SPECTRA FOR LINE TO NEUTRAL VOLTAGE WAVEFORM FOR A FREQUENCY RATIO OF 6 AND MODULATION INDEX OF 1.0, FOR NATURAL SAMPLED DOUBLE-EDGE P.W.M.

Voltage Waveforms	Sampling Process	Phase Sequence	Harmonic Order											
			1	2	3	4	5	6	7	8	9			
Line to D.C. Neutral	Natural	Reference	$X_B$			$X_B$								
		Reverse		$X_B$								$X_B$		
		In Phase			$X_B$					$X_B$				$X_B$

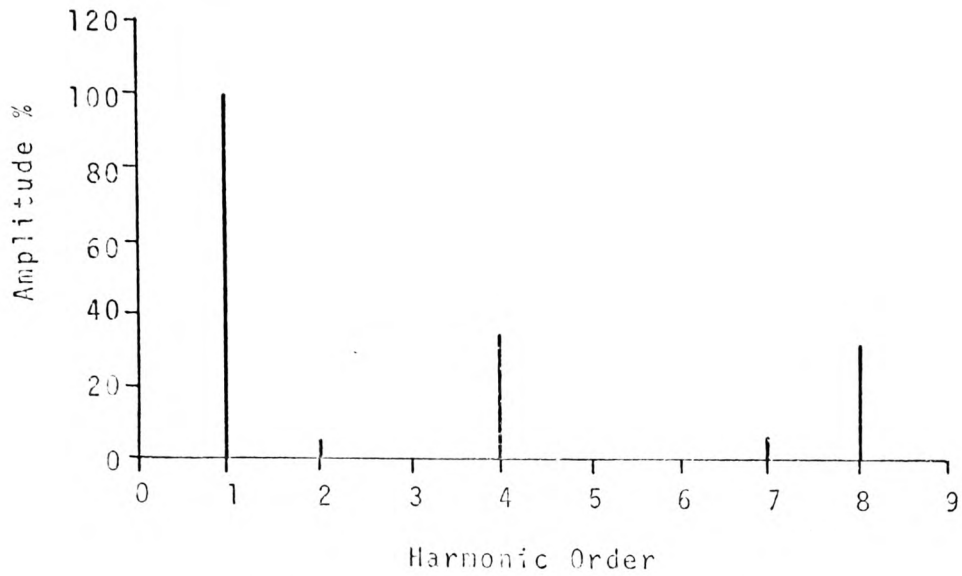
$X_B$  - Respective Harmonic Components Form Balanced Sequence sets

$X_u$  - " " " Unbalanced " "

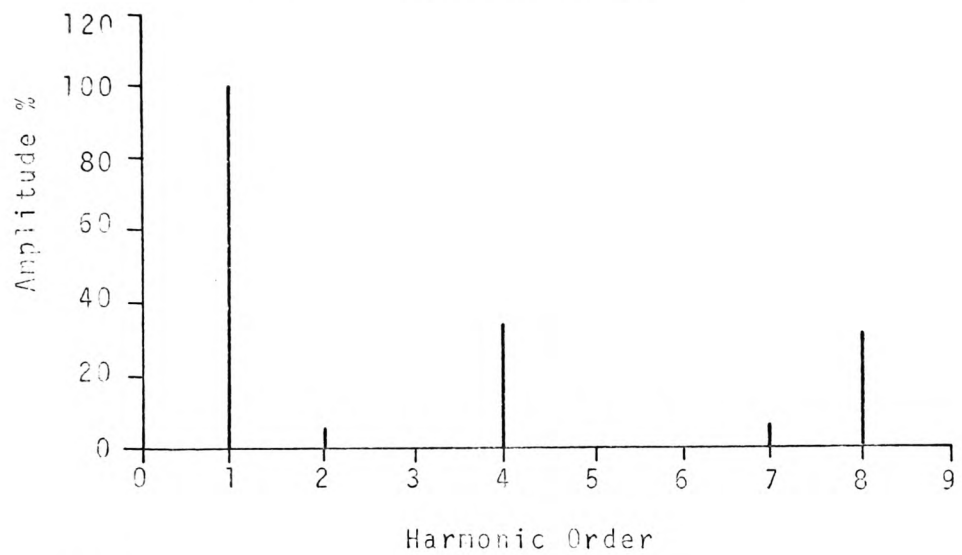
Fig. (4.9b) PHASE SEQUENCE OF RESPECTIVE LINE TO D.C. NEUTRAL VOLTAGE WAVEFORM HARMONICS

FOR FREQUENCY RATIO OF 6 AND MODULATION INDEX OF 1.0, FOR NATURAL SAMPLED DOUBLE-EDGE P.W.M.

Line (A) To Line (B) Voltage  
(Reference)



Line (B) To Line (C) Voltage



Line (C) To Line (A) Voltage

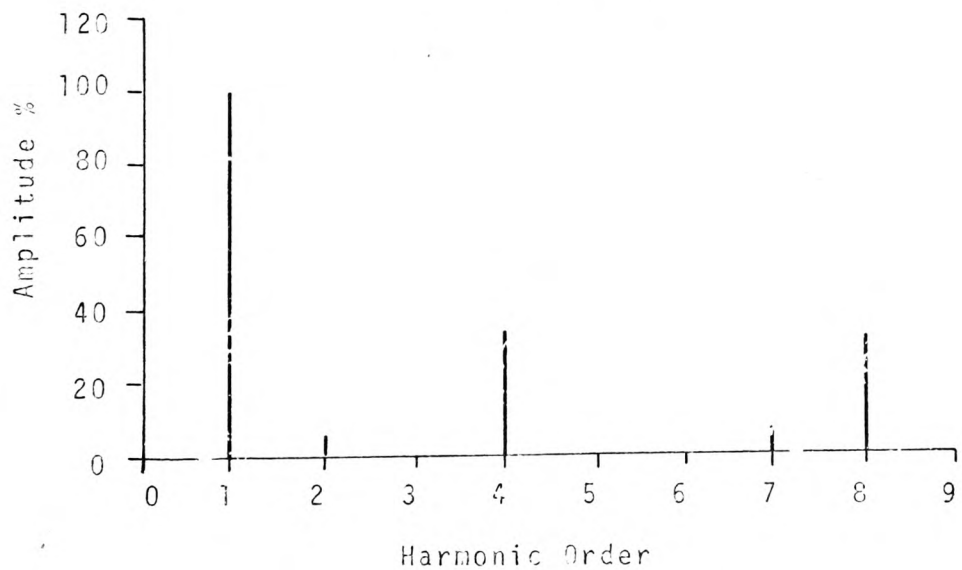
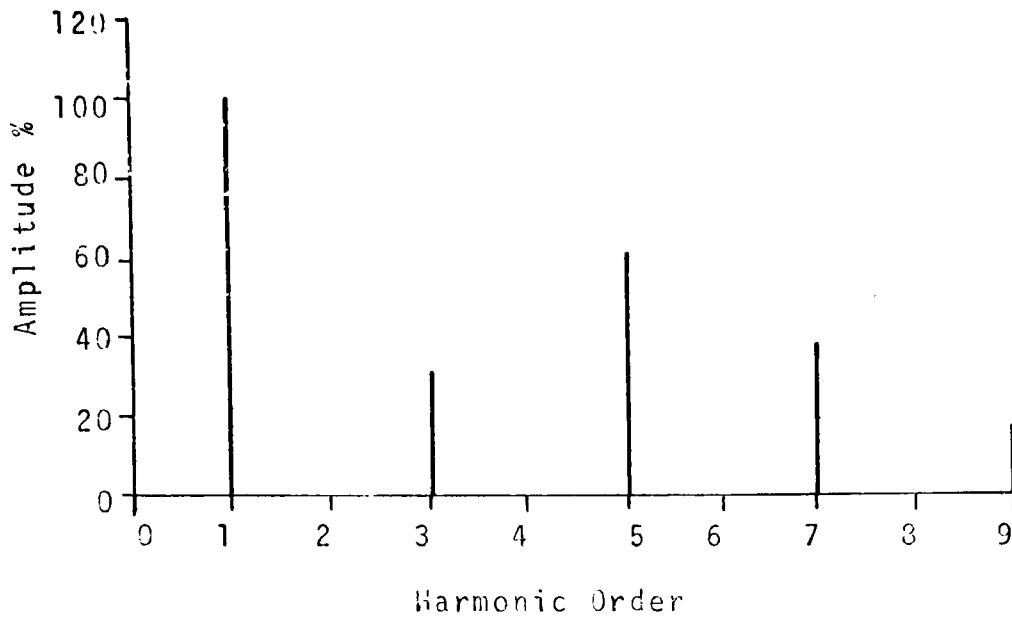


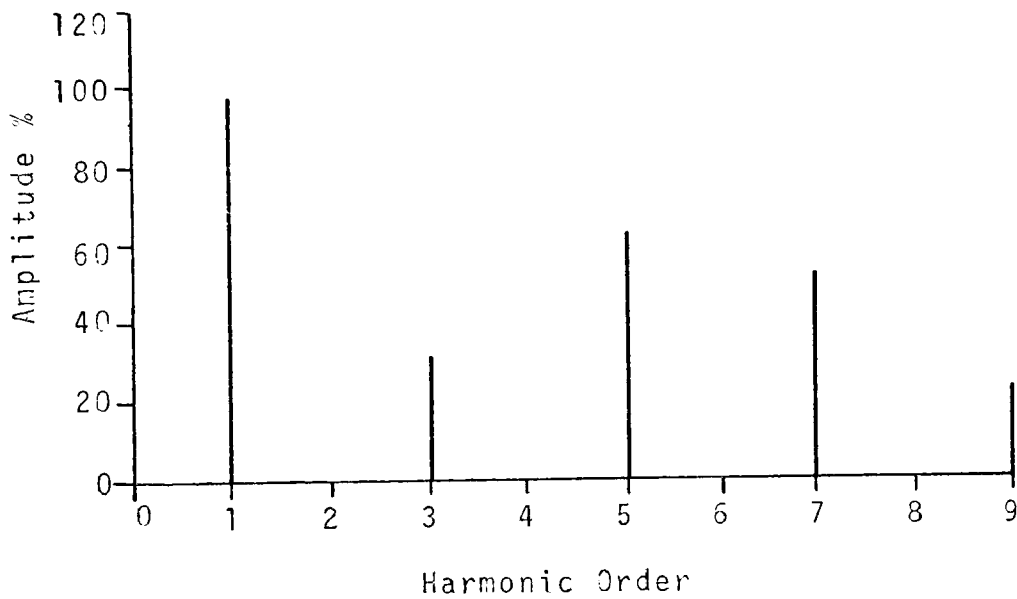
FIG.(4.9c) HARMONIC SPECTRA FOR LINE TO LINE VOLTAGE WAVEFORM FOR A FREQUENCY RATIO OF 6 AND MODULATION INDEX OF 1.0, FOR NATURAL SAMPLED DOUBLE-EDGE P.W.M.



Line (A) To Neutral Voltage  
(Reference)



Line (B) To Neutral Voltage



Line (C) To Neutral Voltage

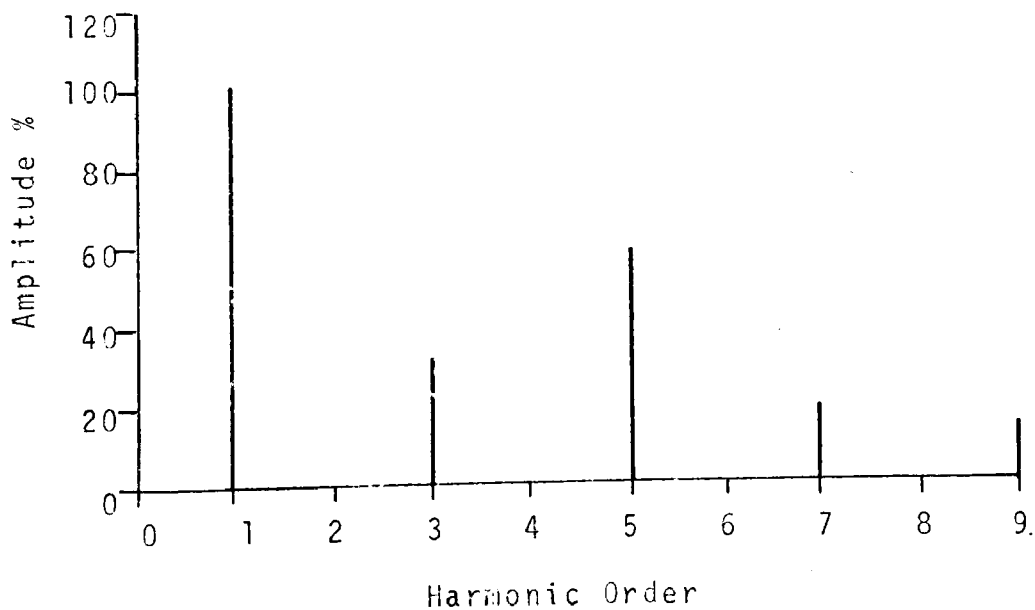


FIG. (4.10a) HARMONIC SPECTRA FOR LINE TO D.C. NEUTRAL VOLTAGE WAVEFORMS FOR A FREQUENCY RATIO OF 5 AND MODULATION INDEX OF 1.0, FOR NATURAL SAMPLED DOUBLE-EDGE P.W.M.

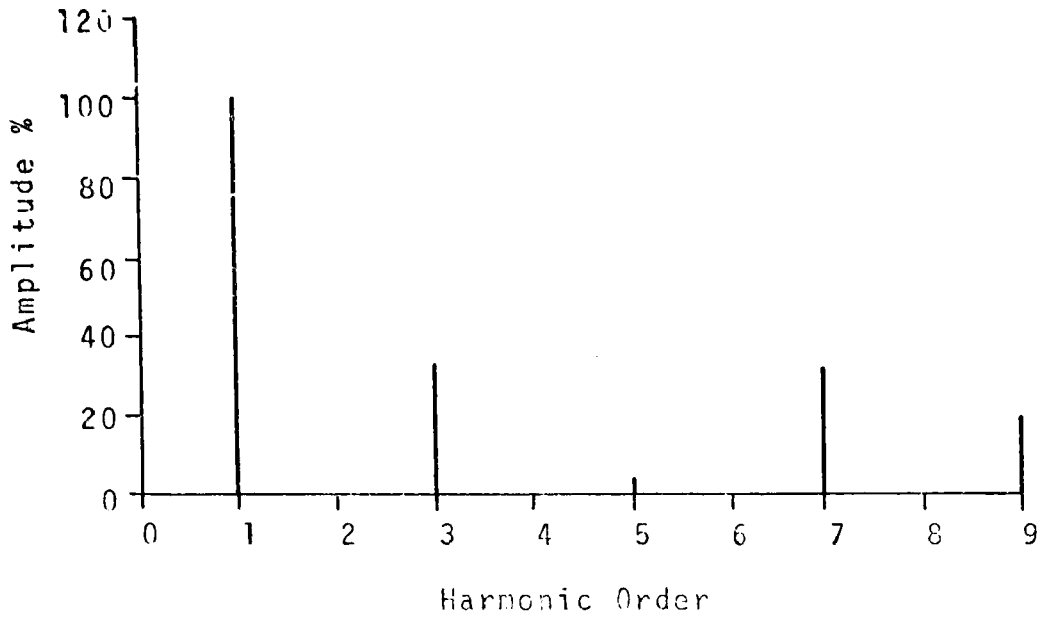
Voltage Waveforms	Sampling Process	Phase Sequence	Harmonic Order											
			1	2	3	4	5	6	7	8	9			
Line to D.C. Neutral	Natural	Reference	Xu		Xu									
		Reverse					Xu					Xu		
		In Phase												Xu

$X_B$  - Respective Harmonic Components Form Balanced Sequence Sets

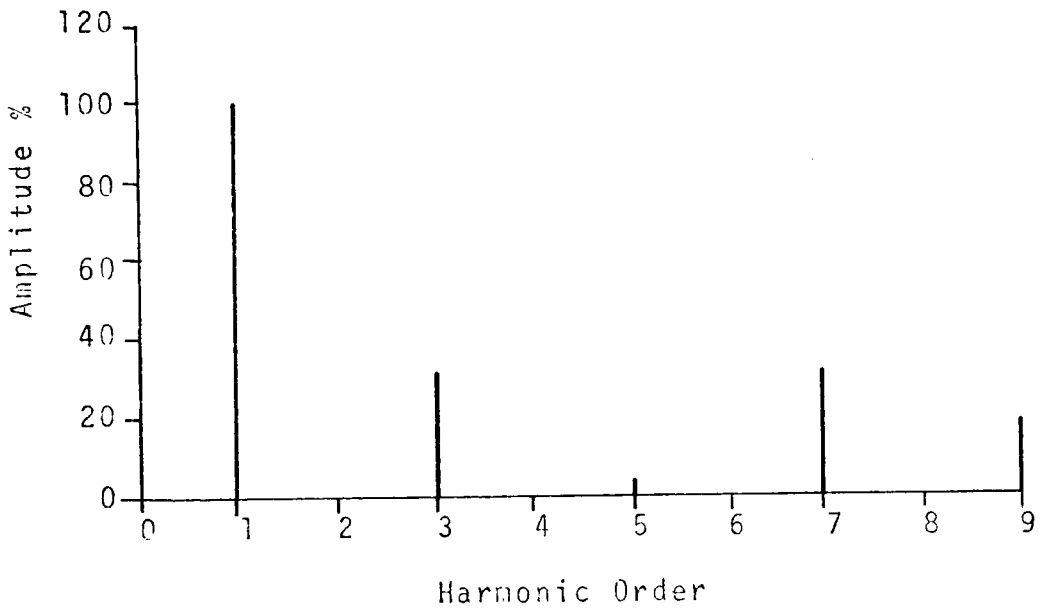
$X_u$  - " " " Unbalanced " "

FIG.(4.10b) PHASE SEQUENCE OF RESPECTIVE LINE TO D.C. NEUTRAL VOLTAGE WAVEFORM HARMONIC FOR FREQUENCY RATIO OF 6, AND MODULATION INDEX OF 1.0, FOR NATURAL SAMPLED DOUBLE-EDGE P.W.M.

Line (A) To Line (B) Voltage



Line (B) To Line (C) Voltage



Line (C) To Line (A) Voltage

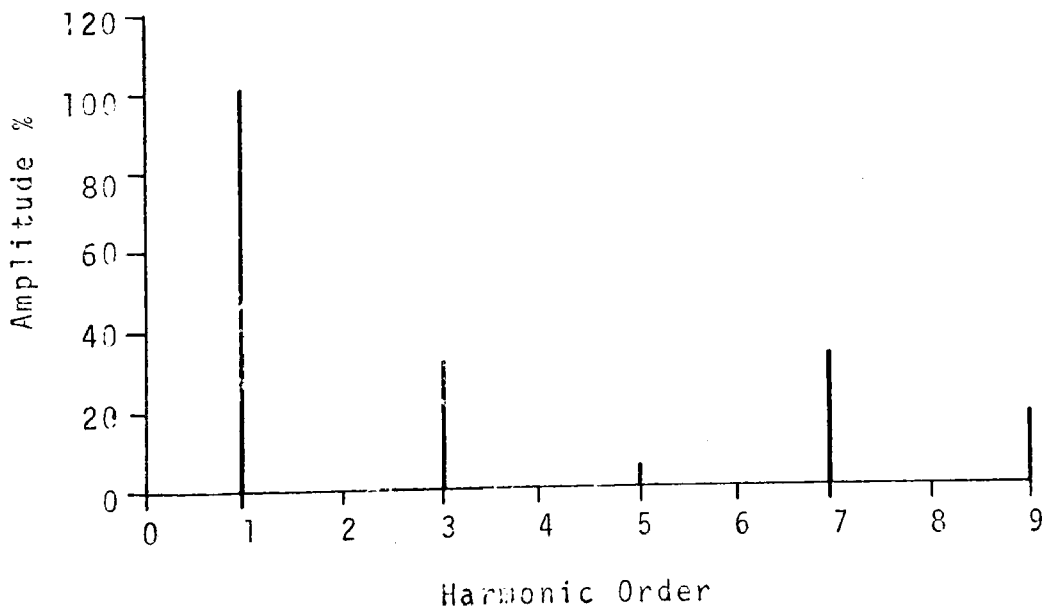
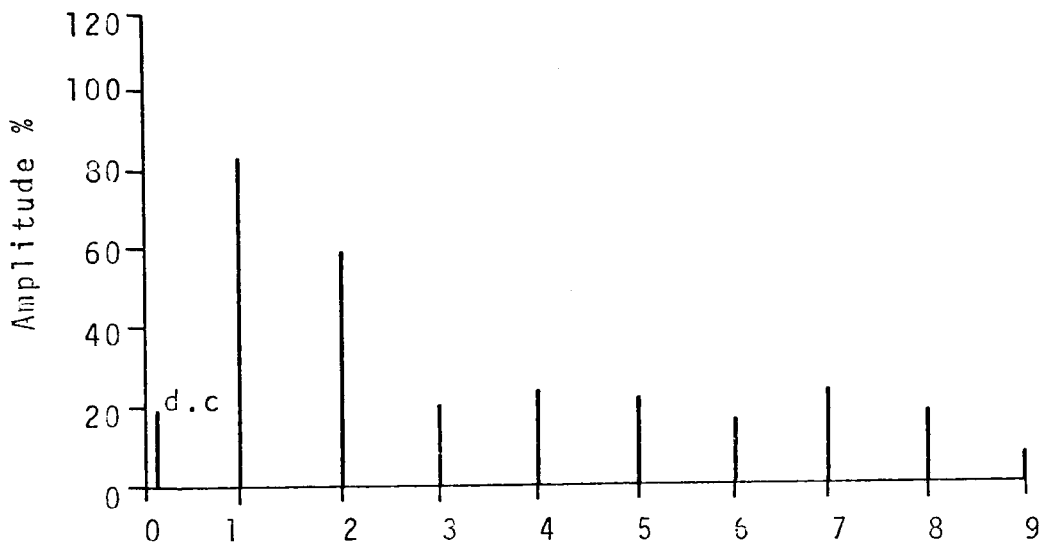


FIG.(4.10) HARMONIC SPECTRA FOR LINE TO LINE VOLTAGE WAVEFORMS FOR FREQUENCY RATIO OF 5 AND MODULATION INDEX OF 1.0 FOR NATURAL SAMPLED DOUBLE-EDGE P.W.M.

Line (A) To Neutral Voltage  
(Reference)



Line (B) To Neutral Voltage



Line (C) To Neutral Voltage

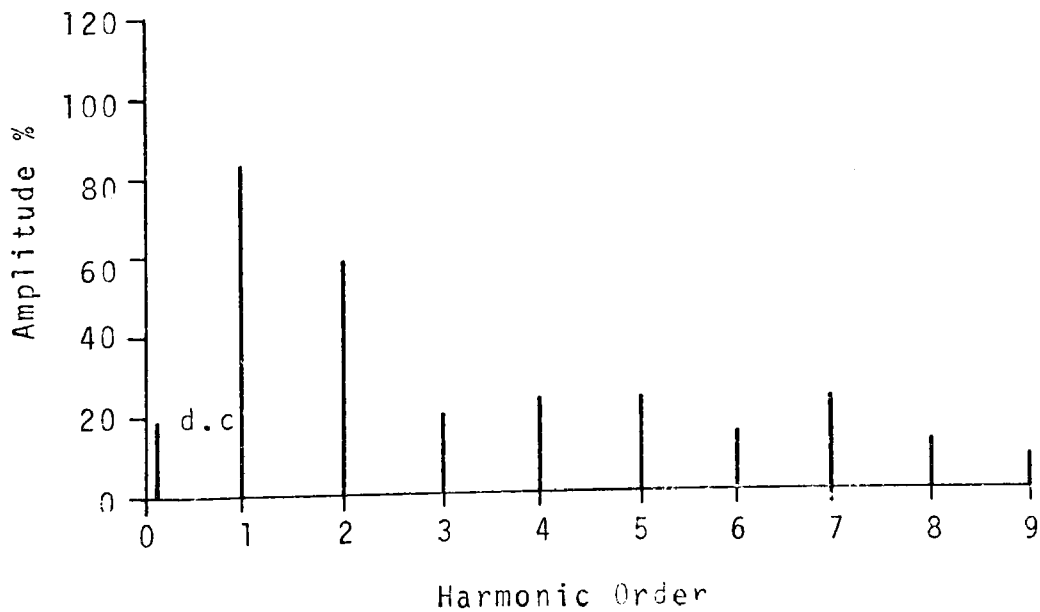


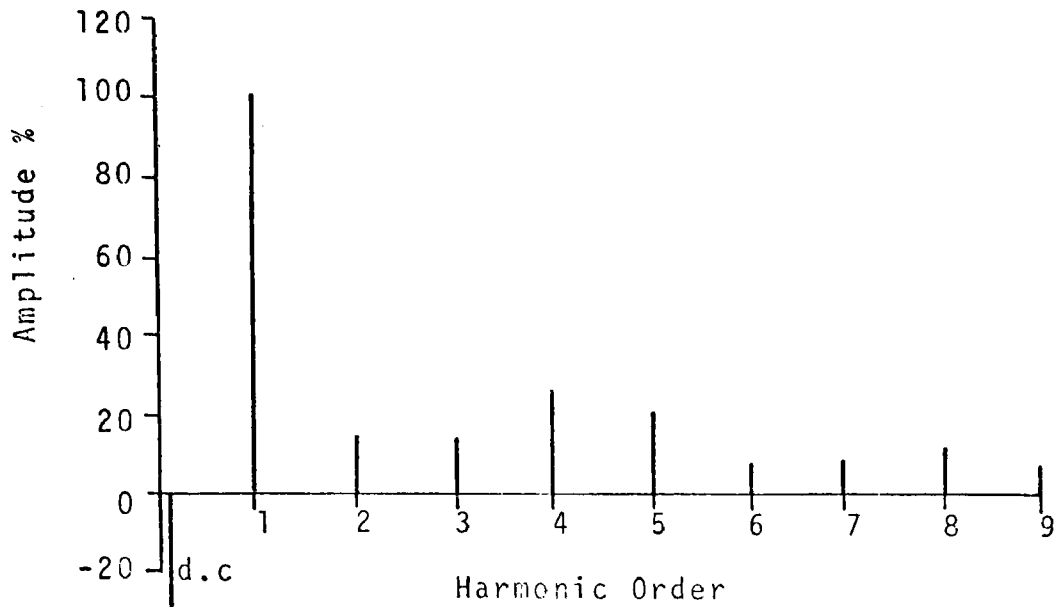
FIG.(4.11a) HARMONIC SPECTRA FOR LINE TO D.C. NEUTRAL VOLTAGE WAVEFORMS FOR A FREQUENCY RATIO OF 2, AND MODULATION INDEX OF 1.0, FOR NATURAL, SAMPLED DOUBLE-EDGE P.W.M.

Voltage Waveforms	Sampling Process	Phase Sequence	Harmonic Order																		
			1	2	3	4	5	6	7	8	9										
Line to D.C. Neutral	Natural	Reference	Xu	Xu			Xu	Xu	Xu	Xu											
		Reverse			Xu	Xu															
		In Phase																			

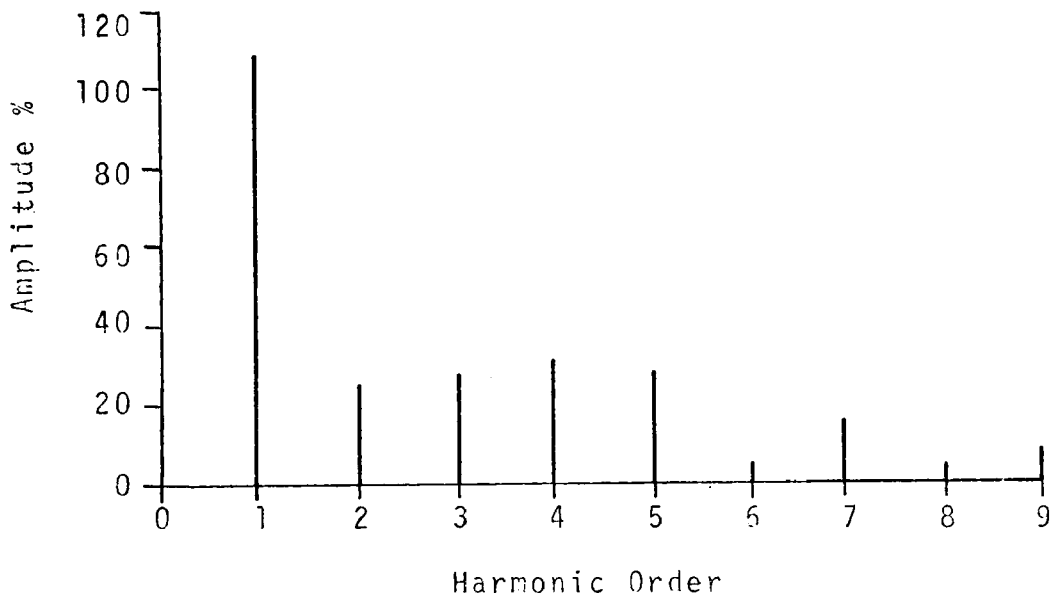
$X_B$  - Respective Harmonic Components Form: Balanced Sequence Sets  
 $X_u$  - " " " Unbalanced " "

Fig. (4.11b) PHASE SEQUENCE OF RESPECTIVE LINE TO D.C. NEUTRAL VOLTAGE WAVEFORM HARMONICS FOR FREQUENCY RATIO OF 2, AND MODULATION INDEX OF 1.0, FOR NATURAL SAMPLED DOUBLE-EDGE P.W.M.

Line (A) To Line (B) Voltage  
(Reference)



Line (B) To Line (C) Voltage



Line (C) To Line (A) Voltage

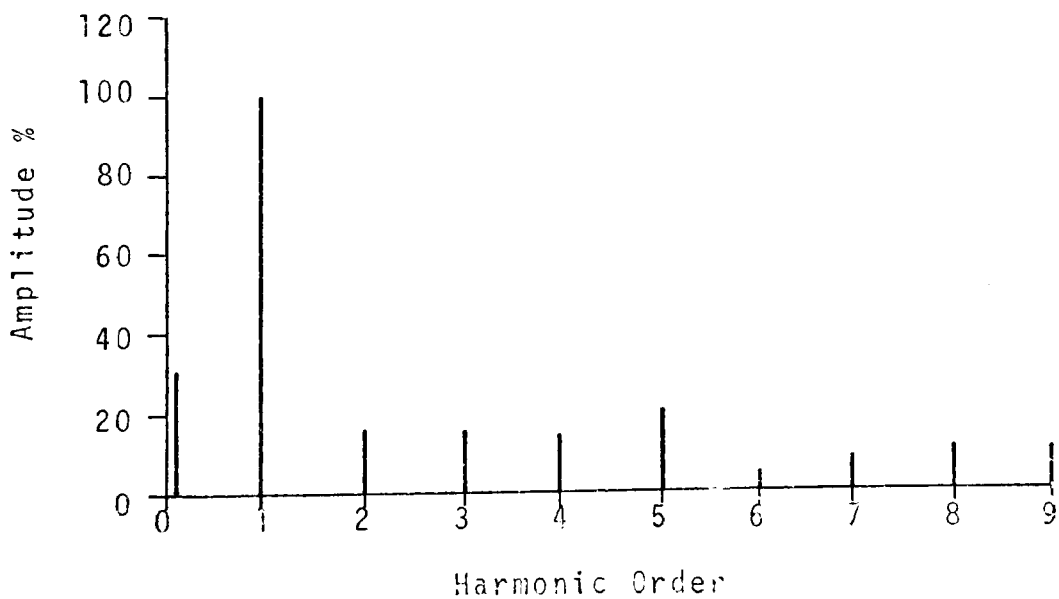


FIG.(4.11c) HARMONIC SPECTRA FOR LINE TO LINE VOLTAGE WAVEFORMS FOR FREQUENCY RATIO OF 2 AND MODULATION INDEX OF 1.0, FOR NATURAL SAMPLED DOUBLE-EDGE P.W.M.

natural sampled double-edge p.w.m, have been shown to agree with the results obtained by experimental investigation. The results obtained from both methods of investigation have demonstrated that the harmonic spectra of the p.w.m, output voltage waveforms from the convertor illustrated in Fig.(4.1) are very dependent upon the value of integer frequency ratio.

It has been shown that the first choice of integer frequency ratio values, are the odd triple-integer values given by:

$$\frac{f_c}{f_m} = 3, 9, 15 \dots 3(2n - 1),$$

because of the following factors:

(i) Positive and negative half-wave symmetry is achieved which eliminates even order harmonics and d.c. components from the output LINE to D.C. NEUTRAL voltage waveforms.

(ii) Odd triplen harmonics of order:  $3(2n - 1)$  which exist in the LINE to D.C. NEUTRAL voltage waveforms, form balanced zero-sequence sets, which results in the cancellation of these harmonics in the LINE to LINE voltage waveform when supplying a three-phase, three-wire load.

The second choice of integer frequency ratio values have been shown to be the even triple-integer values given by:

$$\frac{f_c}{f_m} = 6, 12, 18 \dots 3(2n)$$

These values of frequency ratio have been shown to be inferior to the odd triple-integer values because they introduce even order and odd order harmonics into the LINE to D.C. NEUTRAL voltage waveforms. However, it was also shown that triplen harmonics of order;  $3(n)$ , form balanced zero-sequence sets, which cancel in the LINE to LINE voltage waveforms when

supplying a three-phase, three-wire load.

The third preferred choice of frequency ratio values have been shown to be the odd non-triple integer values, given by:

$$\frac{f_c}{f_m} = 5, 7, 11, \dots, (3n + \frac{1}{2} [3 - (-1)^n])$$

Although it was shown that these values of frequency ratio eliminate d.c. voltage components and harmonics of order;  $2n$ , from the LINE to D.C. NEUTRAL voltage waveform and from the LINE to LINE voltage waveforms, it was also shown that the following disadvantage existed: respective harmonic components in both the LINE to D.C. NEUTRAL voltage waveforms and LINE to LINE voltage waveforms did not form balanced sequence sets.

The least preferred frequency ratio values have been shown to be the even non-triple integer values given by:

$$\frac{f_c}{f_m} = 2, 4, 8, \dots, (3n - \frac{1}{2} [3 + (-1)^n])$$

It was shown that these values of frequency ratio present the following disadvantages: d.c. voltage components, even order harmonics (of order  $2n$ ) and odd order harmonics (of order  $(2n - 1)$ ) all exist in both the LINE to D.C. NEUTRAL voltage waveforms and in the LINE to LINE voltage waveforms.

A relationship between harmonic order and phase sequence was also shown to exist for triple-integer values of frequency ratio, that is to say: for frequency ratio values given by:

$$\frac{f_c}{f_m} = 3, 6, 9, 12, \dots, 3(n),$$

respective harmonic of order:  $(3n - 2)$ ,  $(3n - 1)$  and  $3(n)$ , formed balanced positive-sequence sets, balanced negative-sequence sets and balanced zero-sequence sets respectively,



in both the LINE to D.C. NEUTRAL voltage waveforms and LINE to LINE voltage waveforms. However, for non-triple integer frequency ratio values given by:

$$\frac{fc}{fm} = 3n - \frac{1}{2} [3 + (-1)^n]$$

and

$$\frac{fc}{fm} = 3n + \frac{1}{2} [3 - (-1)^n],$$

respective harmonic components did not form balanced sequence sets and no apparent relationship between phase sequence and harmonic order existed.

#### (4.3) The Application of Regular Sampling to P.W.M.

##### Power Convertors Operating in the Synchronised Mode.

The main object of any power modulator intended for infinitely variable induction motor speed control systems, is to produce a sinusoidal output voltage waveform which is variable in both magnitude and frequency. Such an objective cannot be achieved of course because all power modulators introduce some degree of harmonic distortion. Therefore, consideration must be given to the most acceptable harmonically distorted waveforms. For the convertor shown in Fig.(4.1) the most desirable voltage waveforms between each LINE to D.C. NEUTRAL would consist of fundamental components which form a balanced positive-sequence set, plus the 'minimum' number of harmonic components - where the respective harmonic components form balanced zero-sequence sets:

$$V_{an} = V_{dc} + \hat{V}_1 \sin \omega_m t + \dots + \hat{V}_{n-1} \sin(n-1)\omega_m t + \hat{V}_n \sin n\omega_m t \quad \text{----(4.1)}$$

$$V_{bn} = V_{dc} + \hat{V}_1 \sin(\omega_m t - 120^\circ) + \dots + \hat{V}_{n-1} \sin(n-1)\omega_m t + \hat{V}_n \sin n\omega_m t \quad \text{--(4.2)}$$

$$V_{cn} = V_{dc} + \hat{V}_1 \sin(\omega_m t + 120^\circ) + \dots + \hat{V}_{n-1} \sin(n-1)\omega_m t + \hat{V}_n \sin n\omega_m t \quad \text{-----(4.3)}$$

When such hypothetical waveforms are applied to a balanced three-phase, three-wire load all the remaining harmonics with the exception of the wanted harmonic components, would cancel in the LINE to LINE voltage of the convertor shown in Fig.

(4.1) such that:

$$V_{an} - V_{bn} = \sqrt{3} \hat{V}_1 \sin(\omega_m t + 30^\circ) \quad \text{---- (4.4)}$$

$$V_{bn} - V_{cn} = \sqrt{3} \hat{V}_1 \sin(\omega_m t - 90^\circ) \quad \text{---- (4.5)}$$

$$V_{cn} - V_{an} = \sqrt{3} \hat{V}_1 \sin(\omega_m t + 150^\circ) \quad \text{---- (4.6)}$$

Therefore, the currents flowing in each phase of the load would correspond to the fundamental harmonic voltages only. Should respective super-harmonics (harmonics of higher order than the fundamental components) in equations (4.1), (4.2) and (4.3) form balanced positive-sequence sets or balanced negative-sequence sets, 'no cancellation' will occur in the LINE to LINE voltage waveform. However, when respective super-harmonics in equations (4.1), (4.2) and (4.3) are unbalanced in 'phase' or 'magnitude' or both, 'partial cancellation' can occur.

Therefore, there remains two possible means of improving the harmonic spectra of the LINE to LINE voltage waveforms without the addition of extra power components:

(i) the amplitudes of the harmonics in the LINE to D.C. NEUTRAL voltage waveforms can be reduced, or (ii) the phase of respective harmonic components in the LINE to D.C. NEUTRAL voltage waveforms can be made equal or near equal such that

respective harmonics form zero-sequence sets which cancel in the LINE to LINE voltage waveforms. It has been shown in both Section (3.7) and Section (4.2) that the sampling process in prior-art p.w.m. power convertors is natural sampling. However, it was shown in Section (3.9) that there is an alternative sampling process known as 'regular sampling', which is common in communication systems, but which has not previously been applied to p.w.m. power convertors. It was therefore decided to investigate the application of regular sampling to the double-edge p.w.m. process, and observe whether regular sampling improves the harmonic spectra of the output p.w.m. voltage waveforms at low values of carrier frequency/modulating frequency ratio.

#### (4.3.1) Analytical Investigation Into Regular Sampled, Double-Edge P.W.M. Systems

Two forms of regular sampled double-edge p.w.m. were presented in Sections (3.9.3) and (3.9.4) of Chapter (3): (i) regular sampled symmetrical double-edge p.w.m. and (ii) regular sampled asymmetrical double-edge p.w.m. respectively. The generation of three-phase p.w.m. control waveforms from a single-phase carrier wave and three-phase regular sampled modulating waves by both these processes is achieved by comparing each phase of the regular sampled modulating wave with a single phase carrier wave, as described in Section (3.9). It is once again important to emphasise that when the p.w.m. control waveforms are made to drive the power convertor illustrated in Fig. (4.1) the switching instants of the control waveforms will be representative of the switching instants of

the LINE to D.C. NEUTRAL voltage waveforms of the power convertor. Therefore, computer programs were written which determined the switching instants of the p.w.m. waveforms and which calculated harmonic spectra for both the LINE to D.C. NEUTRAL voltage waveforms and LINE to LINE voltage waveforms. The details of the computer programs are included in Appendix ( 3).

(4.3.1.1) Odd Triple-Integer Values of  
Frequency Ratio

From the computed results shown in Figures: (4.12), (4.13), (4.14) and (4.15) and from further computed results for odd triple-integer values of frequency ratio given by:

$$\frac{f_c}{f_m} = 3(2n - 1)$$

the following conclusions can be drawn:

(i) Regular sampled, symmetrical double-edge p.w.m. is inferior to regular sampled asymmetrical double-edge p.w.m. because the symmetrical p.w.m. process introduces both even order and odd order harmonics in the LINE to LINE voltage spectra. The amplitude of the most significant harmonics (the harmonics nearest the fundamental) in the LINE to LINE voltage spectra are also considerably larger for the symmetrical p.w.m. process than for the asymmetrical p.w.m. process.

(ii) For both regular sampled, double-edge p.w.m. processes the triplen harmonics of order,  $3n$ , which existed in the LINE to D.C. NEUTRAL voltage waveforms, formed balanced zero-sequence sets, which will therefore cancel in the LINE to LINE voltage spectra when supplying a three-wire, three-phase load.

(iii) Respective harmonics which existed in the three LINE

Harmonic Order	Line To D.C. Neutral Components			Line to Line Components			Frequency Ratio $\frac{f_c}{f_m}$	Mod. Index.
	$V_{AN}$	$V_{BN}$	$V_{CN}$	$V_{AB}$	$V_{BC}$	$V_{CA}$		
D.C.	0.0	0.0	0.0	0.0	0.0	0.0		
1	100 / $-4^\circ$	100 / $-124^\circ$	100 / $116^\circ$	100 / $26^\circ$	100 / $-94^\circ$	100 / $146^\circ$		
2	58 / $26^\circ$	58 / $146^\circ$	58 / $-94^\circ$	58 / $-4^\circ$	58 / $116^\circ$	58 / $-124^\circ$		
3	72 / $-90^\circ$	72 / $-90^\circ$	72 / $-90^\circ$	0.0	0.0	0.0	3.0	1.0
4	52 / $52^\circ$	52 / $-68^\circ$	52 / $172^\circ$	52 / $82^\circ$	52 / $-38^\circ$	52 / $-158^\circ$		
5	43 / $-35^\circ$	43 / $85^\circ$	43 / $-155^\circ$	43 / $-65^\circ$	43 / $55^\circ$	43 / $175^\circ$		
6	0.0	0.0	0.0	0.0	0.0	0.0		
7	22 / $87^\circ$	22 / $-33^\circ$	22 / $-153^\circ$	22 / $117^\circ$	22 / $-3^\circ$	22 / $-123^\circ$		
8	32 / $-76^\circ$	32 / $44^\circ$	32 / $164^\circ$	32 / $-106^\circ$	32 / $14^\circ$	32 / $134^\circ$		
9	3 / $-90^\circ$	3 / $-90^\circ$	3 / $-90^\circ$	0.0	0.0	0.0		

FIG. (4.12) AMPLITUDE AND PHASE OF HARMONIC COMPONENTS OF LINE TO D.C. NEUTRAL VOLTAGE WAVEFORMS AND LINE TO LINE VOLTAGE WAVEFORMS FOR REGULAR SAMPLED SYMMETRICAL DOUBLE-EDGE P.W.M

Voltage Waveforms	Sampling Process	Phase Sequence	Harmonic Order											
			1	2	3	4	5	6	7	8	9			
Line To D.C. Neutral	Regular	Reference	$X_B$			$X_B$								
		Reverse		$X_B$				$X_B$						
		In Phase			$X_B$								$X_B$	
Line to Line	Regular	Reference	$X_B$			$X_B$								
		Reverse		$X_B$				$X_B$					$X_B$	
		In Phase			$X_B$									$X_B$

$X_B$  - Balanced Sequence Components

$X_u$  - Unbalanced " "

FIG. (4.13) PHASE SEQUENCE CHART FOR RESPECTIVE HARMONICS OF LINE TO D.C. NEUTRAL VOLTAGE WAVEFORMS AND LINE TO LINE VOLTAGE WAVEFORM FOR REGULAR SAMPLED, SYMMETRICAL DOUBLE-EDGE P.W.M.

Harmonic Order	Line To D.C. Neutral Components				Line To Line Components			Frequency Ratio $\frac{f_c}{f_m}$	Mod. Index.
	V <sub>AN</sub>	V <sub>BN</sub>	V <sub>CN</sub>	V <sub>AB</sub>	V <sub>BC</sub>	V <sub>CA</sub>			
D.C.	0.0	0.0	0.0	0.0	0.0	0.0	0.0		
1	100/ <u>-30°</u>	100/ <u>-150°</u>	100/ <u>90°</u>	100/ <u>0°</u>	100/ <u>-120°</u>	100/ <u>120°</u>			
2	0.0	0.0	0.0	0.0	0.0	0.0			
3	55/ <u>-90°</u>	55/ <u>-90°</u>	55/ <u>-90°</u>	0.0	0.0	0.0			
4	0.0	0.0	0.0	0.0	0.0	0.0	3.0	1.0	
5	7/ <u>-150°</u>	7/ <u>-30°</u>	7/ <u>90°</u>	7/ <u>-180°</u>	7/ <u>-60°</u>	7/ <u>60°</u>			
6	0.0	0.0	0.0	0.0	0.0	0.0			
7	32/ <u>150°</u>	32/ <u>30°</u>	32/ <u>-90°</u>	32/ <u>-180°</u>	32/ <u>60°</u>	32/ <u>-60°</u>			
8	0.0	0.0	0.0	0.0	0.0	0.0			
9	2/ <u>-90°</u>	2/ <u>-90°</u>	2/ <u>-90°</u>	0.0	0.0	0.0			

FIG. (4.14) AMPLITUDE AND PHASE OF HARMONIC COMPONENTS OF LINE TO D.C. NEUTRAL VOLTAGE WAVEFORMS AND LINE TO LINE VOLTAGE WAVEFORMS FOR REGULAR SAMPLED ASYMMETRICAL DOUBLE-EDGE P.W.M.

Voltage Waveforms	Sampling Process	Phase Sequence	Harmonic Order																
			1	2	3	4	5	6	7	8	9								
Line To D.C.Neutral	Regular	Reference	$X_B$																
		Reverse					$X_B$												
		In Phase							$X_B$										
Line To Line	Regular	Reference	$X_B$																
		Reverse								$X_B$									
		In Phase																	

$X_B$  - Balanced Sequence Components

$X_u$  - Unbalanced " " "

FIG. (4.15) PHASE SEQUENCE CHART FOR RESPECTIVE HARMONICS OF LINE TO D.C. NEUTRAL VOLTAGE WAVEFORMS AND LINE TO LINE VOLTAGE WAVEFORMS FOR REGULAR SAMPLED ASYMMETRICAL DOUBLE-EDGE P.W.M.



to LINE voltage waveforms of order:  $(3n - 2)$  and  $(3n - 1)$ , formed balanced positive-sequence sets and balanced negative-sequence sets respectively.

When the computed results for the natural sampled double-edge p.w.m. process illustrated in Fig.(4.4) are compared with the computed results illustrated in Fig.(4.12) and Fig.(4.14), it is immediately apparent that the regular sampled asymmetrical double-edge p.w.m. process is superior to both the natural sampled double-edge p.w.m. process and the regular sampled symmetrical double-edge p.w.m. process. It is equally apparent that the regular sampled, symmetrical double-edge p.w.m. process is inferior to the natural sampled double-edge p.w.m. process.

#### (4.3.1.2) Even Triple-Integer Values of Frequency Ratio

From the computed results for even triple-integer values of frequency ratio given by:

$$\frac{f_c}{f_m} = 3(2n),$$

the following conclusions became apparent.

(i) Regular sampled, asymmetrical p.w.m. is superior to regular sampled symmetrical p.w.m. because it considerably reduces the amplitude of the most significant harmonics in the LINE to LINE voltage spectra.

(ii) Respective harmonics of order,  $3n$ , in the LINE to D.C. NEUTRAL voltage waveforms again formed balanced zero-sequence sets, which therefore cancelled in the LINE to LINE voltage waveforms.

(iii) Respective harmonics in the LINE to LINE voltage waveforms of order:  $(3n - 2)$  and  $(3n - 1)$  again formed

balanced positive-sequence sets and balanced negative-sequence sets respectively.

The regular sampled, asymmetrical double-edge p.w.m. process was again found to be significantly superior to the natural sampled double-edge p.w.m. process, however, the regular sampled, symmetrical double-edge p.w.m. process was again found to be inferior to the natural sampled double-edge p.w.m. process.

#### (4.3.1.3) Odd Non-triple Integer Values of Frequency Ratio

The odd non-triple integer values of frequency ratio are given by:

$$\frac{f_c}{f_m} = 3n + \frac{1}{2} [3 - (-1)^n],$$

From the computed results for these values of frequency ratio, the following conclusions were drawn:

(i) Regular sampled, asymmetrical double-edge p.w.m. is again superior to the regular sampled, symmetrical double-edge p.w.m. process because the symmetrical p.w.m. process introduced both even order and odd order harmonics in the LINE to D.C. NEUTRAL voltage waveform, whereas, the asymmetrical p.w.m. process introduced odd order harmonics only in the LINE to D.C. NEUTRAL voltage waveforms.

(ii) The amplitudes of the most significant harmonics in the LINE to LINE voltage for the asymmetrical double-edge p.w.m. process, were considerably less than the amplitude of corresponding harmonics for the symmetrical double-edge p.w.m. process.

It is of considerable importance to add that both regular

sampled p.w.m. processes, completely eradicated the 'amplitude' and 'phase' unbalance of the fundamental harmonic components, which occurred in the natural sampled, double-edge p.w.m. process, for these values of frequency ratio. It was again observed from the computed results that the regular sampled, asymmetrical double-edge p.w.m. process was considerably superior to both the regular sampled, symmetrical double-edge p.w.m. process and the natural sampled double-edge p.w.m. process. However, the voltage harmonic spectra for the regular sampled symmetrical p.w.m. process were again considerably inferior to the voltage harmonic spectra of the natural sampled double-edge p.w.m. process.

(4.3.1.4) Even Non-triple Integer Values of Frequency Ratio

These values of frequency ratio are given by:

$$\frac{f_c}{f_m} = 3n - \frac{1}{2} [3 + (-1)^n],$$

From the computed results for these values of frequency ratio, the following conclusions became apparent:

(i) Regular sampled, asymmetrical double-edge p.w.m. was again superior to regular sampled, symmetrical double-edge p.w.m. because it reduced the amplitudes of the most significant harmonic components.

(ii) The regular sampled, asymmetrical p.w.m. process also eliminated the d.c. components from the LINE to LINE voltage waveforms which occurred in the natural sampled double-edge p.w.m. process.

(iii) The amplitude and phase unbalance of the wanted harmonic components which occurred in the natural sampled,

double-edge p.w.m. process were completely eradicated by the regular sampled asymmetrical double-edge p.w.m. process.

#### (4.3.1.5) Interim Conclusions

The analytical investigation has demonstrated that the novel regular sampled, asymmetrical double-edge p.w.m. process, is considerably superior to both the novel regular sampled, symmetrical double-edge p.w.m. process and the prior-art natural sampled, double-edge p.w.m. process for all values of integer frequency ratio. However, the novel regular sampled, symmetrical double-edge p.w.m. process was found to be inferior to the prior-art natural sampled double-edge p.w.m. process for all integer values of frequency ratio.

#### (4.3.2) Experimental Investigation Into the Regular Sampled Asymmetrical Double-Edge P.W.M. Process

Because this novel p.w.m. process has been found to be considerably superior to the prior-art, natural sampled double-edge p.w.m. process, it was decided to investigate this process experimentally and compare the experimental results with the experimentally determined results for the natural sampled double-edge p.w.m. process presented in Section (4.2.2).

##### (4.3.2.1) Control Circuit for Regular Sampled Asymmetrical Double-Edge P.W.M.

The regular sampled asymmetrical double-edge p.w.m. control waveform (or switching function) was achieved by the circuit represented in block diagram form in Fig.(4.16). A schematic

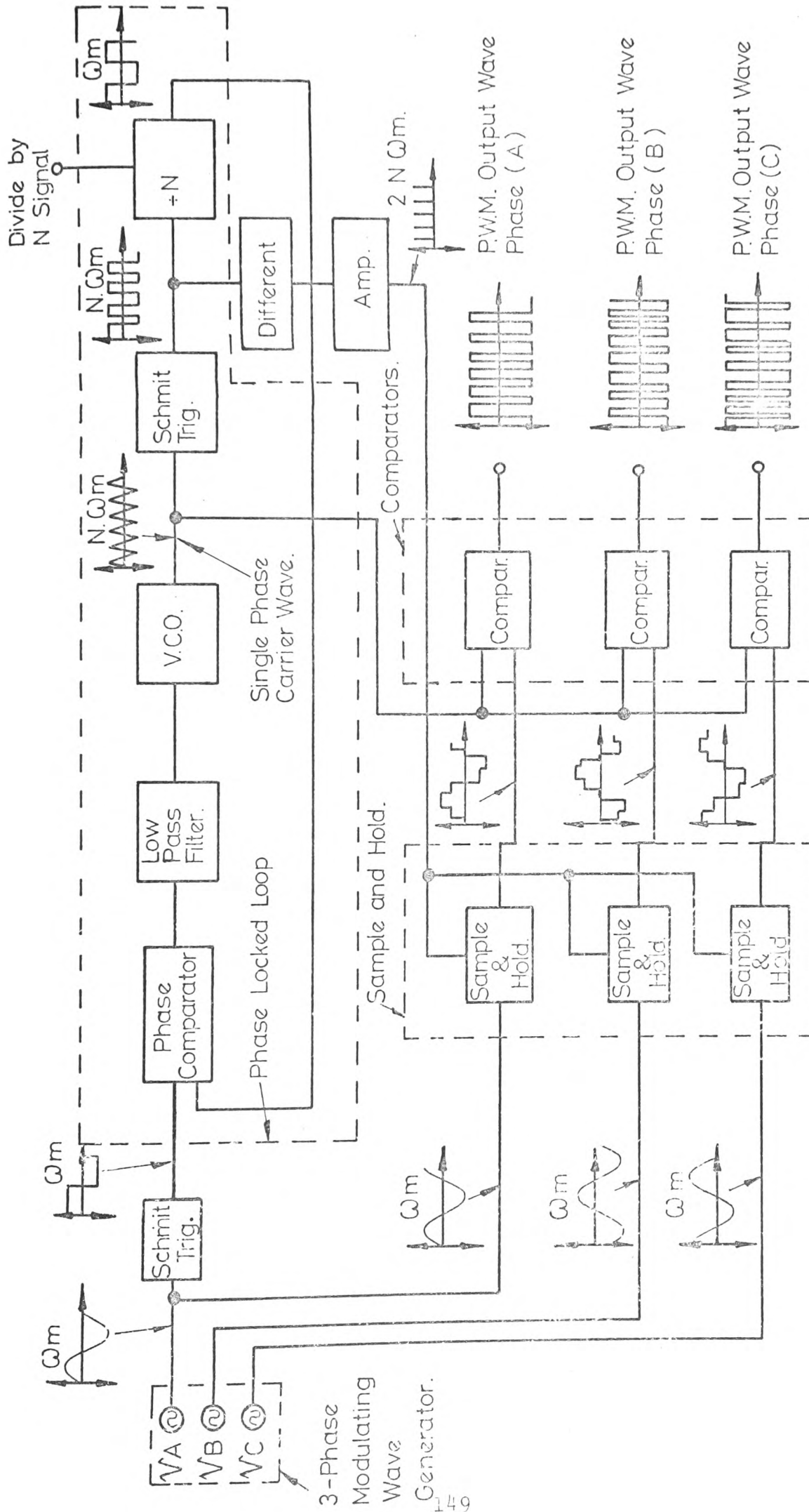
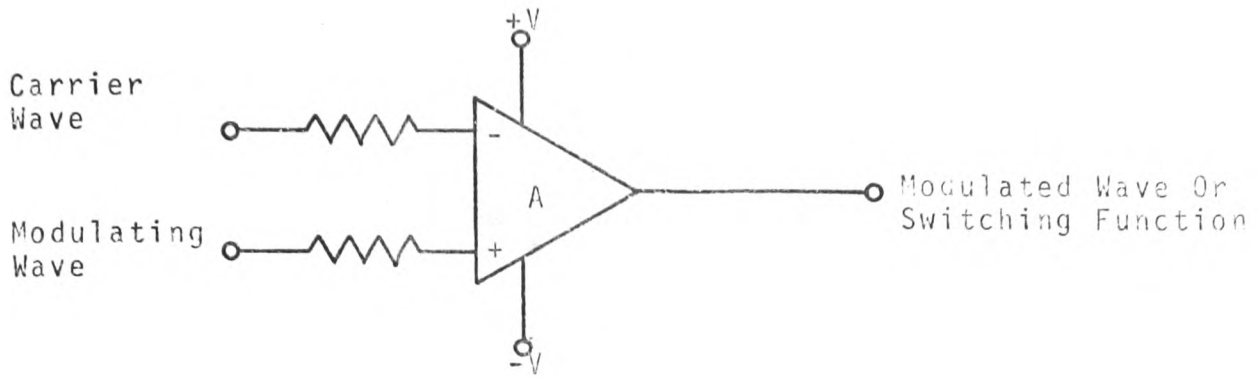


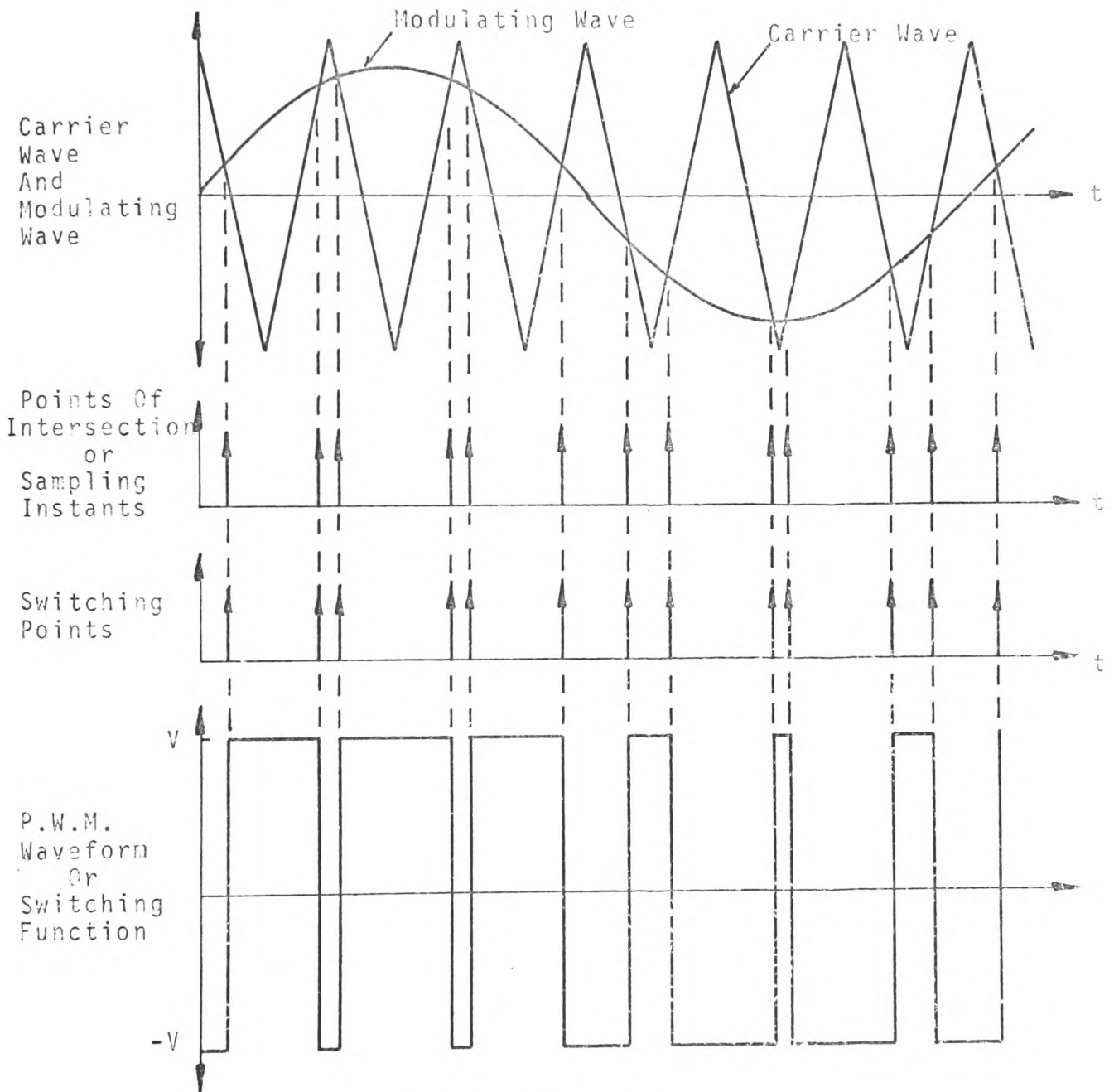
FIG.(4.16) BLOCK DIAGRAM OF CONTROL CIRCUIT FOR REGULARLY SAMPLED ASYMMETRICAL DOUBLE-EDGE PWM.

diagram of this circuit is included in Appendix (4), It may be seen from Fig.(4.16) that the control circuit mainly consists of: a three-phase signal generator, a phase-locked loop, three sampled-and-hold circuits and three voltage comparator circuits. The three-phase modulating wave generator supplies three output waveforms displaced in time-phase by  $-120^\circ$  and  $120^\circ$  respectively, where both the amplitude and frequency of the output waveforms can be varied. The phase-locked-loop generates a triangular carrier wave which is synchronised with the PHASE (A) output wave of the modulating wave generator and is at 'N' times its frequency ( $N.\omega_m$ ). The three sampled-and-hold circuits regularly samples the three output modulating waves at twice the frequency of the triangular carrier wave ( $2N.\omega_m$ ). The three regular sampled modulating waves are then compared with the single-phase triangular carrier wave in the three comparators circuits. The three p.w.m.control output waveforms (or p.w.m.switching functions) are then made to supply three  $1\text{ k}\Omega$  resistors connected in star as for the natural sampled control circuit presented in Section (4.2.2).

It is of considerable importance at this point to re-emphasise, that in prior-art p.w.m.power convertors, the control waveform (or switching function) has been achieved by making a direct comparison between the sinusoidal modulating wave and the triangular carrier wave as illustrated in Fig.(4.17). However, it may be seen from Fig.(4.18) that the novel regular sampled asymmetrical double-edge p.w.m. control wave is realized by comparing the triangular carrier

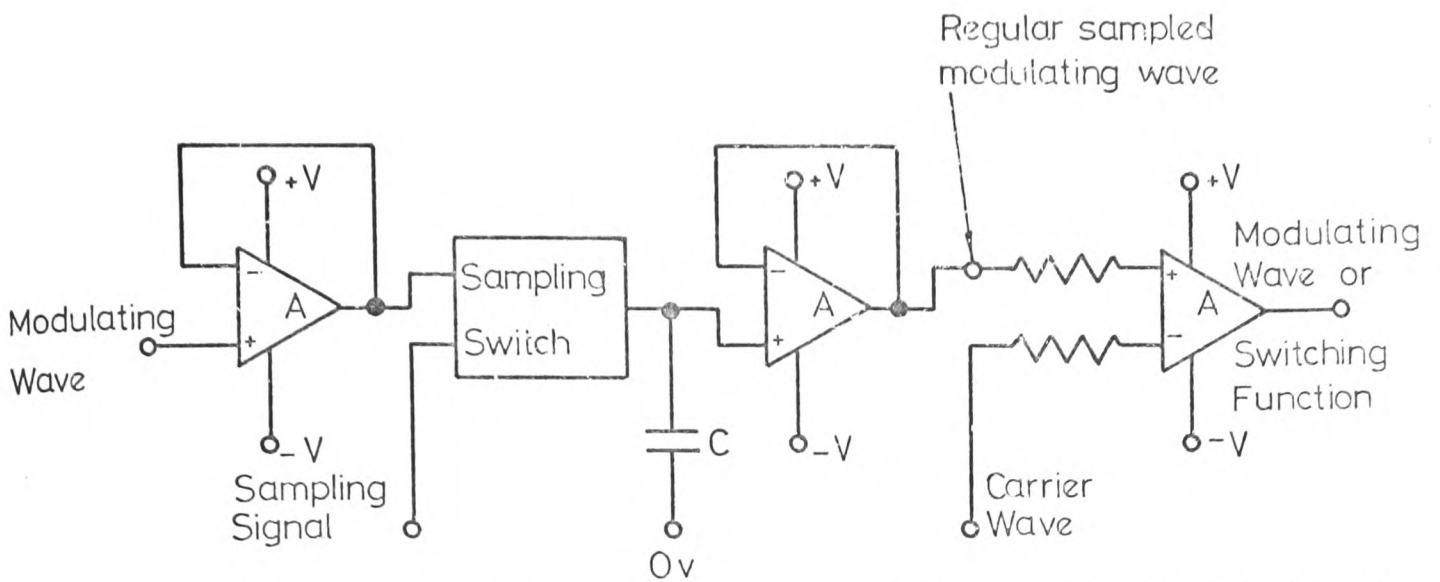


(a) Comparator Circuit

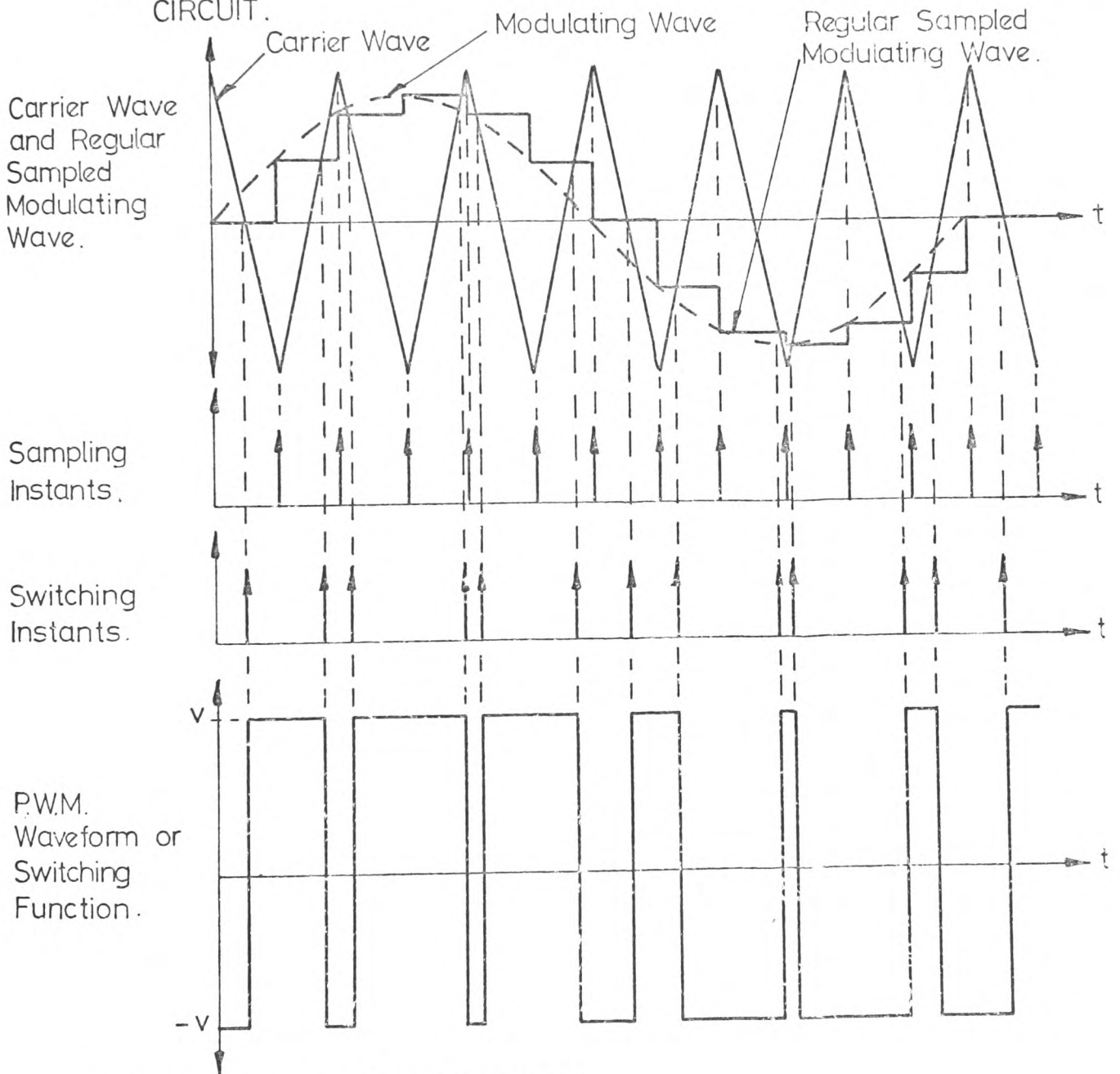


(b) P.W.M. Modulation Process

FIG(4.17) NATURAL SAMPLED DOUBLE-EDGE P.W.M. PROCESS



(a) REGULAR SAMPLED ASYMMETRICAL DOUBLE-EDGE MODULATING CIRCUIT.



(b) P.W.M. MODULATION PROCESS

(4.18) REGULAR SAMPLED ASYMMETRICAL DOUBLE-EDGE P.W.M. PROCESS



wave with the regular sampled modulating wave. This process which is shown in Fig.(4.18) is achieved by the inclusion of only one sample-and-hold circuit per phase, between the modulating wave generator and the comparator circuit. When; one cycle of the natural sampled double-edge p.w.m. waveform is compared with a corresponding cycle of the regular sampled asymmetrical double-edge p.w.m. waveform (Fig.(4.19)), it is immediately apparent that the symmetry of the two waveforms is different. It is this change in the symmetry of the p.w.m. waveform resulting from the regular sampling process which improves the harmonic spectrum of the p.w.m. output waveform. The degree of superiority of the harmonic spectra for the regular sampled asymmetrical double-edge p.w.m. system for the various values of integer frequency ratio, will be enlarged upon in the following Sections of this chapter.

#### (4.3.2.2) Harmonic Spectra

The harmonic spectra presented in the succeeding Sections of this Chapter are for the three LINE to D.C. NEUTRAL voltages, and the three LINE to LINE voltages, as illustrated in Fig. (4.1). The measurements technique used to determine the 'magnitude' and 'phase' of each harmonic component is the same as that described in Section (4.2.2.1). It is important to note that in the spectral diagrams for each of the three LINE to D.C. NEUTRAL voltages, the amplitude of each harmonic component is expressed as a percentage of the amplitude of the fundamental harmonic component of the LINE (A) to D.C. NEUTRAL voltage. Similarly the amplitude of each harmonic component of the three LINE to LINE voltages is expressed as

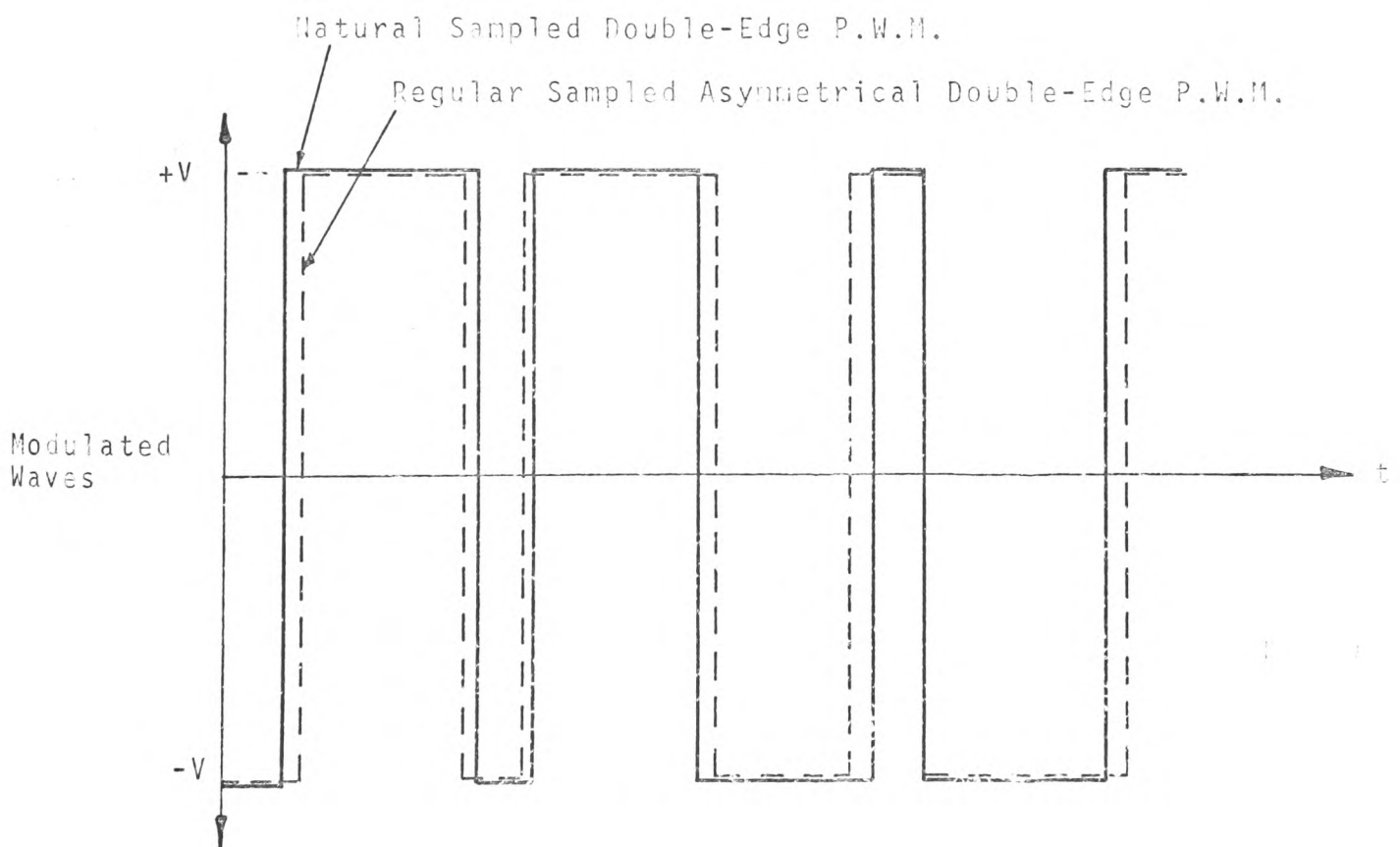
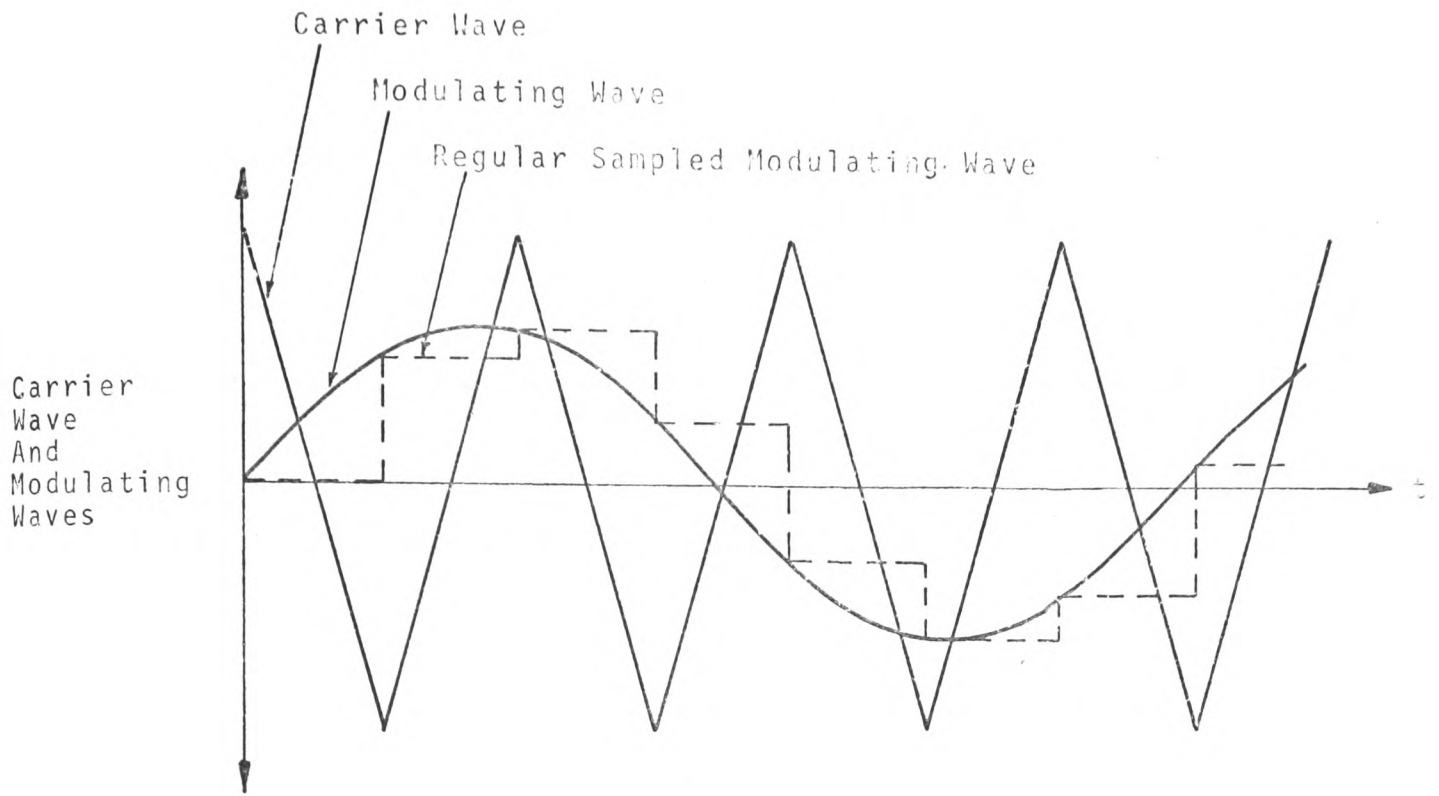


FIG.(4.19) COMPARISON OF NATURAL SAMPLED DOUBLE-EDGE P.W.M. WITH REGULAR SAMPLED ASYMMETRICAL DOUBLE-EDGE P.W.M.

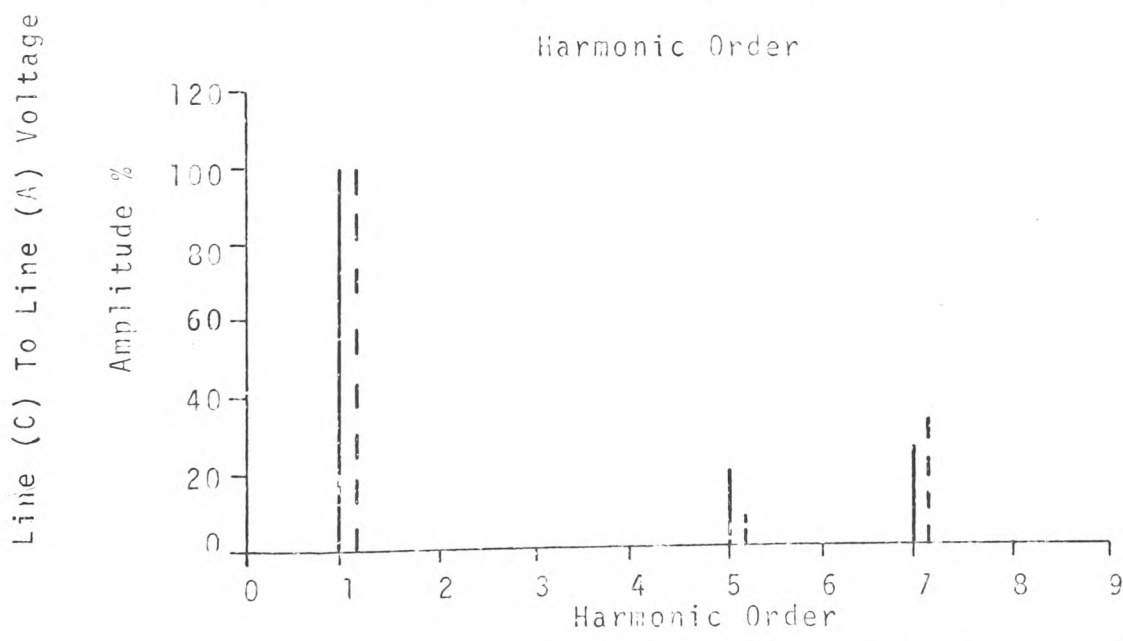
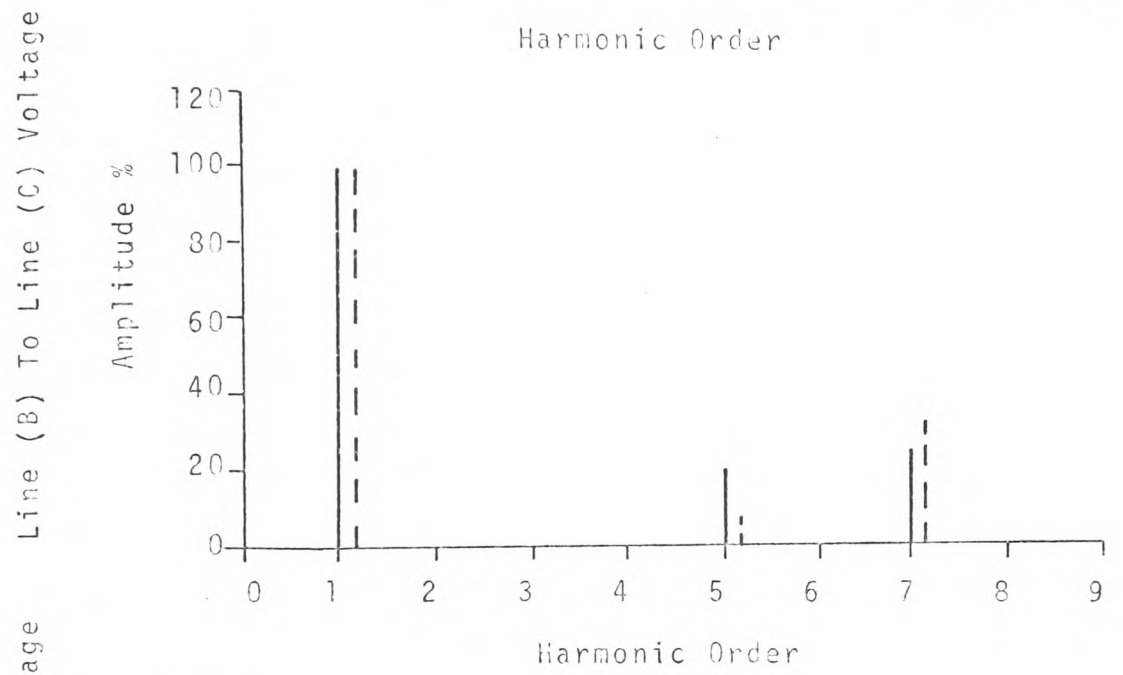
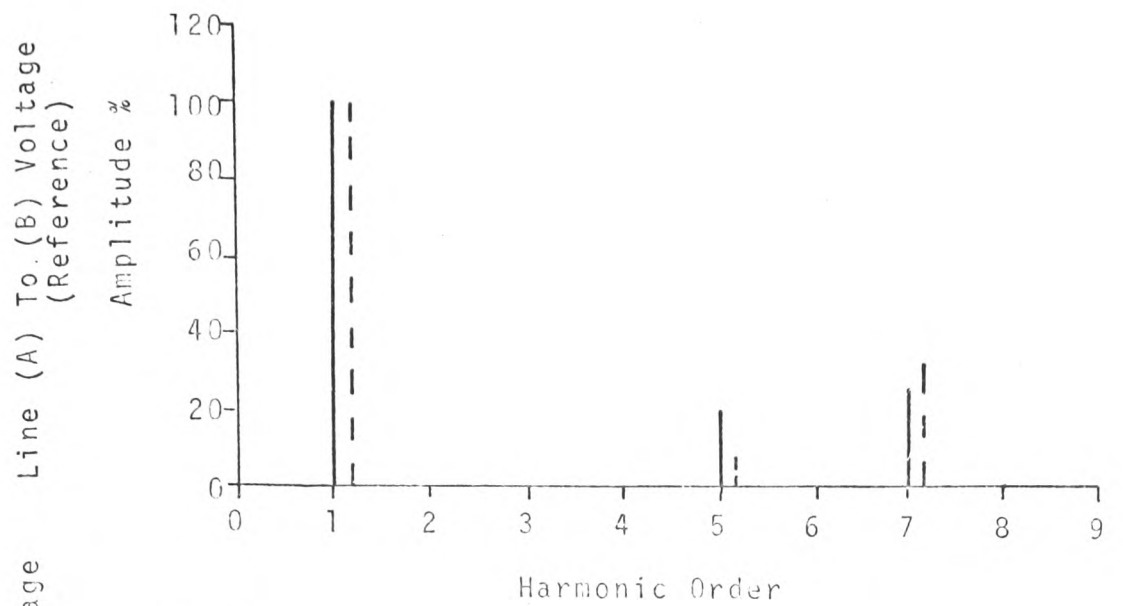
a percentage of the amplitude of the fundamental harmonic component of the LINE (A) to LINE (B) voltage.

(4.3.2.2a) Odd Triple-Integer Frequency  
Ratio's

It is of particular interest to observe from the harmonic spectra illustrated in Fig.(4.20) and the phase-sequence chart shown in Fig.(4.21) which are both for the LINE to LINE voltage waveforms, that the wanted harmonic components form balanced positive- sequence sets and that all triplen harmonics do in fact cancel. It is also quite evident that respective harmonics of order  $(3n - 1)$  and  $(3n - 2)$  respectively, do not cancel. What is also of considerable importance is that the most significant harmonic (the 5th) is reduced by 12%. It is important to note that this reduction in the amplitude of the most significant harmonic is not due to partial cancellation in the LINE to LINE voltage, but is entirely due to the regular sampled asymmetrical double-edge p.w.m.process. This property of the regular sampled asymmetrical double-edge p.w.m.process of always reducing the amplitude of the most significant harmonic components is illustrated further by Fig.(4.22).

(4.3.2.2b) Even Triple-Integer Frequency  
Ratio's

It is again of particular interest to note from the harmonic spectra illustrated in Fig. (4.23), that the most significant harmonic for the natural sampled double-edge p.w.m.process is the 'second' which has an amplitude of 4%, while the next most significant harmonic component is the 'fourth' which has an amplitude of 34%. However, for the



————— Natural Sampled Double-Edge P.W.M.  
 - - - - - Regular Sampled Asymmetrical Double-Edge P.W.M.

FIG.(4.20) HARMONIC SPECTRA FOR LINE TO LINE VOLTAGE WAVEFORM FOR FREQUENCY RATIO OF 3 AND MODULATION INDEX OF 1.0

Sampling Process	Phase Sequence	Harmonic Order												
		1	2	3	4	5	6	7	8	9				
Natural	Reference	$X_B$												
	Reverse					$X_B$						$X_B$		
	In Phase													
Regular	Reference	$X_B$										$X_B$		
	Reverse									$X_B$				
	In Phase													

$X_B$  - Respective Harmonic Component Form Balanced Sequence Sets.

FIG. (4.21) PHASE SEQUENCE OF RESPECTIVE LINE TO LINE VOLTAGE HARMONICS FOR FREQUENCY RATIO OF 3 AND MODULATION INDEX OF 1.0.

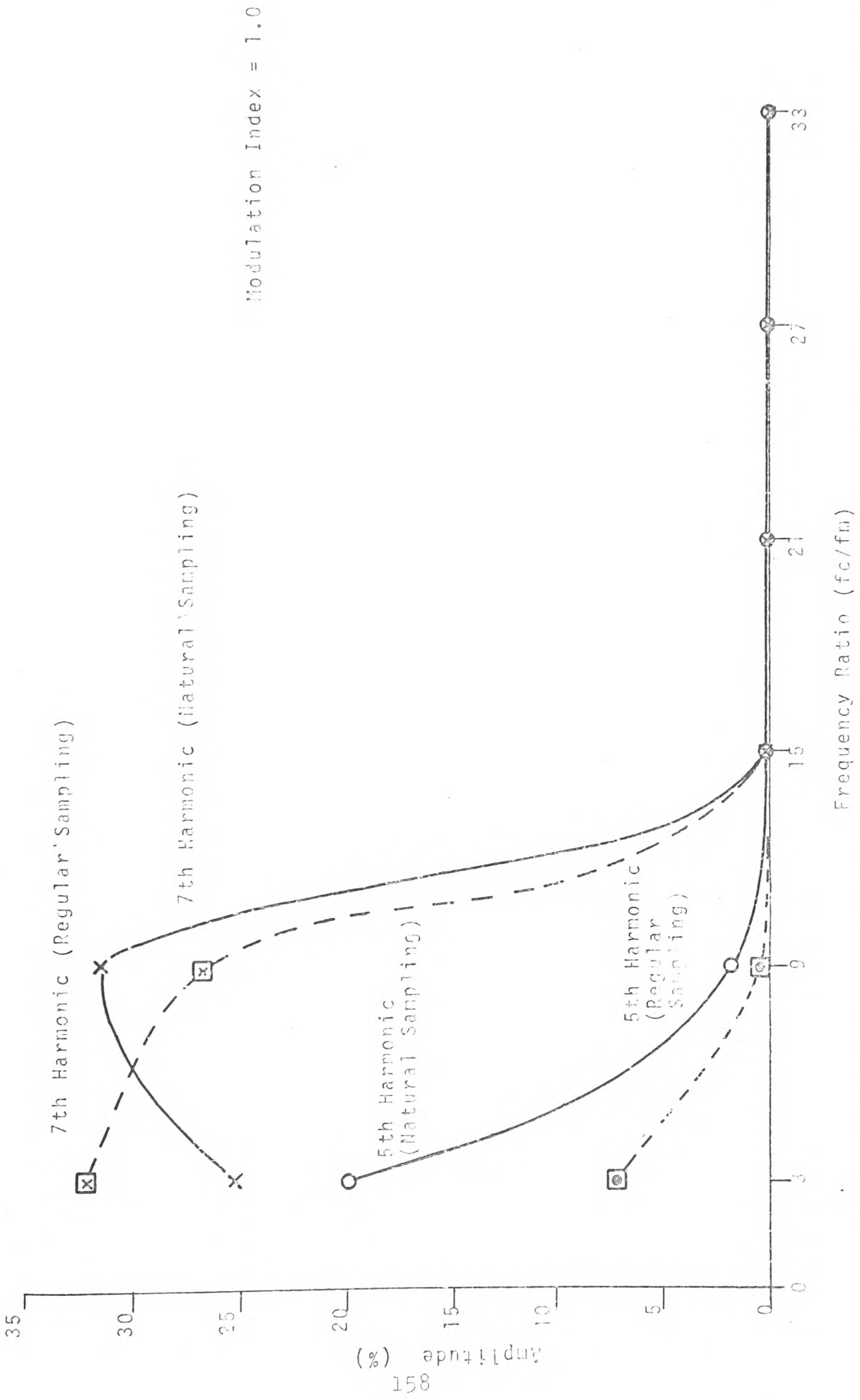
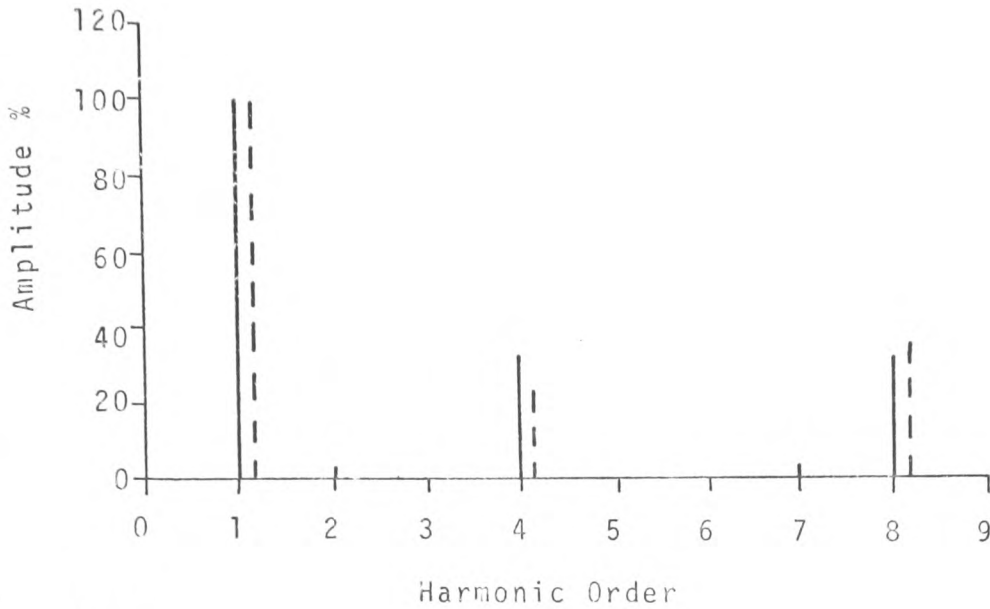
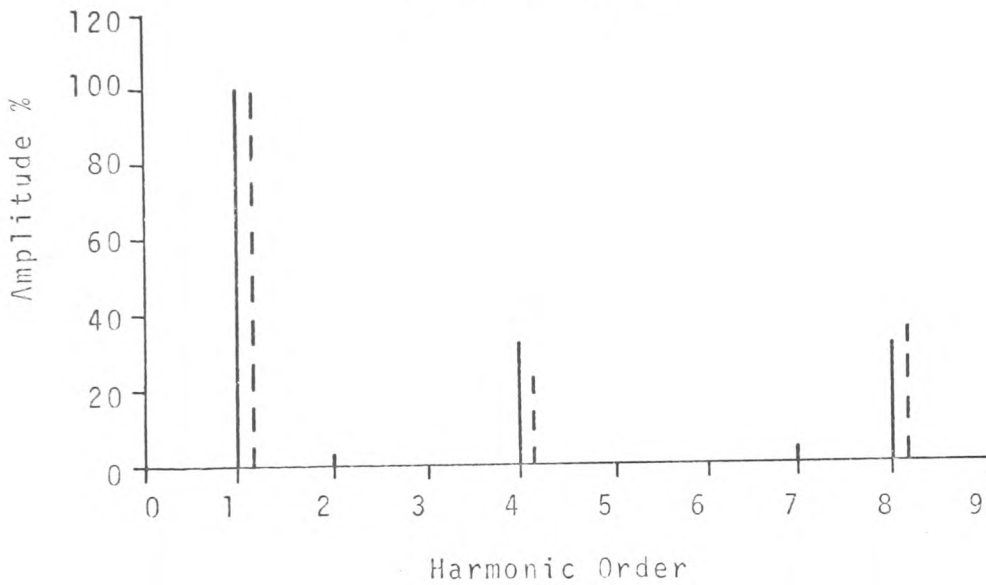


FIG. (4.22) VARIATION IN PERCENTAGE AMPLITUDE OF 5TH AND 7TH HARMONICS WITH FREQUENCY RATIO FOR NATURAL SAMPLED DOUBLE-EDGE P.W.M. AND REGULAR SAMPLED ASYMMETRICAL DOUBLE-EDGE P.W.M.

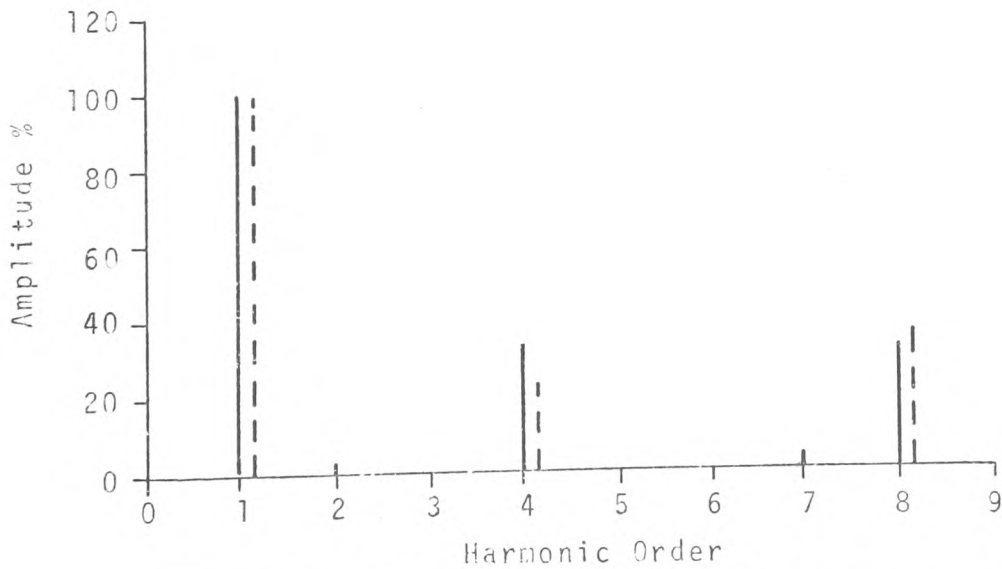
Line (A) To Line (B) Voltage  
(Reference)



Line (B) To Line (C) Voltage



Line (C) To Line (A) Voltage



—————

Natural Sampled Double-Edge P.W.M.

- - - - -

Regular Sampled Asymmetrical Double-Edge P.W.M.

FIG.(4.23) HARMONIC SPECTRA FOR LINE TO LINE VOLTAGE WAVEFORM FOR FREQUENCY RATIO OF 5 AND MODULATION INDEX OF 1.0

Sampling Process	Phase Sequence	Harmonic Order								
		1	2	3	4	5	6	7	8	9
Natural	Reference	$X_B$			$X_B$			$X_B$		
	Reverse		$X_B$						$X_B$	
	In Phase									
Regular	Reference	$X_B$			$X_B$					
	Reverse								$X_B$	
	In Phase									

$X_B$  - Respective Harmonic Components Form Balanced Sequence Sets.

FIG. (4.24) PHASE SEQUENCE OF RESPECTIVE LINE TO LINE VOLTAGE HARMONICS FOR FREQUENCY RATIO OF 6 AND MODULATION INDEX OF 1.0



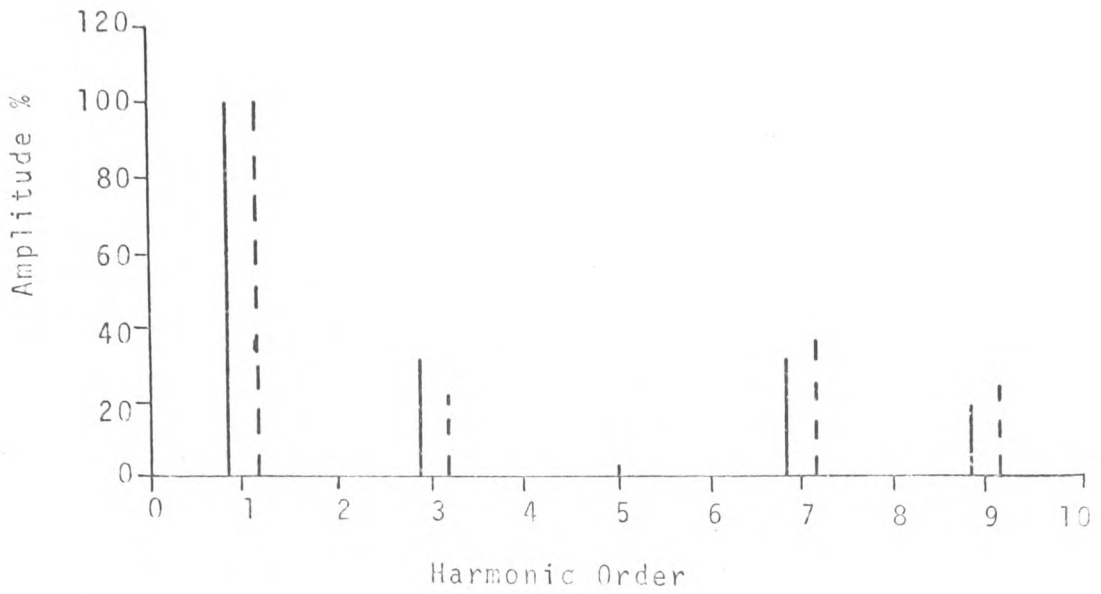
regular sampled asymmetrical double-edge p.w.m. process it may be seen that the harmonic of most significance is the 'fourth' which has an amplitude of 24%. It may also be seen from Fig.(4.23) that triplen harmonics do in fact cancel in the LINE to LINE voltage, while harmonic components of order  $(3n - 2)$  and  $(3n - 1)$  respectively, do not cancel.

It may therefore be concluded that for even triple-integer multiple values of frequency ratio, regular sampled asymmetrical double-edge p.w.m. is superior to the natural sampled double-edge p.w.m. process because it once again reduces the amplitude of the most significant harmonic components.

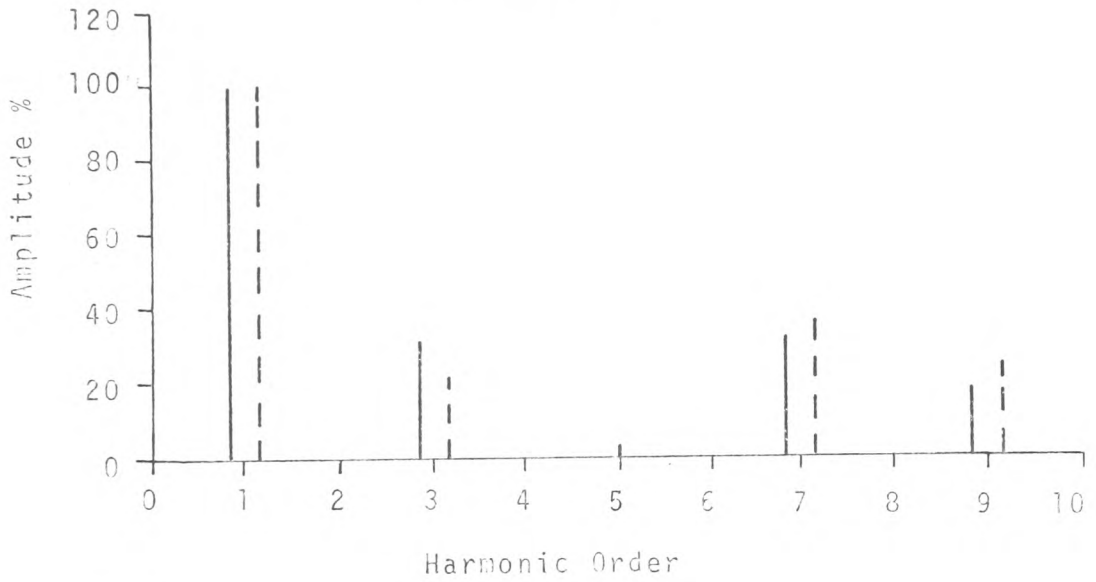
(4.3.2.2c) Odd-Non-Triple-Integer  
Frequency-Ratio's

The results shown in Figures (4.25) and (4.26) illustrates that for the natural sampled double-edge p.w.m. process, amplitude unbalance of 2% occurs between the fundamental components of the three respective LINE to LINE voltage waveforms. It may also be seen that the amplitudes of the 5th harmonics have been reduced to approximately 4% by partial cancellation. However, it is also evident that no three harmonics of the same order in the three respective LINE to LINE voltage waveforms produce balanced sequence sets. Whereas, for the regular sampled asymmetrical double-edge p.w.m. process it is quite evident that the respective fundamental components form balanced positive-sequence sets, 'third' harmonic components form balanced positive-sequence sets and the 'seventh' harmonic components form balanced negative-sequence sets:

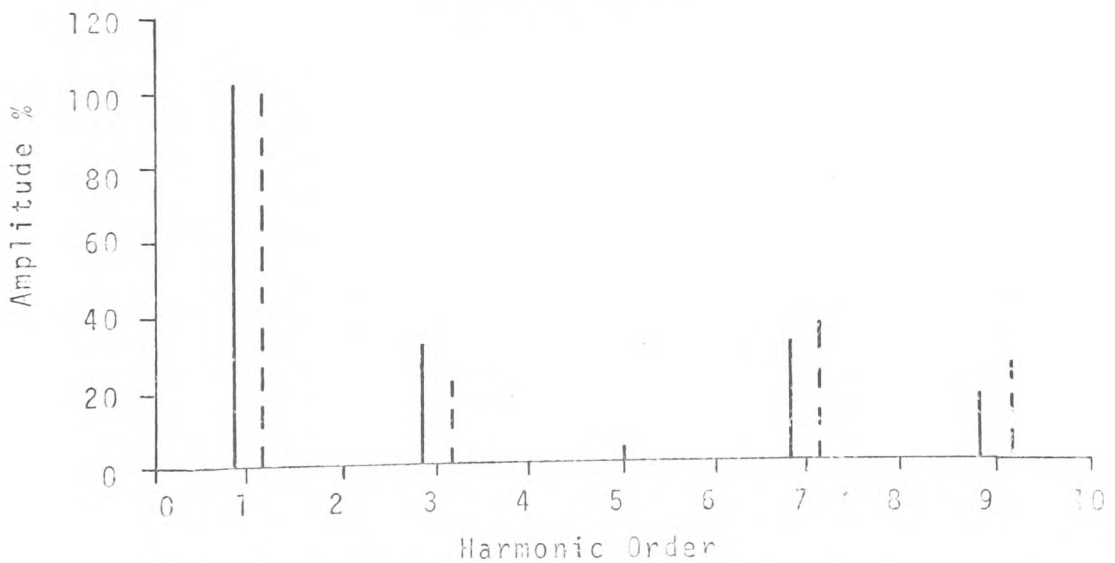
Line (A) To Line (B) Voltage  
(Reference)



Line (B) To Line (C) Voltage



Line (C) To Line (A) Voltage



\_\_\_\_\_ Natural Sampled Double-Edge P.W.M.  
 - - - - - Regular Sampled Asymmetrical Double-Edge P.W.M.

FIG. (4.25) HARMONIC SPECTRA FOR LINE TO LINE VOLTAGE WAVEFORM FOR FREQUENCY RATIO OF 5 AND MODULATION INDEX OF 1.0

Sampling Process	Phase Sequence	Harmonic Order												
		1	2	3	4	5	6	7	8	9				
Natural	Reference	Xu		Xu		Xu								
	Reverse							Xu						Xu
	In Phase													
Regular	Reference	X <sub>B</sub>						X <sub>B</sub>						
	Reverse											X <sub>B</sub>		X <sub>B</sub>
	In Phase													

X<sub>B</sub> - Respective Harmonic Components Form Balanced Sequence Sets

Xu - " " " Unbalanced " "

FIG. (4.26) PHASE SEQUENCE OF RESPECTIVE LINE TO LINE VOLTAGE HARMONICS FOR FREQUENCY RATIO OF 5 AND MODULATION INDEX OF 1.0

It is also of considerable importance to note once again that the regular sampled asymmetrical double-edge p.w.m.process reduces the amplitude of the most significant harmonics: the 'third' by 10% while the 'fifth' is completely eliminated.

(4.3.2.2d) Even Non-Triple Integer  
Frequency Ratio's

It is of considerable importance to note from the LINE to LINE voltage spectra and the LINE to LINE harmonic sequence charts illustrated in Figures (4.27) and (4.28) respectively that:

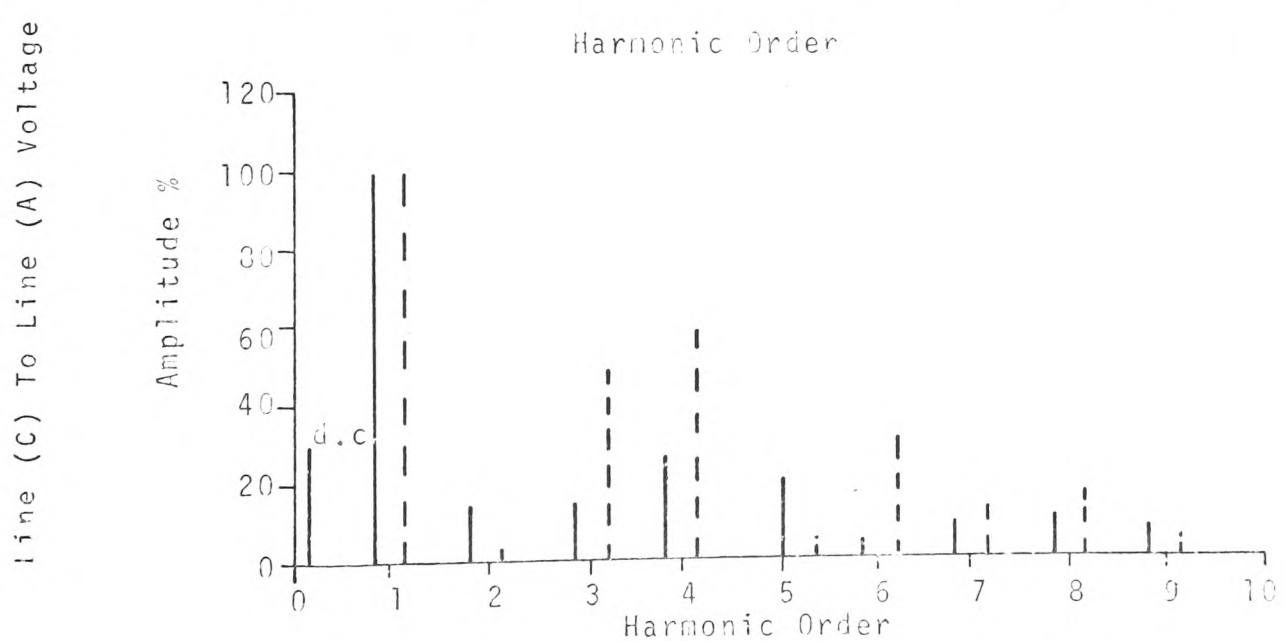
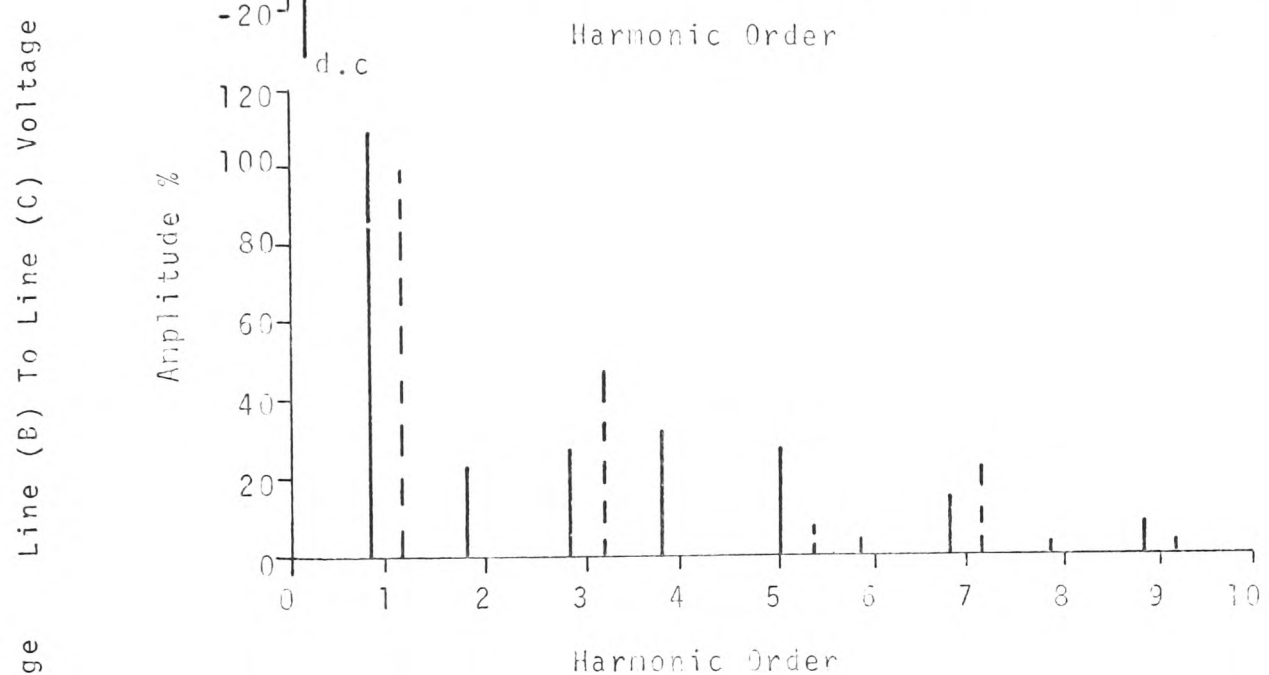
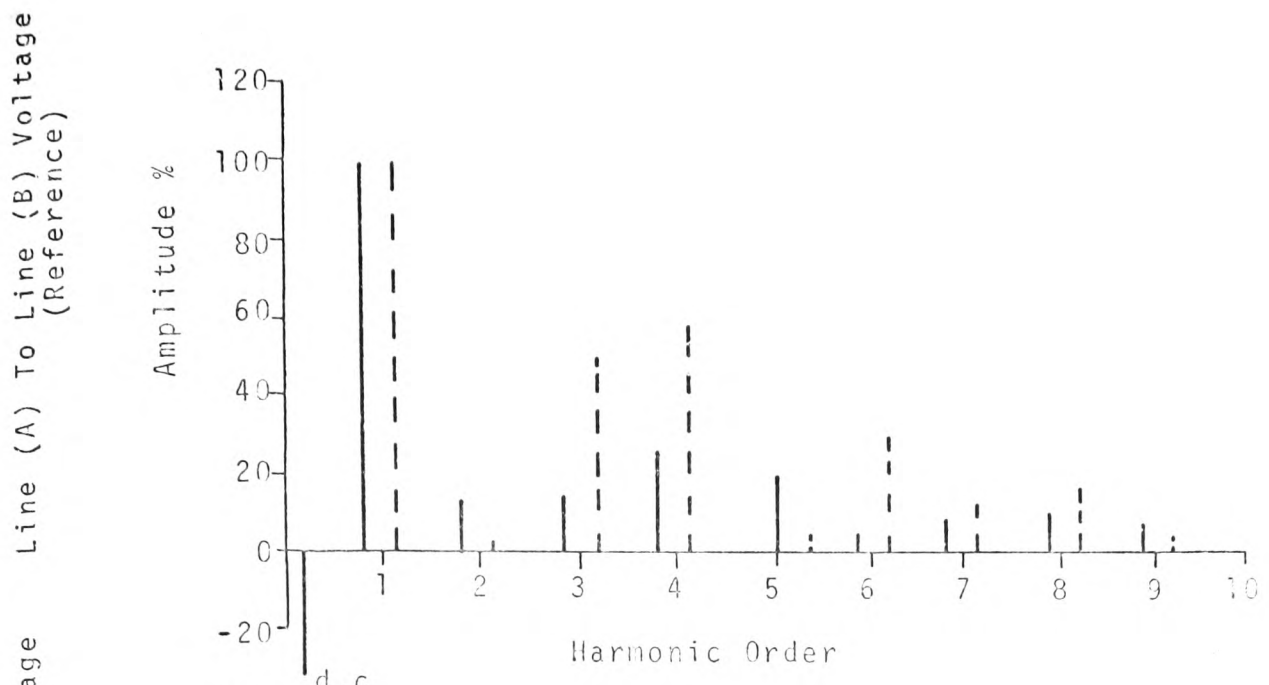
(i) D.C. Components of 29% in amplitude can exist in the LINE to LINE voltage waveform for the natural sampled system, whereas, such components are completely eliminated in the regular sampled system.

(ii) For the regular sampled asymmetrical double-edge p.w.m.process the fundamental harmonic components form a balanced positive-sequence set. However, for the natural sampled double-edge p.w.m.process, the fundamental components form an unbalanced positive-sequence set where the amplitude unbalance alone can amount to 11%.

(iii) The regular sampled asymmetrical double-edge p.w.m. process again reduces the amplitude of the most significant harmonic (the second) by approximately 11%. when compared with the natural sampled system.

(4.3.3) Amplitude Control of the Fundamental  
Harmonic Components

It has been shown earlier, that an essential requirement of a power modulator intended for induction motor speed



— Natural Sampled Double-Edge P.W.M.  
 - - - Regular Sampled Asymmetrical Double-Edge P.W.M.

FIG.(4.27) HARMONIC SPECTRA FOR LINE TO LINE VOLTAGE WAVEFORM FOR FREQUENCY RATIO OF 2 AND MODULATION INDEX OF 1.0  
 165

Sampling Process	Phase Sequence	Harmonic Order													
		1	2	3	4	5	6	7	8	9					
Natural	Reference	Xu				Xu									Xu
	Reverse		Xu		Xu			Xu			Xu			Xu	
	In Phase														
Regular	Reference	X <sub>B</sub>										Xu			
	Reverse					Xu				Xu					Xu
	In Phase														

X<sub>B</sub> - Respective Harmonic Components Form Balanced Sequence Sets  
 Xu - " " " " Unbalanced "

FIG. (4.28) PHASE SEQUENCE OF RESPECTIVE LINE TO LINE VOLTAGE HARMONICS FOR FREQUENCY RATIO OF 2 AND MODULATION INDEX OF 1.0

control systems, is that both the frequency and magnitude of the wanted harmonic components be variable. For constant torque applications the ratio of the magnitude of the wanted harmonic component to its frequency must be maintained approximately constant. It was shown in Section (3.3) that for the natural sampled double-edge p.w.m. process, the magnitude of the wanted harmonic component is proportional to the peak-value of the modulating wave. It may be seen from Fig.(4.29) that for both the natural sampled double-edge p.w.m. process and the regular sampled asymmetrical double-edge p.w.m. process that the amplitude of the wanted harmonic component is directly proportional to the modulation index for all values of integer frequency ratio.

#### (4.4) Interim Conclusions

From the results presented in this chapter and further results which have been determined, the following conclusions can be drawn:

(i) For odd and even triple-integer values of frequency ratio, fundamental relationships relating the phase-sequence of respective harmonics in the LINE to D.C. NEUTRAL voltage waveform or LINE to LINE voltage waveform have become evident.

(ii) For non-triple integer values of frequency ratio no relationship appears to exist for the phase-sequence of respective harmonics in the LINE to D.C. NEUTRAL voltage nor in the LINE to LINE voltage.

(iii) Complete cancellation of harmonics in the LINE to LINE voltage can only be achieved when harmonics of the same order form balanced zero-sequence sets in the LINE to D.C. NEUTRAL voltage. However, partial cancellation of harmonics

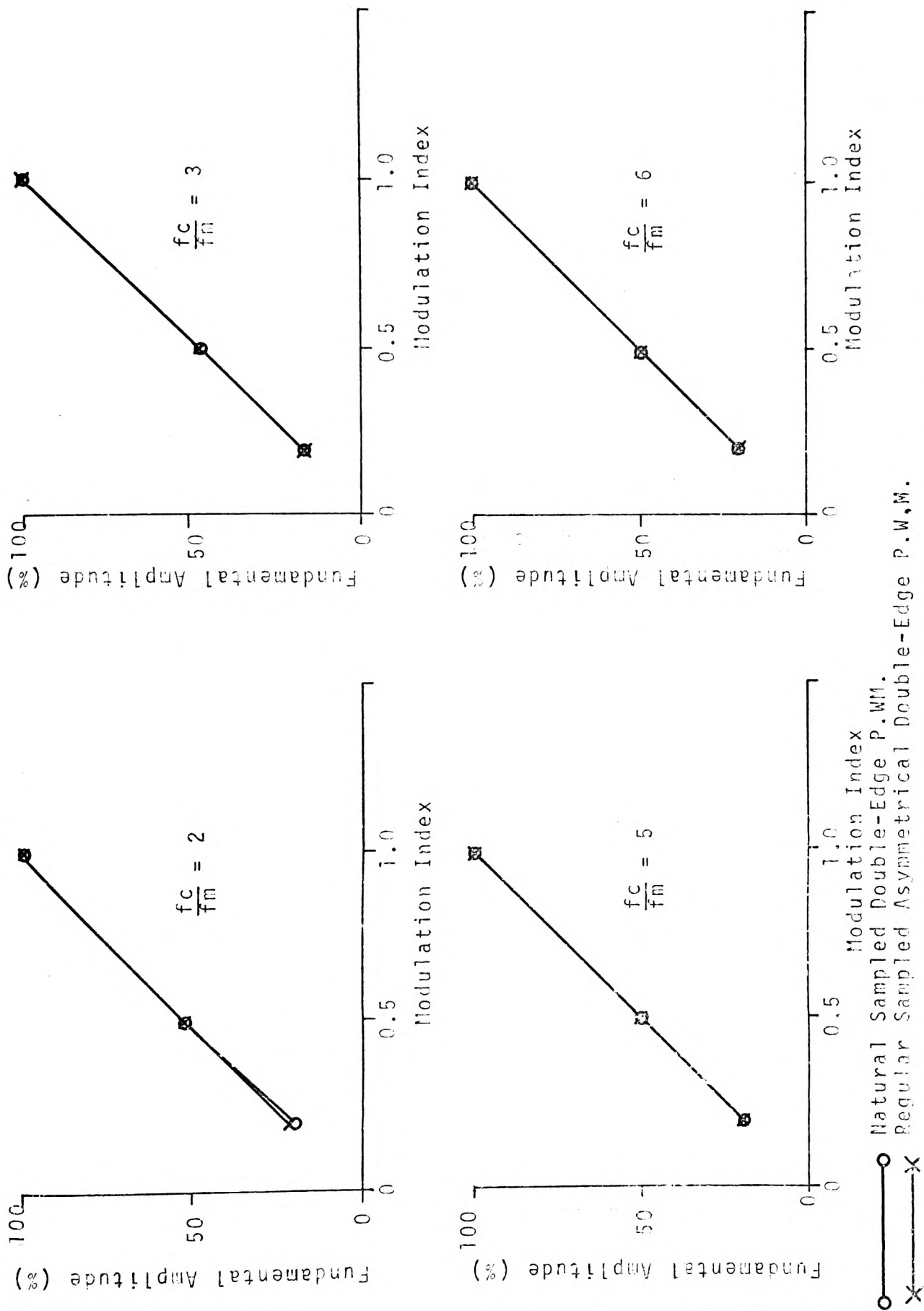


FIG. (4.29) VARIATION IN AMPLITUDE OF FUNDAMENTAL COMPONENT WITH MODULATION INDEX

○ Natural Sampled Double-Edge P.W.M.  
 × Regular Sampled Asymmetrical Double-Edge P.W.M.



in the LINE to LINE voltage can occur when harmonics of the same order in the LINE to D.C. NEUTRAL voltage form unbalanced sequence sets.

(iv) The amplitude and phase unbalance of the wanted harmonic components for non-triple integer values of frequency ratio which occurred in all prior-art p.w.m. systems, is completely eradicated by the proposed regular sampled asymmetrical double-edge p.w.m. process. Similarly the d.c. components in the LINE to D.C. NEUTRAL voltage waveforms which occurred in existing double-edge p.w.m. systems for even non-triple integer values of frequency ratio are also eliminated by the regular sampled, asymmetrical double-edge p.w.m. system.

(v) The novel regular sampled asymmetrical double-edge p.w.m. process always considerably reduces the amplitudes of the most significant harmonic components for all integer values of frequency ratio and modulation index.

(5) A NOVEL ASYNCHRONOUS MODE CONTROL SCHEME FOR A P.W.M. POWER CONVERTOR.

(5.1) Introduction

Almost all prior-art p.w.m. power convertors have operated in the synchronous mode such that the ratio of carrier frequency to modulating frequency has taken integer values only. The synchronous mode of operation requires the modulating wave and carrier wave to be synchronised in time-phase and it was shown in Chapter (4) that such a requirement necessitates the use of a phase-locked-loop circuit. However, the main disadvantage of a phase-locked-loop is that it adds complexity to the control circuit and only remains 'locked' over a specified range of frequency ratio's, therefore imposing limitations on the ratio of carrier frequency to modulating frequency. If, however, the carrier frequency is set at a constant value which is greater than the maximum required frequency of the wanted harmonic component of the output modulated waveform (to satisfy the sampling theorem), and the modulating wave and carrier wave are asynchronous, then varying the frequency of the modulating wave provides a range of frequency ratio between unity and infinity, that is to say:

$$1 < \frac{f_c}{f_m} < \infty \quad \text{----(5.1)}$$

where  $f_c = \text{Constant}$ .

Although the constant-carrier-frequency asynchronous-mode p.w.m. control scheme appears to be the most logical system to use for infinitely variable induction motor speed control systems, the literature available<sup>(21)</sup> suggest that such a means of generating p.w.m. waveforms is virtually useless for

all applications, because, sub-harmonic components, d.c. components and a 'beat effect' occurs in the output frequencies. However, the magnitudes of these undesirable components relative to the amplitude of the wanted harmonic component does not appear to have been determined, the effects of frequency ratio variation on these unwanted components and 'beat effect' phenomena have also avoided analysis in the literature. Indeed, it is not clear in the literature whether the 'beat effect' mentioned occurs in the output complex voltage waveform or in the magnitude of the wanted harmonic component of the output complex voltage. It was therefore decided to investigate the asynchronous mode of operation.

(5.2) The Natural Sampled Asynchronous Mode of  
Generating P.W.M Control Waveforms.

The prior-art technique of generating double-edge p.w.m. control waveforms is shown diagrammatically in Fig.(5.1) and graphically in Fig.(5.2). It is important to note that the modulating-wave-generator and carrier-wave-generator are entirely asynchronous. This means the triangular carrier wave and the three-phase modulating waves illustrated in Fig.(5.2) have no known time-phase relationship, whereas, with the previous synchronised-mode system the carrier wave and three-phase modulating waves were synchronised in time-phase. It may also be seen from Fig.(5.3) (drawn for one-phase only) that the points of instantaneous intersection between the carrier wave and modulating wave (the sampling points) coincide with the switching points of the width-modulated-output-wave. This constitutes natural sampling as described in Section (3.7) of this thesis. It is also of considerable importance

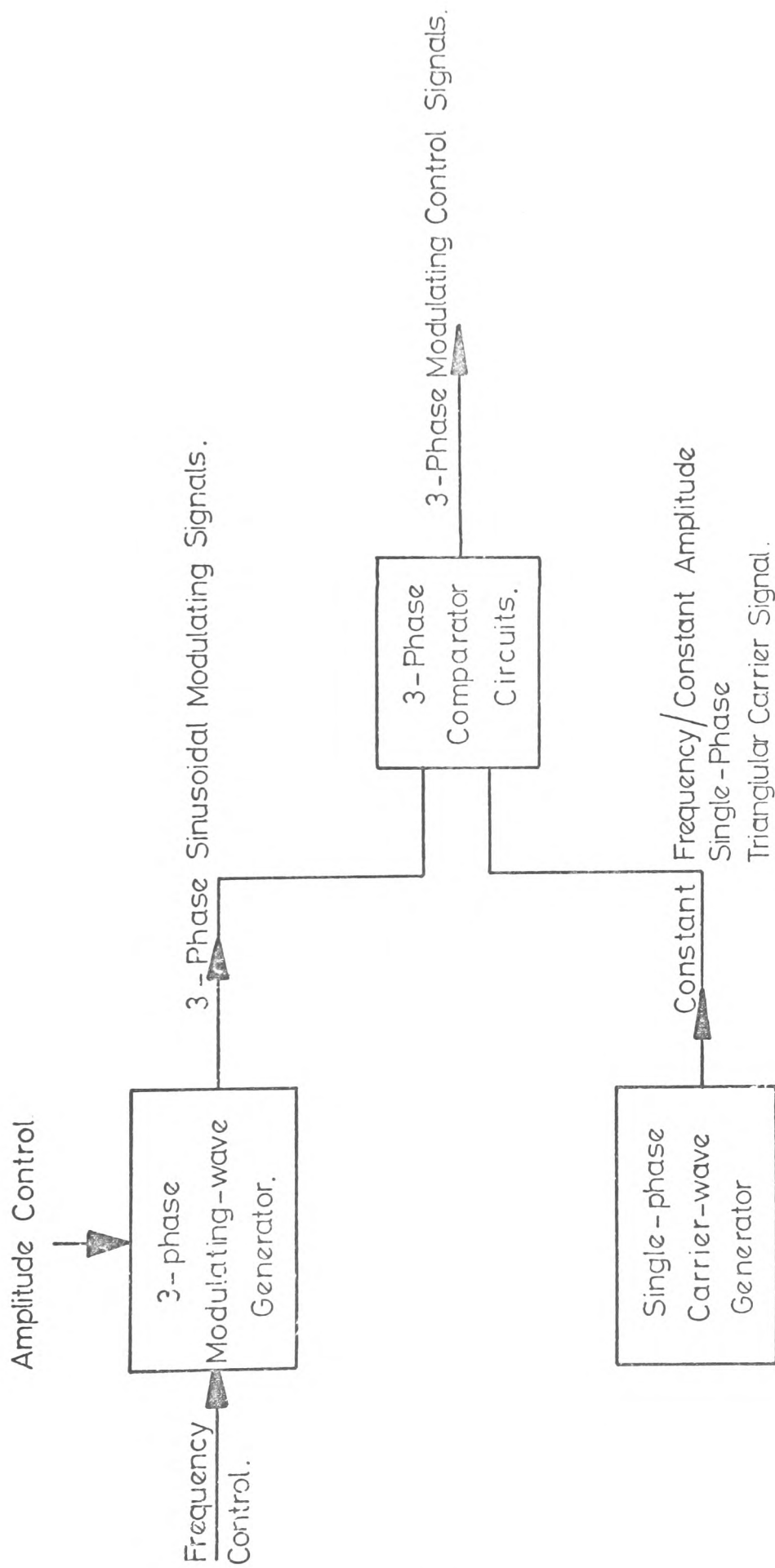
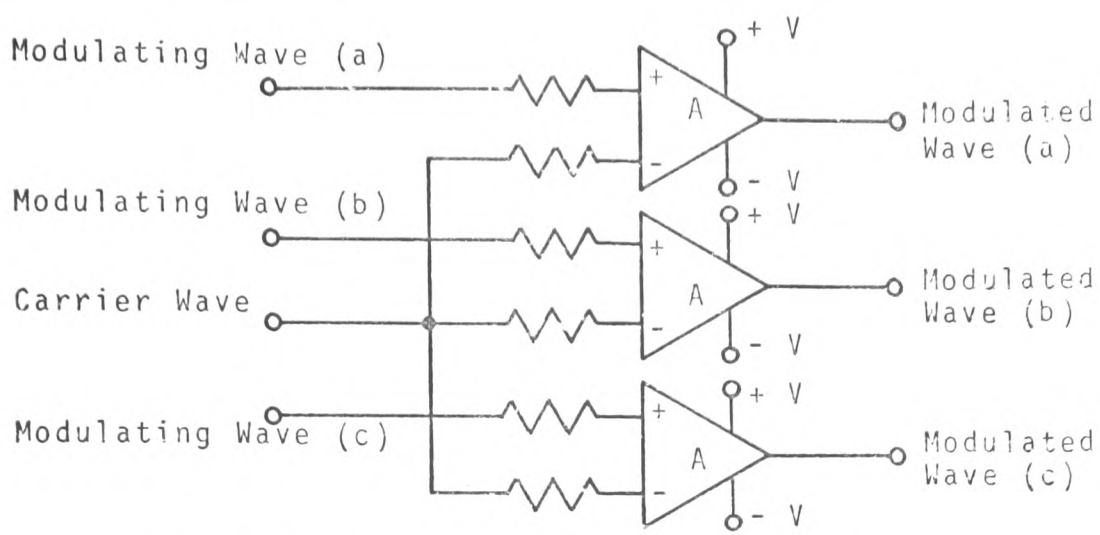
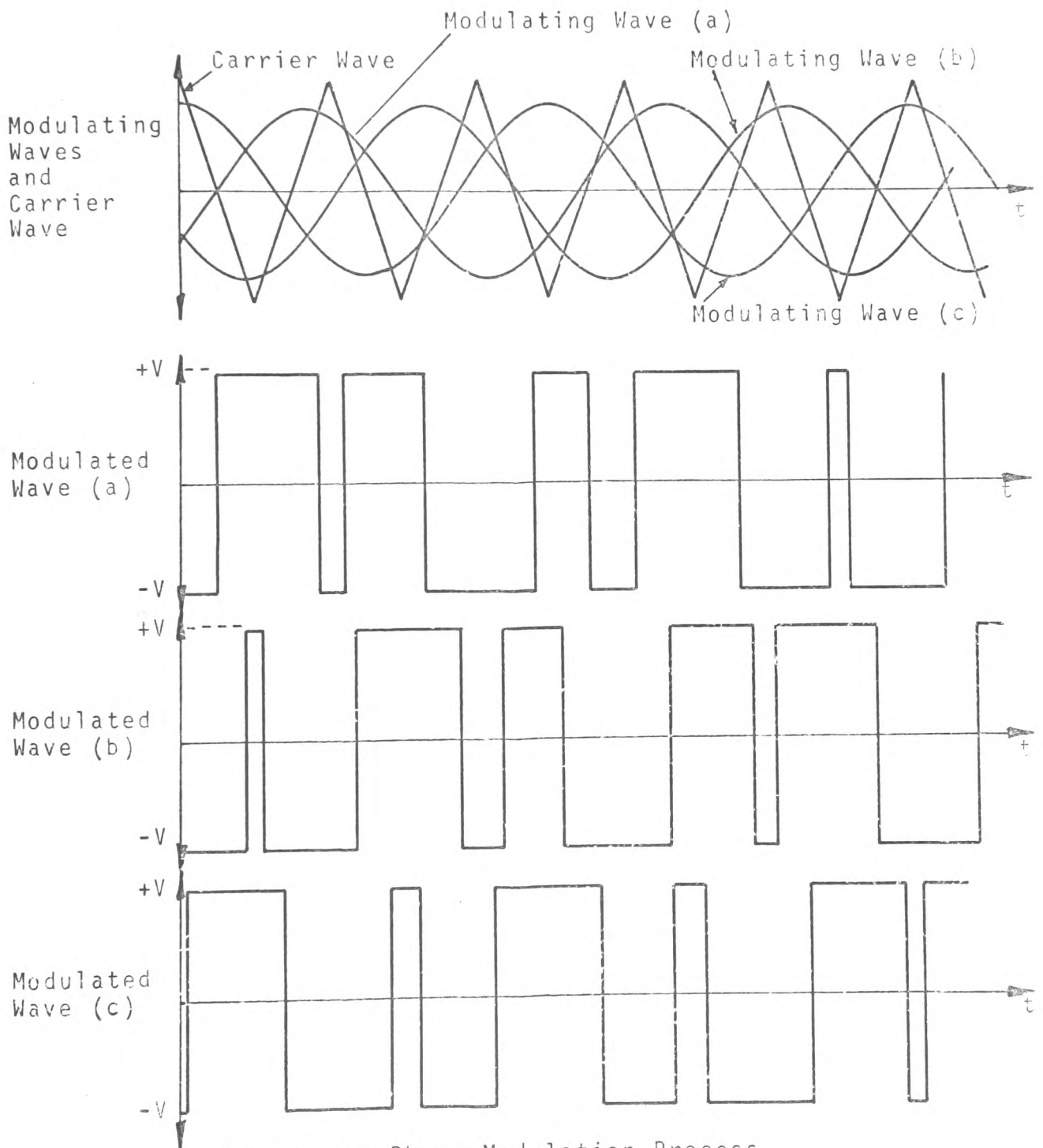


FIG.(5.1) BLOCK DIAGRAM OF ASYNCHRONOUS-MODE, NATURAL SAMPLED, DOUBLE-EDGE P.W.M. CONTROL SYSTEM.

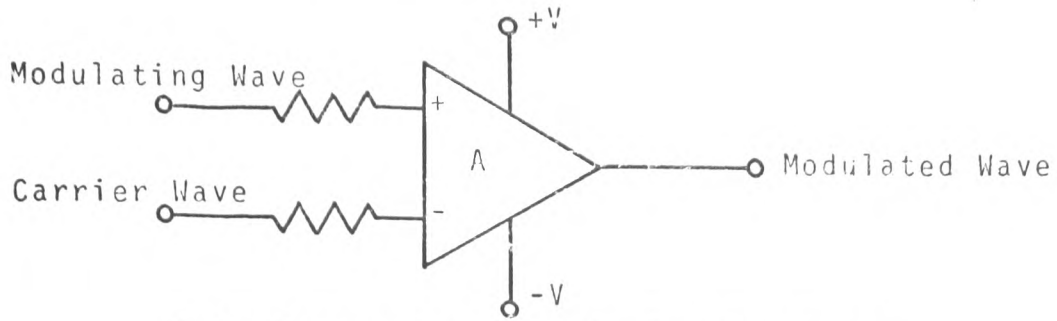


(a) Three-Phase Comparator Circuit.

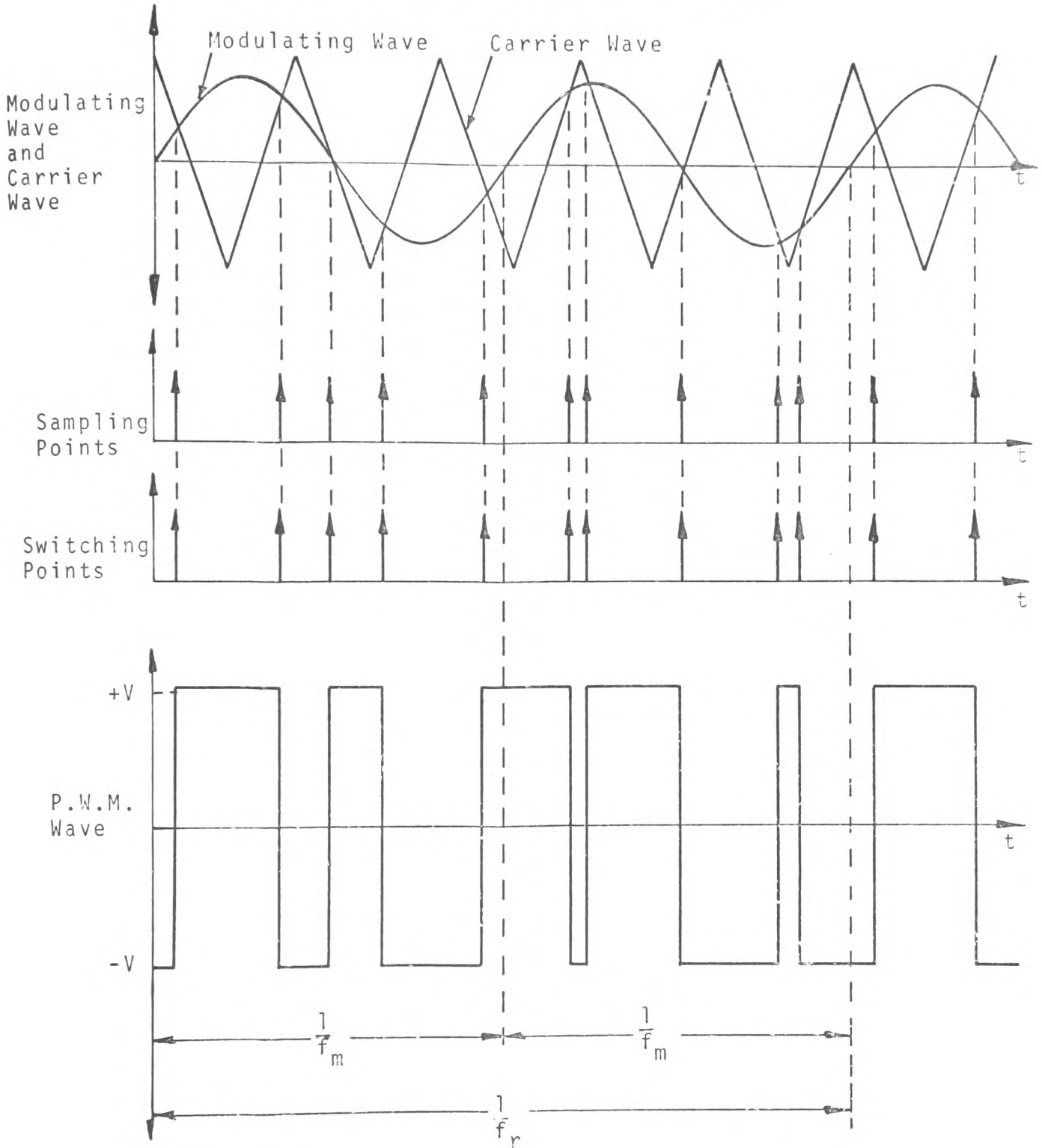


(b) Three-Phase Modulation Process

FIG.(5.2) ASYNCHRONOUS NCD NATURAL SAMPLED DOUBLE-EDGE P.W.M. PROCESS.



(a) Comparator Circuit For One Phase



(b) Modulation Process For One Phase

FIG.(5.3) ASYNCHRONOUS MODE NATURAL SAMPLED DOUBLE-EDGE P.W.M. PROCESS.

to note that the p.w.m. output waveform over a period of time corresponding to one cycle of the modulating wave (between  $t = 0$  and  $t = \frac{1}{f_m}$ ) is different from the p.w.m. waveform over the period of time corresponding to the succeeding cycle of the modulating wave (from  $t = \frac{1}{f_m}$  to  $t = \frac{2}{f_m}$ ), in fact it is quite evident that the p.w.m. waveform pattern only starts to repeat itself after a period of time,  $T = \frac{2}{f_m}$ . The time-period  $\frac{2}{f_m}$ , is therefore the fundamental-repetition-time,  $T_r$ , or the frequency,  $\frac{1}{T_r}$ , which in the case illustrated is equal to  $\frac{f_m}{2}$ , is the fundamental repetition frequency,  $f_r$ . Although  $f_r = \frac{f_m}{2}$  in the case illustrated in Fig.(5.3), this relationship is not true for all values of frequency ratio, indeed it will be shown in the succeeding Section that the relationship between the fundamental repetition frequency,  $f_r$ , and the ratio of carrier frequency to modulating frequency,  $\frac{f_c}{f_m}$ , is different for each value of  $\frac{f_c}{f_m}$ .

(5.2.1) Relationship Between Fundamental Repetition Frequency and Frequency Ratio

From the previous Section it is now quite evident that when the ratio of carrier frequency to modulating frequency is equal to non-integer values, that is to say:

$$\frac{f_c}{f_m} \neq n, \text{ where } n = \text{any integer value.}$$

then the fundamental repetition frequency,  $f_r$ , of the modulated waveform will always be different from the frequency of the modulating waveform,  $f_m$ , whereas, for the synchronised-mode of operation presented in Chapter (4), the repetition frequency of the modulated wave always equaled the frequency

of the modulating wave. Therefore, for the asynchronous-mode of operation, the first harmonic component of the p.w.m. voltage-waveform-spectra will not be of the same frequency as the modulating signal, but will in fact be equal to the fundamental repetition frequency of the output modulated waveform. It is therefore, of considerable importance that a relationship be established between the ratio of carrier frequency to modulating frequency,  $\frac{f_c}{f_m}$ , and the fundamental repetition frequency,  $f_r$ , of the modulated wave.

The constant-carrier-frequency asynchronous-mode p.w.m. system, which is the system being presented in this Chapter, is designed such that the carrier frequency,  $f_c$ , is maintained at a constant value, and the modulating frequency,  $f_m$ , varied between the limits:

$$0 < f_m < f_c \quad \text{----(5.2)}$$

The upper limit of the modulating frequency is of course determined by: (1) the sampling theorem, (2) the maximum required frequency of the wanted harmonic component of the output modulated waveform and (3) the amount of harmonic distortion of the output modulated waveform considered to be acceptable. Therefore, it is intuitively obvious that when the p.w.m. power convertor is made to drive a three-phase induction motor, where the speed of the motor is required to be smoothly increased from zero to a maximum value corresponding to the frequency,  $f_c$ , then the ratio of the carrier frequency to modulating frequency,  $\frac{f_c}{f_m}$ , must decrease from infinity to unity, that is to say:

$$1 < \frac{f_c}{f_m} < \infty \quad \text{----(5.3)}$$



which means the frequency ratio,  $\frac{f_c}{f_m}$ , must pass through integer and non-integer values. It would therefore appear that there is a possibility that a required motor speed could occur when  $\frac{f_c}{f_m}$  equals an integer value, thus inferring that at this desired speed the fundamental repetition frequency,  $f_r$ , would be equal to the modulating frequency,  $f_m$ . However,, it must not be forgotten that the modulating-wave-generator and carrier-wave-generator are entirely asynchronous. Therefore, the slightest shift in frequency of either generator will result in the value of  $\frac{f_c}{f_m}$  moving away from the integer value, thus confirming what has been determined experimentally: simply that the frequency ratio,  $\frac{f_c}{f_m}$ , passes through integer values but never settles on a true integer value.

According to the literature (6) the fundamental repetition frequency,  $f_r$ , of a modulated waveform, is equal to the highest 'common factor' (the largest number that will divide into two or more other numbers an integer number of times) of the carrier frequency and modulating frequency. Therefore, for the p.w.m. process illustrated in Fig.(5.4) where the carrier frequency equals 1000 Hz. and the modulating frequency equals 300 Hz, then the fundamental repetition frequency is 100 Hz, which means the wanted harmonic component is the 3rd harmonic of frequency 300 Hz, Now, rather than determine the 'harmonic order' of the wanted component from the values of carrier frequency and modulating frequency, it is far simpler to work in terms of frequency ratio. By referring to Fig.(5.4) once again, it may be seen that,  $\frac{f_c}{f_m} = \frac{1000}{300} = \frac{10}{3}$  which can be taken to mean: for 10 cycles of the carrier wave 3 cycles of the wanted component occurs, whereas, only 1 cycle of the

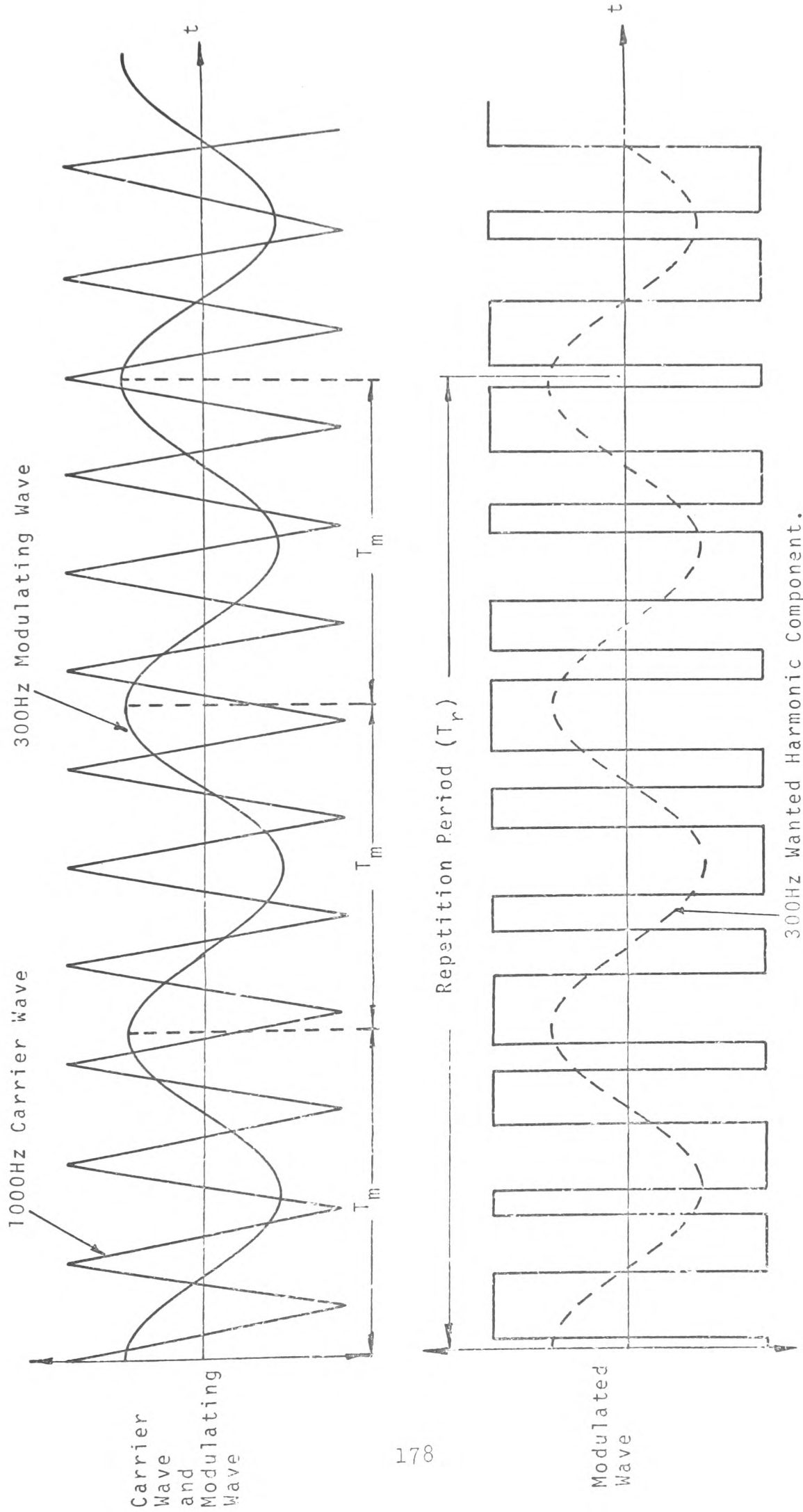


FIG. (5.4) OUTPUT MODULATED WAVEFORM FOR CARRIER FREQUENCY OF 1000HZ AND MODULATING FREQUENCY OF 300HZ.

fundamental exists. Therefore, for any non-integer value of frequency ratio the 'order' of the wanted harmonic component can be determined in terms of the fundamental harmonic component. For a further example consider the frequency ratio:

$$\frac{f_c}{f_m} = 4 \frac{1}{1000} = \frac{4001}{1000}$$

then for 4001 cycles of the carrier wave, 1000 cycles of the wanted harmonic component exists, whereas only one cycle of the fundamental component occurs. This means the 'order' of the wanted harmonic component is '1000'. Therefore, for this particular value of frequency ratio 999 sub-harmonic components (harmonic components of lower frequency order than the wanted component) can exist. Although this novel technique of expressing 'harmonic order' from the non-integer value of frequency ratio only, is very convenient when discussing harmonic spectra, it is however, very important to note, that to determine the absolute value of the fundamental repetition frequency and the frequency interval between adjacent harmonic components, either the absolute value of the carrier frequency or modulating frequency must be known. This will be expanded further in the Section devoted to the analysis of the 'beat effect' phenomena.

(5.2.2) Analytical Investigation Into The  
Natural Sampled Asynchronous Mode of  
Generating Double-Edge P.W.M. Waveforms.

Because of the limited amount of literature on the asynchronous-mode of operation and the vagueness of its contents, it was decided to make an analytical investigation

into the natural sampled asynchronous-mode p.w.m. process by means of a digital computer. The computer programs written for this purpose, calculate the amplitude and phase of respective harmonics for non-integer values of frequency ratio. A facility was also provided which simulated the random time-phase displacement between the carrier wave and modulating waves. Details of the computer programs are included in Appendix (1).

(5.2.2.1) Effects of Random Time-Phase Displacement Between Carrier Wave and Modulating Wave

It has been emphasised in the preceding Sections of this Chapter, that the time-phase displacement between the carrier wave and modulating wave is entirely random. The literature available<sup>(19), (21)</sup> suggests that this random time-phase displacement can result in the 'amplitudes' and 'phases' of the wanted harmonic components becoming unbalanced when three-phase modulating waves are compared with a single-phase carrier wave. It was therefore decided to investigate this problem analytically and determine the degree of unbalance.

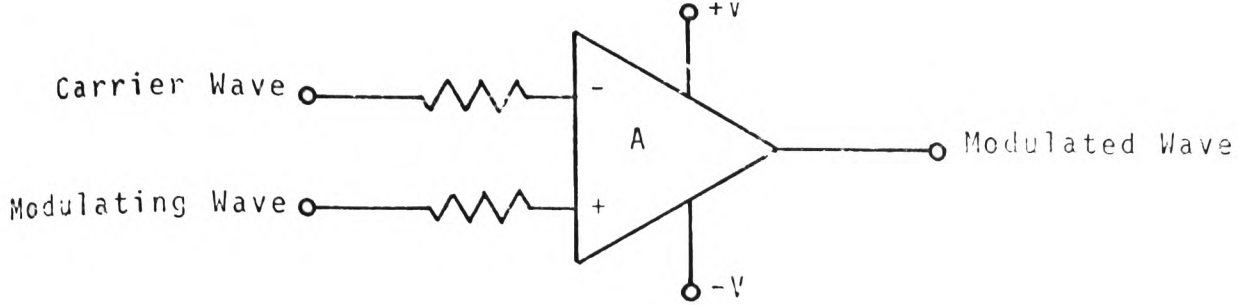
Consider the natural sampled double-edge p.w.m. process illustrated in Fig.(5.5), where the three modulating waves are defined by:

$$v_{ma} = A \sin(\omega_m t + \phi_1) \quad \text{----(5.4)}$$

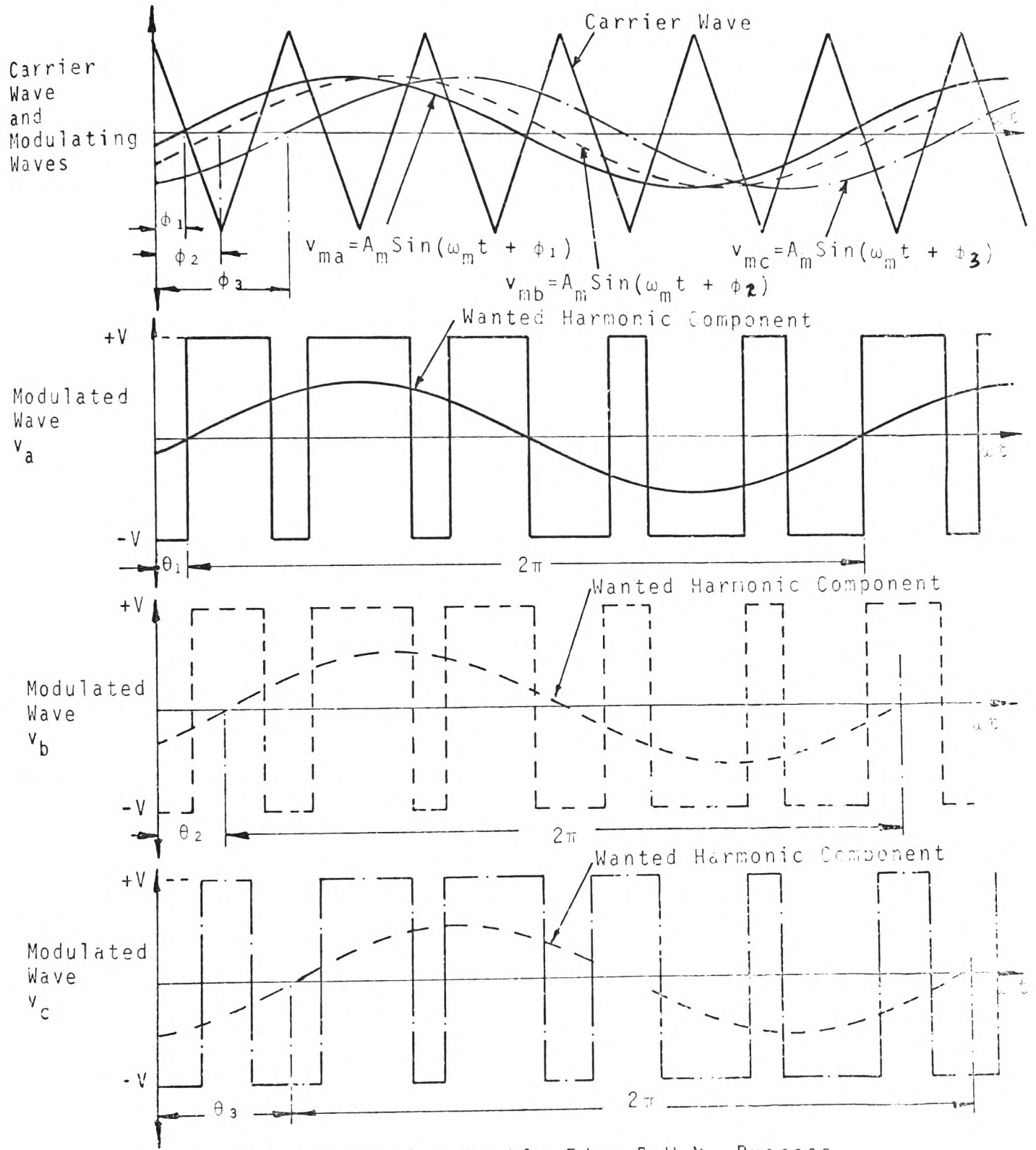
$$v_{mb} = A \sin(\omega_m t + \phi_2) \quad \text{----(5.5)}$$

and 
$$v_{mc} = A \sin(\omega_m t + \phi_3) \quad \text{----(5.6)}$$

Now the three wanted harmonic components of the three modulated waves can be defined by:



(a) Comparator Circuit For One Phase



(b) Natural Sampled Double-Edge P.W.M. Process

FIG.(5.5) THE EFFECT OF THE RANDOM TIME-PHASE DISPLACEMENT BETWEEN THE CARRIER WAVE AND MODULATING WAVE UPON THE NATURAL SAMPLED DOUBLE-EDGE P.W.M. PROCESS.

$$v_a = E_1 \sin(\omega t + \theta_1) \quad \text{----(5.7)}$$

$$v_b = B_2 \sin(\omega t + \theta_2) \quad \text{----(5.8)}$$

$$v_c = B_3 \sin(\omega t + \theta_3) \quad \text{----(5.9)}$$

It was found by computer analysis that for the natural sampled double-edge p.w.m. process:

$$\begin{aligned} B_1 &= B_2 = B_3, \\ \text{and } \theta_1 &= \phi_1, \theta_2 = \phi_2, \theta_3 = \phi_3 \end{aligned} \quad \text{----(5.10)}$$

provided:

$$\begin{aligned} \phi_2 - \phi_1 &= 120^\circ, \phi_3 - \phi_2 = 120^\circ \\ &\text{----(5.11)} \end{aligned}$$

$$\text{and } \frac{f_c}{f_m} = \frac{3n}{m}$$

where n and m equals any integer value. This applies for all values of modulation index  $\left\{ \frac{\text{Peak value of Carrier wave}}{\text{Peak value of modulating wave}} \right\}$  between zero and unity. Therefore, if it is assumed that the three-phase modulating waves are always balanced in both phase and amplitude, which is normally the case in practice, then the three wanted components of the three modulated waves will also be balanced in both 'phase' and 'amplitude' provided the numerator of the frequency ratio,  $\frac{f_c}{f_m}$ , is a triple-integer multiple (3,6,9,12 etc.). It is also appropriate at this point to note that fundamental amplitude and phase unbalance of the wanted harmonic components, occurred in the synchronised mode natural sampled double-edge p.w.m. process when the frequency ratio,  $\frac{f_c}{f_m}$ , did not equal a triple-integer multiple. This was enlarged upon in Chapter (4) of this thesis. One exception to the rules depicted by eq.(5.10) and eq.(5.11) occurs for a frequency ratio of:  $\frac{f_c}{f_m} = \frac{3}{2}$  and a modulation index of unity. These values lead to considerable unbalance of the

three wanted harmonic components, whereas, a frequency ratio of:  $\frac{f_c}{f_m} = \frac{3}{2}$  and a modulation index of 0.5, does not cause unbalance of the wanted harmonic components. In fact, the degree of amplitude and phase unbalance for a frequency ratio of:  $\frac{f_c}{f_m} = \frac{3}{2}$  and a modulation index of unity, was found to be of the order: 7% and 11° respectively.

It can therefore be concluded that the amplitude and/or phase unbalance of the wanted harmonic components which exists in the asynchronous-mode, natural sampled p.w.m. system, is not due to the random time-phase displacement between the carrier wave and modulating waves, but, is entirely due to the natural sampling process.

#### (5.2.2.2) Desirability for Balanced Harmonic Spectra

Consider the three-phase power convertor illustrated in Fig.(4.1), Chapter (4), which is again shown in Fig.(5.6). It was shown in Chapter (4) that for the synchronised mode of operation, the most desirable harmonic spectra of the three LINE to D.C. NEUTRAL voltage waveforms, consisted of three fundamental harmonic components which formed a balanced positive-sequence set, plus super-harmonics which formed balanced zero-sequence sets. This allowed the respective zero-sequence sets to cancel in the LINE to LINE voltage waveform, such that a balanced three-wire, three-phase load connected between the LINES would draw balanced positive-sequence currents only. However, it has already been shown in this Chapter that for the asynchronous-mode of operation the output voltage spectra can contain sub-harmonic components

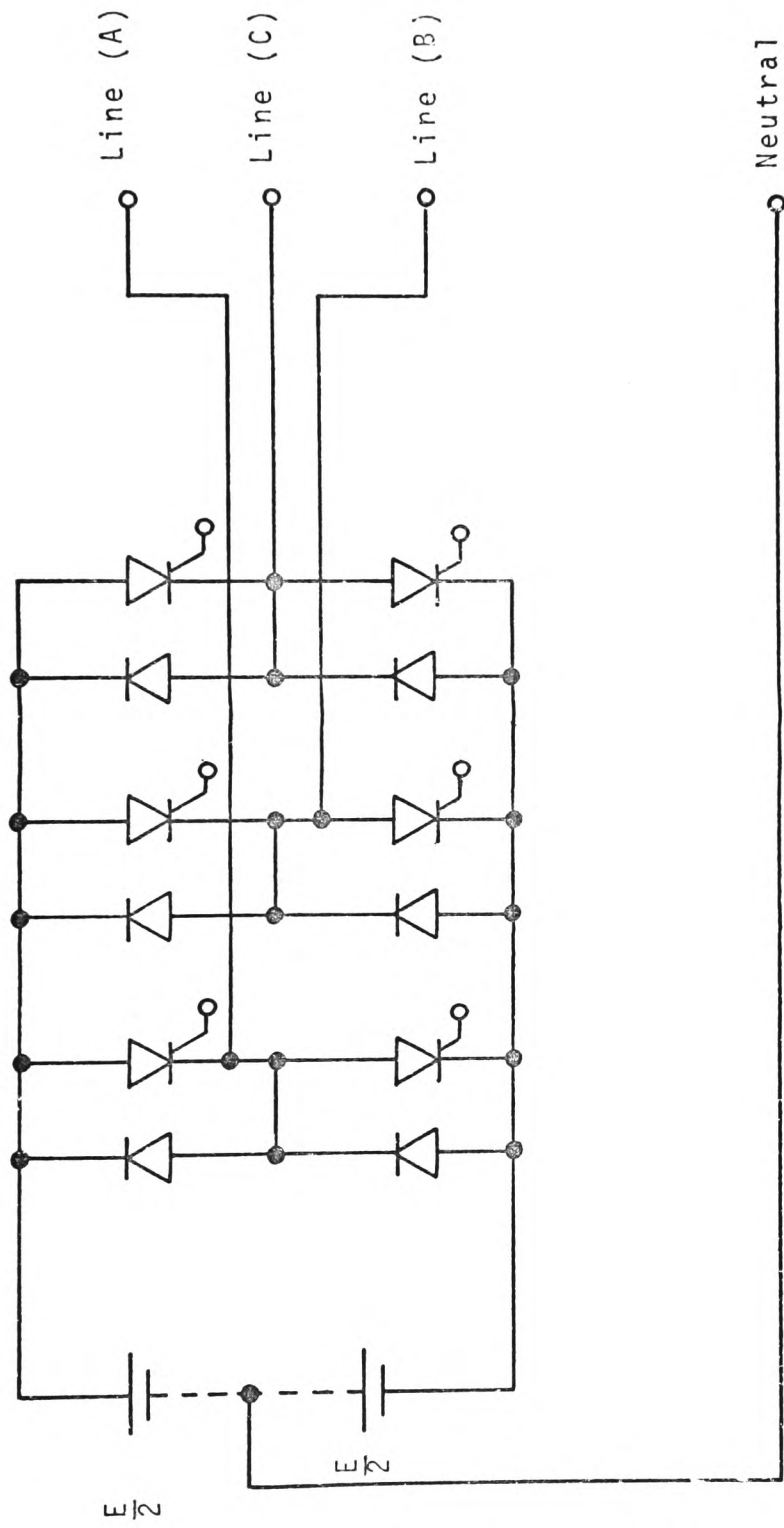


FIG. (5.6) THREE-PHASE MODULATOR (EXCLUDING COMMUTATING COMPONENTS).



as well as super-harmonic components. Therefore, the most desirable harmonic spectra of the three LINE to D.C. NEUTRAL voltage waveforms would be as follows:

$$v_{an} = V_{d.c.} + \hat{V}_1 \sin \omega_r t + \dots + \hat{V}_n \sin n \omega_r t + \hat{V} \sin \omega_m t \\ + \dots + \hat{V}_m \sin m \omega_r t \quad \text{----(5.12)}$$

$$v_{bn} = V_{d.c.} + \hat{V}_1 \sin \omega_r t + \dots + \hat{V}_n \sin n \omega_r t + \hat{V} \sin(\omega_m t - \frac{2\pi}{3}) \\ + \dots + \hat{V}_m \sin m \omega_r t \quad \text{----(5.13)}$$

$$v_{cn} = V_{d.c.} + \hat{V}_1 \sin \omega_r t + \dots + \hat{V}_n \sin n \omega_r t + \hat{V} \sin(\omega_m t + \frac{2\pi}{3}) \\ + \dots + \hat{V}_m \sin m \omega_r t \quad \text{----(5.14)}$$

the three LINE to LINE voltage waveforms would then be given by:

$$v_{ab} = \sqrt{3} \cdot \hat{V} \sin(\omega_m t + \frac{\pi}{6}) \quad \text{----(5.15)}$$

$$v_{bc} = \sqrt{3} \cdot \hat{V} \sin(\omega_m t - \frac{\pi}{2}) \quad \text{----(5.16)}$$

$$v_{ca} = \sqrt{3} \cdot \hat{V} \sin(\omega_m t + \frac{5\pi}{6}) \quad \text{----(5.17)}$$

Such hypothetical LINE to D.C. NEUTRAL voltage waveform spectra are, of course, not possible in practical systems, as was stated in Chapter (4). Therefore, consideration must be given to the p.w.m. process which produces the most acceptable harmonic spectra for all non-integer values of frequency ratio. Such an investigation can be best achieved by dividing the LINE to D.C. NEUTRAL voltage spectra into four areas of study: (i) d.c. components, (ii) sub-harmonic components (iii) wanted harmonic components and (iv) super-harmonic components.

### (5.2.2.2a) D.C. Components

When the three d.c. components in the three LINE to D.C. NEUTRAL voltage waveforms described by equations: (5.12), (5.13) and (5.14) respectively, are not equal, d.c. components will exist in the LINE to LINE voltages. Therefore, when three-phase, three-wire loads are connected between the three LINES shown in Fig.(5.6), d.c. components of current will flow in the load. When the load is inductive such that the impedance of each phase of the load is of the type:

$$Z_L = R + j.\omega.L.$$

where

$$\omega.L. \gg R, \text{ and } R \rightarrow 0.$$

then small components of direct voltage can circulate large components of direct current, because the reactance,  $\omega.L.$ ; presents no impedance to the flow of direct current. Therefore, for induction motor drive applications d.c. components of voltage in the output LINE to LINE modulated voltage are clearly undesirable.

Because the frequency ratio,  $\frac{f_c}{f_m}$ , has an infinite number of values it is not possible to present results for all the possible values of  $\frac{f_c}{f_m}$ . However, it may be seen from the computed results illustrated in Figures (5.7), (5.8) and (5.9) that d.c. components greater or equal to 1.0% of the wanted harmonic component of the LINE (A) to LINE (B) voltage do exist for values of  $\frac{f_c}{f_m} < 9$ , for the natural sampled double-edge p.w.m. process. Therefore, if the figure of 1.0% is taken as the criterion of acceptability so far as d.c. components alone are concerned, the minimum value of frequency

D.C. Components In Line To Line Voltage Waveforms As % of Wanted Harmonic Components			Frequency Ratio $\frac{f_c}{f_m}$	Mod. Index
$V_{AB}$	$V_{BC}$	$V_{CA}$		
			1.0	1.0
			1.2	
			1.4	
-5.0		5.0	1.6	
			1.8	
-29.0		29.0	2.0	
			2.2	
			2.4	
			2.6	
			2.8	
			3.0	
			3.2	
			3.4	
			3.6	
			3.8	
-20		2.0	4.0	
			4.2	
			4.4	
			4.6	
			4.8	
			5.0	
			5.2	
			5.4	
			5.6	
			5.8	
			6.0	
			6.2	
			6.4	
			6.6	
			6.8	
			7.0	
			7.2	
			7.4	
			7.6	
			7.8	
			8.0	

FIG.(5.7) D.C. COMPONENTS IN LINE TO LINE VOLTAGE WAVEFORMS AS % OF WANTED HARMONIC COMPONENTS FOR MODULATION INDEX OF 1.0

D.C. Components In Line To Line Voltage Waveforms As % of Wanted Harmonic Components			Freq. Ratio $\frac{f_c}{f_m}$	Mod. Index
$V_{AB}$	$V_{BC}$	$V_{CA}$		
			1.0	0.5
			1.2	
			1.4	
- 1.0		1.0	1.6	
			1.8	
-15.0		15.0	2.0	
			2.2	
			2.4	
			2.6	
			2.8	
			3.0	
			3.2	
			3.4	
			3.6	
			3.8	
- 1.0		1.0	4.0	
			4.2	
			4.4	
			4.6	
			4.8	
			5.0	
- 1.0		1.0	5.2	
			5.4	
			5.6	
			5.8	
			6.0	
			6.2	
			6.4	
			6.6	
			6.8	
			7.0	
			7.2	
			7.4	
			7.6	
			7.8	
1.0		- 1.0	8.0	

FIG.(5.8) D.C. COMPONENTS IN LINE TO LINE VOLTAGE WAVEFORMS AS % OF WANTED HARMONIC COMPONENTS FOR MODULATION INDEX OF 0.5

D.C. Components IN Line To Line Voltage Waveforms As % Of Wanted Harmonic Components			Frequency Ratio $\frac{f_c}{f_m}$	Mod. Index
$V_{AB}$	$V_{BC}$	$V_{CA}$		
			1.0	0.2
			1.2	
			1.4	
			1.6	
			1.8	
-9.0		9.0	2.0	
			2.2	
1.0	-1.0		2.4	
			2.6	
1.0		1.0	2.8	
			3.0	
-1.0		1.0	3.2	
			3.4	
			3.6	
			3.8	
			4.0	
			4.2	
			4.4	
			4.6	
			4.8	
			5.0	
-1.0		1.0	5.2	
			5.4	
			5.6	
			5.8	
			6.0	
			6.2	
-1.0		1.0	6.4	
			6.6	
1.0		-1.0	6.8	
			7.0	
			7.2	
			7.4	
			7.6	
			7.8	
2.0		-2.0	8.0	

FIG.(5.9) D.C. COMPONENTS IN LINE TO LINE VOLTAGE WAVEFORMS AS % OF WANTED HARMONIC COMPONENTS FOR MODULATION INDEX OF 0.2

ratio is:  $\frac{f_c}{f_m} \geq 9$ . This minimum value of frequency ratio therefore imposes limitations on the operating frequency range of the power convertor. For example, consider the carrier frequency is set at 300 Hz, and the power convertor is required to supply an output voltage whose wanted component has a frequency of 120 Hz, then  $\frac{f_c}{f_m} = \frac{5}{2}$ , which is outside the limits:

$$9 < \frac{f_c}{f_m} < \infty,$$

in fact, the maximum frequency of the wanted harmonic component of the output modulated voltage is limited to approximately 33Hz. Therefore, to achieve an output wanted harmonic component of 120 Hz, requires the frequency of the carrier wave to be increased to approximately 1080 Hz, which means the number of commutations in the power convertor are increased by 360%. This increase in the number of commutations in the power convertor causes the efficiency of the power convertor to decrease. The design complexity of the power convertors also increases with increase in the frequency of operation. Therefore, power convertors operating at high frequencies is clearly undesirable.

#### (5.2.2.2b) Sub-Harmonic Components

It has been shown in previous Sections of this Chapter, that when the fundamental repetition frequency of the output modulated waveform is different from the frequency of the modulating wave, sub-harmonic components of voltage can occur in the harmonic spectra of the output modulated voltage. Therefore, if the three LINE to D.C. NEUTRAL voltages:  $V_{an}$ ,

$V_{bn}$ , and  $V_{cn}$ , of the convertor illustrated in Fig.(5.6) contain sub-harmonic components, where respective sub-harmonic components in the three voltages do not form balanced zero-sequence sets, complete cancellation of the sub-harmonic components in the LINE to LINE voltages:  $V_{ab}$ ,  $V_{bc}$ , and  $V_{ca}$ , will not occur. When the impedance of each phase of a three-phase, three-wire load is again of the type:

$$Z_L = R + j. \omega.L.$$

where  $\omega.L. \gg R$  and  $R \rightarrow 0$ .

then the inductive reactance opposing the flow of sub-harmonic currents can be very much less than the inductive reactance opposing the flow of the wanted harmonic components of current (harmonic component of current of same frequency as modulating wave). Therefore, small sub-harmonic voltages can circulate large sub-harmonic currents. For induction motor drive applications it is once again evident, that sub-harmonic components in the output modulated voltage are totally undesirable.

It was found by computer analysis that for the natural sampled double-edge p.w.m.process, sub-harmonic voltage components do in fact exist in the output voltage spectra for low non-integer values of frequency ratio. Fig.(5.10) illustrates the first, nine harmonic voltage components in both the LINE to D.C. NEUTRAL voltage waveforms and LINE to LINE voltage waveforms, where the amplitudes of the harmonics are expressed as percentages of the amplitudes of the wanted component (The 5th harmonic component). It is interesting to note from Fig.(5.11) that respective sub-harmonic components, respective wanted harmonic components and respective super-

Harmonic Order	Line To D.C. Neutral Components						Line To Line Components			Frequency Ratio $\frac{f_c}{f_m}$	Mod. Index
	$V_{AN}$	$V_{BN}$	$V_{CN}$	$V_{AB}$	$V_{BC}$	$V_{CA}$					
D.C.	-9.0	-9.0	-9.0								
1	18/0°	18/120°	18/-120°	18/-30°	18/90°	18/-150°					
2	19/90°	19/-30°	19/-150°	19/120°	19/0°	19/-120°					
3	23/180°	23/180°	23/180°								
4	31/-90°	31/30°	31/150°	31/-120°	31/0°	31/120°					1.0
5	100/0°	100/-120°	100/120°	100/30°	100/-90°	100/150°					
6	64/-90°	64/-90°	64/-90°								
7	23/0°	23/120°	23/-120°	23/-30°	23/90°	23/-150°					
8	12/90°	12/-30°	12/-150°	12/120°	12/0°	12/-120°					
9	7/180°	7/180°	7/180°								

FIG. (5.10) PERCENTAGE AMPLITUDE AND PHASE OF HARMONICS IN BOTH LINE TO D.C. NEUTRAL VOLTAGE WAVEFORM AND LINE TO LINE VOLTAGE WAVEFORM FOR NATURAL SAMPLED DOUBLE-EDGE P.W.M.



Voltage Waveform	Sampling Process	Phase Sequence	Harmonic Order												
			1	2	3	4	5	6	7	8	9				
LINE		Reference		$X_B$				$X_B$					$X_B$		
TO	NATURAL	Reverse	$X_B$			$X_B$					$X_B$				
D.C. NEUTRAL		In Phase			$X_B$				$X_B$						$X_B$
LINE		Reference		$X_B$									$X_B$		
TO	NATURAL	Reverse	$X_B$				$X_B$							$X_B$	
LINE		In Phase													

$X_B$  - Respective harmonic components are balanced.

$X_u$  - " " " " Unbalanced.

FIG.(5.11) PHASE SEQUENCE CHART OF RESPECTIVE HARMONICS IN BOTH LINE TO D.C. NEUTRAL VOLTAGE WAVEFORM AND LINE TO LINE VOLTAGE WAVEFORM.

harmonic components all form balanced sequence sets. The triplen order harmonics in the LINE to D.C. NEUTRAL voltage waveforms, again form balanced zero-sequence sets, which means cancellation of these components in the LINE to LINE voltage waveforms will occur. From the computed results illustrated in Fig.(5.10) and further computed results the following relationships became apparent:

(1) All triplen order harmonics (3rd, 6th, 9th, ---, 3n) always cancel in the LINE to LINE voltage, provided the numerator of the frequency ratio fraction,  $\frac{f_c}{f_m}$ , is a triple-integer multiple, that is to say:

$$\text{when } \frac{f_c}{f_m} = \frac{3n}{m}, \text{ and } 3n > m,$$

then harmonics of order, 3n, cancel in the LINE to LINE voltage.

(2) All even order harmonics (2nd, 4th, 6th, ---, 2n) are eliminated from the LINE to D.C. NEUTRAL voltage and therefore from the LINE to LINE voltage when:

$$\frac{f_c}{f_m} = \frac{(2n - 1)}{(2m - 1)}, \text{ where } n > m,$$

(3) When  $\frac{f_c}{f_m} = \frac{(2n - 1)}{2m}$ , where  $n > m$ ,

both even order and odd order harmonics can be present in the LINE to LINE voltage.

(4) When  $\frac{f_c}{f_m} = \frac{2n}{(2m - 1)}$  and  $n > m$

both even order and odd order harmonics can again be present in the LINE to LINE voltage.

From the computed results illustrated in Fig. (5.12) and from further computed results, it became evident that for low values of modulation index, sub-harmonic voltage components equal to 1% or more of the wanted harmonic component, exist in

Harmonic Order	Line to D.C. Neutral Components			Line to Line Components			Frequency Ratio $\frac{f_c}{f_m}$	Mod. Index
	$V_{AN}$	$V_{BN}$	$V_{CN}$	$V_{AB}$	$V_{BC}$	$V_{CA}$		
D.C.	- 1.0			- 1.0				
1		$1.0/\underline{165^\circ}$	$1.0/\underline{-165^\circ}$	$1.0/\underline{-13^\circ}$		$1.0/\underline{-167^\circ}$		
2		$1.0/\underline{100^\circ}$	$1.0/\underline{80^\circ}$	$1.0/\underline{-84^\circ}$		$1.0/\underline{78^\circ}$		
3							$9 \frac{1}{5}$	0.2
4								
5	$100/\underline{0^\circ}$	$100/\underline{-120^\circ}$	$100/\underline{120^\circ}$	$100/\underline{30^\circ}$		$100/\underline{-90^\circ}$		
6								
7	$1.0/\underline{180^\circ}$			$1.0/\underline{-169^\circ}$		$1.0/\underline{-110^\circ}$		
8	$1.0/\underline{97^\circ}$	$1.0/\underline{-82^\circ}$	$1.0/\underline{-98^\circ}$	$1.0/\underline{98^\circ}$		$1.0/\underline{-86^\circ}$		
9	$1.0/\underline{0^\circ}$	$1.0/\underline{42^\circ}$	$1.0/\underline{-42^\circ}$					

FIG. (5.12) PERCENTAGE AMPLITUDE AND PHASE OF HARMONIC COMPONENTS IN BOTH THE LINE TO D.C. NEUTRAL VOLTAGE WAVEFORM AND LINE TO LINE VOLTAGE WAVEFORMS FOR NATURAL SAMPLED DOUBLE-EDGE P.W.M.

the LINE to LINE voltage spectra for non-integer values of frequency ratio below 'ten'. Therefore, if a sub-harmonic component amplitude of less than 1% is taken as the criterion for acceptability, then the limiting value of minimum frequency ratio is given by:

$$\frac{f_c}{f_m} \geq 10.$$

This means the usable range of frequency ratio is bounded by the limits:

$$10 < \frac{f_c}{f_m} < \infty$$

which results in the same consequences described in Section (5.2.3.1.). Once again sub-harmonic components in the LINE to LINE voltage spectrum, are clearly undesirable.

#### (5.2.2.2c) Wanted Harmonic Components

For the asynchronous mode of generating p.w.m. waveforms, it has been shown (Section 5.2.2.2)) that the wanted harmonic components are of the same frequency as the modulating wave. For three-phase, induction motor drive applications it is particularly important that the three wanted harmonic components form a balanced positive-sequence set, for all values of frequency ratio and modulation index. It was found by means of computer analysis, that the degree of amplitude and/or phase unbalance between respective wanted harmonic components was less than 1% and/or 1° respectively, for nearly all non-integer-values of frequency ratio which lie within the limitations of the sampling theorem. In fact it is true to say that the degree of unbalance between wanted harmonic components is greater for the synchronous-mode of operation (integer values of frequency ratio) than for the

asynchronous-mode of operation (non-integer values of frequency ratio). However for reasons of theoretical argumentation, it must be added that 'true-balance' of the wanted harmonic components only occurred for non-integer values of frequency ratio given by:

$$\frac{f_c}{f_m} = \frac{3n}{m} \text{ and } 3n > m$$

where m and n are both any integer values.

#### (5.2.2.2d) Super-Harmonic Components

Super-harmonic components are considerably more important in the asynchronous-mode of operation than in the synchronous-mode of operation because of the frequency interval between adjacent harmonics (the fundamental repetition frequency). It was shown in Chapter (4) that the minimum value of frequency between any two harmonics is the modulating frequency, provided the mode of operation was synchronous. However, it was shown in this Chapter that for the asynchronous-mode of operation the minimum value of frequency between any two harmonics is the repetition frequency, which can be very much less than the modulating frequency. Consider  $f_c = 550$  Hz and  $f_m = 250$  Hz, then the fundamental repetition frequency is:  $f_r = 50$  Hz. Therefore, the frequency interval between adjacent harmonics is 50 Hz.

From the computed results illustrated in Figures (5.10) and (5.12), and from further computed results, it was found that the conditions for the existence and cancellation of super-harmonics were mainly the same as the conditions which apply to sub-harmonics; that is to say:

- (i) All triplen harmonics (of order: 3,6,9, ---,3n) which

exist in the LINE to D.C. NEUTRAL voltages, completely cancel in the LINE to LINE voltage, provided:

$$\frac{f_c}{f_m} = \frac{3n}{m} \text{ and } 3n > m.$$

(ii) All even harmonics (of order: 2,4,6, ---,2n) are eliminated from the LINE to D.C. NEUTRAL voltages and therefore from the LINE to LINE voltages provided:

$$\frac{f_c}{f_m} = \frac{(2n - 1)}{(2m - 1)}, \text{ where } n > m$$

(iii) Both even order and odd order harmonics can be present in the LINE to LINE voltage waveforms when:

$$(a) \frac{f_c}{f_m} = \frac{(2n - 1)}{2m}, \text{ where } n > m$$

or

$$(b) \frac{f_c}{f_m} = \frac{2n}{(2m - 1)}, \text{ where } n > m$$

(iv) The higher the value of frequency ratio,  $\frac{f_c}{f_m}$ , the smaller the amplitude of the most significant harmonics.

### (5.2.3) Interim Conclusions

It has been shown analytically that the natural sampled, prior-art technique of generating double-edge p.w.m. waveforms in the asynchronous-mode, introduces many undesirable features:

(1) Direct voltage components are introduced into the harmonic spectra of the LINE to LINE voltage waveforms when:

$$\frac{f_c}{f_m} < 9.$$

(2) Similarly sub-harmonic components of voltage exist in the LINE to LINE voltage waveforms for values of,  $\frac{f_c}{f_m}$ , less than 'ten'.

(3) Slight amplitude unbalance and/or phase unbalance between the wanted harmonic components has been shown to exist for certain low, non-integer values of frequency ratio.

(5.3) The Application of Regular Sampling Techniques  
To the Asynchronous Mode of Generating P.W.M.  
Control Waveforms.

It was shown in Chapter (4), that the application of regular sampling techniques, completely eradicated the many undesirable features of the prior-art, natural sampled, synchronised-mode p.w.m. control schemes. It was therefore thought that the application of the same techniques to the prior-art asynchronous-mode p.w.m. control schemes may again overcome the many disadvantages which have been shown to exist. It is of particular importance at this point, to again emphasise, that the application of regular sampling techniques to p.w.m. power convertor control circuits, is entirely novel.

(5.3.1) Analytical Investigation Into the Application  
of Regular Sampling Techniques to the  
Asynchronous Mode of Generating Double-Edge  
P.W.M. Waveforms

Harmonic spectra for both the LINE to D.C. NEUTRAL voltage waveforms and LINE to LINE voltage waveforms were computed for both the regular sampled symmetrical double-edge p.w.m. process and the regular sampled asymmetrical double-edge p.w.m. process for non-integer values of frequency ratio.

(5.3.1.1) D.C. Components

The computed results for both the regular sampled symmetrical modulation process and regular sampled asymmetrical modulation process demonstrated that the direct voltage components were completely eliminated from the harmonic spectra

of the output modulated voltage waveforms for non-integer values of frequency ratio.

#### (5.3.1.2) Sub-Harmonic Voltage Components

Fig.(5.13) illustrates the first twenty harmonics of the LINE to LINE voltage waveforms for the natural sampled double-edge p.w.m.process, the regular sampled symmetrical p.w.m. process and regular sampled asymmetrical p.w.m.process for frequency ratio values of:  $1\frac{1}{17}$ ,  $2\frac{1}{17}$ , and  $3\frac{1}{17}$ , and a modulation index of unity. It is quite evident from these results that regular sampling significantly reduces the amplitude of the sub-harmonics voltage components when compared with natural sampling. For a frequency ratio of:  $1\frac{1}{17}$ , the regular sampled symmetrical p.w.m.process proves to be one exception. The reason for this exception is that  $\frac{f_c}{f_m} = 1\frac{1}{17}$ , is less than the minimum frequency ratio value  $(\frac{f_c}{f_m} \geq 2)$  specified by the limitation of the regular sampling process when applied to symmetrical p.w.m. This point was enlarged upon in Section (3.9.5) of Chapter (3) in this thesis.

Therefore from the results illustrated in Fig.(5.13) and further computed results it can be concluded that the application of regular sampling techniques approximately eliminates all sub-harmonic voltage components for all values of frequency ratio greater than 'two'  $(\frac{f_c}{f_m} > 2)$  and all values of modulation index between 'zero' and 'unity'. It is important to again emphasise at this point that for the natural sampled p.w.m.process, sub-harmonic voltage components only became insignificant for values of frequency ratio greater than "ten"  $(\frac{f_c}{f_m} > 10)$



Sampling Process	Freq. Ratio	Harmonic Order																			
		1	2	3	4	5	6	7	8	9	10	11	12	13	14	15	16	17	18	19	20
Natural (Double-Edge)		29	26		19	13	3	1		8	9			7	2		19	100		30	13
Regular (Sym. Mod.)	$\frac{1}{17}$	1524	12											1	13		446	100		93	506
Regular (Asym. Mod.)															1		39	100		93	45
Natural (Double-Edge)		32				1		1								3		100			
Regular (Sym. Mod.)	$\frac{2}{17}$																	100	95		
Regular (Asym. Mod.)																		100			
Natural (Double-Edge)																	2	100	32	3	1
Regular (Sym. Mod.)	$\frac{3}{17}$																	100	8		
Regular (Asym. Mod.)																		100	14		

FIG. (5.13) AMPLITUDE OF HARMONIC COMPONENTS IN LINE TO LINE VOLTAGE WAVEFORMS EXPRESSED AS PERCENTAGES OF THE WANTED HARMONIC COMPONENTS FOR A MODULATION INDEX OF UNITY.

#### (5.3.1.3) Wanted Harmonic Components

It was shown in Section (5.2.2.2c) of this thesis that for natural sampled p.w.m. at non-integer values of frequency ratio, the degree of amplitude and/or phase unbalance between respective wanted harmonic components was generally insignificant. However, for the few cases where unbalance did occur, the regular sampled asymmetrical double-edge p.w.m. process completely eradicated these undesirable effects.

#### (5.3.1.4) Super-Harmonic Components

It may be seen from Fig.(5.13), that for a frequency ratio of  $2\frac{1}{17}$ , the first twenty harmonic components in the LINE to LINE voltage waveforms for both natural sampled double-edge p.w.m. and regular sampled asymmetrical double-edge p.w.m, does not contain super-harmonic components, whereas, for the regular sampled symmetrical double-edge p.w.m. process a super-harmonic of 95% is included. Fig.(5.14) further illustrated the harmonic elimination property of the regular sampled asymmetrical double-edge p.w.m. process.

It may therefore be concluded, that the regular sampled asymmetrical double-edge p.w.m. process is considerably superior to both the natural sampled double-edge p.w.m. process and the regular sampled symmetrical double-edge p.w.m. process so far as the elimination of super-harmonic components is concerned.

#### (5.3.1.5) Interim Conclusions

The analytical results have shown that the regular sampled asymmetrical double-edge p.w.m. process is superior to existing p.w.m. processes because:

- (i) It completely eradicates direct voltage components from

Sampling Process	Freq. Ratio	Harmonic Order																			
		1	2	3	4	5	6	7	8	9	10	11	12	13	14	15	16	17	18	19	20
Natural (Double-Edge)			2	100	32	3	1														
Regular (Sym. Mod.)	$\frac{1}{3\frac{1}{4}}$			100	10			21	46	1							3	30	34	1	1
Regular (Asym. Mod.)				100	15																
Natural (Double-Edge)				2	100	32	3	1													
Regular (Sym. Mod.)	$\frac{1}{3\frac{1}{5}}$				100	9				22	47	1									3
Regular (Asym. Mod)					100	15															
Natural (Double-Edge)					2	100	32	3	1												
Regular (Sym. Mod.)	$\frac{1}{3\frac{1}{6}}$					100	9					22	48	1							
Regular (Asym. Mod.)						100	7														

FIG. (5.14) PERCENTAGE AMPLITUDE OF HARMONIC COMPONENTS IN LINE TO LINE VOLTAGE WAVEFORMS FOR A MODULATION INDEX OF UNITY.

the output LINE to LINE voltage waveforms.

(ii) The amplitudes of sub-harmonic voltage components are reduced to an insignificant value which allows the useable frequency range of the p.w.m. control generator to be increased from:

$$10 < \frac{f_c}{f_m} < \infty$$

to

$$2 < \frac{f_c}{f_m} < \infty$$

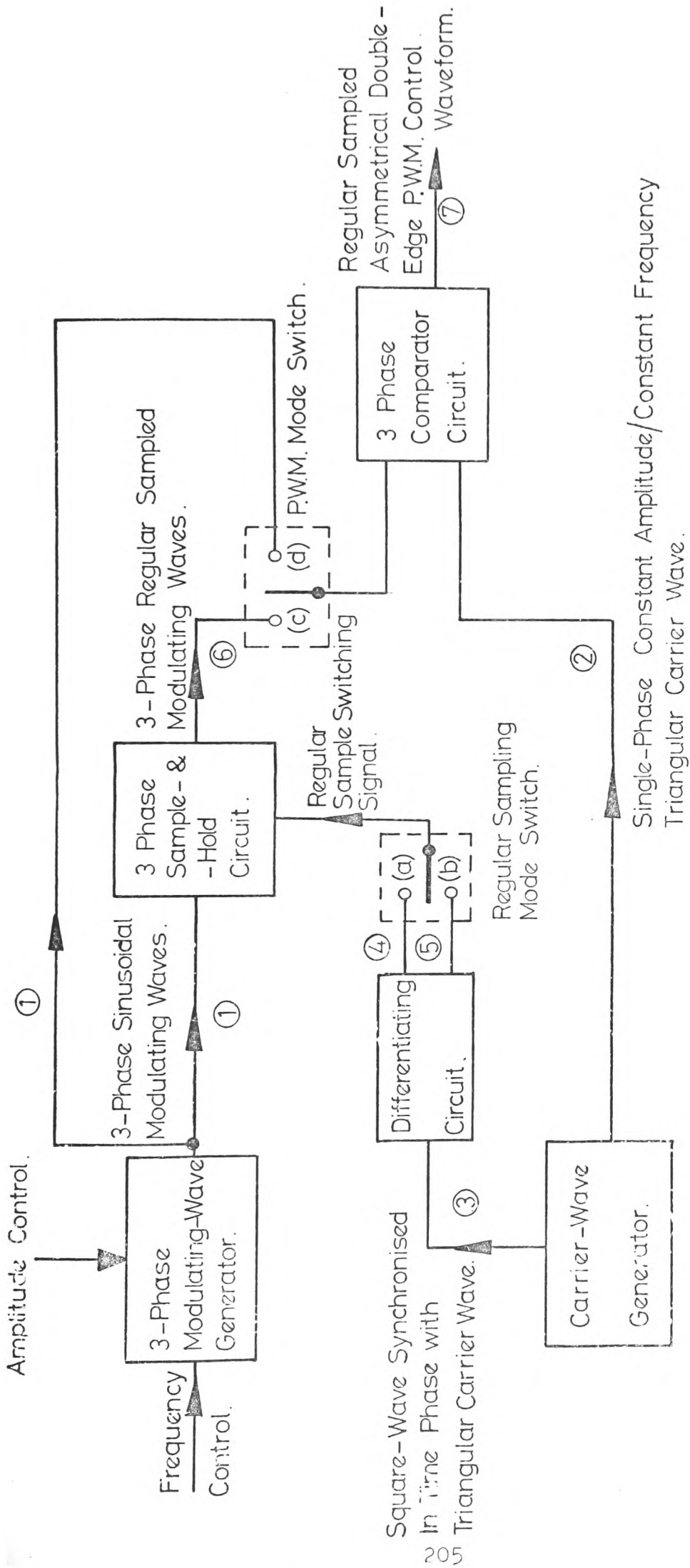
(iii) The most significant super-harmonic voltage components in the output LINE to LINE voltage waveforms are reduced in amplitude to an insignificant value.

#### (5.3.2) Experimental Investigation Into the Three Double-Edge P.W.M. Control Schemes

A light electronic control circuit was constructed which simulated the natural sampled double-edge p.w.m. process, the regular sampled symmetrical double-edge p.w.m. process and the regular sampled asymmetrical double-edge p.w.m. process. This circuit provided a means of comparing the analytical results for the three p.w.m. processes with the experimental results and also allowed a direct comparison to be made of the experimental results for the three p.w.m. processes.

##### (5.3.2.1) Light Electronic Control System which Simulated the Three P.W.M. Processes.

A block diagram of this control system is shown in Fig. (5.15a), and it is particularly interesting to observe that when the novel regular sampled p.w.m. control schemes are compared with the prior-art p.w.m. control scheme illustrated in Fig.(5.1), it is again immediately apparent, that regular



FIG(5 15a) BLOCK DIAGRAM OF LIGHT ELECTRONIC CONTROL CIRCUIT WHICH SIMULATES

THE THREE DOUBLE - EDGE P.W.M. PROCESSES.

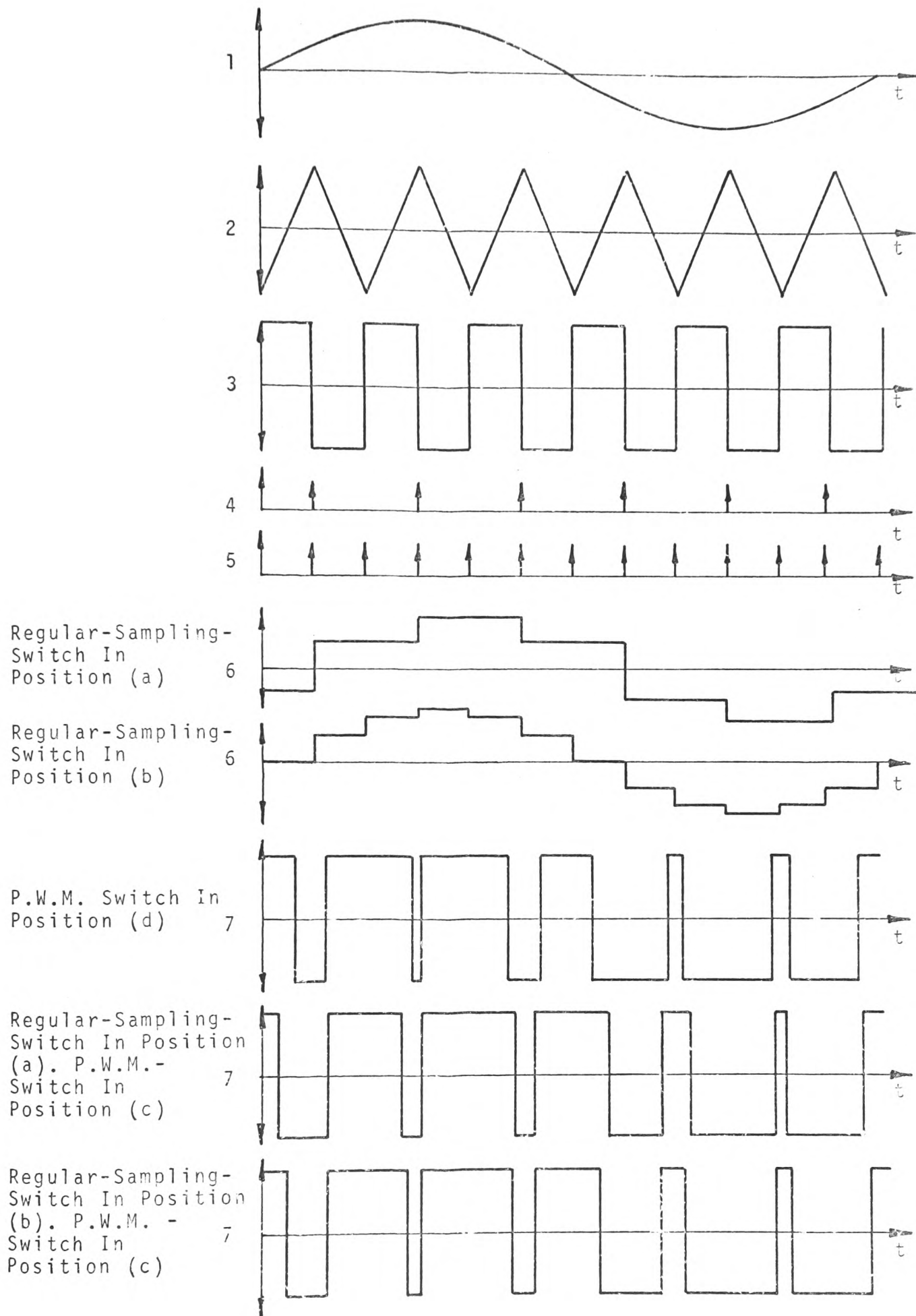
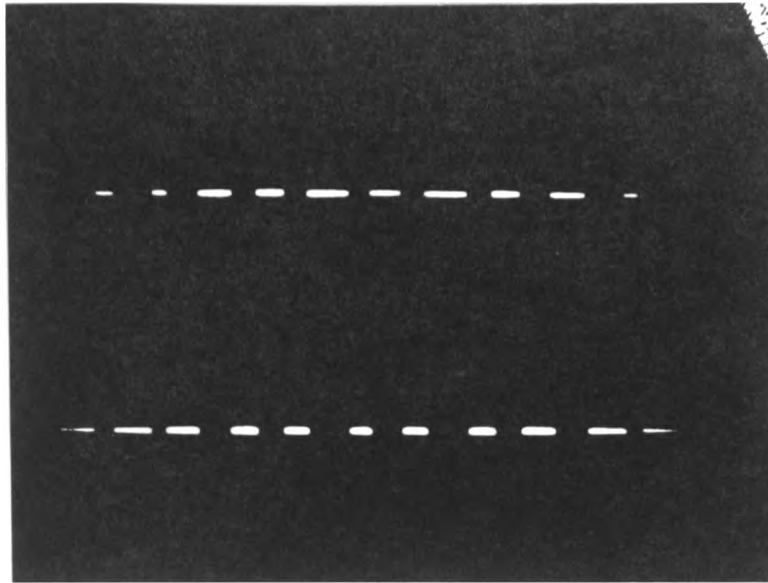
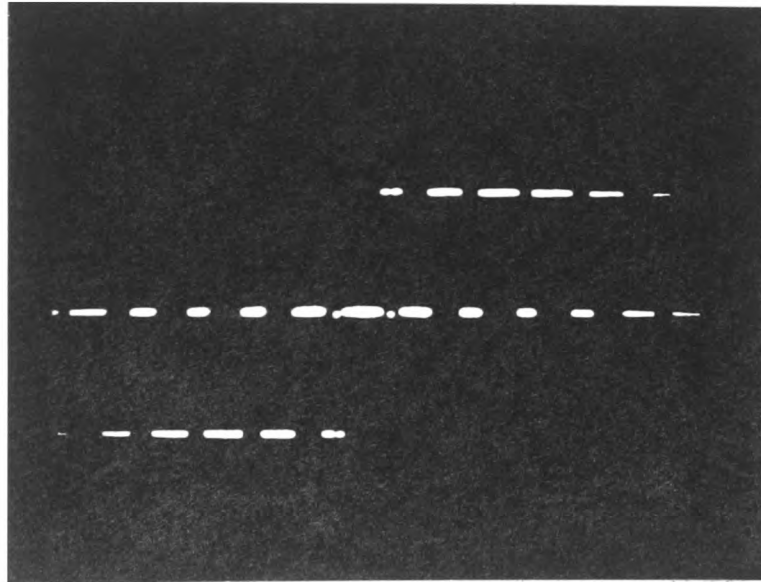


FIG.(5.15b) WAVEFORMS AT POINTS INDEICATED ON BLOCK DIAGRAM ILLUSTRATED IN FIG.(5.15a) FOR ONE PHASE ONLY.

sampled symmetrical and asymmetrical double-edge p.w.m, is achieved at a cost of only three sample-and-hold circuits. The three-phase modulating wave generator generates three-phase sinusoidal waveforms which are variable in both amplitude and phase. The three-phase sample-and-hold circuits regularly samples the three-phase modulating waves at the carrier frequency or twice the carrier frequency. The single-phase carrier-wave generator generates both a rectangular waveform and an isosceles-triangular-waveform where both waveforms are of constant amplitude and frequency and synchronised in time-phase. The differentiating circuit supplies the regular sample switching pulses to the three-phase sample-and-hold circuit. The three-phase comparator circuit compares the modulating wave or regular sampled modulating wave with the single phase carrier wave and thus produces the p.w.m control waves. The p.w.m mode-switch selects either natural sampled p.w.m or regular sampled p.w.m whereas, the regular sampling switch selects either regular sampled symmetrical p.w.m or regular sampled asymmetrical p.w.m. The waveforms at the various numbered points in the block diagram are illustrated in Fig.(5.15b). The three-phase comparator circuit was made to supply three,  $1k\Omega$  resistors connected in star as illustrated in Fig.(5.16). Oscillograms of the true LINE to LINE and LINE to D.C. NEUTRAL voltage waveforms are illustrated in PLATE (5.1). A schematic diagram of the light electronic control scheme illustrated in Fig.(5.15a) is included in Appendix (5).



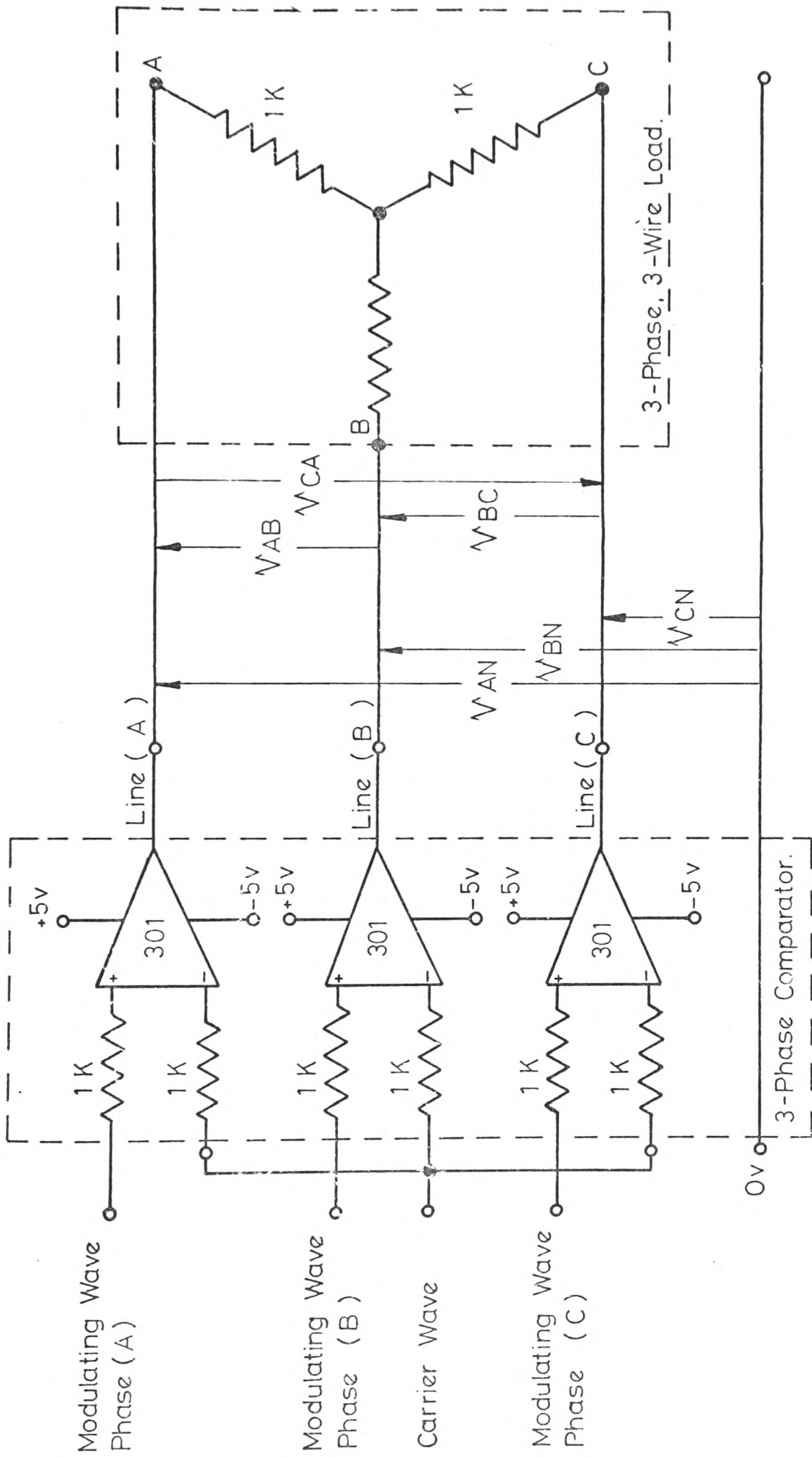
Line To D.C. Neutral Voltage Waveforms



Line To Line Voltage Waveforms

PLATE (5.1). OSCILLOGRAMS OF LINE TO NEUTRAL AND  
LINE TO LINE VOLTAGES





$V_{AN}$ ,  $V_{BN}$ ,  $V_{CN}$  = Line to D.C. Neutral Voltages.  $V_{AB}$ ,  $V_{BC}$ ,  $V_{CA}$  = Line to Line Voltages.

NATURAL SAMPLED DOUBLE-EDGE P.W.M. CONTROL CIRCUIT SUPPLYING 3-PHASE 3-WIRE LOAD.

### (5.3.2.2) Measurements Technique

The measurements technique used for the asynchronous-mode of operation was the same as the measurements technique used for the synchronous mode of operation described in Section (4.2.2.1) of this thesis. However, it is important to again emphasise that the carrier wave and modulating waves were synchronised in time-phase in the synchronous-mode of operation, whereas, the carrier wave and modulating waves are asynchronous in the asynchronous-mode being presented in this chapter. Because of this asynchronism between the carrier wave and modulating waves the measuring of harmonic amplitudes and phase was complicated by a 'beat effect' of the meter movement of the waveform analyser.

When the wave analyser was connected between LINES or between a LINE and the D.C. NEUTRAL of the circuit illustrated in Fig.(5.16) and the carrier frequency to modulating frequency ratio set to a low non-integer value  $\left(\frac{f_c}{f_m} < 4\right)$ , it was observed for both natural sampled double-edge p.w.m. and regular sampled symmetrical double-edge p.w.m. that the meter-movement oscillated when the wave analyser had been tuned to the wanted harmonic component. However, for the regular sampled asymmetrical double-edge p.w.m. process it was observed that the amplitude of oscillation of the meter movement was practically eliminated. It was therefore decided to investigate the 'beating effect' of the meter movement.

### (5.3.2.3) Beat Effect Phenomenon

Basically there are two possible means by which the 'beat effect' can occur: (i) the meter movement responds to two or

more harmonic components where the amplitudes of the harmonic components remain constant, or (ii) the meter movement responds to one harmonic component where the amplitude of the harmonic component is varying with time. Any other 'heat effect' must be a result of the combination of these two means.

Because the waveform analysers (Muirhead, D-788A), being used in the experimentation were the most 'selective' at the time, it was only possible to make an analytical investigation. The computer programs which have already been referred to in this thesis were modified to compute: (a) the amplitude of the harmonic components as a percentage of the d.c. supply and (b) the fundamental repetition frequency (fr) of the p.w.m. complex voltage waveforms. The results of the investigation suggested:

(1) The 'beat effect' due to the change in amplitude of the wanted harmonic component resulting from a change in frequency ratio was very small (less than 1%), that is to say: if the frequency ratio was set to  $2\frac{1}{20}$ , for example and the frequency ratio is then assumed to drift to  $2\frac{1}{40}$ , the change in amplitude of the wanted harmonic component was less than 1%.

(2) The fundamental repetition frequency which is the lowest possible frequency interval between adjacent harmonics can be very small for non-integer values of frequency ratio near integer values. For example consider the carrier frequency,  $f_c$ , is set at 300 Hz, then for a frequency ratio,  $\frac{f_c}{f_m} = 3\frac{1}{17}$ , the fundamental repetition frequency,  $f_r$ , is equal to 5.77 Hz, whereas, for a frequency ratio,  $\frac{f_c}{f_m} = 3\frac{1}{2}$ , the

fundamental repetition frequency,  $f_r$ , is equal to 42.86 Hz. This dependence of the fundamental repetition frequency on the value of frequency ratio can be expressed algebraically as follows:

$$\text{let } \frac{f_c}{f_m} = \frac{M}{N}, \text{ where } M > N$$

and where the 'highest common factor' of M and N is unity,

$$\text{then, } \frac{f_m}{f_r} = N \text{ or } f_m = N \cdot f_r$$

$$\text{therefore, } N \cdot f_r = \frac{N}{M} \cdot f_c \text{ or } f_r = \frac{f_c}{M},$$

$$\text{therefore, when } M \gg f_c, f_r \rightarrow 0.$$

From the analytical results it may therefore be concluded that the 'beat effect' phenomenon of the meter movement of the waveform analyser is entirely due to the presence of the wanted harmonic component plus sub-harmonic components and/or super-harmonic components lying within the 10 Hz flat-top selective pass-band of the waveform analyser. Therefore, it may also be concluded that the reason for the observed 'beat effect' in the natural sampled double-edge p.w.m. process for values of frequency ratio given by:

$$1 < \frac{f_c}{f_m} < 4$$

was due to sub-harmonics and super-harmonics lying within the 10 Hz pass-band of the wave analyser; whereas, the reason for the observed 'beat effect' in the regular sampled symmetrical double-edge p.w.m. process was due to the presence of the wanted harmonic component and the large super-harmonic components only, lying within the 10 Hz pass-band. Similarly the reason for the absence of the 'beat effect' in the regular sampled asymmetrical double-edge p.w.m. process was

because the wanted harmonic component only existed in the 10 Hz pass-band of the wave analyser; the sub-harmonic components and most significant super-harmonic components being eliminated by the asymmetrical p.w.m. process. This supports the computed harmonic spectra illustrated in both Fig.(5.13) and Fig.(5.14).

#### (5.3.2.4) Experimental Results

Because of the 'beat effect' phenomenon experimental results could only be determined for values of frequency ratio where the fundamental repetition frequency was greater than the 10 Hz. pass-band of the waveform analyser, or, where sub-harmonic components and super-harmonic components inside the 10 Hz pass-band cancelled or were eliminated by the modulation process. To reduce the possibility of more than one harmonic component lying within the pass-band of the waveform analyser, the carrier frequency,  $f_c$ , was set at 4000 Hz. Whilst such a high value of carrier frequency is possible with the p.w.m. control waveform generator, such a high value is not possible when the p.w.m. control generator is made to drive the thyristor power convertor. This point will be enlarged upon in Chapter (6). In order to eliminate the possibility of a change in the chosen value of frequency ratio as a result of frequency drift, the carrier frequency and modulating frequency were held rigorously constant. Fig.(5.17), Fig.(5.18) and Fig.(5.19) illustrates and compares experimental results with analytical results for the three double-edge p.w.m. processes, where it may be seen that good correlation is achieved. The slight difference which exists between the theoretical results and experimental results are probably due to slight non-linearities

$$f_c = 4000 \text{ Hz}, \quad \frac{f_c}{f_m} = 2\frac{1}{9}$$

Modulation Index = 1.0

— Theoretical

- - - Experimental

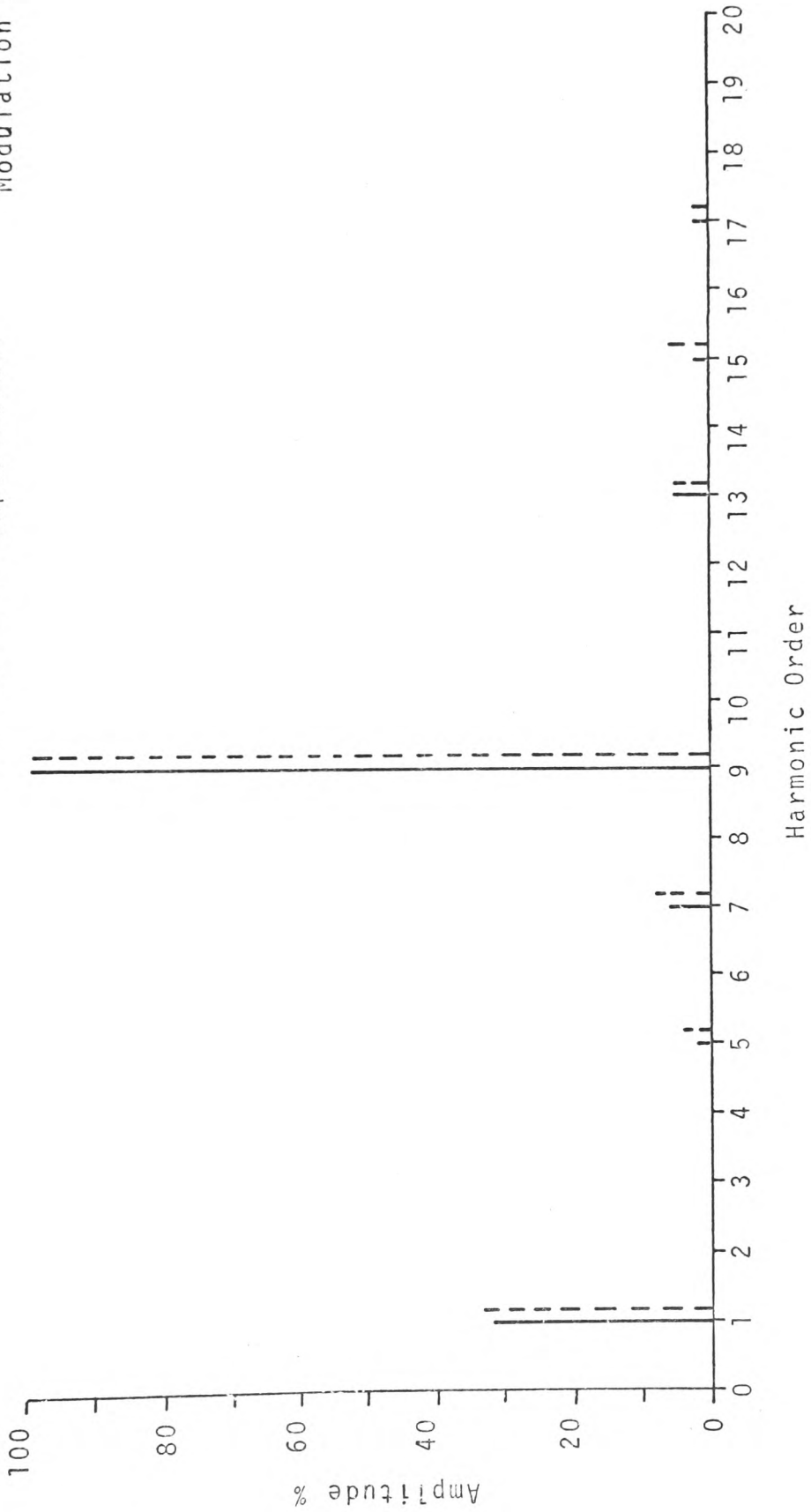


FIG. (5.17) LINE TO LINE VOLTAGE WAVEFORM HARMONICS FOR NATURAL SAMPLED DOUBLE-EDGE P.W.M.

$$f_c = 4000 \text{ Hz}, \frac{f_c}{f_m} = 2\frac{1}{9}$$

Modulation Index = 1.0

Theoretical

Experimental

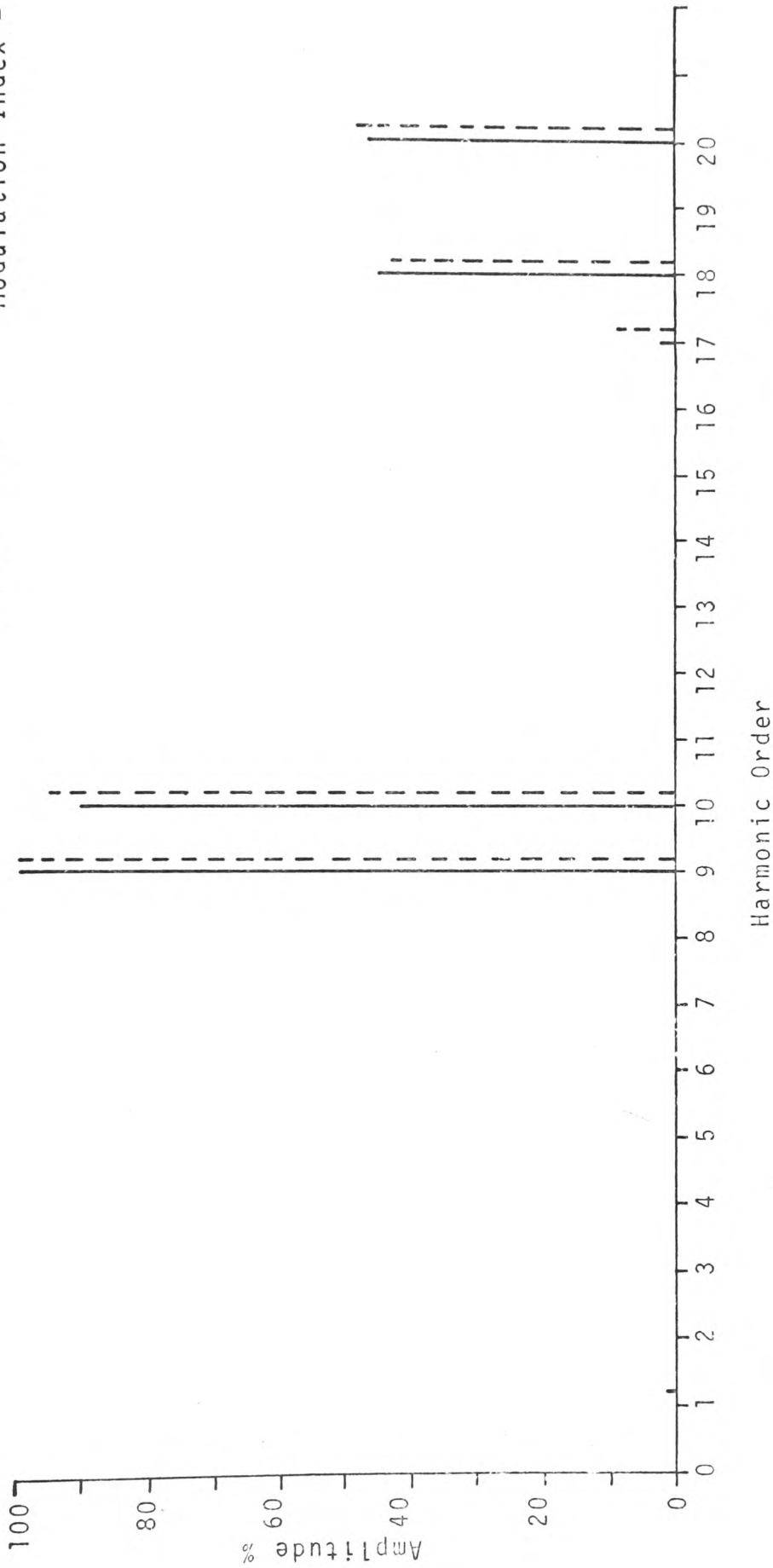


FIG. (5.18) LINE TO LINE VOLTAGE WAVEFORM HARMONICS FOR REGULAR SAMPLED SYMMETRICAL DOUBLE-EDGE P.W.M.

$f_c = 4000. \text{ Hz}, \frac{f_c}{f_m} = 29$

Modulation Index = 1.0

— Theoretical

- - - Experimental

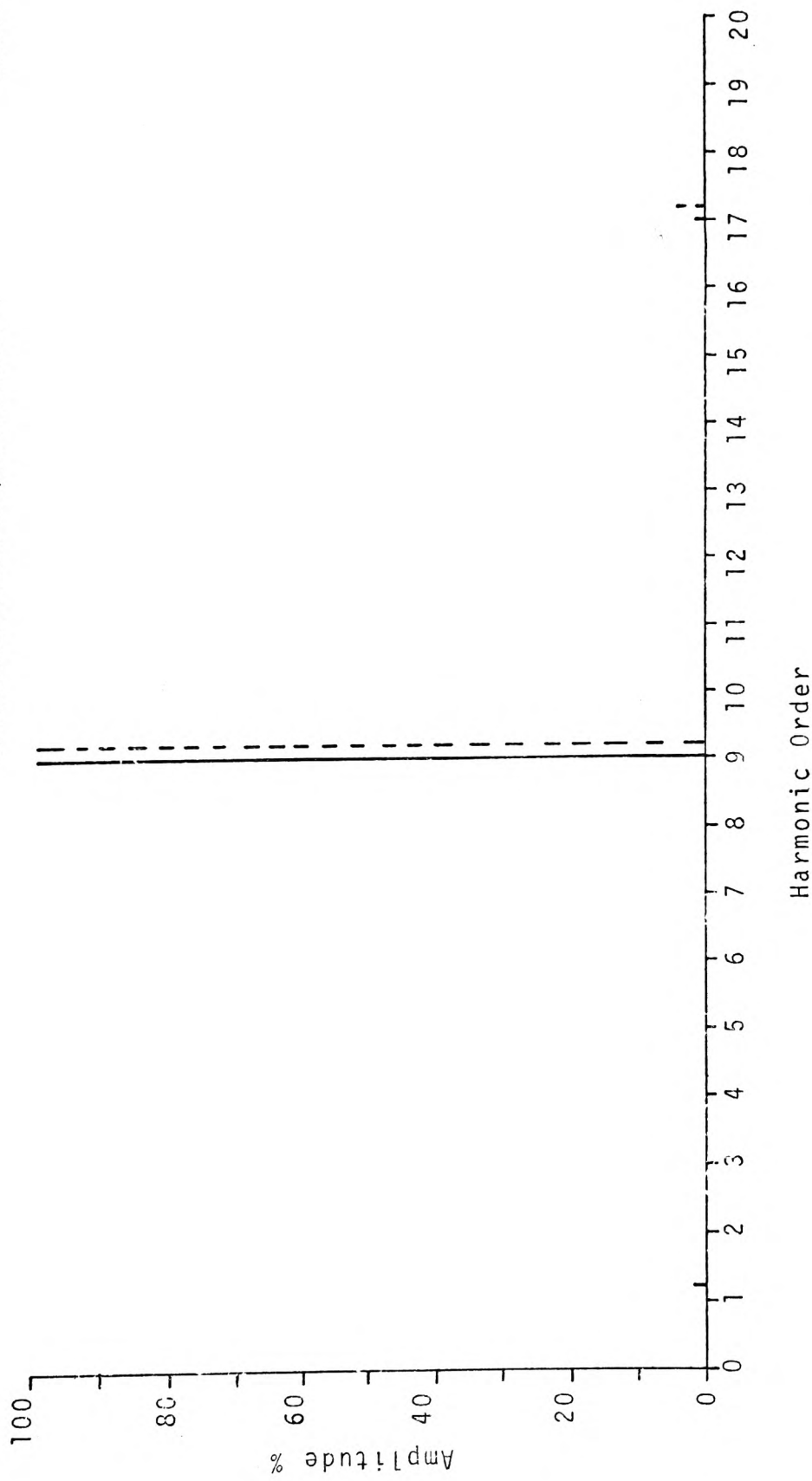


FIG.(5.19) LINE TO LINE VOLTAGE WAVEFORM HARMONICS FOR REGULAR SAMPLED ASYMMETRICAL DOUBLE-EDGE P.W.M.



in the physical p.w.m. processes.

### (5.3.3) Interim Conclusions

An asynchronous p.w.m. control scheme has been introduced, which allows the frequency ratio to theoretically vary between the limits:

$$1 < \frac{f_c}{f_m} < \infty$$

However, it has been shown that the practical range of frequency ratio variation for the prior-art natural sampled double-edge p.w.m. process is limited to:

$$10 < \frac{f_c}{f_m} < \infty$$

because of the presence of sub-harmonics and d.c. components in the output p.w.m. voltage spectra. It has been shown that the application of regular sampling, which is a well known concept in telecommunications practice but which has not previously been applied to p.w.m. power convertor control circuits, eradicates the undesirable sub-harmonic and d.c. components from the output p.w.m. voltage spectra which increases the practical range of frequency ratio variation to:

$$2 < \frac{f_c}{f_m} < \infty$$

The 'beat effect' phenomenon which has been known to exist in prior-art asynchronous-mode p.w.m. convertor systems but which has not previously been investigated has now been analysed, and it has been demonstrated that the novel regular sampled asynchronous-mode p.w.m. control scheme almost eliminates this undesirable phenomenon for all non-integer values of frequency ratio.

## (6) POWER CONVERTOR AND TRIGGER PULSE CIRCUITS

### (6.1) Introduction

The two preceding chapters of this thesis have demonstrated both analytically and experimentally that the application of regular sampling techniques to the p.w.m. control signal generator circuits, eradicates many of the undesirable features which have existed in prior-art synchronous-mode and asynchronous-mode p.w.m. systems. It therefore only remains to be shown that the novel regular sampled asymmetrical double-edge p.w.m. process also improves the output voltage harmonic spectra of the thyristor power convertor. However, because the p.w.m. power convertor is basically a power amplifier, the percentage amplitude of the harmonic voltage components at the output of the power convertor should be identical to the percentage amplitude of the harmonic voltage components at the output of the p.w.m. control signal generator, provided, the power convertor has a flat-top frequency response. It is this aspect of the project which will be investigated in this chapter.

The investigation was aided by the design and construction of a '5 KVA, 240 volt three-phase, auxiliary impulse commutated thyristor inverter'. A photograph of the convertor is shown in PLATE (6.1). This particular convertor configuration was chosen for the reasons given in Section (2.3) of this thesis.

### (6.2) Design Details of the Practical P.W.M. Power Convertor

A schematic layout of the complete power convertor is shown in Fig.(6.1). The power circuit and gating circuit can be

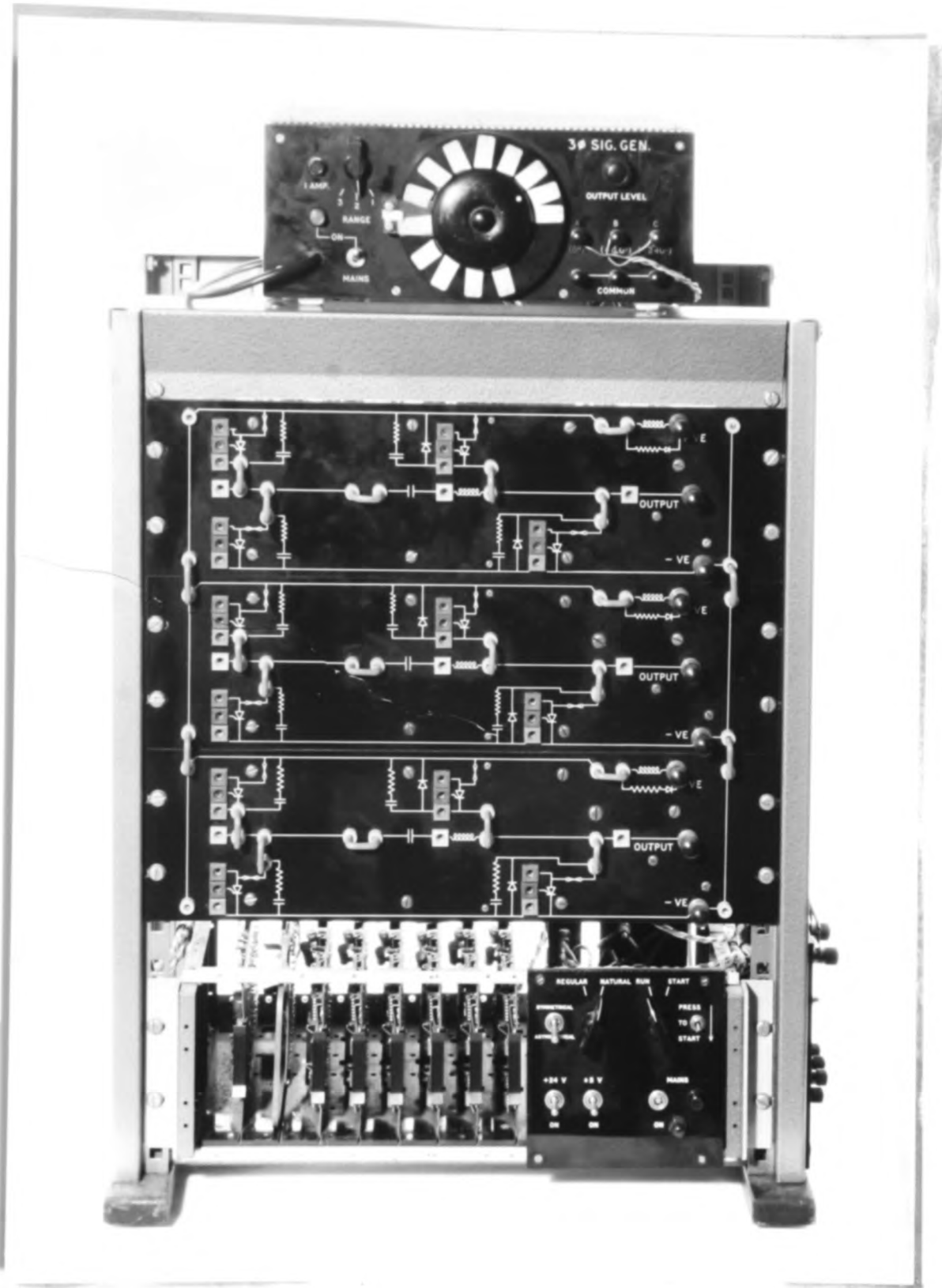


PLATE (6.1). 3-PHASE, 240 VOLT, 7KVA POWER CONVERTOR

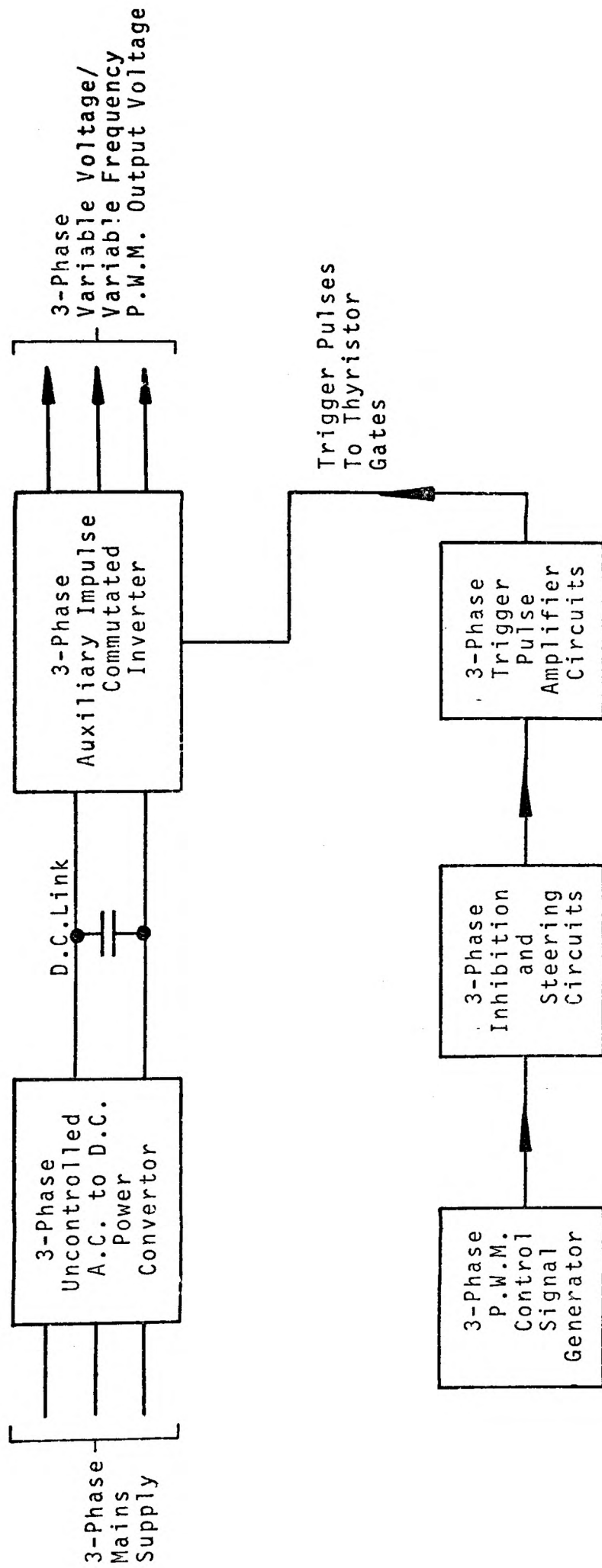


FIG.(6.1) SCHEMATIC LAYOUT DIAGRAM OF PRACTICAL POWER CONVERTOR.

divided into several sections, each section performing a distinct function within the overall system. It was therefore decided to describe each section of the system separately.

(6.2.1) Three-Phase Uncontrolled A.C. to D.C. Power Convertor

A circuit diagram of this section of the convertor is shown in Fig.(6.2). It may be seen to consist of a three-phase diode bridge (Mullard Three-Phase Rectifier Diode Stack, Type OSK40 - 600), across the output of which is connected an electrolytic capacitor (5,000 $\mu$ F, 350 volts). The capacitors were inserted for mainly two reasons: (1) to smooth the d.c. link voltage and (2) to receive the V.Ar. from the inverter when supplying an inductive load. The convertor provided a maximum d.c. link voltage of mean-value 228 volts, with a full-load ripple-factor and regulation of 1.4% and 8% respectively.

(6.2.2) Three-Phase Auxiliary Impulse Commutated Thyristor Inverter

It may be seen from the circuit diagram illustrated in Fig.(6.3) that the three-phase thyristor power inverter basically consists of three identical single-phase, half-bridge auxiliary impulse commutated circuits. The reasons for the choice of the half-bridge auxiliary impulse commutated inverter along with a description of its operation, was presented in Section (2.3) of this thesis. All thyristors used in the power inverter were of inverter-grade (Mullard, Type: BTW30 - 600), whereas, the diodes were of the fast-recovery type (Mullard Type: BYX30 - 600). Both the 10 $\mu$ H,  $\frac{di}{dt}$  - limit -

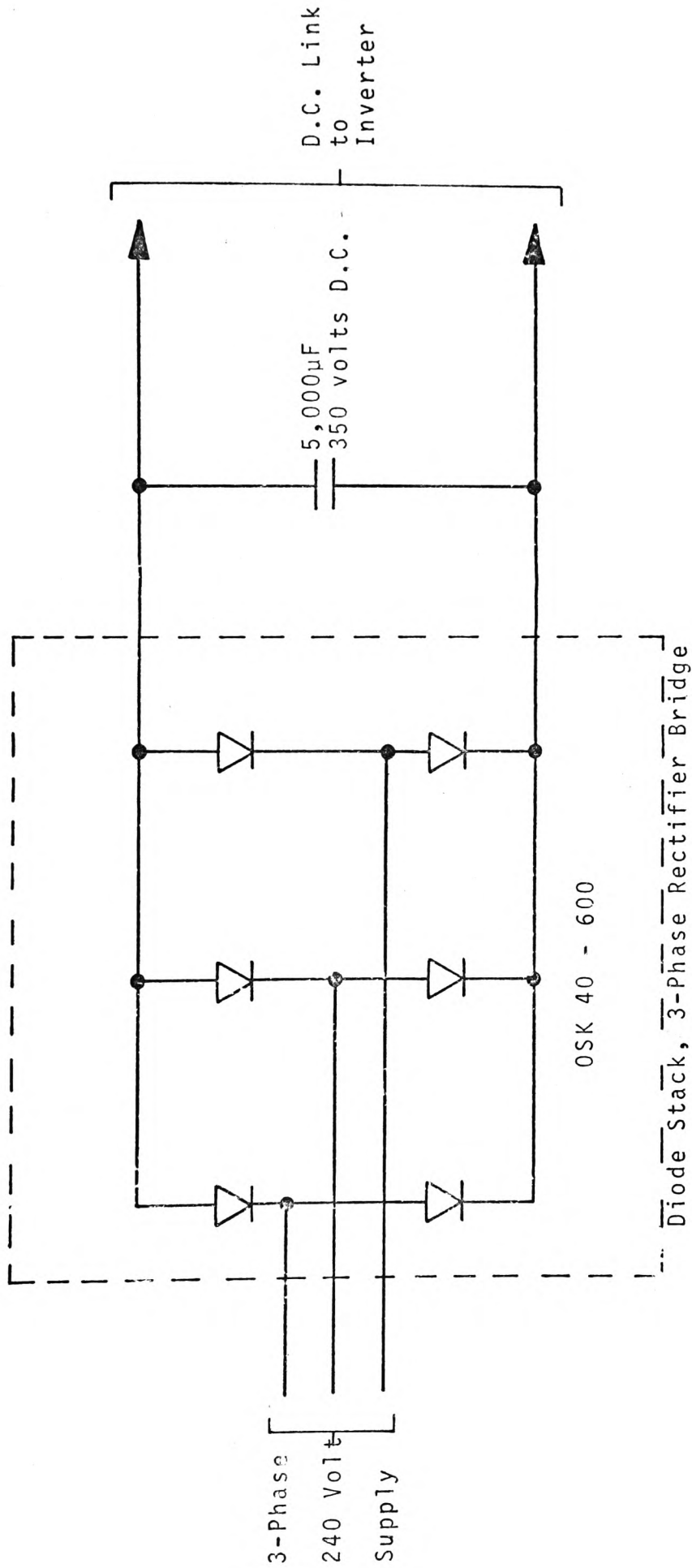


FIG. (5.2) CIRCUIT DIAGRAM OF UNCONTROLLED A.C. TO D.C. CONVERTOR.

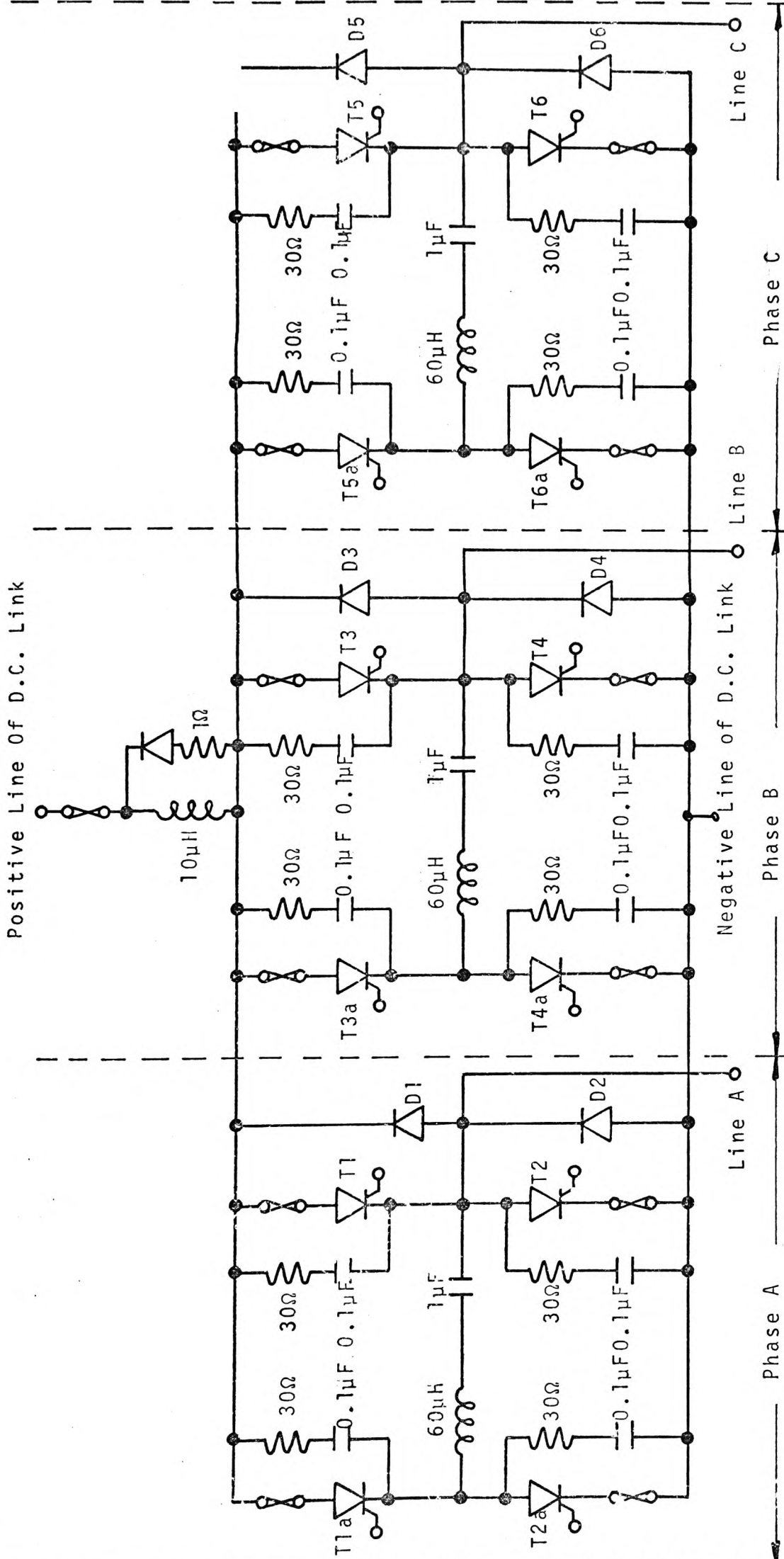


FIG. (6.3) 3-PHASE AUXILIARY IMPULSE COMMUTATED THYRISTOR INVERTER

inductor and the 60 $\mu$ H commutating -choke were of the air-cored type. The 1 $\mu$ F commutating capacitor and the 0.1 $\mu$ F snubber capacitor were both of the resin moulded metallised polycarbonate type (I.T.T Types: P.M.A.1.0 M400 and P.M.A.O.1 M400 respectively). The values of the various components were determined by means of the design equations included in Ref.( 5 ).

Each of the three half-bridge circuits of the three-phase inverter were controlled by each respective phase of the three-phase p.w.m.control generator via steering circuits and trigger-pulse-amplifiers. The possibility of short circuits occurring between the d.c. link bus-bars was prevented by inhibition circuits.

### (6.2.3) Inhibition Circuits and Steering Circuits

The switching sequence and commutating sequence of the thyristors in each phase of the power convertor, are determined by the polarity of the pulses of the respective p.w.m.control waveform from the three-phase p.w.m.control signal generator. However, because series connected thyristors exist across the d.c. link bus-bars, it became necessary to detect the conduction-state of these thyristors and so prevent the possibility of short circuits occurring.

Consider:

G(T1) = trigger pulses applied to gate of  
thyristor T1

G(T2a)= trigger pulses applied to gate of  
thyristor T2a.

G(T2) = trigger pulses applied to gate of  
thyristor T2.



$G(T1a)$  = trigger pulses applied to gate of thyristor T1a  
 $(P.W.M)$  = p.w.m control signal is at (+V)  
 $(\overline{P.W.M})$  = " " " " " (-V)  
 $(T1)$  = thyristor T1 is in ON - state  
 $(T2)$  = " T2 " " " "  
 $(T1a)$  = " T1a " " " "  
 $(T2a)$  = " T2a " " " "  
 $(\overline{T1})$  = " T1 " " OFF - state  
 $(\overline{T2})$  = " T2 " " " "  
 $(\overline{T1a})$  = " T1a " " " "  
 $(\overline{T2a})$  = " T2a " " " "

then the conditions for triggering of the thyristors in phase (A) of the power convertors without the possibility of short circuits occuring can be expressed in terms of Boolean algebra as follows:

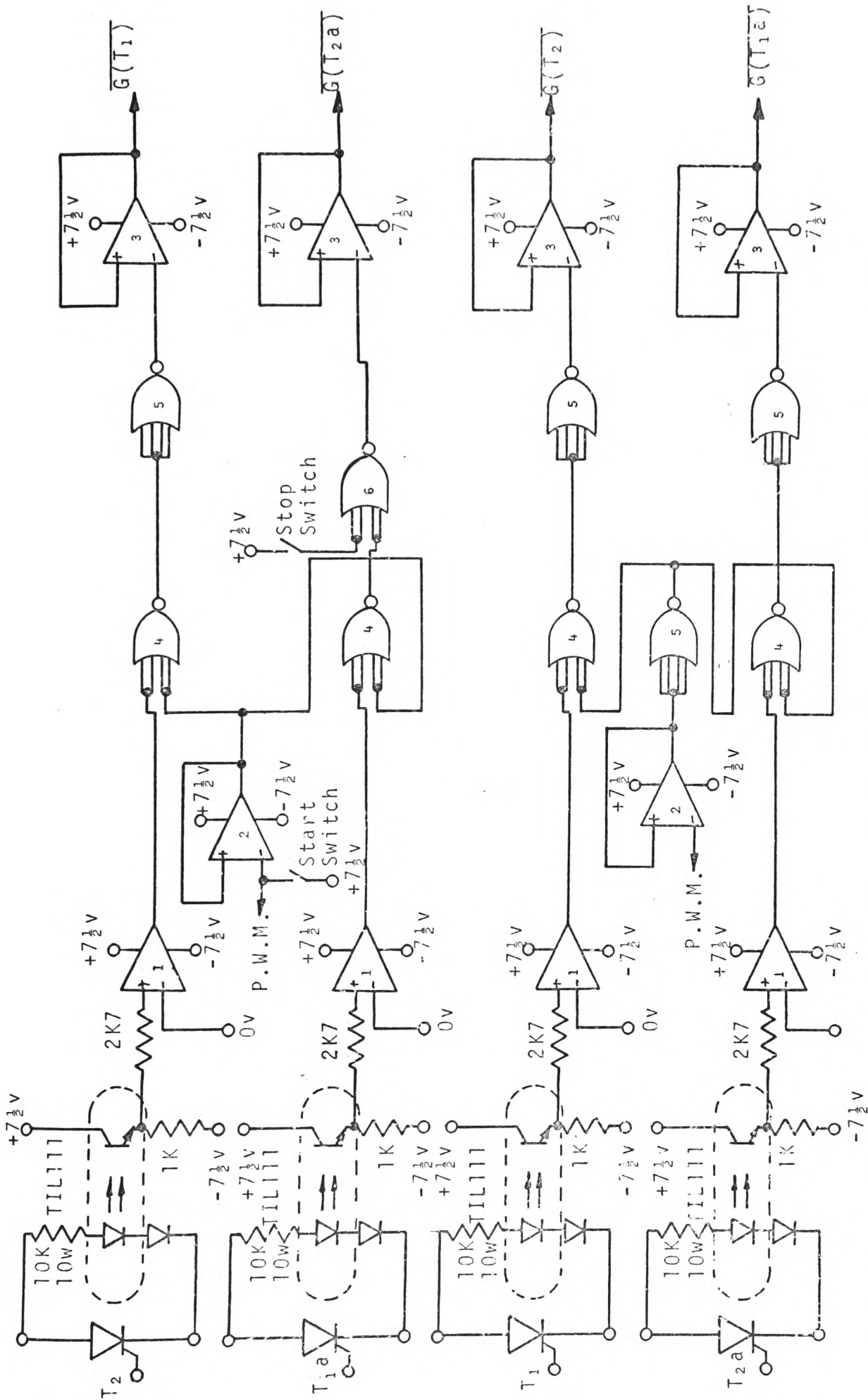
$$G(T1) = (P.W.M) \cdot (\overline{T2}) = \overline{(P.W.M) \cdot (T2)} \quad \text{---(6.1)}$$

$$G(T2a) = (P.W.M) \cdot (\overline{T1a}) = \overline{(P.W.M) \cdot (T1a)} \quad \text{---(6.2)}$$

$$G(T2) = (\overline{P.W.M}) \cdot (\overline{T1}) = \overline{(P.W.M) \cdot (T1)} \quad \text{---(6.3)}$$

$$G(T1a) = (\overline{P.W.M}) \cdot (\overline{T2a}) = \overline{(P.W.M) \cdot (T2a)} \quad \text{---(6.4)}$$

The triggering requirements for thyristors T1 and T2a, T2 and T1a are determined by equations (6.1) and (6.2) and equations (6.3) and (6.4) respectively. The practical implementation of these conditions is illustrated in Fig.(6.4). The conduction-state of the thyristors was detected by the opto-coupling devices (TIL111). When the thyristors were in the non-conducting-state positive output voltage signals existed



(1), (2) & (3) - Operational Amplifier, Type-741  
 (4), (5) & (6) - Dual, 4-Input NOR Gate, Type - MC14002  
 P.W.M. - To Control Signal Generator  
 $G(T_1)$ ,  $G(T_{2a})$ ,  $G(T_2)$ ,  $G(T_{1a})$  - Gate Control Signals To Trigger Pulse Amplifiers.

FIG. (6.4) INHIBITION AND STEERING CIRCUITS FOR PHASE (A) OF THE THREE-PHASE POWER INVERTER.

(logic "1") whereas, when the thyristors were in the conducting-state the output voltage signals from the opto-couplers were negative (logic "0"). The output voltage signals from the opto-couplers were amplified by the open-loop amplifiers (1). The output voltage signals from the open-loop amplifiers, along with the buffered (2) p.w.m control signals or their negation (5) were then applied to the input of CMOS NOR-gates (4). The output signals from the NOR-gates (4) were then buffered (3) and applied to the inputs of the trigger pulse amplifiers.

The start switches provided a means of initially charging the commutating capacitors. With the p.w.m control signals isolated from the buffer amplifiers and the start-switches closed, thyristors: T1, T4 and T6 were triggered into conduction. The start switches were then opened, but the three thyristors remained in conduction. The application of the p.w.m control signals to the buffer amplifiers (2) along with the logic control signals from the opto-couplers (T1L111) via open loop amplifiers (1) supplied the trigger-pulse amplifiers via NOR-gates (4) and buffer amplifiers (3), with the appropriate control signals.

Shut-down of the power inverter was achieved by means of the stop switches. With the p.w.m control signals removed from the inputs to the buffer amplifier (2), the stop switches were closed which resulted in the application of trigger pulses to the three auxiliary thyristors: T2a, T4a and T6a. The triggering of these auxiliary thyristors caused the commutation of any of the three main thyristors: T2, T4 and

T6, which might have been conducting. Therefore, because all return paths for the load-current to the negative bus-bar were closed, anyone of the main thyristors: T1, T3 and T5, which might have been conducting were also commutated.

#### (6.2.4) Trigger\_Pulse\_Amplifiers

The output trigger pulse control signals:  $\overline{G(T1)}$ ,  $\overline{G(T2a)}$ ,  $\overline{G(T2)}$ , and  $\overline{G(T1a)}$  from the inhibition and steering circuits were applied to the gates of the respective thyristors (T1, T2a, T2 and T1a) via: common emitter amplifiers, trigger pulse amplifiers and pulse transformers. The power amplification stage of the control circuits is illustrated in Fig.(6.5). The common emitter amplifier stages inverts the input trigger control signals ( $\overline{G(T1)}$ ,  $\overline{G(T2a)}$ ,  $\overline{G(T2)}$  and  $\overline{G(T1a)}$ ) and changes the voltage level of the control signal from 5 volts to 24 volts. The output voltage control signals were fed directly to the inputs of the trigger pulse amplifiers. The trigger pulse amplifiers were circuit modules (Mullard, 61 Series, Type - UPA61) which mainly consisted of: a voltage level detector circuit, a pulse amplifier and an emitter follower, which were interconnected as shown. The output pulses from the trigger pulse modules were supplied to the gates of respective thyristors via pulse transformer modules (Mullard, 61 Series, Type - TT61). The pulse transformers provided isolation of the power convertor circuit from the light current control and drive circuits. The synchronisation of the thyristor-gate-trigger-pulses with the p.w.m control signal for one phase is illustrated in Fig.(6.6). The mark/space ratio and pulse

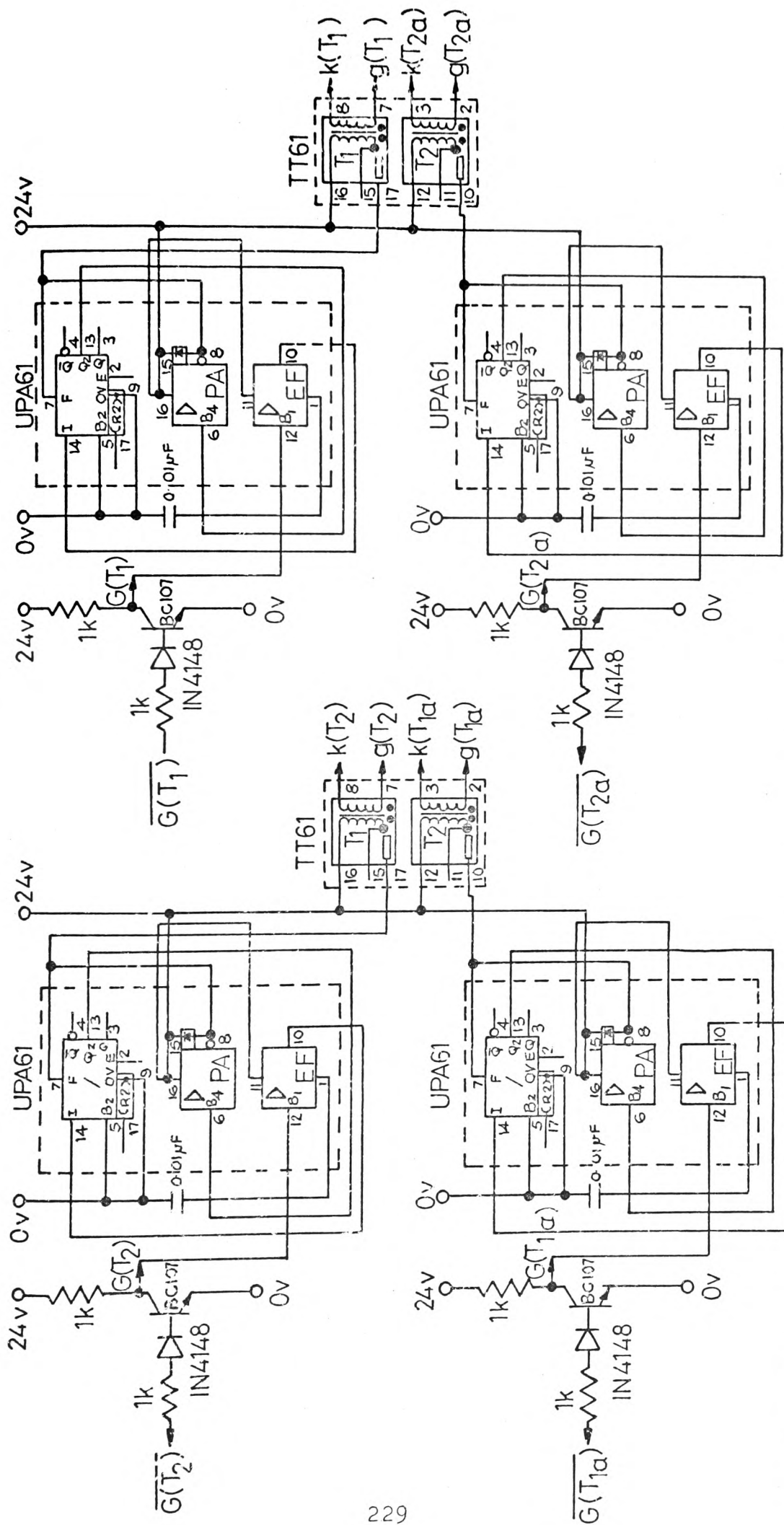
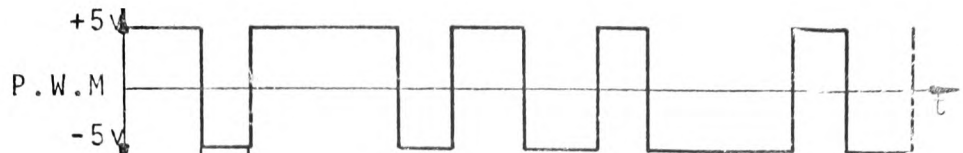


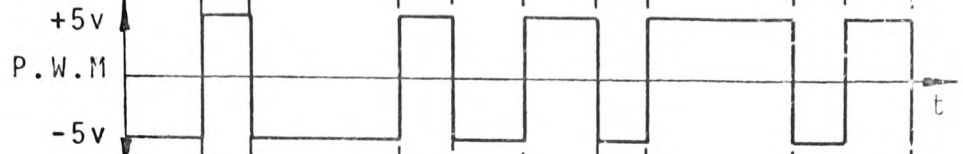
FIG.(6.5) TRIGGER PULSE AMPLIFIER CIRCUITS FOR PHASE (A) OF THREE-PHASE POWER INVERTER.

$G(T_1)$ ,  $G(T_{2a})$ ,  $G(T_2)$  and  $G(T_{1a})$  : Gate Control Pulses From Inhibition and Steering Circuits  
 $g(T_1)$  : To Gate of Thyristor  $T_1$ ,  $g(T_{2a})$  : To Gate of Thyristor  $T_{2a}$ ,  $g(T_2)$  : To Gate of Thyristor  $T_2$ ,  
 $g(T_{1a})$  : To Gate of Thyristor  $T_{1a}$ ,  $k(T_1)$  : To Cathode of Thyristor  $T_1$ ,  $k(T_{2a})$  : To Cathode of Thyristor  $T_{2a}$ ,  
 $k(T_2)$  : To Cathode of Thyristor  $T_2$ ,  $k(T_{1a})$  : To Cathode of Thyristor  $T_{1a}$ .

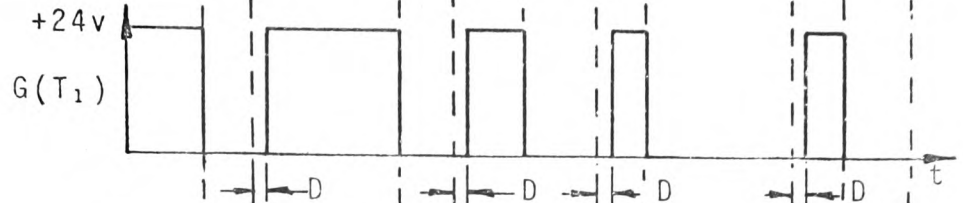
Control Signal  
From P.W.M.  
Generator



Negation of  
P.W.M.  
Control Signal



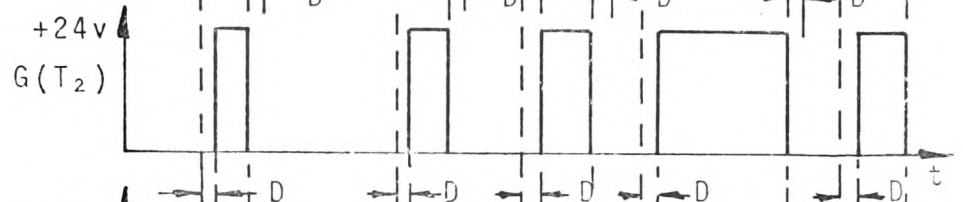
Output Control  
Pulses From  
C.E. Amplifier



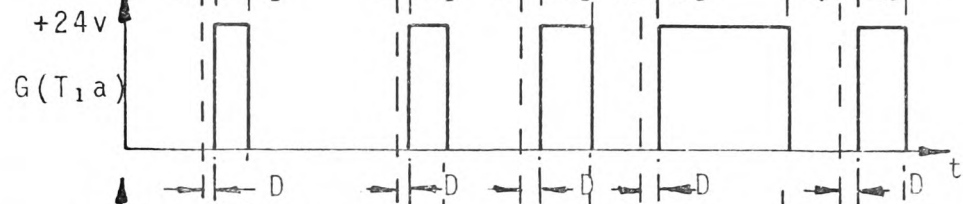
Output Control  
Pulses From  
C.E. Amplifier



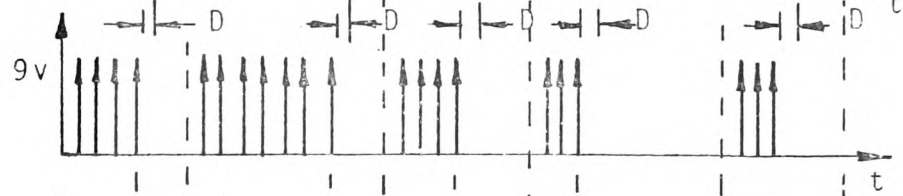
Output Control  
Pulses From  
C.E. Amplifier



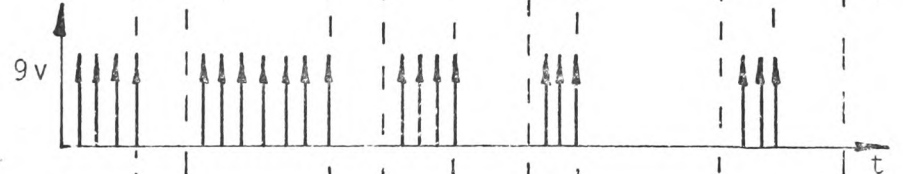
Output Control  
Pulses From  
C.E. Amplifier



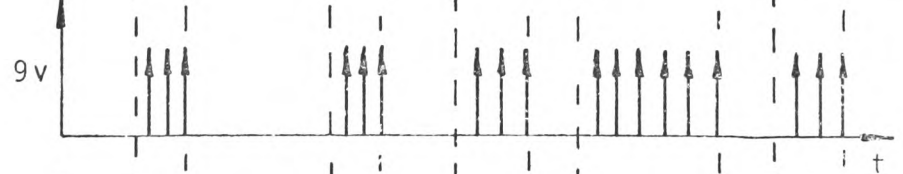
Trigger Pulses  
To Gate Of  
Thyristor T<sub>1</sub>



Trigger Pulses  
To Gate Of  
Thyristor T<sub>2a</sub>



Trigger Pulses  
To Gate Of  
Thyristor T<sub>2</sub>



Trigger Pulses  
To Gate Of  
Thyristor T<sub>1a</sub>

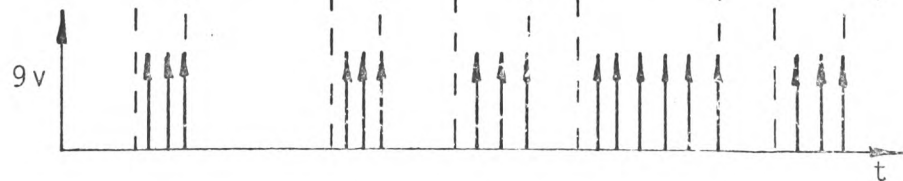


FIG.(6.6) SYNCHRONISATION OF THYRISTOR GATE TRIGGER PULSES WITH THE P.W.M. CONTROL SIGNAL.

duration of the trigger pulses was designed for 1:2 and 20 $\mu$  secs. respectively. The 20 $\mu$  second pulse duration time was achieved by means of the 0.01 $\mu$  F. capacitors. The time-delay, D, between the edges of the p.w.m control signal (P.W.M.) and the output voltage control pulses from the common emitter (C.E) amplifiers was due to the presence of the inhibition signals at the inputs to the NOR-gates in the inhibition and steering circuits.

### (6.3) Experimental Results

The three-phase power inverter was made to supply a three phase, three-wire resistive load. LINE to LINE voltage harmonic spectra were measured for both the synchronous-mode of operation and asynchronous-mode of operation for both the natural sampled double-edge p.w.m process and the regular sampled asymmetrical double-edge p.w.m process. The amplitudes of the harmonic voltage components were measured by means of a low frequency wave analyser. The measurements technique was the same as the technique described in both Chapters (4) and (5) of this thesis. The d.c. link voltage to the inverter was adjusted to approximately 100 volts by means of a three-phase variac at the input to the three-phase diode bridge rectifier.

This value of voltage was then held constant for both modes of operation. Because the commutating capability of the thyristor inverter was designed for a maximum frequency of 500 Hz, it was decided to limit the frequency of the carrier signal to approximately 300 Hz.

#### (6.3.1) Synchronous-Mode of Operation

This mode of operation was achieved by driving the thyristor

power inverter by means of the synchronous-mode p.w.m control signal generators described in Sections (4.2.3) and (4.3.2) of this thesis. The frequency of the fundamental harmonic component and the depth of modulation was selected by means of the three-phase, sinusoidal modulating wave generator, whereas, the frequency ratio was chosen by the selector switch of the programmable divide by "N" counter.

$$(6.3.1.1) \quad f_m = 20 \text{ Hz}, \frac{f_c}{f_m} = 3, \text{ Mod.Index} = 0.5$$


---

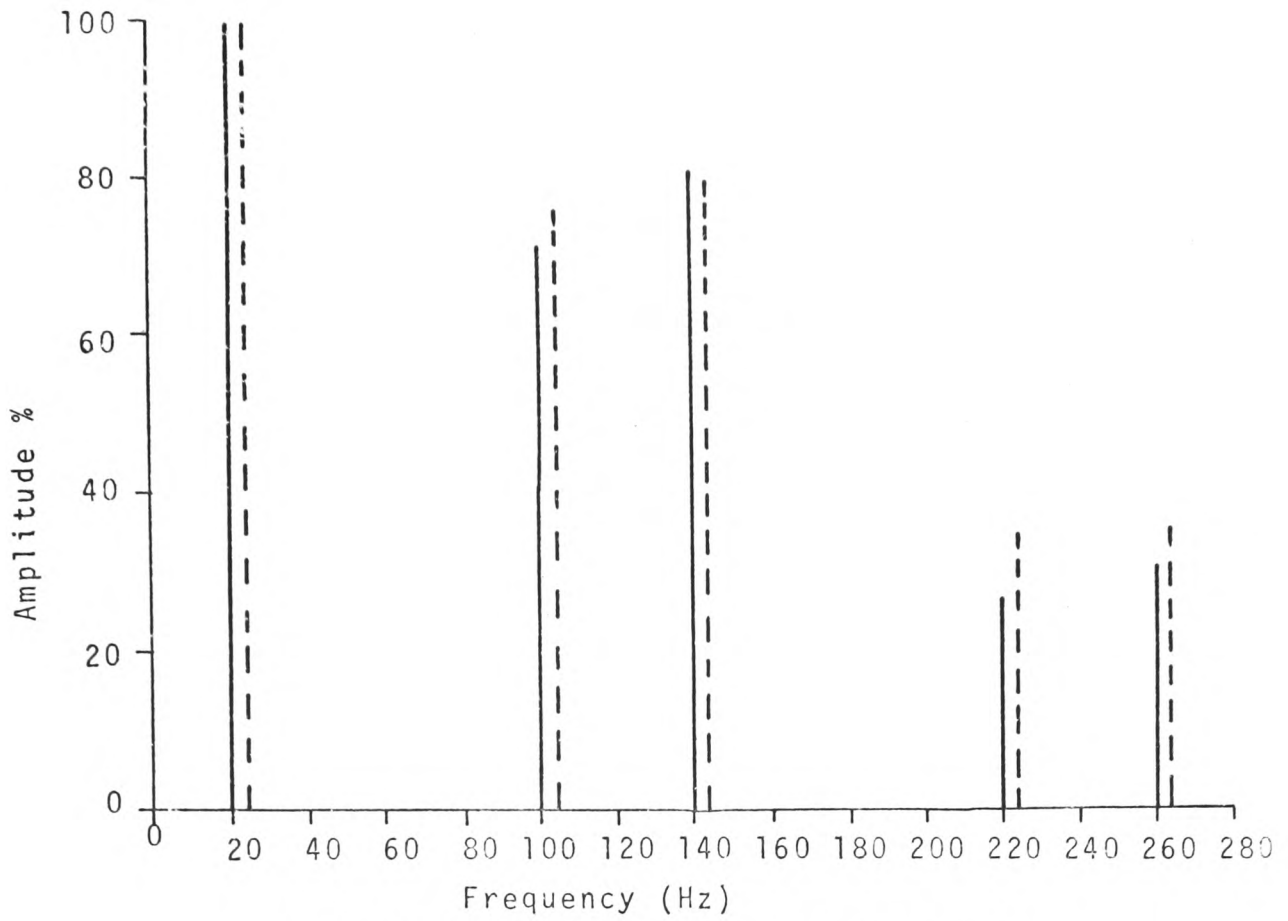
From the results illustrated in Fig.(6.7a) and Fig.(6.7b) it may be seen that for both natural sampling, and regular sampling good correlation exists between the computed results and the experimental results. It may also be seen that the regular sampling asymmetrical double-edge p.w.m process reduces the amplitude of the most significant harmonic: the 100 Hz component was reduced by approximately 35%. However, the 140 Hz component is increased by approximately 22%. For both modulation process, the wanted components formed a balanced positive-sequence set.

$$(6.3.1.2) \quad f_m = 30 \text{ Hz}, \frac{f_c}{f_m} = 4, \text{ Mod.Index} = 0.5$$

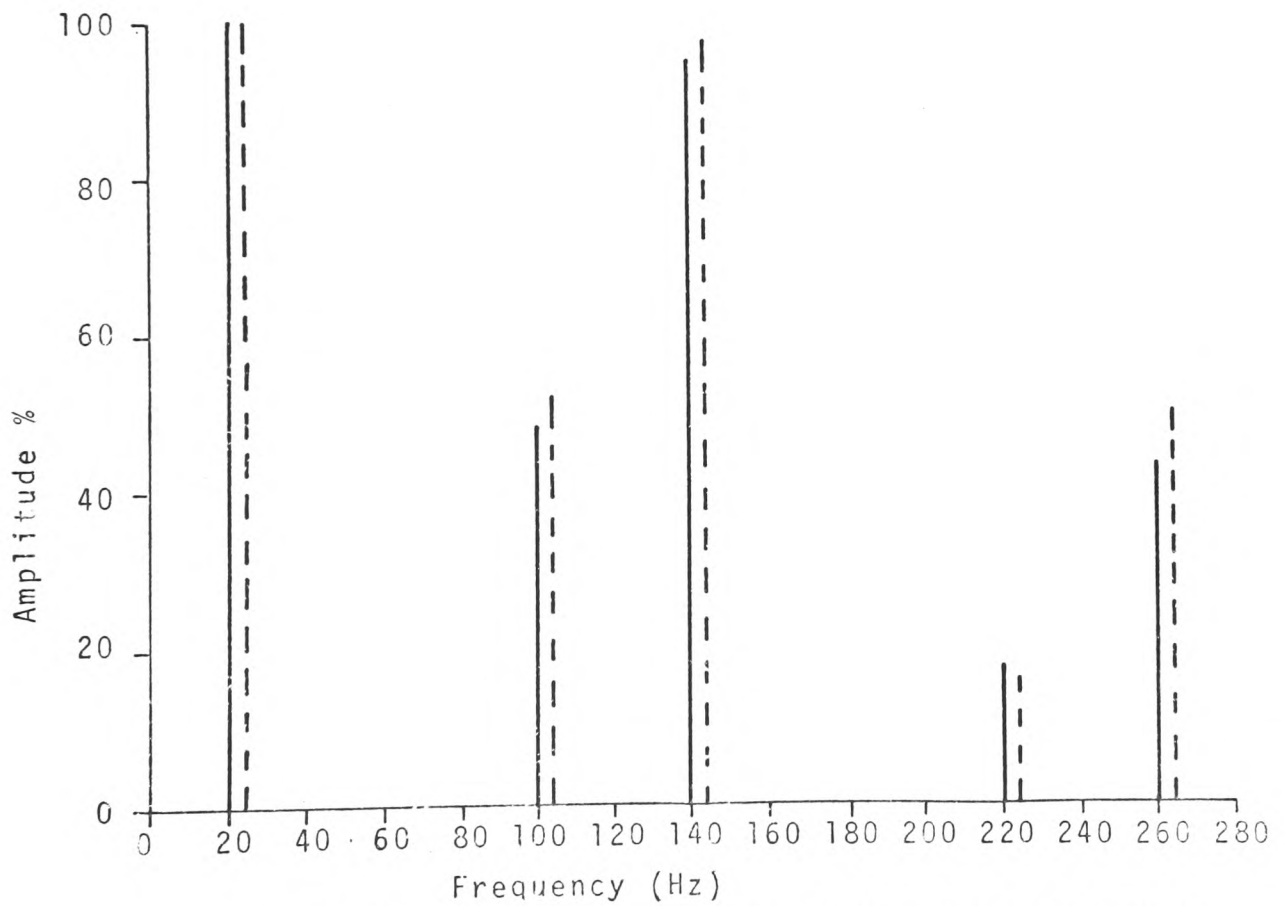

---

The results shown in Fig.(6.8a) and Fig.(6.8b) again illustrates the good correlation between theoretical results and experimental results. It is equally apparent that the regular sampled asymmetrical double-edge p.w.m process reduces the amplitude of the 60 Hz component by approximately 60%, whereas, the 150 Hz component is eliminated. For the natural sampled p.w.m process it was found that slight amplitude unbalance existed between the fundamental harmonic components,





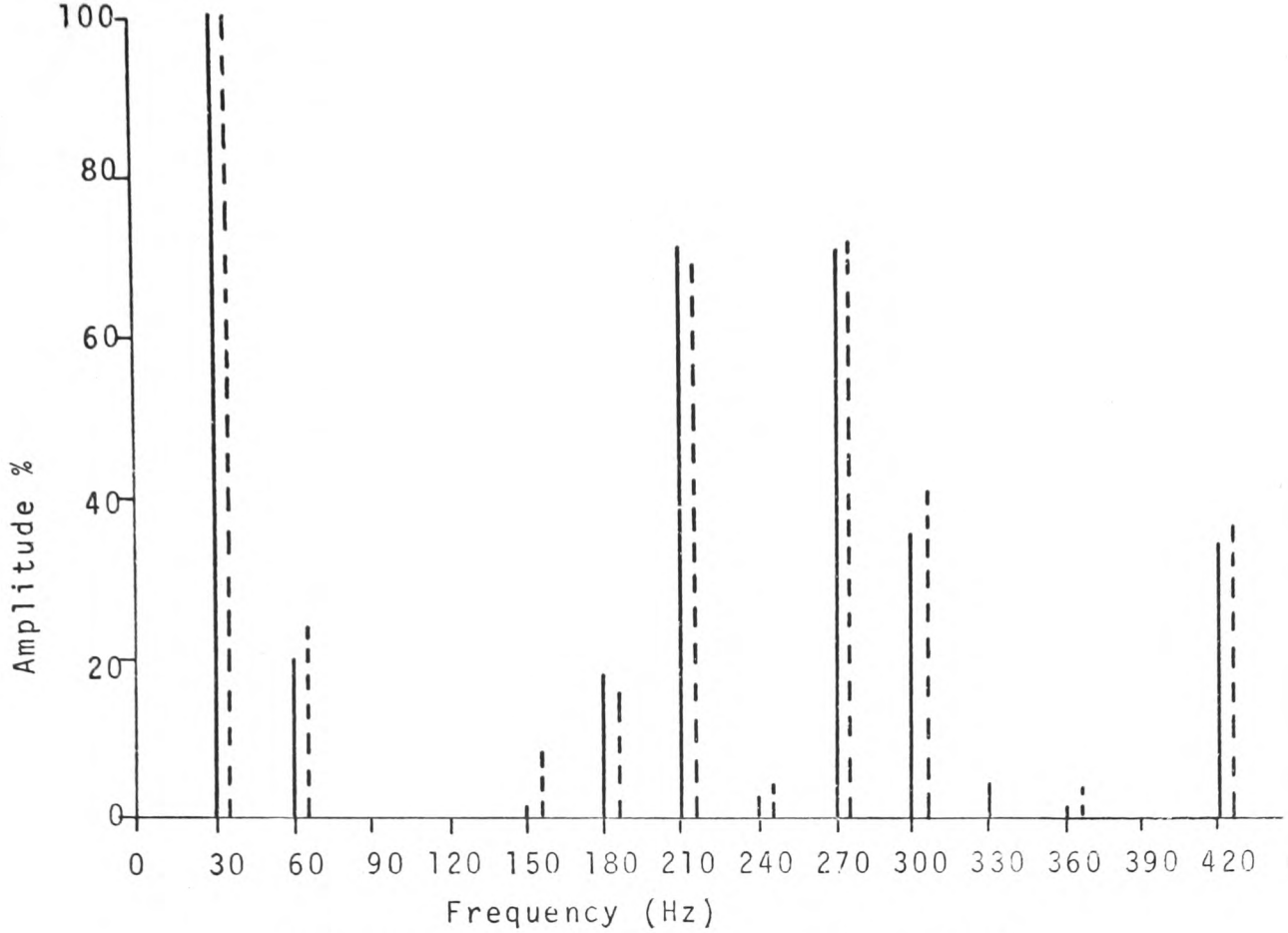
(a) Natural Sampling Double-Edge P.W.M.



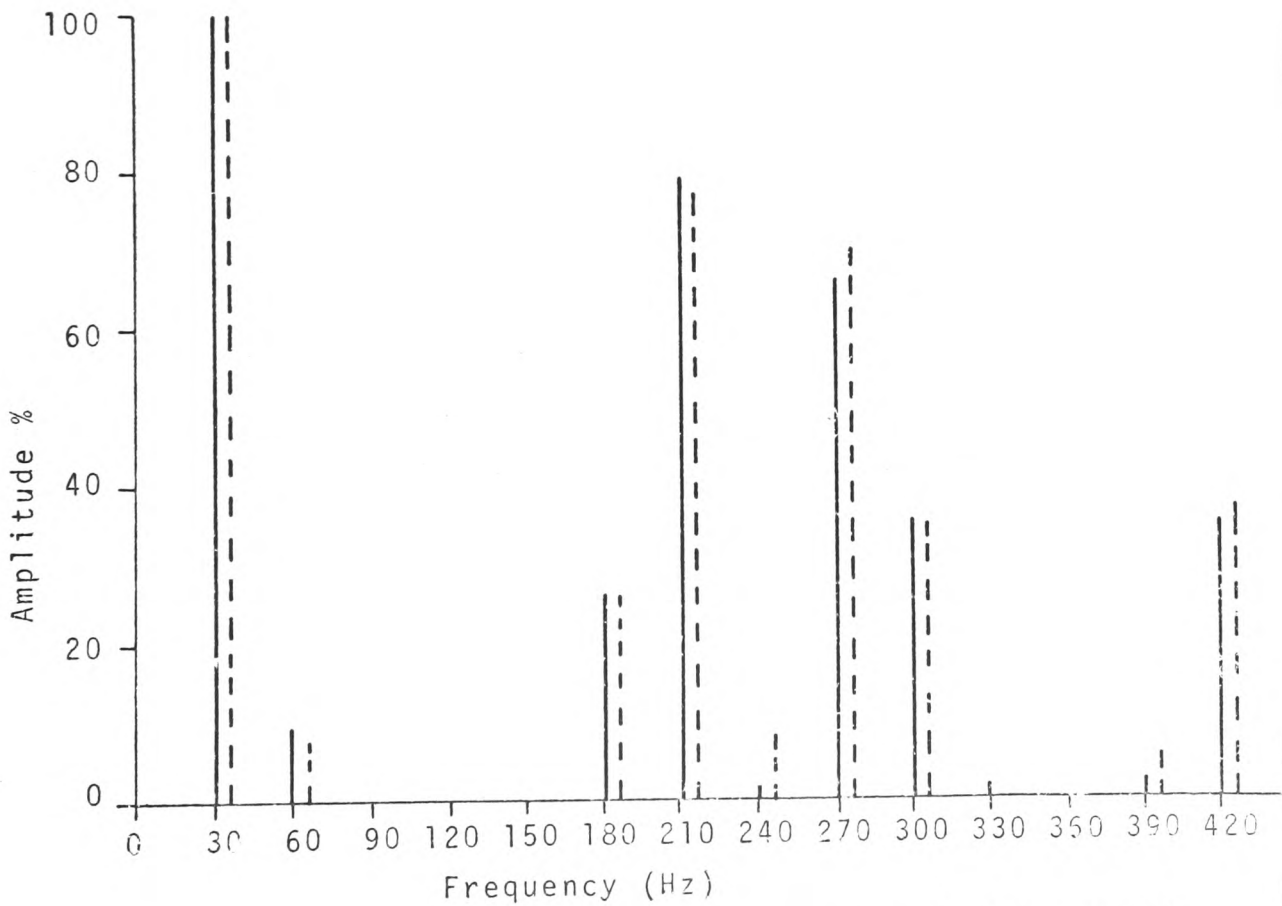
(b) Regular Sampled Asymmetrical Double-Edge P.W.M.

— Theoretical  
 - - - Experimental

FIG.(6.7) LINE TO LINE VOLTAGE HARMONICS FOR  $f_m = 20$  Hz,  $\frac{f_c}{f_m} = 3$ , AND MODULATION INDEX = 0.5



(a) Natural Sampled Double-Edge P.W.M.



(b) Regular Sampled Asymmetrical Double-Edge P.W.M.

— Theoretical  
 - - - Experimental

FIG. (6.8) LINE TO LINE VOLTAGE HARMONICS FOR  $f_m = 30$  Hz,  $\frac{f_c}{f_m} = 4$ , AND MODULATION INDEX = 0.5

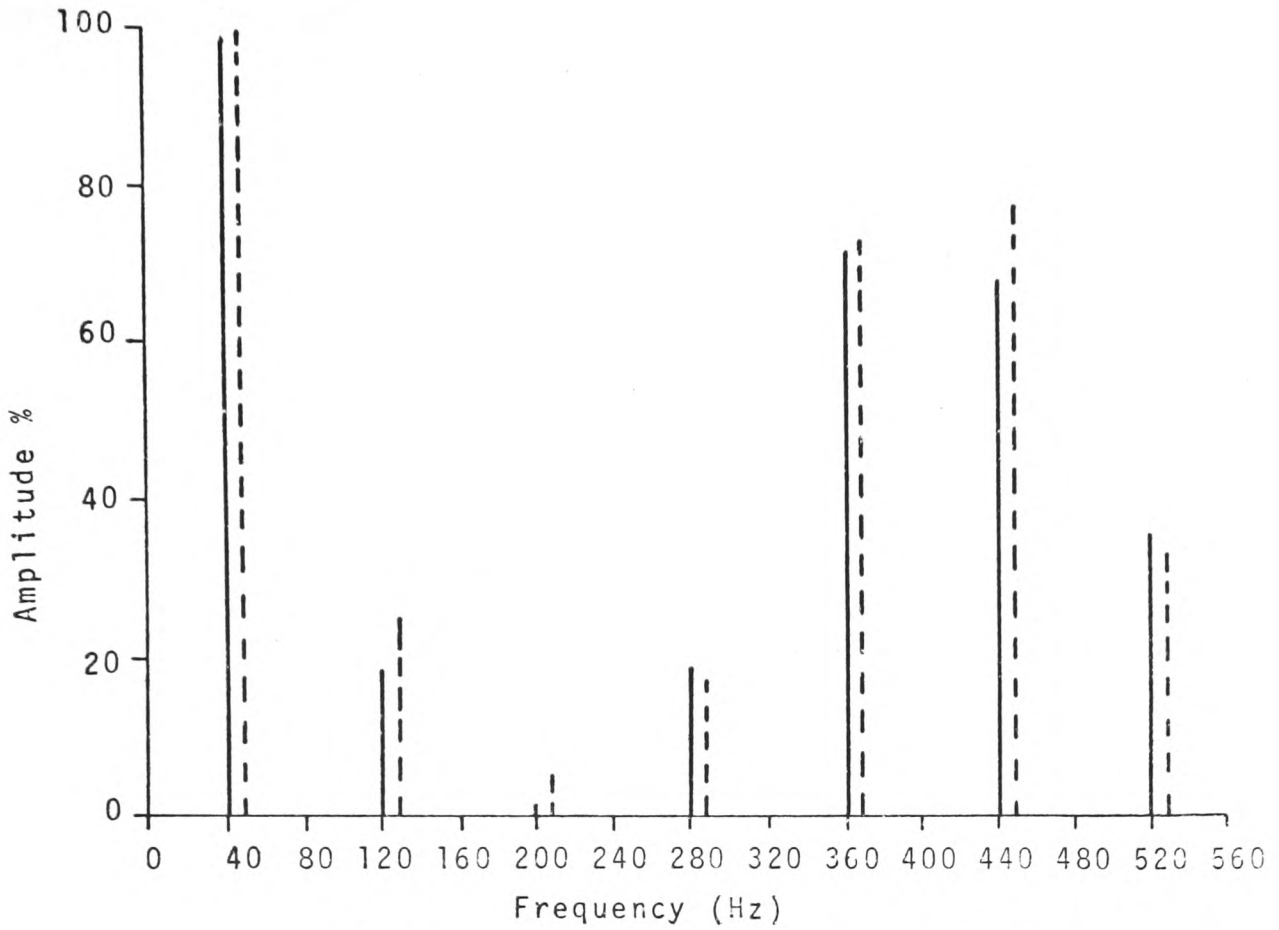
whereas, for the regular sampled p.w.m process unbalance of the wanted harmonic components could not be detected. Similarly the natural sampled p.w.m process introduced small d.c. components (approximately 1%) into the LINE to LINE voltage, whereas, d.c. components could not be detected in the regular sampled p.w.m. process.

$$(6.3.1.3) \quad \underline{\underline{f_c = 40 \text{ Hz}, \frac{f_c}{f_m} = 5, \text{Mod Index} = 0.5}}}$$

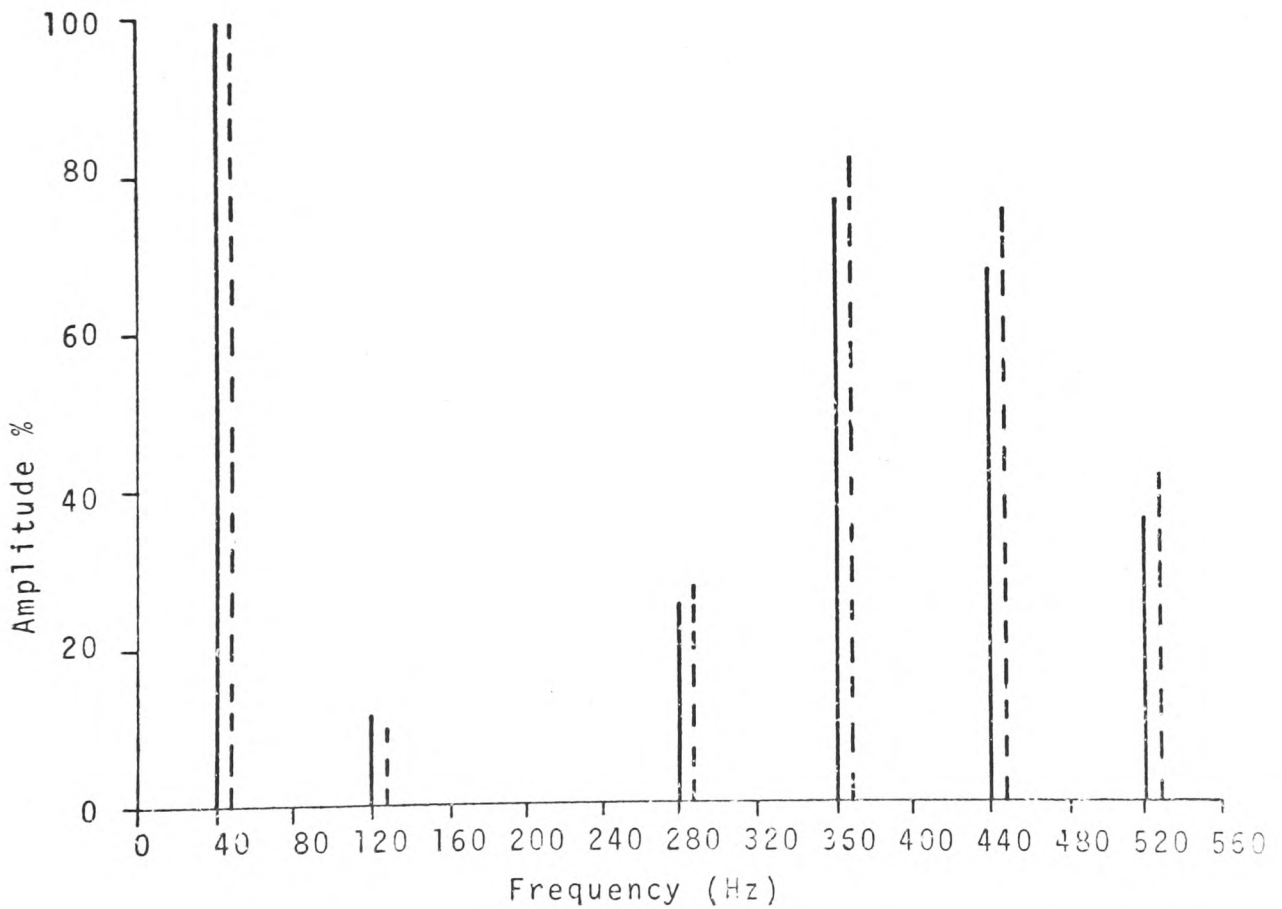
Fig.(6.9a) and Fig.(6.9b) illustrates the theoretical and experimental results for these values of modulating frequency, frequency ratio and modulation index, and it is immediately apparent that good correlation again exists between the theoretical and experimental results for each p.w.m process. The regular sampling process may again be seen to reduce the amplitude of the most significant harmonic components (the 120 Hz component) by approximately 50%, whereas, the 200 Hz component is eliminated. For the natural sampled p.w.m process the amplitudes of the wanted harmonic component were found to be unbalanced by approximately 2%, whereas, for the regular sampled p.w.m process, the wanted harmonic components again formed a balanced positive-sequence set.

(6.3.1.4) Relationship Between Amplitude of Fundamental Component and Modulation Index

The amplitude of the fundamental harmonic component of the output LINE to LINE voltage was recorded for various values of modulation index between zero and unity and for different values of integer frequency ratio. The relationship between the amplitude of the fundamental component and modulation



(a) Natural Sampled Double-Edge P.W.M.



(b) Regular Sampled Asymmetrical Double-Edge P.W.M.

— Theoretical  
 - - - Experimental

FIG. (6.9) LINE TO LINE VOLTAGE HARMONICS FOR  $f_m = 40\text{Hz}$ ,  $\frac{f_c}{f_m} = 5$ , AND MODULATION INDEX = 0.5

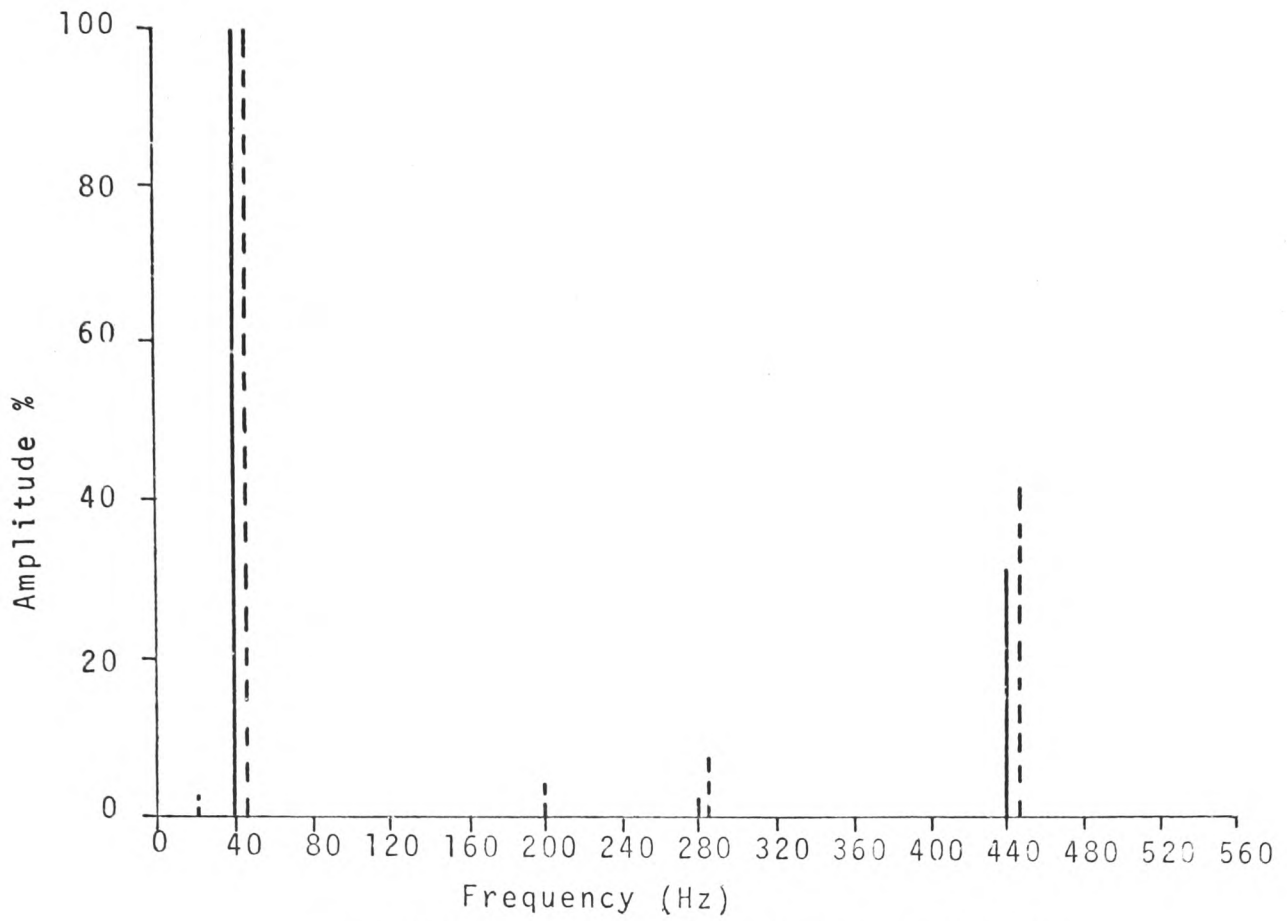
index was found to be strictly linear for both the natural sampled double-edge p.w.m process and the regular sampled asymmetrical double-edge p.w.m process.

### (6.3.2) Asynchronous-Mode of Operation

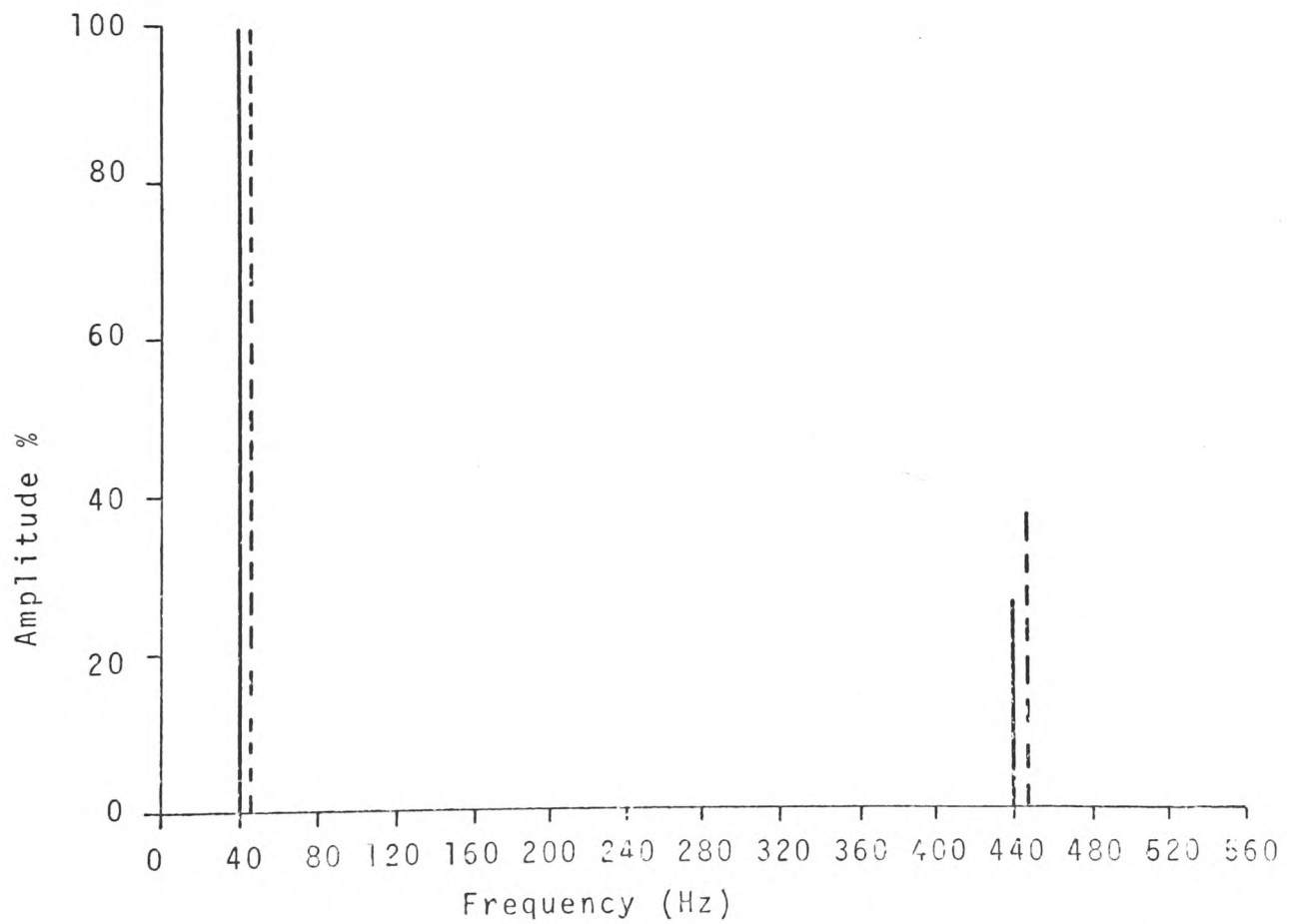
The power inverter stage was driven by the asynchronous p.w.m control scheme presented in Section (5.3.2) of this thesis. The magnitude and frequency of the wanted harmonic component of the output LINE to LINE p.w.m voltage waveform from the power inverter was again varied by varying the magnitude and frequency of the sinusoidal three-phase modulating wave generator. The frequency of the single-phase triangular carrier wave was maintained constant at 300 Hz. The carrier frequency and chosen values of modulating frequency were held rigorously constant when the measurement of harmonic components was being made. This was done to avoid any change in the fundamental repetition frequency as a result of frequency drift.

#### (6.3.2.1) $f_c = 40$ Hz, Modulation Index = 0.95

From the results illustrated in Fig.(6.10) it may be seen that reasonable correlation exists between the theoretical results and experimental results. It may also be seen that the novel regular sampled asymmetrical double-edge p.w.m process is again superior to the prior-art natural sampled p.w.m process, because, it eliminates the small 20 Hz sub-harmonic component, and the 200 Hz and 280 Hz super-harmonic components. However, the 40 Hz wanted harmonic components formed balanced positive-sequence sets for both p.w.m processes.



(a) Natural Sampled Double-Edge P.W.M.



(b) Regular Sampled Asymmetrical Double-Edge P.W.M.

— Theoretical  
 - - - Experimental

FIG.(6.10) LINE TO LINE VOLTAGE HARMONICS FOR  $f_m=40$  Hz, AND MODULATION INDEX = 0.95.

(6.3.2.2) fm = 90 Hz, Modulation Index = 0.95

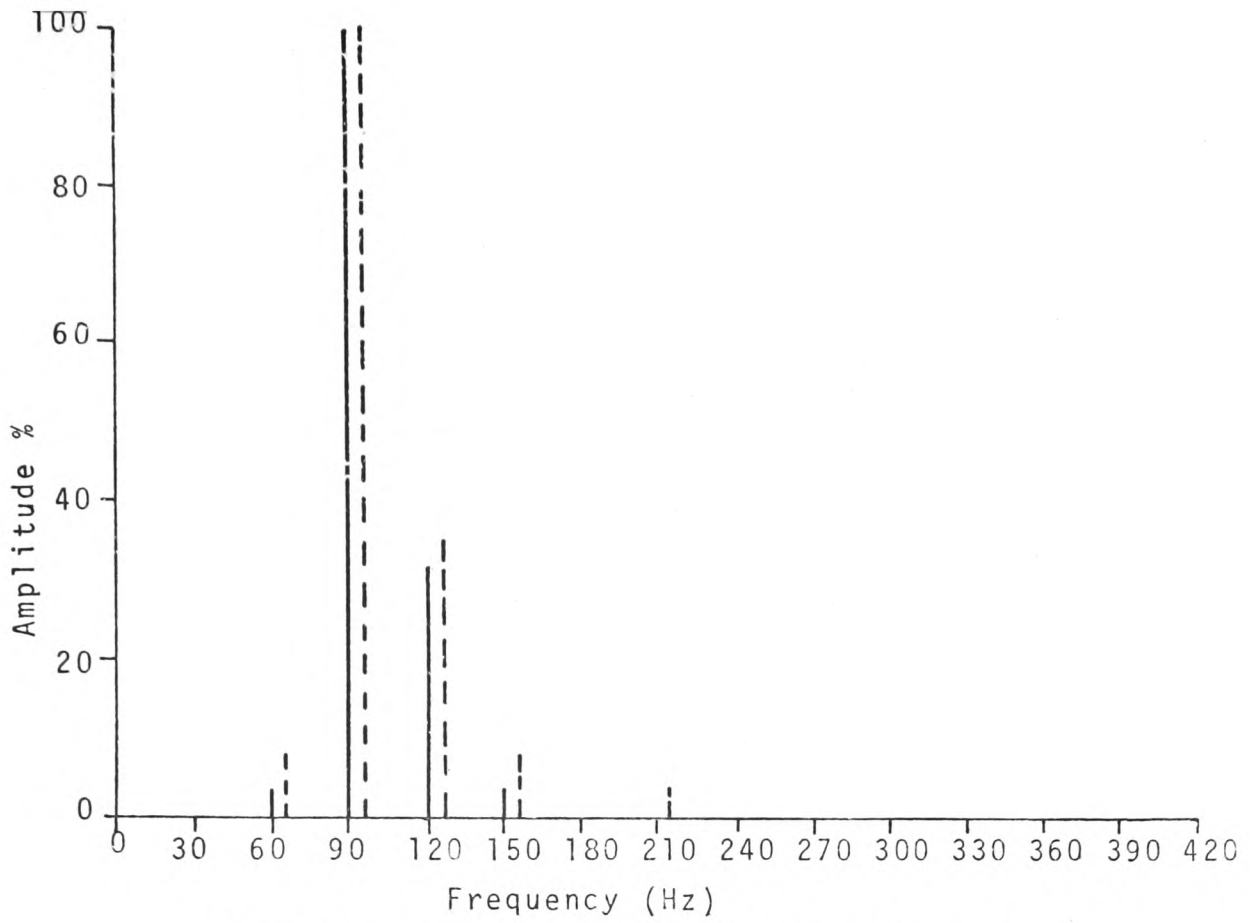
The results illustrated in Fig.(6.11) again demonstrates the superiority of the novel regular sampled asymmetrical double-edge p.w.m process over the prior-art natural sampled double-edge p.w.m process. The 60 Hz. sub-harmonic component, 150 Hz and 240 Hz super-harmonic components are totally eliminated, whereas, the 120 Hz super-harmonic component is reduced by approximately 20%. For both p.w.m processes, the 90 Hz wanted harmonic components again formed balanced positive-sequence sets.

(6.3.2.3) fm = 140 Hz, Modulation Index = 0.95

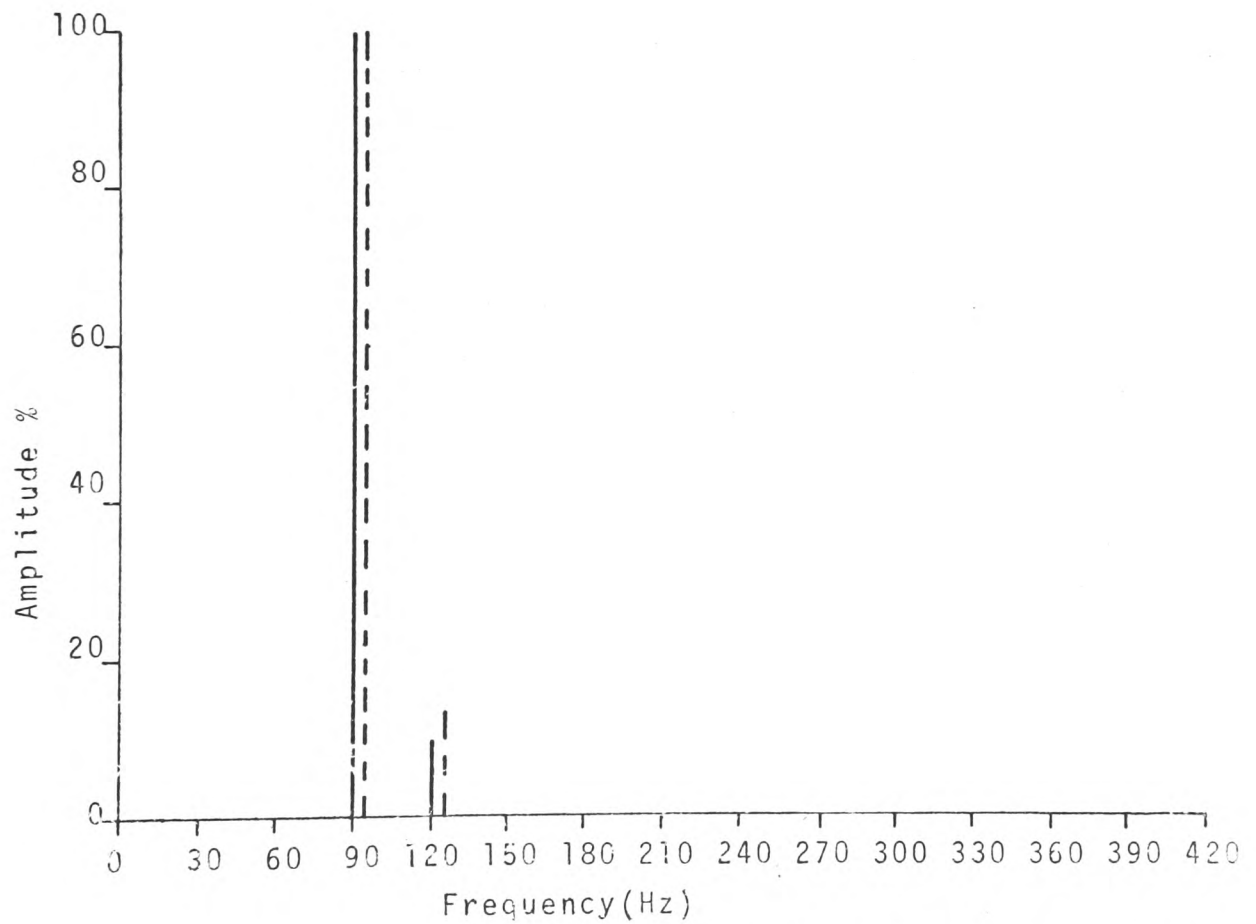
It may be seen from Fig.(6.12a) that when the frequency of the modulating wave was increased to 140 Hz, the natural sampling process introduced a 20 Hz sub-harmonic component of approximately 30%, and a 100 Hz sub-harmonic component of approximately 6%. However it may be seen from Fig.(6.12b) that the novel regular sampled asymmetrical p.w.m process almost eliminates the 20 Hz, sub-harmonic component and totally eliminates the 100 Hz sub-harmonic component. It is equally apparent that the regular sampling process almost eliminates the 220 Hz and 260 Hz super-harmonic components which existed in the natural sampled system.

(6.3.3) Interim Conclusions

A three-phase auxiliary impulse commutated thyristor inverter, which incorporated inhibition in the gating circuits has been presented. The inhibition was a success because it greatly reduced the commutation failures which occurred when the power inverter was driven without inhibition.



(a) Natural Sampled Double-Edge P.W.M.

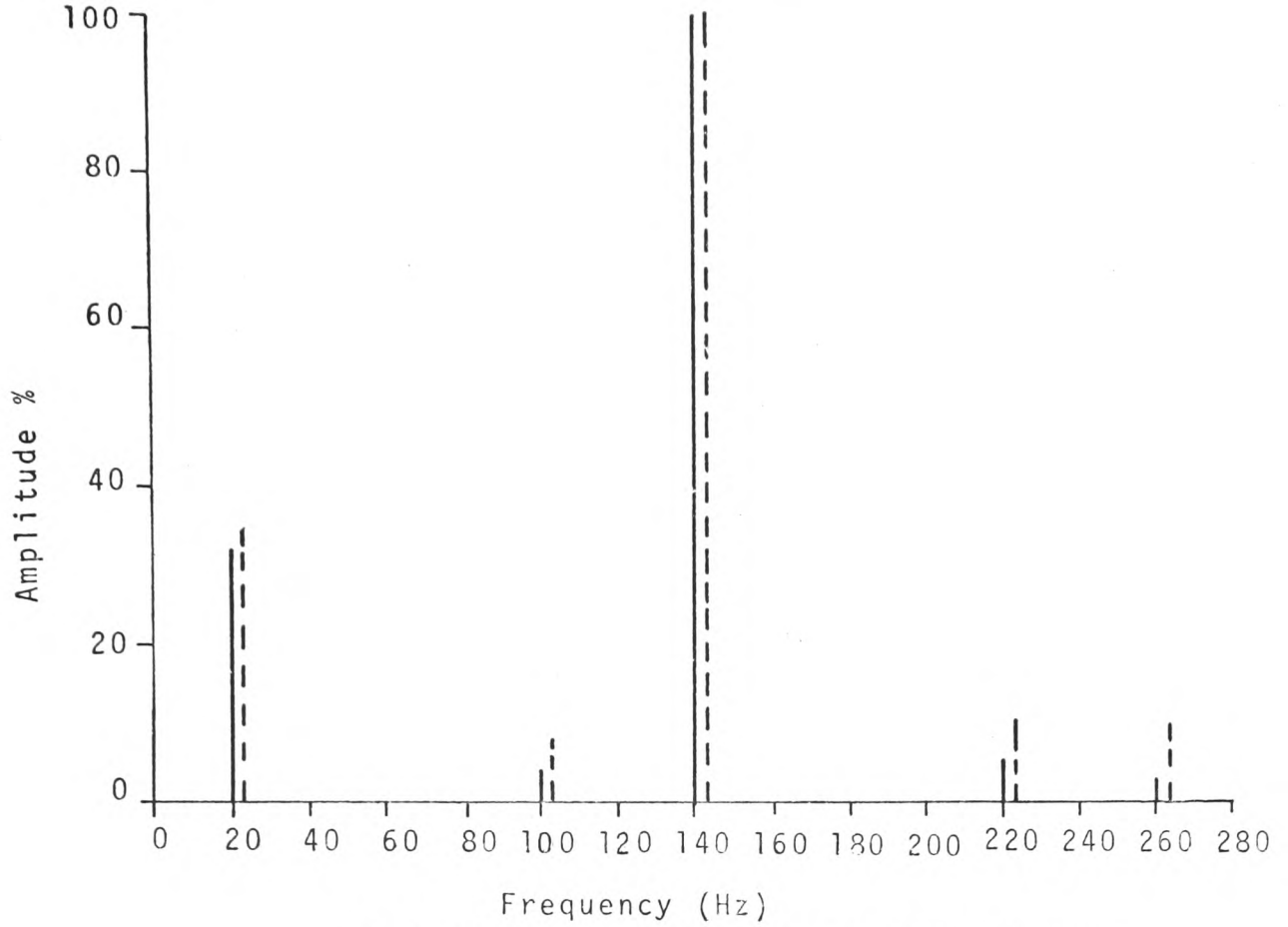


(b) Regular Sampled Asymmetrical Double-Edge P.W.M.

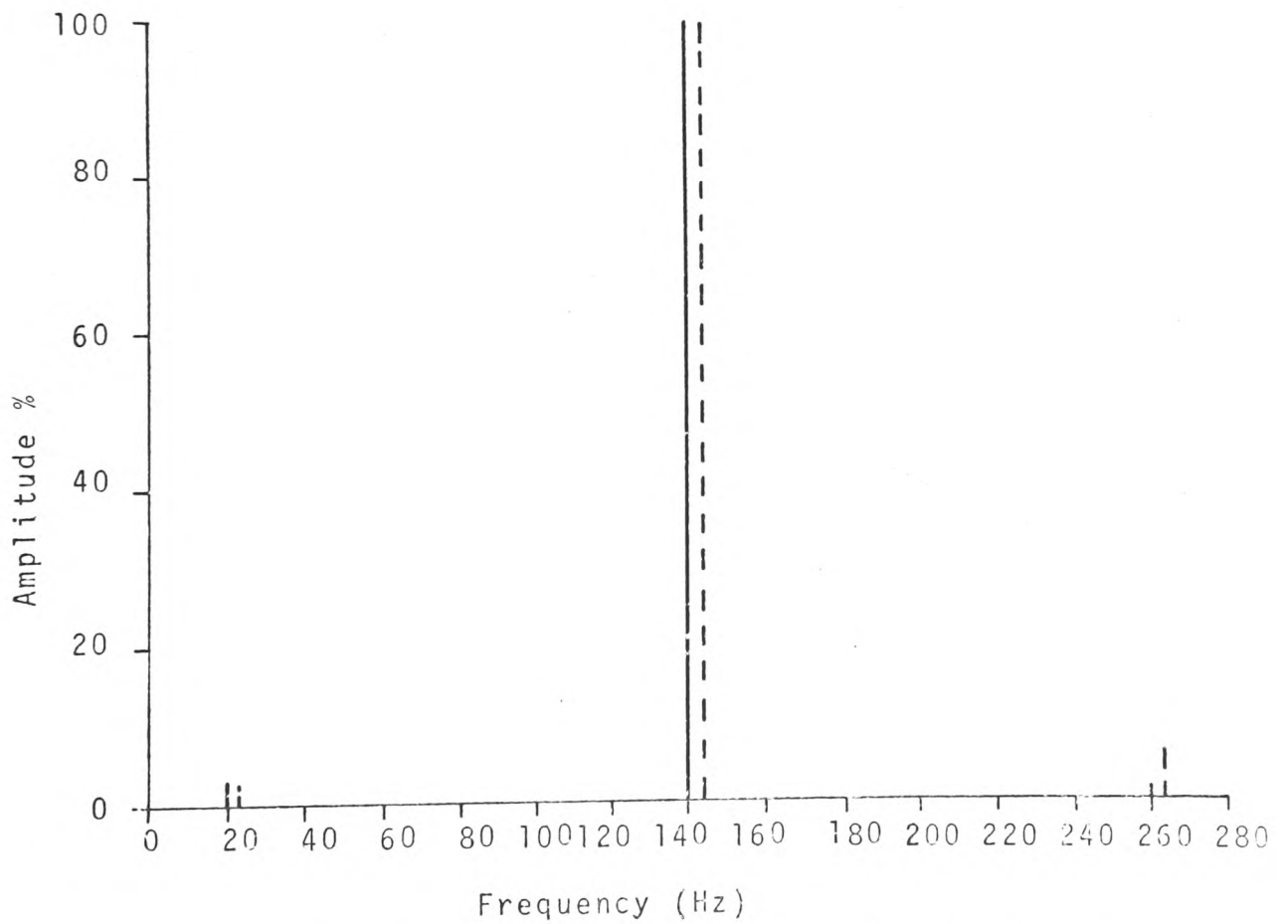
— Theoretical  
 - - - Experimental

FIG.(6.11) LINE TO LINE VOLTAGE HARMONICS FOR  $f_m=90$  Hz, AND MODULATION INDEX = 0.95





(a) Natural Sampled Double-Edge P.W.M.



(b) Regular Sampled Asymmetrical Double-Edge P.W.M.

— Theoretical  
 - - - Experimental

FIG. (6.12) LINE TO LINE VOLTAGE HARMONICS FOR  $f_m=140$  Hz AND MODULATION INDEX = 0.95

Good correlation was achieved between the theoretical results and the experimental results measured at the output of the power inverter. The degree of correlation was greater for the regular sampling p.w.m process than for the natural sampled p.w.m process. This difference was probably attributable to the comparator comparing a triangular waveform with a horizontal line in the regular sampled system, whereas the comparator compared a triangular waveform with a sinewave in the natural sampled system.

The novel regular sampled asymmetrical p.w.m process again reduced or eliminated the most significant harmonic components which existed in the prior-art natural sampled p.w.m process, thus increasing the allowable frequency range of operation. It is also of considerable importance to note that many of the sub-harmonic components introduced by the natural sampled system were of reverse phase-sequence.

## (7) CONCLUSIONS

The fundamental rules of frequency changing have been established, and it has been shown that all power inverters are basically pulse modulators. The various pulse modulation processes have been analysed, and it has been shown that the p.w.m. process is most suited to power modulators intended for infinitely variable induction motor speed control systems. Prior-art harmonic elimination techniques in power inverters have been analysed and it has been demonstrated that such techniques are not applicable to variable voltage/variable frequency invertors without requiring added power components and transformers. The addition of such components increases the cost of power inverters and decreases their attractiveness, thus making the inverter/induction motor speed control system less competitive with the d.c. motor/thyristor drive systems.

The modulation process in existing p.w.m power inverters has been studied in depth, and it has been shown that natural sampling is inherent in these systems. Although natural sampling is a well established concept in communication systems, it does not appear to have been previously identified in existing p.w.m. power inverters. The limitations of the natural sampling processes were therefore investigated, and it was shown that for a modulation index of unity the minimum values of frequency ratio for single-edge p.w.m. and double-edge p.w.m. were:  $\pi$  and  $\frac{\pi}{2}$  respectively. However, regular sampling which is also a well established technique in communication practice but which has not previously been applied to p.w.m. power inverters, was introduced and it was found that the minimum values of frequency ratio for the

regular sampled 'symmetrical' and 'asymmetrical' p.w.m processes were 'two' and 'one' respectively. It was also shown that regular sampling can be achieved at a cost of only one sample-and-hold circuit per phase.

The natural sampled single-edge and double-edge p.w.m processes were analysed by means of a digital computer, and it was found that the double-edge p.w.m process was superior to the single-edge process for all values of integer frequency ratio for mainly two reasons: (a) for single-edge p.w.m even order and odd order harmonics are always present in the LINE to LINE voltage spectra, (b) less harmonic cancellation occurs in single-edge p.w.m systems than in double-edge p.w.m systems.

The synchronous mode of generating natural sampled double-edge p.w.m, regular sampled symmetrical double-edge p.w.m and regular sampled asymmetrical double-edge p.w.m was analysed by means of a digital computer. The theoretical results were initially verified by means of a light current p.w.m control signal generator which simulated the three p.w.m processes. It was found that the theoretical results and experimental results provided good correlation. However, the novel regular sampled asymmetrical p.w.m process proved to be the most superior of the three double-edge p.w.m processes for the following reasons:

- (1) Direct voltage components were completely eliminated from the LINE to LINE voltage waveforms for all integer values of frequency ratio.

- (2) The amplitude and phase unbalance of the fundamental harmonic components which occurred for low non-triple integer

values of frequency ratio was eliminated.

(3) The amplitudes of the most significant unwanted harmonic components were reduced by a considerable amount for all low integer values of frequency ratio.

The amplitude of the fundamental harmonic component for both the prior-art natural sampled p.w.m process and the novel regular sampled asymmetrical double-edge p.w.m process was found to be directly proportional to the modulation index for all integer values of frequency ratio.

The asynchronous mode of p.w.m was investigated analytically by means of a digital computer. It was found that for the prior-art natural sampled p.w.m process, sub-harmonic voltage components and direct voltage components were introduced into the output LINE to LINE voltage spectra for frequency ratio values less than 'ten'. However, the analytical results again demonstrated that the novel regular sampled asymmetrical p.w.m process completely eradicated the direct voltage components and reduced the amplitudes of the unwanted sub-harmonic voltage components to an insignificant value (less than 1% of wanted component), thus, allowing the minimum value of frequency ratio to be reduced to approximately 'two'. A light current p.w.m control circuit was constructed which simulated the two p.w.m processes in the asynchronous mode. The experimental results obtained from the light current control circuit, verified the theoretical results for both p.w.m processes. The 'beat effect' phenomena was investigated and it was shown to be due to the variation in the fundamental repetition frequency' resulting from

frequency drift. Any amplitude or phase unbalance of the wanted harmonic components was also shown to be due to the natural sampling process and not the asynchronous mode of operation. The results of the investigation also illustrated that the novel regular sampled asymmetrical double-edge p.w.m process almost eradicated the 'beat effect' phenomena because it eliminated or reduced sub-harmonic components and the most significant super-harmonic components which lay within the pass-band of the waveform analyser when the sampling process was natural.

A three-phase, 5KVA, auxiliary impulse commutated thyristor power converter was designed and constructed and made to supply a three-phase, three-wire resistive load. The convertor was designed for a maximum carrier frequency of 300 Hz, which is a typical value for present day p.w.m. thyristor inverters. The light current synchronous mode and asynchronous mode p.w.m control circuits were made to drive the power inverter via: inhibition circuits, steering circuits and trigger-pulse amplifiers. Harmonic voltage spectra were measured for both the synchronous mode of operation and asynchronous mode of operation and for both the natural sampled double-edge p.w.m process and regular sampled asymmetrical double-edge p.w.m process. The experimentally determined harmonic spectra for the power converter agreed with both the computed spectra and the experimental spectra for the light current p.w.m generator circuits. This confirmed that the frequency response of the power convertor was flat-topped.

It may therefore be concluded that the philosophy of

applying sampling techniques which are common in communication engineering but which have not previously been applied to p.w.m power convertors, considerably increases the usable frequency range of p.w.m power convertors without decreasing the efficiency of the convertors or increasing the number of power components and cost.

## (8) ACKNOWLEDGEMENTS

The author gratefully acknowledges the advice and encouragement of Professor B.M. Bird, Head of the Electrical Engineering Department, of the University of Bristol who supervised the research to which this thesis relates.

The advice and co-operation of Dr. S.R. Bowes, Lecturer in the Electrical Engineering Department of the University of Bristol is also warmly appreciated.

Great appreciation is expressed to Dr. R.Murray Shelley, Principal Lecturer in Electrical Engineering at the Polytechnic of Wales, for his enthusiasm and encouragement.

The author also wishes to express his thanks to the Principal, Head of the Electrical Engineering Department and the Governing Body of the Polytechnic of Wales for supporting his application for registration with the C.N.A.A. and provision of the examination facilities.

Great appreciation and thanks are also expressed to the Principal, Dean of the Faculty of Science and Technology and the Governing Body of the Gwent College of Higher Education for the secondment of the author to the University of Bristol to pursue the investigation to which this thesis relates.

The author also wishes to express his thanks to the University of Bristol for the facilities provided and to the technical staff of the Electrical Engineering Department for the construction of much of the experimental equipment.



(9) REFERENCES

1. TUCKER, D.G. : Modulators and frequency changers, 1953, Macdonald & Co. Ltd.,
2. RIDGE, J. : Two New Methods of Motor Speed Control; Ph.D.Thesis University of Bristol, 1971.
3. RAWCLIFFE, G.H., BURBRIDGE, R.F. and FONG, W. : Induction Motor Speed Changing by Pole Amplitude Modulation; 1958, Proc. I.E.E. Vol. 105A, p.411.
4. PELLY, B.R. : Thyristor Phase-Controlled Convertors and Cycloconvertors;1971 Interscience, Wiley.
5. BEDFORD, B.B. and HOFT, R.G : Principles of Inverter Circuits, Wiley.
6. BIRD, B.M. and FORD, J.S. : Improvements in the Phase Controlled Cyclconverter Using Communication Principles; 1974, Proc.I.E.E. Vol. 121, No.10, p.1146.
7. GRANT, D. : An A.C. Variable Speed Drive Employing Communication Principles; Ph.D.Thesis University of Bristol, 1974.
8. BLACK, H.S. : Modulation Theory, 1953, D.Van Nostrand.
9. STARR, A.T. : Telecommunications; 1964, Pitman.
10. KRETZMER, E.R : Distortion in Pulse-Duration Modulation; Nov.1974, Proc. Inst. Radio Eng., Vol.35, No.11, p.p 1230-1235.

11. JACKSON, S.P. : Multiple Pulse Modulation in Static Inverters Reduces Selected Output Harmonics and Provides Smooth Adjustment of Fundamentals; 1970, IEEE Transactions on Industry and General Applications, Vol.IGA-6, No.4.
12. PATEL, H.S. and HOFT, R.G. : Generalized Techniques of Harmonic Elimination and Voltage Control in Thyristor Inverters:Part 1-Harmonic Elimination; 1973, IEEE Transactions on Industry Applications, Vol.1A-9, No.3.
13. BOWES, S.R.,and BIRD, B.M. : Asymmetric and Symmetric Uniform-Sampled Pulse-Width-Modulated Inverters; 1975,.British Patent.
14. DANFOSS A/S : A Waveform Generator for providing Width-Modulated Square Waves; British Patent 1,202,466, 1970.
15. JACOVIDES, L.J : Analysis of Induction Motor Drives with a Nonsinusoidal Supply Voltage using Fourier Analysis; 1973, IEEE Trans. on Ind.Appl., Vol.1A-9 No. 6.
16. THE ENGLISH ELECTRIC COMPANY : Electric Inverting Apparatus; British Patent 1,190,847. 1970.

17. SCHÖNING, A. and STEMLER. H. :  
Static Frequency Changers with  
Sub-Harmonic Control in Conjunction  
with reversible variable-speed A.C.  
Drives; The Brown Boveri Review,  
Aug./Sept., 1964.
18. KNIGHT, M.A. and TORKILDSEN, R.A. :  
One-kVA, Three-Phase dc-ac Inverter  
with Digital Control; 1969, IEEE Trans.  
on Aerospace and Electronic Systems.  
Vol. AES-5, No.6.
19. LEVERANCE, N.C. : Fourier Analysis of Pulse Width  
Modulated Inverter Wave Forms;  
1970, IEEE Ind. and Gen. Appls.  
Group Milwaukee Section.
20. FITCH, E. : The Spectrum of Modulated Pulses;  
1947, Proc. of the Inst. of Rad.  
Eng., p.p 556-564.
21. MEIER, U and MOKRYTZKI, B. :  
Voltage Control Thru Pulse Width  
Modulation; 1970. IEEE Ind.& Gen.  
Appls. Group Milwaukee Section.
22. DEWAN, S.B. and FORSYTHE, J.B. :  
Harmonic Analysis of a Synchronized  
Pulse-Width-Modulated Three-Phase  
Inverter; 1974, IEEE Trans. on Ind.  
Appls.Vol.1A-10 No. 1.

APPENDIX (1)

Computer Programmes for :

Natural Sampled Leading-Edge P.W.M.

Natural Sampled Trailing-Edge P.W.M.

Natural Sampled Double-Edge P.W.M.

```

BEGIN
| COMMENT PWM ANALYSIS SAMPLING NATURAL;
| COMMENT LEADING EDGE MODULATION;
| REAL ARRAY ANG,G,DC,GR,A,B,E,D,H(1::500);
| INTEGER F,R,I;
| REAL C,ANS,L,K,M,Z;
| REAL ARRAY X,Y (1::500);
| LIBRARY OUTPUT;
| LIBRARY SIGN;
| PROCEDURE DOT;
| BEGIN
|   FOR J:=1 UNTIL H+1 DO
|     BEGIN
|       L:=100;
|       FOR G:=(J-1)*100 UNTIL J*100 DO
|         BEGIN
|           K:=G*2*PI/((H/F)*(100))-Z;
|           ANS:=(R/20)*SIN(K-W)-J+K*(H/(2*F*PI))+0.5;
|           IF ABS(ANS)<L THEN
|             BEGIN
|               L:=ABS(ANS);
|               X(J):=K;
|             END;
|           END;
|         BEGIN
|           Y(J):=J*2*PI/(H/F)-Z;
|         END;
|         FREEPOINT(4);
|         OUTR(X(J)*180/PI);
|         SAMELINE;
|         SPACES(3);
|         OUTR(Y(J)*180/PI);
|         NEWLINE;
|       END;
|     LINES(4);
|     FOR N:=1 STEP 1 UNTIL 20 DO
|       BEGIN
|         A(N):=G(N):=0;
|       END;
|     FOR N:=1 STEP 1 UNTIL 20 DO
|       BEGIN
|         FOR J:=1 UNTIL H DO
|           BEGIN
|             A(N):=(SIN(Y(J)+N/F)-SIN(X(J)+N/F))/(PI*N)+A(N);
|             B(N):=(COS(X(J)+N/F)-COS(Y(J)+N/F))/(PI*N)+B(N);
|           END;
|         F=FREEPOINT(5);
|         OUTI(H);
|         SAMELINE;
|         SPACES(3);

```

```

| | OUTR(A(N));
| | SAMELINE;
| | SPACES(3);
| | OUTR(B(N));
| | NEWLINE;
| | H(N):=SQRT(A(N)*A(N)+B(N)*B(N));
| | IF ABS(B(N))<0.0001 THEN B(N):=SIGN(B(N))*0.0001;
| | IF ABS(B(N))=0.0 THEN B(N):=0.0001;
| | ANG(N):=ARCTAN(A(N)/B(N));
| END;
| LINES(3);
| FOR N:=1 STEP 1 UNTIL 20 DO
| BEGIN
| | IF ((N+1) REM 10)=0 THEN LINES(2);
| | SAMELINE;
| | FREEPOINT(5);
| | SPACES(4);
| | OUTI(H);
| | SPACES(2);
| | OUTR(H(N));
| | SPACES(3);
| | OUTR(H(N)*100/H(F));
| | SPACES(2);
| | OUTR(ANG(N)*180/PI);
| END;
| LINES(3);
| FOR J:=1 UNTIL N DO
| BEGIN
| | G(J):=0;
| END;
| G(1):=(2*Y(1)-X(1)-X(2))/(2*PI*F);
| DC(1):=G(1)/2;
| FOR J:=2 UNTIL N DO
| BEGIN
| | G(J):=(2*Y(J)-X(J)-X(J+1))/(2*PI*F)+G(J-1);
| | DC(J):=G(J)/2;
| END;
| FREEPOINT(5);
| SPACES(6);
| OUTR(DC(N));
| SAMELINE;
| SPACES(6);
| OUTR(DC(N)*100/H(F));
| LINES(3);
| END;
| F:=5;
| FOR PH:=9,14,19,24,29,34,39,44,49 DO
| FOR RR:=10,5,2 DO
| BEGIN
| | H:=PH;

```

```

R:=ERR;
DIGITS(2);
OUTR(PH/F);
LINES(3);
OUTI(R);
LINES(3);
W:=4*PI/3;
Z:=0;
DOT;
FOR N:=1 UNTIL 20 DO
BEGIN
|   E(N):=A(N);
|   D(N):=B(N);
END;
FOR J:=1 UNTIL H DO
BEGIN
|   GR(J):=RG(J);
END;
W:=0;
Z:=0;
DOT;
FOR N:=1 UNTIL 20 DO
BEGIN
|   A(N):=E(N)-A(N);
|   B(N):=D(N)-B(N);
|   F:=DEPOINT(5);
|   OUTI(H);
|   SAMELINE;
|   SPACES(3);
|   OUTR(A(N));
|   SAMELINE;
|   SPACES(3);
|   OUTR(B(N));
|   NEWLINE;
|   H(N):=SQRT(A(N)2+B(N)2);
|   IF ABS(B(N))<0.0001 THEN B(N):=SIGN(B(N))*0.0001;
|   IF ABS(B(N))=0.0 THEN B(N):=0.0001;
|   ARG(N):=ARCTAN(A(N)/B(N));
END;
LINES(3);
FOR N:=1 STEP 1 UNTIL 20 DO
BEGIN
|   IF ((N+1) REM 10)=0 THEN LINES(2);
|   SAMELINE;
|   FREEPOINT(5);
|   SPACES(4);
|   OUTI(H);
|   SPACES(2);
|   OUTR(H(N));
|   SPACES(3);

```

```
| | |   OUTR(H(N)*100/H(F));  
| | |   SPACES(2);  
| | |   OUTR(ANG(N)*180/PI);  
| | |   END;  
| | |   LINES(3);  
| | |   FOR J:=1 UNTIL N DO  
| | |   BEGIN  
| | |   |   G(J):=GR(J)-G(J);  
| | |   |   DC(J):=RG(J)/2;  
| | |   END;  
| | |   FREEPOINT(5);  
| | |   SPACES(6);  
| | |   OUTR(DC(N));  
| | |   SAMELINE;  
| | |   SPACES(6);  
| | |   OUTR(DC(N)+100/H(F));  
| | |   LINES(3);  
| | END;  
| END.
```



```

BEGIN
| COMMENT PWM ANALYSIS SAMPLING NATURAL;
| COMMENT TRAILING_EDGE MODULATION;
| REAL ARRAY ANG,G,DC,GR,A,B,E,D,H(1::500);
| INTEGER F,R,H;
| REAL C,ANS,L,K,U,Z;
| REAL ARRAY X,Y (1::500);
| LIBRARY OUTPUT;
| LIBRARY SIGN;
| PROCEDURE DOT;
| BEGIN
|   FOR J:=1 UNTIL H+1 DO
|     BEGIN
|       X(J):=(J-1)*2*PI/(H/F)-Z;
|       L:=100;
|       FOR Q:=H(J-1)*100 UNTIL J+100 DO
|         BEGIN
|           K:=H*2*PI/((H/F)*(100))-Z;
|           ANG:=(R/20)*SIN(K-Q)+J*K*(H/(2*F*PI))-0.5;
|           IF ABS(ANS)<L THEN
|             BEGIN
|               L:=ABS(ANS);
|               Y(J):=K;
|             END;
|           END;
|           FREEPOINT(4);
|           OUTR(X(J)*180/PI);
|           SAMELINE;
|           SPACES(3);
|           OUTR(Y(J)*180/PI);
|           NEWLINE;
|         END;
|       LINES(4);
|       FOR N:=1 STEP 1 UNTIL 20 DO
|         BEGIN
|           A(N):=B(N):=0;
|         END;
|       FOR N:=1 STEP 1 UNTIL 20 DO
|         BEGIN
|           FOR J:=1 UNTIL H DO
|             BEGIN
|               A(N):=(SIN(Y(J)*H/F)-SIN(X(J)*H/F))/(PI*N)+A(N);
|               B(N):=(COS(X(J)*H/F)-COS(Y(J)*H/F))/(PI*N)+B(N);
|             END;
|           FREEPOINT(5);
|           OUTI(N);
|           SAMELINE;
|           SPACES(3);
|           OUTR(A(N));
|           SAMELINE;

```

```

|   |   | SPACES(3);
|   |   | OUTR(B(N));
|   |   | NEWLINE;
|   |   | H(N):=SQRT(A(N)*A(N)+B(N)*B(N));
|   |   | IF ABS(B(N))<0.0001 THEN B(N):=SIGN(B(N))*0.0001;
|   |   | IF ABS(B(N))=0.0 THEN B(N):=0.0001;
|   |   | ANG(N):=ARCTAN(A(N)/B(N));
|   |   | END;
|   |   | LINES(3);
|   |   | FOR N:=1 STEP 1 UNTIL 20 DO
|   |   | BEGIN
|   |   |   | IF ((N+1) REM 10)=0 THEN LINES(2);
|   |   |   | SAMELINE;
|   |   |   | FREEPOINT(5);
|   |   |   | SPACES(4);
|   |   |   | OUTI(N);
|   |   |   | SPACES(2);
|   |   |   | OUTR(H(N));
|   |   |   | SPACES(3);
|   |   |   | OUTR(H(N)*100/H(F));
|   |   |   | SPACES(2);
|   |   |   | OUTR(ANG(N)*180/PI);
|   |   |   | END;
|   |   |   | LINES(3);
|   |   |   | FOR J:=1 UNTIL 11 DO
|   |   |   | BEGIN
|   |   |   |   | G(J):=0;
|   |   |   |   | END;
|   |   |   | G(1):=(2*Y(1)-X(1)-X(2))/(2*PI*F);
|   |   |   | DC(1):=G(1)/2;
|   |   |   | FOR J:=2 UNTIL 11 DO
|   |   |   | BEGIN
|   |   |   |   | G(J):=(2*Y(J)-X(J)-X(J+1))/(2*PI*F)+G(J-1);
|   |   |   |   | DC(J):=G(J)/2;
|   |   |   |   | END;
|   |   |   | FREEPOINT(5);
|   |   |   | SPACES(6);
|   |   |   | OUTR(DC(1));
|   |   |   | SAMELINE;
|   |   |   | SPACES(6);
|   |   |   | OUTR(DC(1)*100/H(F));
|   |   |   | LINES(3);
|   |   | END;
|   |   | F:=5;
|   |   | FOR PH:=9,14,19,24,29,34,39,44,49 DO
|   |   | FOR PR:=10,5,2 DO
|   |   | BEGIN
|   |   |   | H:=PH;
|   |   |   | R:=PR;
|   |   |   | DIGITS(2);

```

```
| | OUTR(PM/F);  
| | LINES(3);  
| | OUTI(R);  
| | LINES(3);  
| | W:=4*PI/3;  
| | Z:=0;  
| | DOT;  
| | FOR N:=1 UNTIL 20 DO  
| | BEGIN  
| | | E(N):=A(N);  
| | | D(N):=B(N);  
| | END;  
| | FOR J:=1 UNTIL H DO  
| | BEGIN  
| | | GR(J):=G(J);  
| | END;  
| | W:=0;  
| | Z:=0;  
| | DOT;  
| | FOR N:=1 UNTIL 20 DO  
| | BEGIN  
| | | A(N):=E(N)-A(N);  
| | | B(N):=D(N)-B(N);  
| | | FREEPOINT(5);  
| | | OUTI(N);  
| | | SAMELINE;  
| | | SPACES(3);  
| | | OUTR(A(N));  
| | | SAMELINE;  
| | | SPACES(3);  
| | | OUTR(B(N));  
| | | NEWLINE;  
| | | H(N):=SQRT(A(N)*A(N)+B(N)*B(N));  
| | | IF ABS(B(N))<0.0001 THEN B(N):=SIGN(B(N))*0.0001;  
| | | IF ABS(B(N))=0.0 THEN B(N):=0.0001;  
| | | ANG(N):=ARCTAN(A(N)/B(N));  
| | END;  
| | LINES(3);  
| | FOR F:=1 STEP 1 UNTIL 20 DO  
| | BEGIN  
| | | IF ((F+1) REM 10)=0 THEN LINES(2);  
| | | SAMELINE;  
| | | FREEPOINT(5);  
| | | SPACES(4);  
| | | OUTI(N);  
| | | SPACES(2);  
| | | OUTR(H(N));  
| | | IF ABS(H(F))=0.0 THEN H(F):=0.0001;  
| | | SPACES(3);  
| | | OUTR(H(N)*100/H(F));
```

```
| | | SPACES(2);
| | | OTR(ANG(')+180/PI);
| | | END;
| | | LINES(3);
| | | FOR J:=1 UNTIL N DO
| | | BEGIN
| | | | G(J):=BR(J)-G(J);
| | | | DC(J):=G(J)/2;
| | | | END;
| | | IF ABS(H(F))=0 THEN H(F):=0.0001;
| | | FREEPOINT(3);
| | | SPACES(6);
| | | OTR(DC('));
| | | SAMELINE;
| | | SPACES(6);
| | | OTR(DC(')+100/H(F));
| | | LINES(3);
| | | END;
| | END.
END.
```

```

BEGIN
| COMMENT PWM ANALYSIS SAMPLING NATURAL;
| REAL ARRAY ANG,G,DC,GR,A,B,E,D,H(1:500);
| INTEGER F,R,M;
| REAL C,ANS,L,K,W,Z;
| REAL ARRAY X,Y(1:500);
| LIBRARY OUTPUT;
| LIBRARY SIGN;
| PROCEDURE DOT;
| BEGIN
|   FOR J:=1 UNTIL H+1 DO
|     BEGIN
|       L:=100;
|       FOR Q:=(2*J-2)*1000 UNTIL (2*J-1)*1000 DO
|         BEGIN
|           K:=90*PI/((H/F)+(1000))-Z;
|           ANS:=(R/20)*SIN(K-W)-2*J+1+K*(H/(F*PI))+0.5;
|           IF ABS(ANS)<L THEN
|             BEGIN
|               L:=ABS(ANS);
|               X(J):=K;
|             END;
|           END;
|           L:=100;
|           FOR Q:=(2*J-1)*1000 UNTIL (2*J+0)*1000 DO
|             BEGIN
|               K:=90*PI/((H/F)+(1000))-Z;
|               ANS:=(R/20)*SIN(K-W)+2*J-1-K*(H/(F*PI))+0.5;
|               IF ABS(ANS)<L THEN
|                 BEGIN
|                   L:=ABS(ANS);
|                   Y(J):=K;
|                 END;
|               END;
|             FREEPOINT(4);
|             OUTR(X(J)*180/PI);
|             SAMELINE;
|             SPACES(3);
|             OUTR(Y(J)*180/PI);
|             NEWLINE;
|           END;
|         LINES(4);
|         FOR N:=1 STEP 1 UNTIL 20 DO
|           BEGIN
|             A(N):=B(N):=0;
|           END;
|         FOR N:=1 STEP 1 UNTIL 20 DO
|           BEGIN
|             FOR J:=1 UNTIL H DO
|               BEGIN

```



```

|   L&NES(3);
| END;
| F:=1;
| FOR PH:=3,5,7,9,11,13,15,17,21,27,33 DO
| FOR RR:=10,5,2 DO
| BEGIN
|   H:=PH;
|   R:=RR;
|   DIGITS(2);
|   OUTR(PH/F);
|   LINES(3);
|   OUTI(R);
|   LINES(3);
|   W:=2*PI/3;
|   O:=0;
|   DOT;
|   FOR N:=1 UNTIL 20 DO
|   BEGIN
|     E(N):=A(N);
|     D(N):=B(N);
|   END;
|   FOR J:=1 UNTIL 10 DO
|   BEGIN
|     G(J):=HG(J);
|   END;
|   W:=4*PI/3;
|   O:=0;
|   DOT;
|   FOR N:=1 UNTIL 20 DO
|   BEGIN
|     A(N):=E(N)-A(N);
|     B(N):=D(N)-B(N);
|     FREEDPOINT(5);
|     OUTI(N);
|     SAMELINE;
|     SPACES(3);
|     OUTR(A(N));
|     SAMELINE;
|     SPACES(3);
|     OUTR(B(N));
|     NEWLINE;
|     H(A):=SORT(A(N)*A(N)+B(N)*B(N));
|     IF ABS(B(N))<0.0001 THEN B(N):=SIGN(B(N))*0.0001;
|     IF ABS(B(N))=0 THEN B(N):=0.0001;
|     ARG(N):=ARCTAN(A(N)/B(N));
|   END;
|   LINES(3);
|   FOR N:=1 STEP 1 UNTIL 20 DO
|   BEGIN
|     IF ((N+1) MOD 10)=0 THEN LINES(2);

```

```
| | | SAMELINE;  
| | | FREEPOINT(5);  
| | | SPACES(4);  
| | | OUTI(H);  
| | | SPACES(2);  
| | | OUTR(H(H));  
| | | SPACES(3);  
| | | OUTR(H(H)*100/H(F));  
| | | SPACES(2);  
| | | OUTR(ANG(H)*180/PI);  
| | | END;  
| | | L&NES(3);  
| | | FO- J:=1 UNTIL H DO  
| | | BEGIN  
| | | | G(J):=GR(J)-G(J);  
| | | | DC(J):=HG(J)/2;  
| | | | END;  
| | | | FREEPOINT(5);  
| | | | SPACES(6);  
| | | | OUTR(DC(H));  
| | | | SAMELINE;  
| | | | SPACES(6);  
| | | | OUTR(DC(H)*100/H(F));  
| | | | L&NES(3);  
| | | END;  
| | END.  
END.
```



## APPENDIX (2)

### Control Circuit For Synchronous Mode, Natural Sampled, Double-Edge P.W.M. Process.

It may be seen from Fig.(10.1) that this control circuit mainly consists of a three-phase modulating wave generator, a schmitt trigger, phase locked loop and a three-phase comparator. However, it may also be seen that the phase locked loop circuit consists of: a phase comparator, low pass filter, phase splitter, voltage controlled triangular wave oscillator, schmitt trigger and a programmable divide "N" counter.

#### Three Phase Modulating Wave Generator

This consisted of a standard laboratory three-phase signal generator, whose output voltage waveforms were sinusoidal. The amplitude and frequency of the output voltage signals could be varied in both amplitude and frequency.

#### Schmitt Trigger

This circuit converts the PHASE (A) sinusoidal modulating signal to a rectangular pulse waveform. The circuit consists of two inverter/buffer gates connected in cascade, a 100K feedback resistor and a 1k input resistor. These values of resistance reduced the hysteresis of the circuit to a negligible amount.

#### Phase Locked Loop Circuit

The output signals from the schmitt trigger and divide by "N" counter are fed to the two inputs of the phase comparator, which consists of an exclusive -OR gate. The output error signal from the phase comparator is proportional to the phase and frequency difference between the two input waveforms.

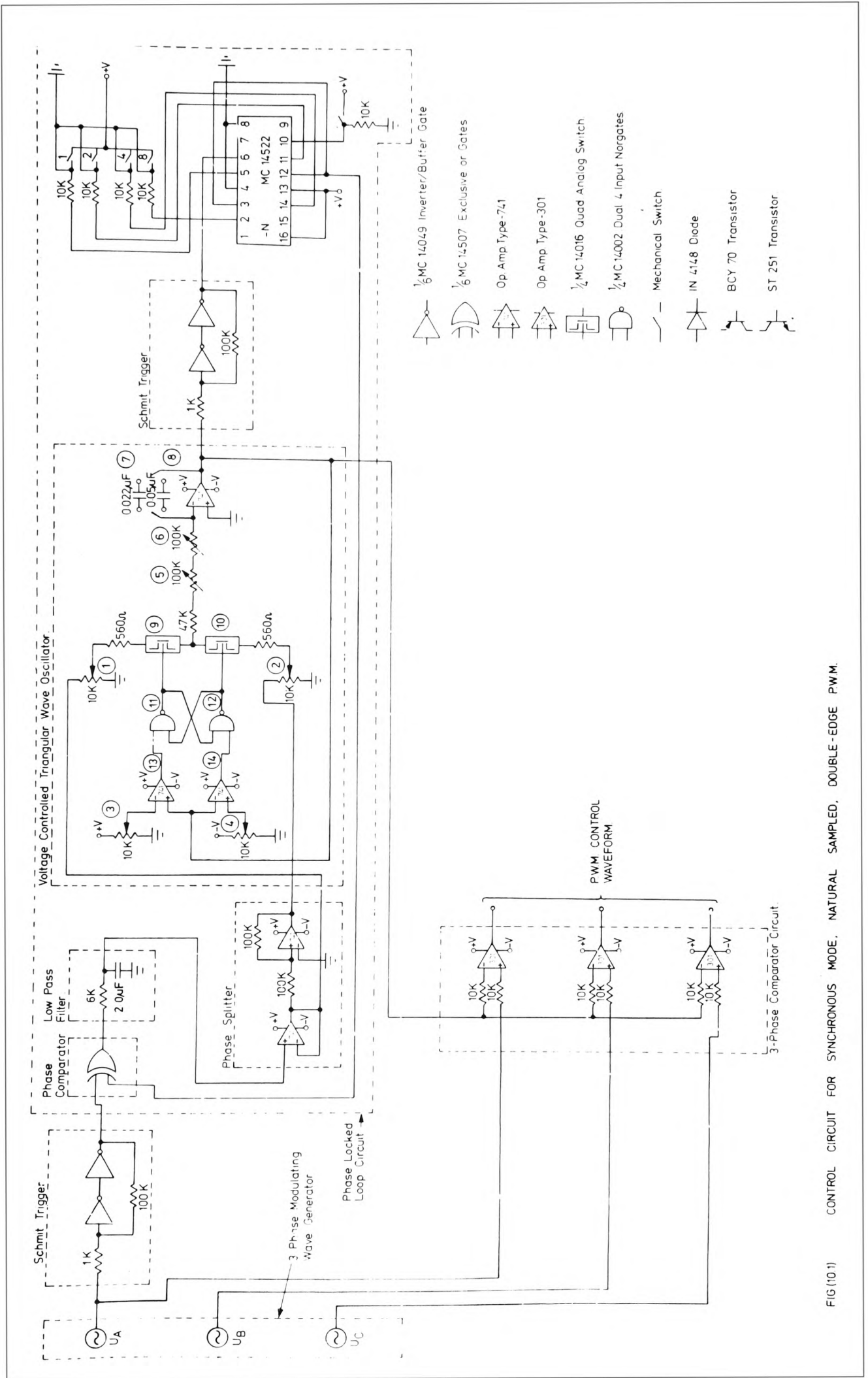


FIG 10.1) CONTROL CIRCUIT FOR SYNCHRONOUS MODE, NATURAL SAMPLED, DOUBLE-EDGE PWM.

The low pass filter filters the output signal from the phase comparator and produces a direct voltage component proportional to the phase error.

The direct voltage component from the low pass filter is fed to the phase splitter which produces two output voltage signals displaced in time phase by  $180^{\circ}$ . The phase splitter circuit consists of a non inverting buffer amplifier and an inverting buffer amplifier connected in cascade.

The output voltage signals from the non-inverting buffer amplifier and inverting buffer amplifier are fed to potentiometers (1) and (2) respectively, of the voltage controlled triangular wave oscillator circuit. This circuit produces an isocetes triangular voltage waveform whose frequency is directly proportional to the direct voltage signals from the phase splitter. The symmetry of the triangular output voltage waveform from the integrator is set by means of potentiometers (1) and (2), whereas, the free-running frequency of the waveform is set by means of potentiometers (5) and (6) and capacitors (7) and (8). The positive and negative voltage levels to which the integrator integrates, are set by potentiometers (3) and (4) respectively. When the voltage levels on potentiometers (3) and (4) are set to +2 volts and -2 volts respectively, and NOR-gate (11) is at "logic 1" then the integrator will integrate to + 2 volts, at which time op-amp (13) will switch to +V causing NOR-gate (11) to go to "logic 0" and NOR-gate (12) to "logic 1", switch (9) then closes and switch (10) opens. This allows the integrator to integrate to -2 volts, at which time op-amp (14) will switch to +V

causing NOR-gate (12) to revert to "logic 0" and NOR-gate (11) to "logic 1". The cyclic process then repeats itself and so produces an output triangular voltage waveform which is symmetrical.

The output signal from the integrator is the triangular carrier signal which is then fed to the input of the three-phase comparators. The frequency of this signal is "N" times the modulating frequency,  $N.\omega_m$ . The output signal from the integrator is also fed to the schmitt trigger circuit, where the triangular waveform is converted to a rectangular pulse waveform.

The output rectangular pulse waveform from the schmitt trigger of frequency ( $\omega_c$ ) is fed to the input of the programmable divide by "N" counter. The output signal from the counter of frequency,  $\frac{\omega_c}{N}$ , is then fed back to the input of the phase comparator circuit where it is phase and frequency locked to the modulating signal of frequency,  $\omega_m$ . By closing switch "1", "2", "4" and "8" and combinations of these switches, the frequency ratio,  $\frac{\omega_c}{\omega_m}$ , can be varied from 1 to 10.

#### Comparator Circuits

The output carrier signal of frequency,  $N.\omega_m$ , from the voltage controlled oscillator circuit is fed to the inputs of the three comparator circuits along with the three modulating signals from the modulating wave generator. The comparator circuits consists of three op-amps (type - 301) in open loop mode which compares the single phase triangular carrier signal with the three sinusoidal modulating signals. The output signals from the three comparators are the three-phase p.w.m. control waveforms.

APPENDIX (3)

Computer Programmes for :

Regular Sampled Symmetrical Double-Edge P.W.M.

Regular Sampled Asymmetrical Double-Edge P.W.M.

```

BEGIN
| COMMENT PWM ANALYSIS SAMPLING REGULAR ;
| COMMENT SYMMETRICAL;
| REAL ARRAY DC,G,GR,ANG,A,B,E,D,H,X,Y (1::500);
| INTEGER F,H,K;
| REAL C,W;
| LIBRARY OUTPUT;
| LIBRARY SIGN;
| PROCEDURE DOT;
| BEGIN
|   FOR J:=1 UNTIL H+1 DO
|     BEGIN
|       C:=PI/(H/F)+(J-1)*2*PI/(H/F);
|       X(J):=C*(PI/(2*H/F))*(1+(SIN(C*W)*(R/10)));
|       Y(J):=C*(PI/(2*H/F))*(1+(SIN(C*W)*(R/10)));
|       FREEPOINT(4);
|       OUTR(X(J)*150/PI);
|       SABLNE;
|       SPACES(3);
|       OUTR(Y(J)*150/PI);
|       NEWLINE;
|     END;
|   LINES(4);
|   FOR N:=1 STEP 1 UNTIL 20 DO
|     BEGIN
|       A(N):=B(N):=0;
|     END;
|   FOR N:=1 STEP 1 UNTIL 20 DO
|     BEGIN
|       ;
|       FOR J:=1 UNTIL H DO
|         BEGIN
|           A(N):=(SIN(Y(J)*H/F)-SIN(X(J)*H/F))/(PI*N)+A(N);
|           B(N):=(COS(X(J)*H/F)-COS(Y(J)*H/F))/(PI*N)+B(N);
|         END;
|       FREEPOINT(5);
|       OUTI(H);
|       SABLNE;
|       SPACES(3);
|       OUTR(A(N));
|       SABLNE;
|       SPACES(3);
|       OUTR(B(N));
|       NEWLINE;
|       H(N):=SQRT(A(N)*A(N)+B(N)*B(N));
|       IF ABS(B(N))<0.0001 THEN B(N):=SIGN(B(N))*0.0001;
|       IF ABS(B(N))=0.0 THEN B(N):=0.0001;
|       ARG(N):=ARCTAN(A(N)/B(N));
|     END;
|   LINES(3);

```

```

FOR N:=1 STEP 1 UNTIL 20 DO
BEGIN
  IF ((N+1) REM 10) = 0 THEN LINES(2);
  SAMELINE;
  FREEPOINT(5);
  SPACES(4);
  OUTI(N);
  SPACES(2);
  OUTR(H(N));
  SPACES(2);
  OUTR(H(N)*100/H(F));
  SPACES(2);
  OUTR(ANG(N)*180/PI);
END;
LINES(3);
FOR J:=1 UNTIL N DO
BEGIN
  G(J):=0;
END;
G(1):=(2*Y(1)-X(1)-X(2))/(2*PI*F);
DC(1):=G(1)/2;
FOR J:=2 UNTIL N DO
BEGIN
  G(J):=(2*Y(J)-X(J)-X(J+1))/(2*PI*F)+G(J-1);
  DC(J):=G(J)/2;
END;
FREEPOINT(5);
SPACES(6);
OUTR(DC(N));
SAMELINE;
SPACES(6);
OUTR(DC(N)*100/H(F));
LINES(3);
END;
F:=1;
FOR PH:=3,5,7,9,11,13,15,17,21,27,33 DO
FOR RR:=10,5,2 DO
BEGIN
  N:=PH;
  R:=RR;
  DIGITS(2);
  OUTR(PH/F);
  LINES(3);
  OUTI(R);
  LINES(3);
  W:=0;
  DOT;
  FOR N:=1 UNTIL 20 DO
  BEGIN
    E(N):=A(N);

```

```

|   D(N):= B(N);
| END;
| FOR J:=1 UNTIL N DO
| BEGIN
|   GR(J):=RG(J);
| END;
| W:=2*PI/3;
| DOT;
| FOR N:=1 UNTIL 20 DO
| BEGIN
|   A(N):= E(N) - A(N);
|   B(N):= D(N) - B(N);
|   FREEPOINT(5);
|   OUTI(N);
|   SAMELINE;
|   SPACES(3);
|   OUTR(A(N));
|   SAMELINE;
|   SPACES(3);
|   OUTR(B(N));
|   NEWLINE;
|   H(N):=SQRT(A(N)*A(N)+B(N)*B(N));
|   IF ABS(B(N))<0.0001 THEN B(N):=SIGN(B(N))*0.0001;
|   IF ABS(B(N))=0.0 THEN B(N):=0.0001;
|   ANG(N):=ARCTAN(A(N)/B(N));
| END;
| LINES(3);
| FOR N:=1 STEP 1 UNTIL 20 DO
| BEGIN
|   IF (((N+1) MOD 10)=0) THEN LINES(2);
|   SAMELINE;
|   FREEPOINT(5);
|   SPACES(4);
|   OUTI(N);
|   SPACES(7);
|   OUTR(H(N));
|   IF ABS(H(N))=0.0 THEN H(N):=0.0001;
|   SPACES(2);
|   OUTR(H(N)*100/H(N));
|   SPACES(2);
|   OUTR(ANG(N)*100/PI);
| END;
| LINES(3);
| FOR J:=1 UNTIL N DO
| BEGIN
|   G(J):=GR(J)-G(J);
|   DC(J):=B(J)/2;
| END;
| FREEPOINT(5);
| SPACES(6);

```



```
| |   OUTP(DC(N));  
| |   IF ABS(H(F))#0.0 THEN H(F):=0.0001;  
| |   SAMELINE;  
| |   SPACES(6);  
| |   OUTP(DC(N)*100/H(F));  
| |   LINES(3);  
|   END;  
END.
```

```

BEGIN
| COMMENT PWD ANALYSIS SAMPLING REGULAR ;
| COMMENT ASYMMETRICAL;
| REAL ARRAY DC, G, GR, ANG, A, B, E, D, H, X, Y (1::500);
| INTEGER F, H, R;
| REAL C, W;
| LIBRARY OUTPUT;
| LIBRARY SIGN;
| PROCEDURE DOT;
| BEGIN
|   FOR J:=1 UNTIL H+1 DO
|     BEGIN
|       C:=PI/(H/F)+(J-1)*2*PI/(H/F);
|       X(J):=C-(PI/(2*H/F))*(1+(SIN((C-PI/(H/F))-W)*(R/10)));
|       ;
|       Y(J):=C+(PI/(2*H/F))*(1+(SIN(C*4)*(R/10)));
|       FREEPOINT(4);
|       OUTR(X(J)*180/PI);
|       SABLIME;
|       SPACES(3);
|       OUTR(Y(J)*180/PI);
|       NEWLINE;
|     END;
|   LINES(4);
|   FOR N:=1 STEP 1 UNTIL 20 DO
|     BEGIN
|       A(N):=B(N):=0;
|     END;
|   FOR N:=1 STEP 1 UNTIL 20 DO
|     BEGIN
|       ;
|       FOR J:=1 UNTIL H DO
|         BEGIN
|           A(N):=(SIN(Y(J)*H/F)-SIN(X(J)*H/F))/(PI*N)+A(N);
|           B(N):=(COS(X(J)*H/F)-COS(Y(J)*H/F))/(PI*N)+B(N);
|         END;
|       FREEPOINT(5);
|       OUTI(N);
|       SABLIME;
|       SPACES(3);
|       OUTR(A(N));
|       SABLIME;
|       SPACES(3);
|       OUTR(B(N));
|       NEWLINE;
|       H(N):=SQRT(A(N)*A(N)+B(N)*B(N));
|       IF ABS(B(N))<0.0001 THEN B(N):=SIGN(B(N))*0.0001;
|       IF ABS(B(N))=0.0 THEN B(N):=0.0001;
|       ANG(N):=ARCTAN(A(N)/B(N));
|     END;

```

```

|   |   | LINES(3);
|   |   | FOR I:=1 STEP 1 UNTIL 20 DO
|   |   | BEGIN
|   |   |   | IF ((H(I) REM 10)=0) THEN LINES(2);
|   |   |   | SAMELINE;
|   |   |   | FREEPOINT(5);
|   |   |   | SPACES(4);
|   |   |   | OUTI(H);
|   |   |   | SPACES(2);
|   |   |   | OUTR(H(H));
|   |   |   | SPACES(2);
|   |   |   | OUTR(H(I)*100/H(F));
|   |   |   | SPACES(2);
|   |   |   | OUTR(ANG(H)*180/PI);
|   |   | END;
|   |   | LINES(3);
|   |   | FOR J:=1 UNTIL H DO
|   |   | BEGIN
|   |   |   | G(J):=0;
|   |   | END;
|   |   | G(1):=(2*Y(1)-X(1)-X(2))/(2*PI*F);
|   |   | DC(1):=G(1)/2;
|   |   | FOR J:=2 UNTIL H DO
|   |   | BEGIN
|   |   |   | G(J):=(2*Y(J)-X(J)-X(J+1))/(2*PI*F)+G(J-1);
|   |   |   | DC(J):=G(J)/2;
|   |   | END;
|   |   | FREEPOINT(5);
|   |   | SPACES(6);
|   |   | OUTR(DC(H));
|   |   | SAMELINE;
|   |   | SPACES(6);
|   |   | OUTR(DC(1)*100/H(F));
|   |   | LINES(3);
|   | END;
|   | F:=1;
|   | FOR PH:=3,5,7,9,11,13,15,17,21,27,33 DO
|   | FOR RR:= 10, 5, 2 DO
|   | BEGIN
|   |   | H:=PH;
|   |   | R:=RR;
|   |   | DIGITS(2);
|   |   | OUTR(PH/F);
|   |   | LINES(3);
|   |   | OUTI(R);
|   |   | LINES(3);
|   |   | W:=0;
|   |   | DOT;
|   |   | FOR N:=1 UNTIL 20 DO
|   |   | BEGIN

```

```

|   |   |   E(N):=A(N);
|   |   |   D(N):= B(N);
|   |   | END;
|   |   | FOR J:=1 UNTIL N DO
|   |   | BEGIN
|   |   |   | GR(J):=G(J);
|   |   |   | END;
|   |   | W:=2*PI/3;
|   |   | DOT;
|   |   | FOR N:=1 UNTIL 20 DO
|   |   | BEGIN
|   |   |   | A(N):= E(N) - A(N);
|   |   |   | B(N):= D(N)- B(N);
|   |   |   | FREEPOINT(5);
|   |   |   | OUTI(N);
|   |   |   | SAMELINE;
|   |   |   | SPACES(3);
|   |   |   | OUTR(A(N));
|   |   |   | SAMELINE;
|   |   |   | SPACES(3);
|   |   |   | OUTR(B(N));
|   |   |   | NEWLINE;
|   |   |   | H(N):=SQRT(A(N)*A(N)+B(N)*B(N));
|   |   |   | IF ABS(B(N))<0.0001 THEN B(N):=SIGN(B(N))*0.0001;
|   |   |   | IF ABS(B(N))=0.0 THEN B(N):=0.0001;
|   |   |   | ANG(N):=ARCTAN(A(N)/B(N));
|   |   | END;
|   |   | LINES(3);
|   |   | FOR N:=1 STEP 1 UNTIL 20 DO
|   |   | BEGIN
|   |   |   | IF ((N+1) REM 10)=0 THEN LINES(2);
|   |   |   | SAMELINE;
|   |   |   | FREEPOINT(5);
|   |   |   | SPACES(4);
|   |   |   | OUTI(N);
|   |   |   | SPACES(2);
|   |   |   | OUTR(H(N));
|   |   |   | SPACES(2);
|   |   |   | OUTR(H(N)*100/H(N));
|   |   |   | SPACES(2);
|   |   |   | OUTR(ANG(N)*180/PI);
|   |   | END;
|   |   | LINES(3);
|   |   | FOR J:=1 UNTIL N DO
|   |   | BEGIN
|   |   |   | G(J):=GR(J)-G(J);
|   |   |   | DC(J):=HG(J)/2;
|   |   | END;
|   |   | FREEPOINT(5);
|   |   | SPACES(6);

```

```
I  I  OUTR(DC(H));  
I  I  SAMELINE;  
I  I  SPACES(6);  
I  I  OUTR(DC(H)+100/H(F));  
I  I  LINES(3);  
I  END;  
END.
```

MIJOB PRINT OF REE001:+TEMP .LISTAL(S0000)/D FOR USER REE001 COMPLETED AT 10:

## APPENDIX (4)

### Control Circuit For Synchronous Mode, Regular Sampled, Asymmetrical Double-Edge P.W.M. Process.

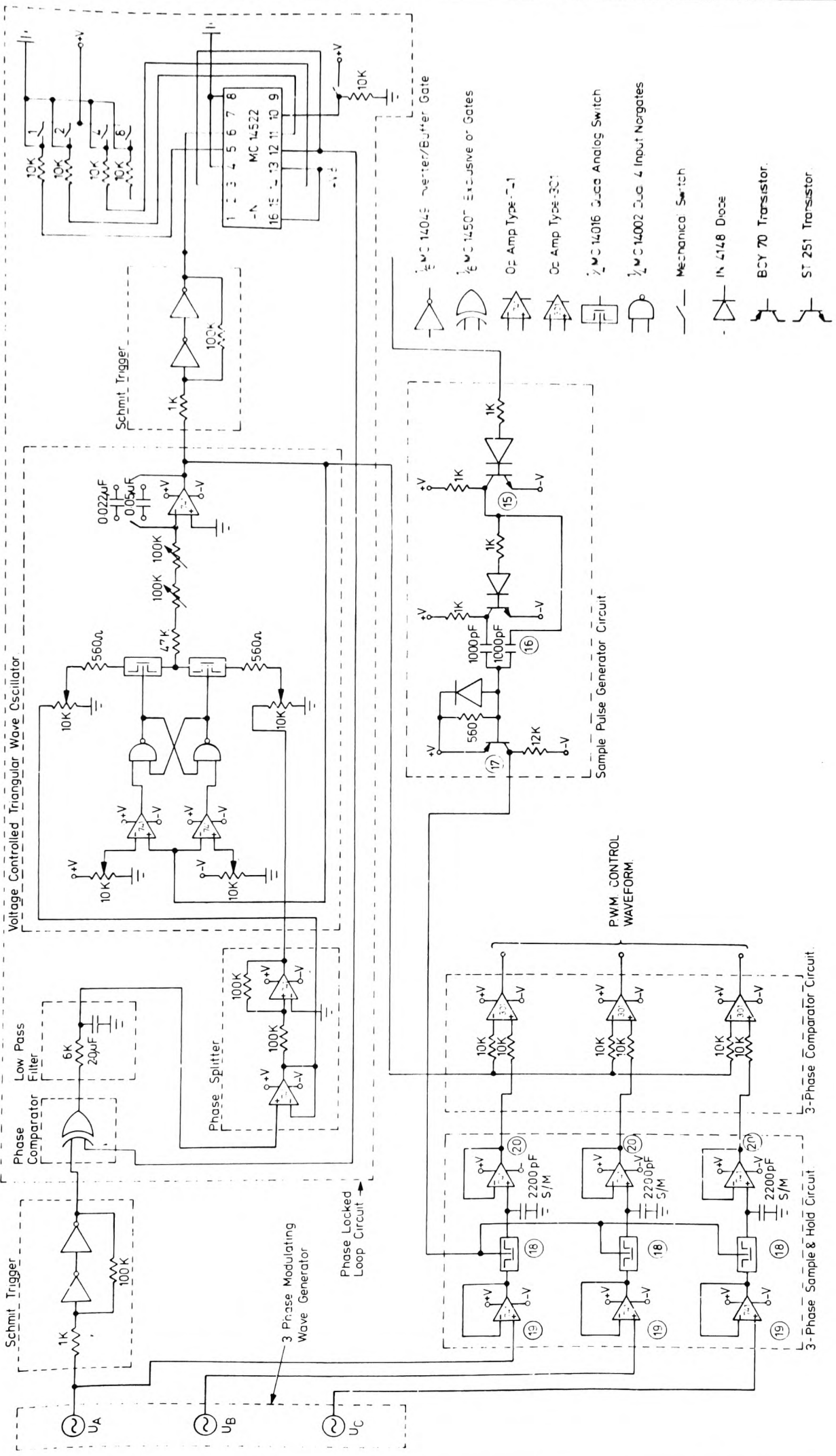
It may be seen from Fig.(10.2) that the control circuit for this p.w.m. process is identical to the circuit for the natural sampled p.w.m. process illustrated in Fig.(10.1) so far as the three-phase modulating wave generator, phase locked loop and comparator circuits are concerned. However, it is equally apparent from Fig.(10.2) that this regular sampled asymmetrical p.w.m. process requires a sample pulse generator circuit and a three-phase sample and hold circuit.

#### Sample Pulse Generator Circuit

The rectangular pulse waveform taken from between the schmitt trigger and divide by "N" programmable counter is fed to the base of a common emitter amplifier (15), which is connected in cascade with a further common emitter amplifier (16). The output signals from the collectors of these amplifiers supply the pulse shaping networks which consists of the two 1000pF capacitors and 560 ohm resistor. The current pulses drawn by the pulse shaping networks are then amplified by the emitter follower amplifier (17). The output pulses from amplifier (17) are synchronised with the output triangular carrier waveform from the phase locked loop and occur at instants corresponding to the positive and negative apices.

#### Sample And Hold Circuit

The output pulses from the sampling pulse generator circuit are fed to the three bi-lateral sampling switches (18). The



FIG(10.2) CONTROL CIRCUIT FOR SYNCHRONOUS MODE, REGULAR SAMPLED, ASYMMETRICAL DOUBLE - EDGE P.W.M

three modulating signals from the non-inverting buffer amplifiers (19) are then sampled at instants in time corresponding to the positive and negative apices of the triangular carrier wave, the samples being stored on the three 2200pF silver mica capacitors. The three regular sampled modulating waves are then fed to the non-inverting inputs of the three comparators, via the buffer amplifiers (20).



## APPENDIX (5)

Control Circuit For Asynchronous Mode, Natural Sampled

Double-Edge P.W.M., Regular Sampled, Symmetrical

Double-Edge P.W.M. and Regular Sampled Asymmetrical

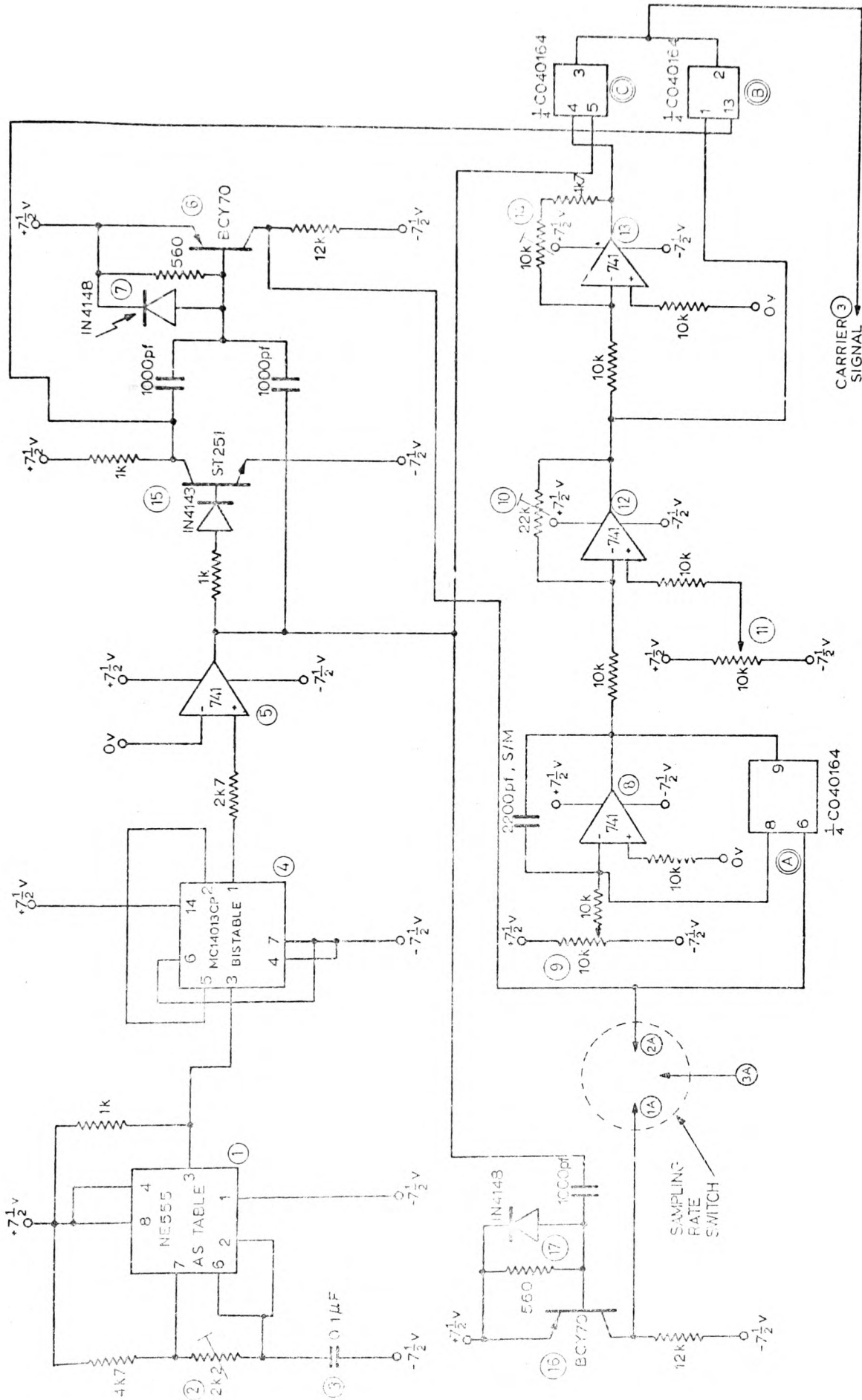
Double-Edge P.W.M.

The circuit which generates the triangular carrier wave and the sampling pulses is illustrated in Fig.(10.3a), whereas, the sample-and-hold circuit and p.w.m. generator circuit is illustrated in Fig.(10.3b).

### Carrier\_Wave\_Generator

Carrier-wave frequency control is achieved using the integrated circuit (I.C.) block (1), operated in the astable mode, as follows.

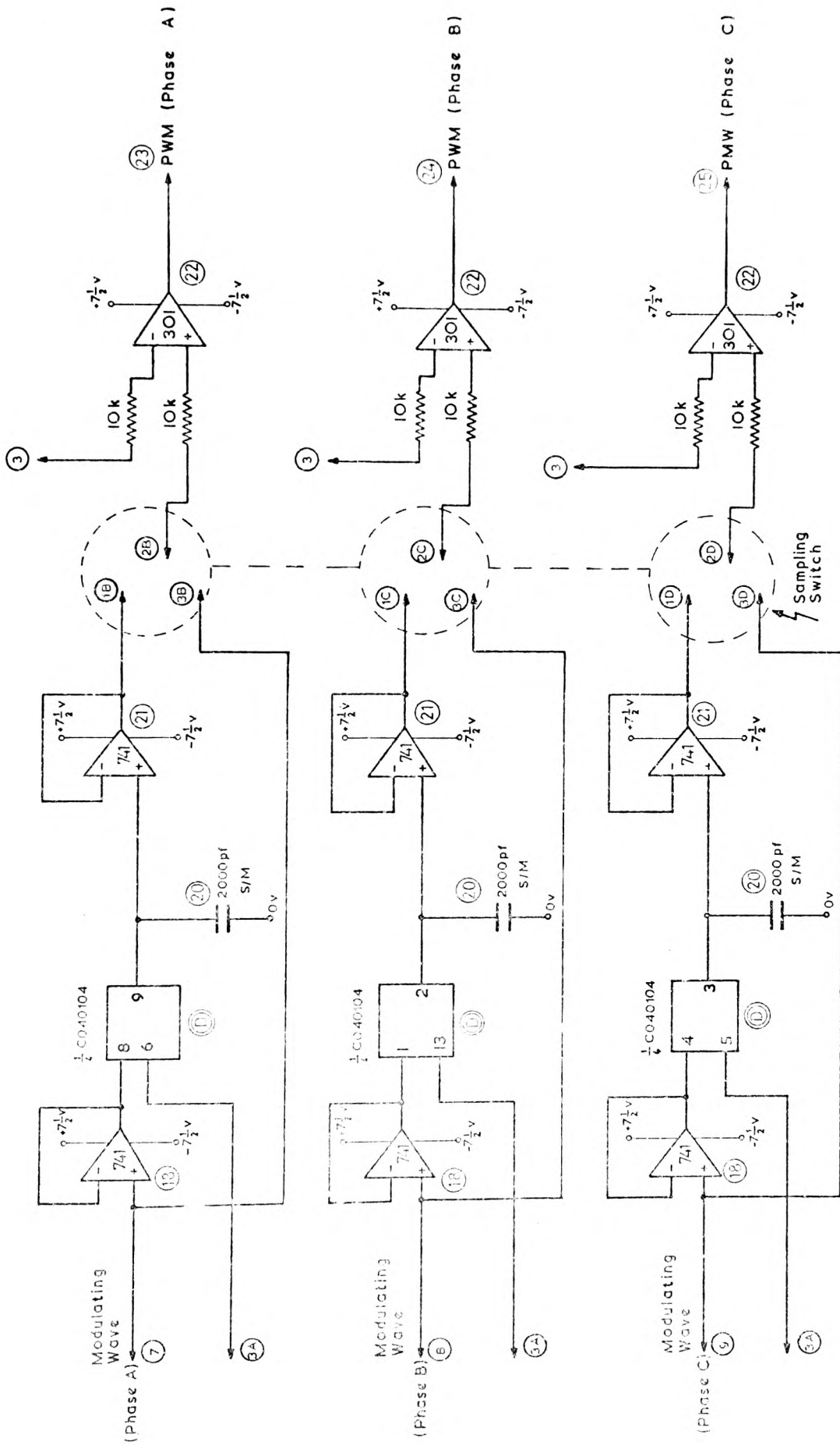
An alternating rectangular waveform voltage is generated by (1), which consists of an I.C. linear timer connected in its astable mode of operation; the mark/space ratio and frequency control is achieved by potentiometer (2) and capacitor (3). Since this device cannot be made to operate with a mark/space ratio of one, its output voltage is fed into the bistable I.C. (4). The output voltage from (4), with a mark/space ratio of one, is fed via open-loop amplifier (5) to the non-inverting pulse amplifier (6) via the pulse shaping network (7). The output pulses from (6) supply terminal (2A) of the sampling switch and the control terminal of switch (A); which is one of four bi-directional CMOS switches contained in one I.C. package. The frequency of operation of switch (A) controls the frequency of the output ramp function voltage of integrator (8). The magnitude of the ramp function voltage of (8) is controlled by potentiometer (9). The voltage from (8) feeds



(ii)

FIG (10.3a) CIRCUIT FOR GENERATING TRIANGULAR WAVE CARRIER SIGNAL & SAMPLING PULSES.

- (1) - FOR SYMMETRICAL MODULATION
- (2) - FOR ASYMMETRICAL MODULATION
- (3) - TO SAMPLE AND HOLD CIRCUITS
- (4) - TO COMPARATOR CIRCUITS



(iii)

(3) - TO MODULATION SWITCH  
 (3) - TO CARRIER SIGNAL  
 (13), (18), (12) - FOR REGULAR SAMPLING  
 (20), (20), (20) - FOR NATURAL SAMPLING  
 (20), (20), (20) - MODULATING WAVE INPUT TO COMPARATOR

(23) - OUTPUT PWM WAVE FOR PHASE A  
 (24) - OUTPUT PWM WAVE FOR PHASE B  
 (25) - OUTPUT PWM WAVE FOR PHASE C  
 (7), (8), (9) - TO 3-PHASE SINUSOIDAL MODULATING WAVE GENERATOR

FIG (10, 3b) PWM WAVEFORM GENERATOR & SAMPLING & HOLD CIRCUITS.

the input of amplifier (12), the gain of which is controlled by potentiometer (10) and the d.c. level of output voltage by potentiometer (11). The voltage from amplifier (12) supplies the input of amplifier (13) and input terminal of switch (B). The gain of amplifier (13) is controlled by potentiometer (14) and its output supplies the input terminal of switch (C). The outputs of switches (B) and (C) are connected together, the voltage at these common terminals providing the triangular carrier signal. The control voltage for switch (C) is derived from the output of open-loop amplifier (5), whereas the control voltage for switch (B) is supplied from the collector of pulse amplifier (15). The frequency of the triangular wave carrier therefore equals half the frequency of the output voltage from bistable (4) which in turn has a frequency equal to half the frequency of the astable (1).

#### Sampling Pulse Generator

This consists of a non-inverting pulse amplifier (16) whose input is obtained from the output of (5) via the pulse shaping network (17). The output from the pulse position modulator supplies terminal (1A) of the sampling rate switch. The output pulses from terminal (3A) of the sampling switch controls the operation of switch (D), which in turn determines the instants at which the modulating wave is sampled. The sample rate is therefore equal to the frequency of the bistable circuit (4) for the asymmetric mode and half the frequency of bistable (4) for the symmetric mode.

### Sample and Hold Circuits

These consist of buffer amplifiers (18) supplied with a variable frequency, variable amplitude three phase modulating wave, from a laboratory three-phase sine wave generator. The outputs from (18) supplies capacitors (20) for the instants during which switches (D) are closed; this is the time duration for which a pulse from the sampling rate switch (3A) exists. The voltage across capacitor (20) supplies the input of buffer amplifier (21). The output from (21) is the regular sampled modulating wave which supplies terminals (1B), (1C) and (1D) of the sampling switch.

For asymmetric double-edge modulation, the frequency of operation of switch (D) is equal to twice the frequency of the triangular carrier wave, whereas for symmetrical double-edge modulation the frequency is equal to the frequency of the triangular carrier wave. The decrease in sampling frequency for the symmetrical regular sampled mode is achieved by removing the output terminals (3A), of the sampling rate switch from (2A) to (1A).

### Comparators

These consist of operational amplifiers (22) supplied at (3) with the triangular carrier wave, and at (2B), (2C) and (2D) with the regular sampled modulating wave. The outputs of (22) are the pulse width modulated voltages (23), (24) and (25). The periods of the pulse-width-modulated voltages (23), (24) and (25) are proportional to the difference between the modulating voltages (2B), (2C) and (2D) and

the triangular carrier voltage (3). This was illustrated graphically in Chapter (3). The amplitudes of the fundamental components of the pulse-width-modulated voltages (23), (24) and (25) are only a function of the amplitude of the modulating voltages (2B), (2C) and (2D) since the amplitude of the carrier voltage (3) is maintained constant.

## LIST OF FIGURES

<u>Figure No.</u>	<u>Page No.</u>
2.1 Time Domain Representation of Pulse Modulation	9
2.2 Unmodulated Pulse Carrier Wave Of Unity Amplitude	10
2.3 Pulse Amplitude Modulation	12
2.4 Pulse Position Modulation	14
2.5 Types of Pulse Width Modulation	16
2.6 Trailing-Edge Pulse Width Modulation	17
2.7 Leading-Edge Pulse Width Modulation	20
2.8 Double-Edge Pulse Width Modulation	22
2.9 Amplitude Modulation of a P.P.M. Wave	26
2.10 Amplitude Modulation of a P.W.M. Wave	29
2.11 Two-Thyristor/Two-D.C. Supply Pulse Convertor	33
2.12 Four-Thyristor/Single-D.C. Supply Pulse Convertor	34
2.13 R.L.C. Commutation Circuit	36
2.14 Auxiliary Impulse Commutated Half-Bridge Circuit	37
2.15 Auxiliary Impulse Commutated Full-Bridge Circuit	39
2.16 Auxiliary Impulse Commutated Bridge Circuits With Feedback Diodes	40
2.17 Switching Function Control of P.W.M. Power Convertor	43
2.18 Switching Function Control of P.A.M. Power Convertor	44

<u>Figure No.</u>		<u>Page No.</u>
2.19	P.W.M. Control For Conduction Angle ( $\gamma$ ) of $120^\circ$	46
2.20	P.W.M. Control For Conduction Angle ( $\gamma$ ) of $60^\circ$	47
2.21	Unmodulated Bipolar Carrier Wave	50
2.22	Width Control Of The Load Voltage Waveform	54
2.23	Multiple Pulse Output Waveform	56
2.24	Increase In The Number Of Commutations With Increase In Frequency Ratio	60
2.25a	Combining Of Two Modulating Waveforms By Means Of A Transformer	62
2.25b	The Combining Of Two P.W.M. Waveforms By Means Of A Transformer In The Time Domain	63
2.26	3-Phase Modulator Excluding Auxiliary Commutating Components	69
3.1	Linear Time - Position Modulation Process	75
3.2	Output Modulated Waveforms For Modulation Indices of: 0.0, 0.5 and 1.0	77
3.3	Leading-Edge P.W.M.	79
3.4	Trailing-Edge P.W.M.	80
3.5	Double-Edge P.W.M.	82
3.6	Limitation Of The Generalised Sampling Theorem Applied To The Natural Sampled Single-Edge P.W.M. Process	87



<u>Figure No.</u>	<u>Page No.</u>
3.7	89
Limitation Of The Generalised Sampling Theorem Applied To The Natural Sampled Double-Edge P.W.M. Process	
3.8	91
Generation Of Regular Sampled Modulating Wave	
3.9	93
Regular Sampled Leading-Edge P.W.M.	
3.10	95
Regular Sampled Trailing-Edge Modulation	
3.11	97
Regular Sampling Symmetrical Double-Edge P.W.M.	
3.12	99
Regular Sampling Asymmetrical Double-Edge Modulation	
4.1	105
3-Phase Modulator (Excluding Auxiliary Commutating Components)	
4.2	107
Amplitude And Phase Of Harmonic Components Of Line To D.C. Neutral Voltage Waveforms And Line To Line Voltage Waveforms For Natural Sampled, Leading-Edge P.W.M.	
4.3	109
Phase-Sequence Chart For Respective Harmonics Of Line To D.C. Neutral Voltage Waveform And Line To Line Voltage Waveform	
4.4	112
Amplitude And Phase Of Harmonic Components Of Line To D.C. Neutral Voltage Waveforms And Line To Line Voltage Waveforms For Natural Sampled Double-Edge P.W.M.	
4.5	113
Phase-Sequence Chart For Respective Harmonics Of Line To D.C. Neutral Voltage Waveform And Line To Line Voltage Waveform	

<u>Figure No.</u>		<u>Page No.</u>
4.6	Block Diagram Of Control Circuit For Natural Sampled Double-Edge P.W.M.	119
4.	Natural Sampled Double-Edge P.W.M. Control Circuit Supplying 3-Phase, 3-Wire Load	121
4.8a	Harmonic Spectra For Line To D.C. Neutral Voltage Waveform For Frequency Ratio Of 3 And Modulation Index of 1.0 For Natural Sampled Double-Edge P.W.M.	123
4.8b	Phase Sequence Of Respective Line To D.C. Neutral Voltage Waveform Harmonics For Frequency Ratio Of 3, And Modulation Index of 1.0 For Natural Sampled Double- Edge P.W.M.	124
4.8c	Harmonic Spectra For Line To Line Voltage Waveform For A Frequency Ratio Of 3 And Modulation Index of 1.0, For Natural Sampled Double-Edge P.W.M.	125
4.9a	Harmonic Spectra For Line To Neutral Voltage Waveform For A Frequency Ratio Of 6 And Modulation Index of 1.0, For Natural Sampled Double-Edge P.W.M.	126
4.9b	Phase Sequence Of Respective Line To D.C. Neutral Voltage Waveform Harmonics For Frequency Ratio of 6 And Modulation Index of 1.0, For Natural Sampled Double- Edge P.W.M.	127

4.9c	Harmonic Spectra For Line To Line Voltage Waveform For A Frequency Ratio of 6 And Modulation Index of 1.0, For Natural Sampled Double-Edge P.W.M.	128
4.10a	Harmonic Spectra For Line To D.C. Neutral Voltage Waveforms For A Frequency Ratio Of 5 And Modulation Index of 1.0, For Natural Sampled Double-Edge P.W.M.	129
4.10b	Phase Sequence Of Respective Line To D.C. Neutral Voltage Waveform Harmonic For Frequency Ratio Of 6, And Modulation Index of 1.0, For Natural Sampled Double-Edge P.W.M.	130
4.10c	Harmonic Spectra For Line To Line Voltage Waveforms For Frequency Ratio Of 5 And Modulation Index of 1.0 For Natural Sampled Double-Edge P.W.M.	131
4.11a	Harmonic Spectra For Line To D.C. Neutral Voltage Waveforms For a Frequency Ratio Of 2, And Modulation Index of 1.0, For Natural Sampled Double-Edge P.W.M.	132
4.11b	Phase Sequence Of Respective Line To D.C. Neutral Voltage Waveform Harmonics For Frequency Ratio Of 2, And Modulation Index of 1.0, For Natural Sampled Double-Edge P.W.M.	133

- 4.11c Harmonic Spectra For Line To Line Voltage Waveforms For Frequency Ratio Of 2, And Modulation Index of 1.0, For Natural Sampled Double-Edge P.W.M. 134
- 4.12 Amplitude And Phase Of Harmonic Components of Line To D.C. Neutral Voltage Waveforms And Line To Line Voltage Waveforms For Regular Sampled Symmetrical Double-Edge P.W.M. 141
- 4.13 Phase Sequence Chart For Respective Harmonics Of Line To D.C. Neutral Voltage Waveforms And Line To Line Voltage Waveform For Regular Sampled, Symmetrical Double-Edge P.W.M. 142
- 4.14 Amplitude And Phase Of Harmonic Components Of Line To D.C. Neutral Voltage Waveforms And Line To Line Voltage Waveforms For Regular Sampled Asymmetrical Double-Edge P.W.M. 143
- 4.15 Phase Sequence Chart For Respective Harmonics Of Line To D.C. Neutral Voltage Waveforms And Line To Line Voltage Waveforms For Regular Sampled Asymmetrical Double-Edge P.W.M. 144
- 4.16 Block Diagram Of Control Circuit For Regularly Sampled Asymmetrical Double-Edge P.W.M. 149
- 4.17 Natural Sampled Double-Edge P.W.M. Process 151

<u>Figure No.</u>	<u>Page No.</u>
4.18 Regular Sampled Asymmetrical Double-Edge P.W.M. Process	152
4.19 Comparison Of Natural Sampled Double-Edge P.W.M. With Regular Sampled Asymmetrical Double-Edge P.W.M.	154
4.20 Harmonic Spectra For Line To Line Voltage Waveform For Frequency Ratio Of 3 And Modulation Index of 1.0	156
4.21 Phase Sequence Of Respective Line To Line Voltage Harmonics For Frequency Ratio Of 3 And Modulation Index of 1.0	157
4.22 Variation In Percentage Amplitude Of 5th and 7th Harmonics With Frequency Ratio For Natural Sampled Double-Edge P.W.M. And Regular Sampled Asymmetrical Double-Edge P.W.M.	158
4.23 Harmonic Spectra For Line To Line Voltage Waveform For Frequency Ratio Of 6 And Modulation Index of 1.0	159
4.24 Phase Sequence Of Respective Line To Line Voltage Harmonics For Frequency Ratio Of 6 And Modulation Index of 1.0	160
4.25 Harmonic Spectra For Line To Line Voltage Waveform For Frequency Ratio of 5 And Modulation Index of 1.0	162
4.26 Phase Sequence Of Respective Line To Line Voltage Harmonics For Frequency Ratio Of 5 and Modulation Index of 1.0	163

4.27	Harmonic Spectra For Line To Line Voltage Waveform For Frequency Ratio Of 2 And Modulation Index of 1.0	165
4.28	Phase Sequence of Respective Line To Line Voltage Harmonics For Frequency Ratio of 2 And Modulation Index of 1.0	166
4.29	Variation In Amplitude Of Fundamental Component With Modulation Index	168
5.1	Block Diagram Of Asynchronous Mode, Natural Sampled Double-Edge P.W.M. Control System	172
5.2	Asynchronous Mode Natural Sampled Double- Edge P.W.M. Process	173
5.3	Asynchronous Mode Natural Sampled Double- Edge P.W.M. Process	174
5.4	Output Modulated Waveform For Carrier Frequency Of 1000Hz And Modulating Frequency of 300 Hz	178
5.5	The Effect Of The Random Time-Phase Displacement Between The Carrier Wave and Modulating Wave Upon The Natural Sampled Double-Edge P.W.M. Process	181
5.6	Three-Phase Modulator (Excluding Commutating Components)	184
5.7	D.C. Components In Line To Line Voltage Waveforms As % of Wanted Harmonic Components For Modulation Index of 1.0	187

5.8	D.C. Components In Line To Line Voltage Waveforms As % of Wanted Harmonic Components For Modulation Index of 0.5	188
5.9	D.C. Components In Line To Line Voltage Waveforms As % of Wanted Harmonic Components For Modulation Index of 0.2	189
5.10	Percentage Amplitude And Phase of Harmonics In Both Line To D.C. Neutral Voltage Waveform And Line To Line Voltage Waveform For Natural Sampled Double-Edge P.W.M.	192
5.11	Phase Sequence Chart of Respective Harmonics in Both Line To D.C. Neutral Voltage Waveform And Line To Line Voltage Waveform	193
5.12	Percentage Amplitude and Phase Of Harmonic Components In Both The Line To D.C. Neutral Voltage Waveform And Line To Line Voltage Waveforms For Natural Sampled Double-Edge P.W.M.	195
5.13	Amplitude Of Harmonic Components In Line To Line Voltage Waveforms Expressed As Percentage Of the Wanted Harmonic Components For A Modulation Index of Unity	201
5.14	Percentage Amplitude of Harmonic Components In Line To Line Voltage Waveforms For A Modulation Index of Unity	203
5.15a	Block Diagram of Light Electronic Control Circuit which Simulates The Three Double- Edge P.W.M. Processes	205

<u>Figure No.</u>		<u>Page No.</u>
5.15b	Waveforms At Points Indicated On Block Diagram Illustrated in Fig.(5.15a) For One Phase Only	206
Plate		
5.1	Oscilllograms Of Line To Neutral And Line To Line Voltages	208
5.16	Natural Sampled Double-Edge P.W.M. Control Circuit Supplying 3-Phase,3-Wire Load	209
5.17	Line To Line Voltage Waveform Harmonics For Natural Sampled Double-Edge P.W.M.	214
5.18	Line To Line Voltage Waveform Harmonics For Regular Sampled Symmetrical Double-Edge P.W.M.	215
5.19	Line To Line Voltage Waveform Harmonics For Regular Sampled Asymmetrical Double-Edge P.W.M.	216
Plate		
6.1	3-Phase, 240 volt, 7KVA Power Convertor	219
6.1	Schematic Layout Diagram of Practical Power Convertor	220
6.2	Circuit Diagram of Uncontrolled A.C. to D.C. Convertor	222
6.3	3-Phase Auxiliary Impulse Commutated Thyristor Invertor	223
6.4	Inhibition and Steering Circuits For Phase (A) Of The Three-Phase Power Inverter	226
6.5	Trigger Pulse Amplifier Circuits For Phase (A) of Threc-Phase Power Inverter	229



<u>Figure No.</u>		<u>Page No.</u>
6.6	Synchronisation of Thyristor Gate Trigger Pulses With The P.W.M. Control Signal	230
6.7	Line To Line Voltage Harmonics For $f_m = 20$ Hz, $\frac{f_c}{f_m} = 3$ , and Modulation Index = 0.5	233
6.8	Line To Line Voltage Harmonics For $f_m = 30$ Hz, $\frac{f_c}{f_m} = 4$ , And Modulation Index = 0.5	234
6.9	Line To Line Voltage Harmonics For $f_m = 40$ Hz, $\frac{f_c}{f_m} = 5$ , And Modulation Index = 0.5	236
6.10	Line To Line Voltage Harmonics For $f_m = 40$ Hz, and Modulation Index = 0.95	238
6.11	Line To Line Voltage Harmonics For $f_m = 90$ Hz, And Modulation Index = 0.95	240
6.12	Line To Line Voltage Harmonics for $f_m = 140$ Hz and Modulation Index = 0.95	241